Structure Activity Relationships of Monomeric and Dimeric Strychnine Analogs as Ligands Targeting Glycine Receptors

Dissertation zur Erlangung des

naturwissenschaftlichen Doktorgrades

der Julius-Maximilians-Universität Würzburg

vorgelegt von

Amal Mahmoud Yassin Mohsen

aus Kuwait

Würzburg, 2016

Eingereicht am ……..
bei der Fakultät für Chemie und Pharmazie

1. Gutachter:……
2. Gutachter:……

der Dissertation

1. Prüfer:……...
2. Prüfer:……
3. Prüfer:……
des öffentlichen Promotionskolloquiums

Tag des öffentlichen Promotionskolloquiums:…….

Doktorurkunde ausgehändigt aus: ……

Die vorliegende Arbeit wurde in der Zeit von 2011 bis 2016 am Institut für Pharmazie und Lebensmittelchemie der Bayerischen Julius-Maximilians-Universität Würzburg unter der Anleitung von **Frau Prof. Dr. Ulrike Holzgrabe** mit finanzieller Unterstützung der Deutschen Forschungsgemeinschaft angefertigt.

ACKNOWLEDGMENTS

First and foremost, I thank **ALLAH** for giving me the strength, patience, and knowledge to complete this work.

Immeasurable appreciation and deepest gratitude for the help and support are extending to the following persons who in one way or another have contributed in making this work possible.

I would like to express my sincere gratitude to Prof. Dr. Ulrike Holzgrabe for giving me the opportunity to prepare my thesis as a member of her research group. Her endless support has been of a great help during these years. Her wide knowledge and her logical way of thinking have been of great value for me. Thanks for providing me with room and facilities to work in her laboratories. She gave me the freedom to explore on my own and at the same time the guidance to recover when my steps weakened.

My endless appreciation goes to Prof. Dr. Darius P. Zlotos for suggesting this project and for his continuous support along my Master and PhD work. Thanks for the constructive help, enthusiasm, valuable comments and inspiration. Thanks for recommending me to work in Professor Holgrabe's research group. I will be always grateful for his support in all levels. His patience, motivation, enthusiasm, and immense knowledge helped me throughout my research and writing of this thesis.

I wish to express my warm and sincere thanks to Professor Anders A. Jensen, Department of Medicinal Chemistry and Drug Design, University of Copenhagen, Denmark; Prof. Hans-Georg Breitinger and Dr. Ulrike Breitinger, GUC; and Prof. Carmen Villmann, Institute for Neurobiology, Würzburg University, Germany, for performing the pharmacological testing. I also thank Prof. Thomas Dandekar and Dr. Edita Sarukhanyan, Bioinformatics, Würzburg University, for molecular modeling studies and for the very pleasant cooperation.

Great thanks goes to all the members of Prof. Holzgrabe group, Dr. Jens Schmitz, Dr. Eberhard Heller, Dr. Ludwig Höllein, Dr. Ines Schmidt, Regina Messerer, Michael Berninger, Dr. Johannes Wiest, Daniela Volpato, Anna Hofmann, Christine Erk, Oliver Wahl, Liana Pogorelaja and Dr. Florian Seufert who were always very helpful in the lab, in NMR measurements and recording of the mass spectra. I also want to thank Lieselotte Moehler, and Christine Ebner for their help, support and for their nice and warm welcoming. Many thanks to Dr. Bernd Reyer and Dr. Curd Schollmayer for the technical support.

I am thankful to Huma Rasheed, Joseph Skaf and Yonah Hebron for their help and support during my PhD journey in Wuerzburg.

I owe a deep since of gratitude to Dr. Mohammad Abdel-Halim, lecturer of pharmaceutical chemistry department, GUC, for his continuous help whenever I was in need. Thanks for all the time and effort he gave me. Without him, completing this work would have been more difficult.

The success of any project depends largely on the encouragement and guidelines of many others. I take this opportunity to express my gratitude to the people who have been instrumental in the successful completion of this project. I am grateful to my laboratory friends Noura Riad and Yasmine Mandour for their nice company, help and support through the whole PhD work in Germany and Egypt. I would like to show my greatest appreciation to my friends Dr. Mostafa Hamed, Amal Ali, Noha Osman and Rasha Rasheed. I am greatly thankful to all my colleagues in the Pharmaceutical Chemistry Department, the German University in Cairo for the support, for being friendly and for encouraging me during the completion of this work specially Islam Eldiasty, Ahmed Kamal, Eman ELsayed, Eman Hafez, Reem Wagdy, Sarah Sameh, Reem Khaled and Menna Hammam.

I dedicate this work to the soul of my father, Mahmoud Yassin, who raised me, educated me, taught me, believed in me and supported me in every step of my life. He has been my ideal role model and for this I dedicate all my achievements to him, and will live my life to make him proud. I would like to thank the greatest

women in my life, my beloved mother, whose patience, struggle and unconditional love gave me the strength and confidence to continue this work. I am grateful for my brother, my backbone, for being supportive. To them I dedicate this thesis.

Amal Mahmoud Yassin Mohsen

Table of Contents

ACKNOWLEDGMENTS I

Table of Contents IV

List of Figures VII

List of Abbreviations I

1. Introduction 3

1.1. Ligand-Gated Ion Channels 3

1.2. Glycine Receptors as Ligand-Gated Ion Channel 4

1.2.1. Glycine Receptors Physiological Functions and Distribution 4

1.2.2. Glycine Receptors Structure 4

1.2.3. Glycine Receptor Subtypes 5

1.2.4. Glycine Binding site 6

1.2.5. Glycine Receptors Gating 7

1.2.6. Glycine Receptors Ligands 9

1.3. Strychnine 12

1.3.1. Strychnine Origin, Physical Properties and Discovery 12

1.3.2. Strychnine Pharmacokinetic Properties 13

1.3.3. Strychnine Pharmacological Actions 13

1.4. Crystal Structure of the Human Glycine Receptor Binding to Strychnine…. 15

1.5. Structure Activity Relationship of Strychnine 17

1.5.1. Strychnine Analogs with Anticonvulsive and muscle relaxant effects…… 17

1.5.2. Structure Activity Relationships of Strychnine Analogs Having Activity at the GlyRs 19

1.6. Strychnine Toxicity and Detoxification 21

1.7. Strychnine's Uses.....22

1.8. Bivalent Ligand Approach 23

1.8.1. Bivalent Ligands Benefits.....24

1.8.2. Some Examples of Bivalent Ligands.....25

1.8.3. Designing Bivalent Ligands 26

1.9. Bivalent Ligands for Ion Channels.....29

1.9.1. Nicotinic Acetylcholine Receptor (nAChR).....29

1.9.2. $5HT_3$ Serotonin Receptors 30

1.9.3. $GABA_A$ Receptors 31

1.9.4. Glycine Receptor Dimeric Ligands 33

2. Aim of work 35

3. References 38

4. Results 46

4.1. Structure–Activity Relationships of Strychnine Analogs at Glycine Receptors.....46

4.2. Oxime Ethers of (E)-11-Isonitrosostrychnine as Highly Potent Glycine Receptor Antagonists.....59

4.3. Dimeric Strychnine Analogs as Bivalent Ligands Targeting Glycine Receptors.....91

5. Overall Discussion and Conclusion 112

6. References 118

7. Summary.....119

8. Zusammenfassung.....122

9. APPENDIX.....126

9.1. NMR Spectra of the Compounds Described in Chapter 4.1 ...127

9.2. NMR Spectra of the Compounds Described in Chapter 4.2 ...137

9.3. NMR Spectra of the Compounds Described in Chapter 4.3 ...153

9.4. LC-MS Chromatograms of the Compounds Described in Chapter 4.3.....161

List of Figures

Figure 1 Binding of the ligand to ligand-gated ions channels followed by opening of the ion channels. 3
Figure 2: (A): Structure of four transmembrane region (4-TM) in receptor subunit, (B): TM2 faces the central pore of the ion channel 5
Figure 3: Structures of homomeric α_1 and heteromeric $\alpha_1\beta$- GlyRs. (A): Schematic drawing of the pentameric arrangement of GlyR subunits in homo-oligomeric α_1 and (B): hetero-oligomeric α1β GlyRs. Binding sites for glycine are indicated in blue 7
Figure 4: Binding of glycine to strychnine-sensitive glycine receptor and the influx of Cl^- ions..... 8
Figure 5: Structures of some glycine receptor antagonists 11
Figure 6: Structure of strychnine with numbering of atoms 12
Figure 7: Schematic diagram illustrating the inhibition of GlyR and chloride ions flow after strychnine binding. 14
Figure 8: Binding of both glycine and strychnine at the same binding site on glycine receptors. 14
Figure 9: Orthosteric binding site of homomeric human GlyR α3 occupied by strychnine. 15
Figure 10: Binding interactions of strychnine at orthosteric binding site of homomeric human GlyR α3. 16
Figure 11: Cryo-microscopy structure of the orthosteric binding site of zebra fish α1 GlyR with strychnine. 17
Figure 12: Structures of strychnine analogs..... 19
Figure 13: Structures of more strychnine analogs 21
Figure 14: General structure of the bivalent ligands..... 23
Figure 15: Some examples of bivalent ligands 25

Figure 16: Structure of the monomer ML10302 with possible spacer attachment points and the structure of 5-HT_4 homo-bivalent ligand based on ML10302 pharmacophores and the possible spacer 27
Figure 17: Structure of KDN-21, a hetero-bivalent ligand targeting δ and κ opioid receptor heterodimers attachment points. 27
Figure 18: Nicotinic acetylcholine bivalent ligands 30
Figure 19: $5HT_3$ serotonin receptor bivalent ligands 31
Figure 20: Some examples of $GABA_AR$ dimeric ligands..... 32
Figure 21: Structures of the reference monomeric propionamide and octanamide and structures of the bivalent ligands derived from 2-aminostrychnine. n= 2, 3, 4, 6, 8, 10..... 33
Figure 22: Strychnine (A) and 2-aminostrychnine (B) in the orthosteric binding pocket of the homomeric α1 glycine* 34
Figure 23: Structures of 9 strychnine derivatives, *(R)*-11-aminostrychnine, *(R)*-Strychnine-11yl propionamide, 11-*(E)*-isonitrososstrychnine and 11 oxime ether..... 36
Figure 24: Structures of potential series of strychnine-derived bivalent ligands of GlyRs 37
Figure 25: Structural modifications applied to strychnine..... 113
Figure 26: Structure-activity relationships of strychnine and its analogs.. 115
Figure 27: Structural modification applied to strychnine. 120

List of Abbreviations

µM	Micromolar
5-HT$_3$R	Serotonin type 3 receptor
Å	Angstrom
Ach	Acetylcholine
Arg	Arginin
BAM22	Bovine adrenal medulla peptide 22
BzR	Benzodiazepine receptor
CNS	Central nervous system
Cys	Cystein
DEPT	Distortionless Enhancement by Polarization Transfer
DIPEA	N,N-Diisopropylethylamine
DMF	Dimethylformamide
DMSO	dimethyl sulphoxide
EC$_{50}$	half maximal effective concentration
ECD	Extracellular domain
ESI	Electrospray ionization (ESI)
G	Gram
GABA	gamma-Aminobutyric acid
GABA$_A$R	GABA type A receptor
Gly	Glycine
GlyA	Strychnine-sensitive glycine receptors
GlyB	Strychnine-insensitive glycine receptor
GlyRN	Neonatal glycine receptor
GlyRs	Glycine receptors
GPCRs	G-Protein coupled receptors
HATU	(1-[Bis(dimethylamino)methylene]-1H-1,2,3-triazolo[4,5-b]pyridinium 3-oxid hexafluorophosphate)
hGlyRs	Human glycine receptors

HH-COSY	^{1}H-^{1}H-Correlation Spectroscopy
HMQC	Heteronuclear Multiple Quantum Coherence
Hr/h	Hour
Hz	Hertz
IC_{50}	half maximal inhibitory concentration
INS	Isonitrososstrychnine
Kd	Dissociation constant
LGICs	Ligand gated ion channels
Mp	Melting point
MS	Mass Spectroscopy
nAChR	Nicotinic acetylcholine receptor
nM	nanomolar
NMR	Nuclear Magnetic Resonance
NOESY	Nuclear Overhauser Enhancement Spectroscopy
ON-O*t*-Bu	Tertiary butyl nitrite
OR	Opioid receptor
Phe	Phenylalanine
Ppm	parts per million
Rt	Room temperature
SNSR	Sensory neuron-specific receptor
t-BuOK	Potassium tertiary butoxide
Thr	Threonin
Tyr	Tyrosine

1. Introduction

1.1. Ligand-Gated Ion Channels

Ligand-gated ion channels (LGICs) are a group of transmembrane ion channel proteins which open/close to allow cations such as Na^+, K^+, Ca^{2+}, or anions such as Cl^- to pass through the membrane in response to the binding of a chemical messenger (i.e. a ligand) such as a neurotransmitter. This permits cells to respond rapidly to changes in their external environment (Figure 1).[1] Therefore, LGICs are known for mediating fast excitatory and inhibitory transmission in the central and peripheral nervous system[2, 3] and this rapid response is measured in a matter of milliseconds.[4] That is why the neurotransmission at most synapses usually involves ion channels.[5] The normal functioning of the CNS depends on the balanced interaction of both excitatory and inhibitory neurons. Glutamate is the principal excitatory while GABA and glycine are the major inhibitory neurotransmitters in the mammalian CNS.

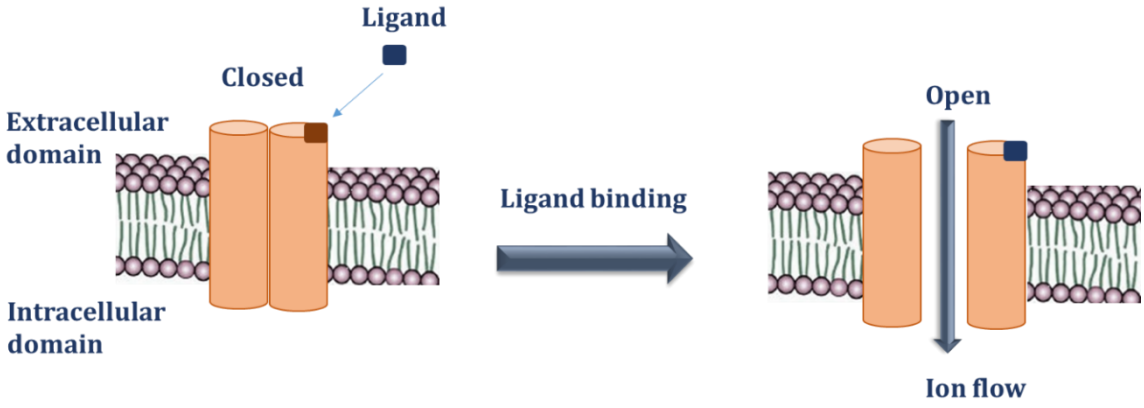

Figure 1: Binding of the ligand to ligand-gated ions channels followed by opening of the ion channels.

1.2. Glycine Receptors as Ligand-Gated Ion Channel

1.2.1. Glycine Receptors Physiological Functions and Distribution

Glycine receptors (GlyRs) were the first neurotransmitter receptor proteins isolated from the mammalian CNS.[6] GlyRs are present in the spinal cord and brain stem where they are chiefly involved in the regulation of motor functions. Additionally, they are found in sensory pathways of the spinal cord, including pain fibers, as well as the auditory and visual system.[2] They are also involved in the inflammatory pain sensitization.[7, 8] Glycine levels are highest in the medulla oblongata, pons and spinal cord regions, in which GlyRs are prominently expressed.[6] Extraneuronal glycine receptors have been found in Kupffer cells from liver and in sperms.[9]

1.2.2. Glycine Receptors Structure

GlyRs topology and the amino acid composition of GlyR subunits classify this receptor as a member of the Cys-loop receptors, that include also the cation-selective nicotinic acetylcholine receptor (nAChR), the serotonin type-3 receptor (5-HT_3R) and the anion-selective GABA type A receptor ($GABA_A$R).[3] They share common transmembrane topology as well as structural and functional features.[5] They are named Cys-loop receptors for the extracellular domain (ECD) of each subunit since it possess a characteristic 13-residue loop formed by a disulfide bond between two cysteine (Cys) residues.[10] The amino terminal in GlyRs, which contains the ligand binding site,[4] and the carboxy terminal of the polypeptide chains are located in the extracellular space (the synaptic cleft), whereas the protein chain transverses the cell membrane four times. This means that each subunit has four transmembrane regions (TM1-TM4) which are hydrophobic in nature.[4] They are connected by a short linker between TM1 and TM2 and a large loop between TM3 and TM4 (Figure 2-A).[6, 8, 11] The subunits are arranged such that the second

transmembrane region (TM2) of each subunit faces the central pore of the ion channel (Figure 2-B).[4, 6]

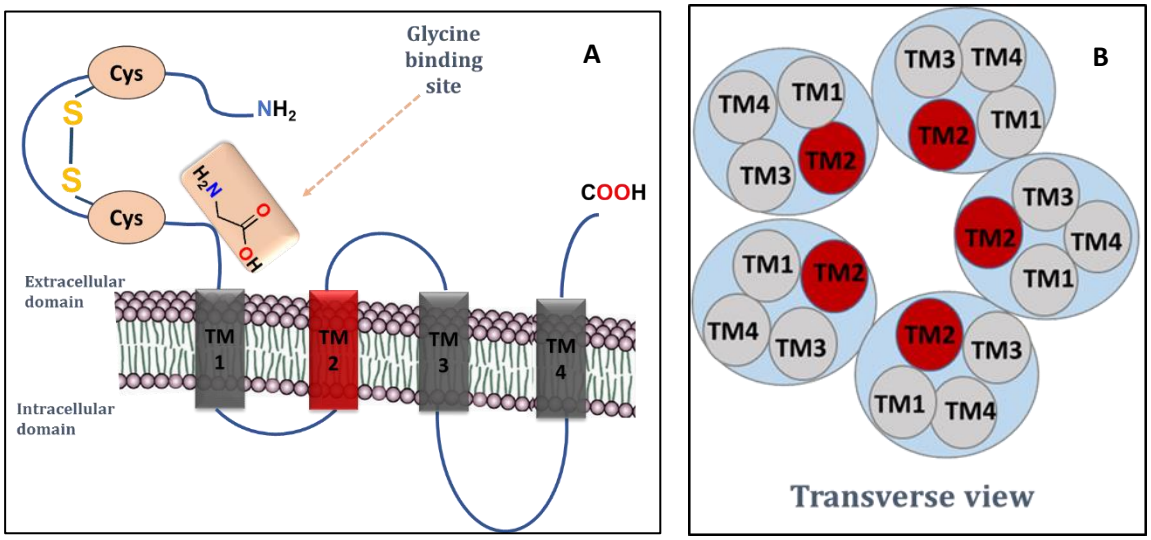

Figure 2: (A): Structure of four transmembrane region (4-TM) in receptor subunit, (B): TM2 faces the central pore of the ion channel (modified from [4] with permission)

1.2.3. Glycine Receptor Subtypes

GlyR complex is composed of two glycosylated integral membrane proteins of 48 kDa (α) and 58 kDa (β) and a peripheral membrane protein of 93 kDa (gephyrin).[8] There are four known isoforms of the α-subunit (α1-4) while there is a single β-subunit.[12] Glycine receptors can be homomeric including only α subunits or heteromeric containing both α and β subunits (Figure 3).

GlyRs are pentameric channels with the five subunits surrounding a central pore[12] in a stoichiometric ratio of two α to three β subunits[5] or three α subunits and two β subunits.[13] The β subunit is unable to form homo-oligomeric receptors.[8] The β subunit anchors the receptor to the cytoskeleton via its attachment to the tubulin binding protein (gephyrin).[14] Gephyrin is believed to mediate synaptic clustering and anchoring at inhibitory synapses by interacting with the subsynaptic cytoskeleton. Therefore, gephyrin restricts the mobility of glycine receptors from

diffusing in the plane of the plasma membrane.[8, 15] The neonatal glycine receptor (GlyRN) appears to be a homopentamer consisting of α_2 subunits, while the adult receptor isoform is a complex heteropentameric glycoprotein of α_1 and β subunits (see Figure 3-B).[2] In contrast to the predominant expression of α subunits in spinal cord and brain stem, the β subunit is widely distributed throughout the central nervous system.[9]

1.2.4. Glycine Binding site

The orthosteric site is located in the amino-terminal domains of the subunits, and the transmembrane regions of the subunits constitute the ion channel domain.[16] The binding site is located at the interface of two adjacent subunits and is surrounded by two loops from the principle (+) subunit, loop C between strands β9 and β10 and loop B between strands β7 and β8 and the β-strands on the complementary (-) subunit. Three residues were identified to be present near TM1 of the human glycine-receptor α1 subunit, Lys200, Tyr202 and Thr204. Additionally, residues Gly160 and Tyr161, were identified as part of the glycine binding pocket. Other residues involved in ligand binding include Ala101, Asn102 and Lys193.[7, 9] The arginine residues located at the (–) interfaces of the α and β subunits (α1 Arg65, β Arg86) are found to form strong ionic interactions with the α-carboxyl group of glycine. Moreover, the acidic residues at their (+) interfaces (α1 Glu157, β Glu180) interact with its α-amino group. The homomeric GlyRs have five identical ligand binding sites for agonists and antagonists at all subunit interfaces. On the other hand, the interfaces of heterooligomeric GlyRs are heterogeneous (αβ, βα and ββ), and evidence that all interfaces contribute to agonist binding is lacking.[6] Equilibrium radioligand binding studies and whole-cell current measurements, propose that glycine and strychnine bind to partially overlapping sites on the receptor.[7, 9]

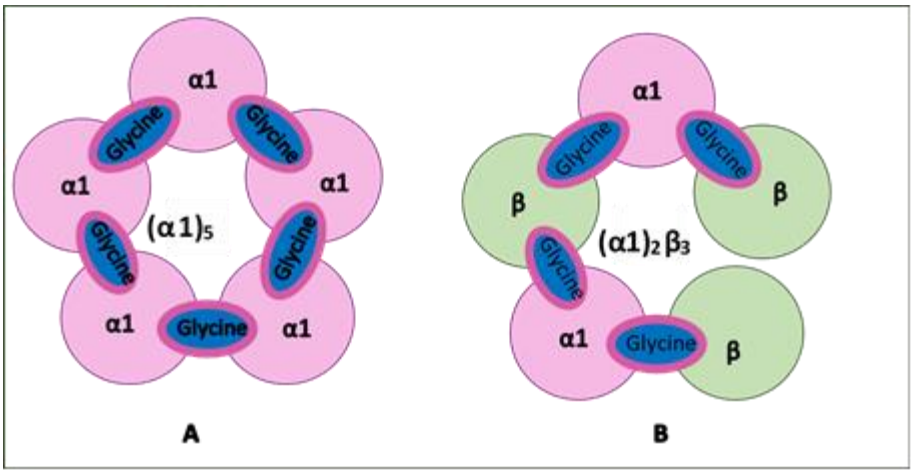

Figure 3: Structures of homomeric α_1 and heteromeric $\alpha_1\beta$- GlyRs. (A): Schematic drawing of the pentameric arrangement of GlyR subunits in homo-oligomeric α_1 and (B): hetero-oligomeric $\alpha1\beta$ GlyRs. Binding sites for glycine are indicated in blue (modified from[6] with permission)

1.2.5. Glycine Receptors Gating

Glycine is the major inhibitory transmitter in the CNS.[3] Glycine-mediated inhibitory neurotransmission is essential for reflex responses, voluntary motor control and the processing of sensory signals in the mammalian CNS.[17] It acts through two receptors: a strychnine-sensitive glycine receptor (GlyA) and a strychnine-insensitive glycine receptor (GlyB). GlyA is localized in the post synaptic membrane of inhibitory glycinergic neurons, whereas GlyB is associated with the excitatory (NMDA) receptor. Glycine therefore has a dual action on neuronal excitability[18] and serves both inhibitory and excitatory functions within the CNS.[19]

1.2.5.1. Strychnine-Sensitive Glycine Receptor (GlyA)

Glycine binds to GlyA receptors on inhibitory neurons and terminates action potentials. Its binding causes conformational changes in the receptor which opens the central pore allowing chloride ions influx flowing down their concentration

gradient.[4, 5] The resulting change in the ionic composition across the membrane of the neuron alters the postsynaptic potential, producing hyperpolarization of the postsynaptic membrane (Figure 4). This prevents depolarization and neuronal firing induced by excitatory neurotransmitters.[5, 8]

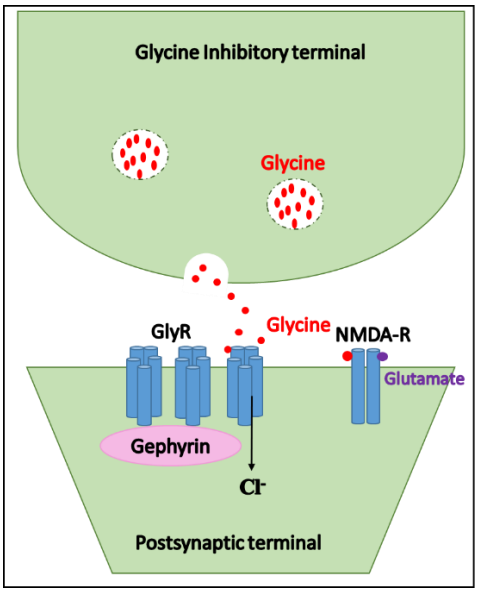

Figure 4: Binding of glycine to strychnine-sensitive glycine receptor and the influx of Cl^- ions.[9] (with permission)

The expression of chloride transporters, and thus the chloride potential in neurons, is developmentally regulated. Embryonic glycine receptors are in fact excitatory due to elevated levels of intracellular chloride in early development.[9] Therefore, glycine receptors have been known to be depolarizing during development. The functional meaning of the developmental switch from excitatory to inhibitory glycine receptor action remains to be elucidated.[8]

1.2.5.2. Strychnine-Insensitive Glycine Receptor (GlyB)

GlyB are NMDA receptors which are ligand-gated ion channel that belong to the glutamate receptor family and possess a high affinity glycine binding site (K_D = 100 nM). Glycine is co-agonist of GlyB receptor (Figure 4).[2]

1.2.6. Glycine Receptors Ligands

1.2.6.1. Agonists

Whereas glycine is the principal physiological agonist at GlyRs[8], taurine and β-alanine have been proposed as endogenous glycine-receptor agonists. However, their affinities and efficacies are lower than that of glycine.[9, 19] Interestingly, low concentrations of these amino acids have been found to antagonize the response to the natural agonist glycine.[20] Glycine receptor agonists are ranked by their potency to activate the receptor as follows: glycine> ß-alanine >taurine> L- and D-α-alanine >L-serine >D-serine.[2]

To date, the only non-amino acid glycinergic agonist identified is cesium. Moreover, there is evidence that the antihelminthic and anticonvulsant, avermectin $B1_{\alpha}$, may also activate GlyRs.[3, 17]

1.2.6.2. Allosteric Potentiators

Allosteric potentiators are effector molecules that potentiate the receptor activity by binding at a site other than the receptor's active site (allosteric binding site). The principal excitatory transmitter glutamate has been reported to allosterically potentiate GlyRs; this may be important for balancing excitation and inhibition in the CNS.[11] Ivermectin and related avermectins also modulate the gating activity of GlyRs.[3] Glucose and fructose were found to be positive modulator of the receptor, reducing the average EC_{50} for glycine up to 4.5-fold.[21] Additionally, high

concentrations of ethanol was reported to enhance the function of brain GlyRs.[17, 22] Moreover, neurosteroids and general anesthetics such as isoflurane and hydrocortisol potentiate GlyR currents. It was also reported that zinc strongly potentiates glycine currents by increasing the apparent glycine affinity at the GlyR at concentrations from 20 nM to 10 mM but reduces glycine affinity at higher concentrations (>20 mM).[6, 11, 17]

1.2.6.3. Antagonists

Localization and characterization of glycine receptors as well as demonstration of their involvement in the CNS inhibitory signal transmission were greatly facilitated by the availability of the selective high-affinity ligand strychnine.[2] Strychnine is a highly selective and extremely potent competitive antagonist of glycine, p-alanine and taurine. The structurally related alkaloid, brucine, also potently and selectively antagonizes glycine-activated currents. A series of opiate alkaloids related to morphine have also been shown to have considerable selectivity for the GlyR over the GABAR, although many of these compounds also have effects on central opioid receptors.[17]

Picrotoxin is an alkaloid that is known to be a potent antagonist at both $GABA_A$ receptors and homomeric GlyRs. However, heteromeric GlyR, consisting of α and β subunits, display a 50-100 fold reduced sensitivity to picrotoxin block.[15]

A series of benzodiazepines such as flunitrazepam, bromazepam, and nitrazepam were found to be potent antagonists of GlyR. Bicuculline is a noncompetitive antagonist of the GlyR. Additionally, its structurally related convulsant alkaloid, laudanosine, selectively antagonizes glycine responses. Steroids such as RU 5135 and progesterone are also selective glycine antagonist.[17] Moreover, the cannabinoids, anandamide and 2-arachidonoylglycerol inhibit glycine currents. Interestingly, at low glycine concentrations, nanomolar

concentrations of anandamide and 2-arachidonoylglycerol were found to potentiate glycine-mediated currents.[11] Cyanotriphenylborate (CTB) and ginkgolide B act as a GlyR ion channel blockers (Figure 5).[17]

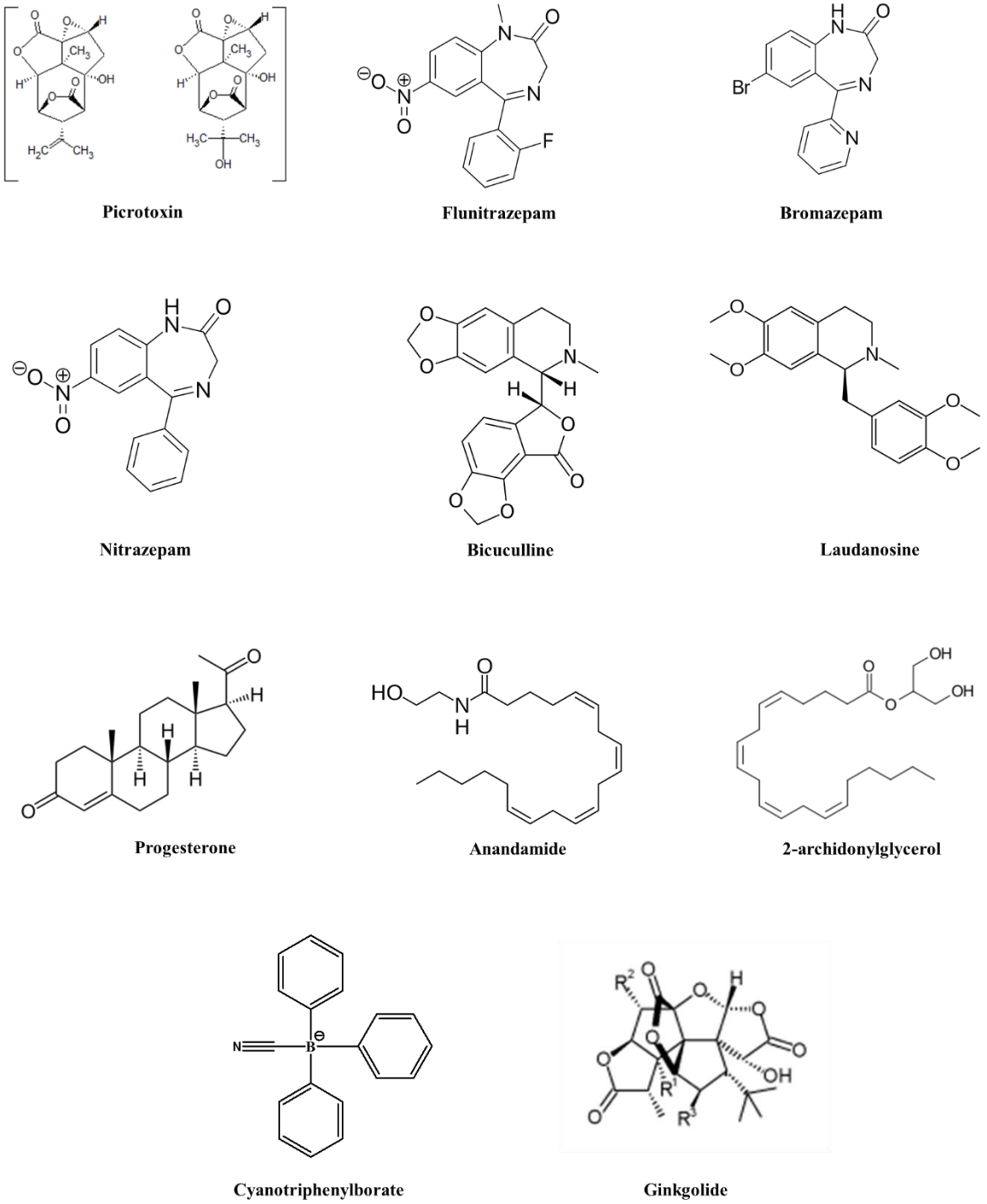

Figure 5: Structures of some glycine receptor antagonists

1.3. Strychnine

1.3.1. Strychnine Origin, Physical Properties and Discovery

Strychnine (Figure 6) was isolated from the seeds, bark and roots of the Indian tree *Strychnos nux vomica* and other members of the Strychnos plant family (Longaniaceae) in 1818.[23] Seeds of *Strychnos nux vomica* contain 1.4–3% strychnine.[23, 24] Strychnine is a white crystalline, odorless, bitter-tasting compound and a deadly poison. Strychnine is an indole alkaloid with 24 skeletal atoms and a molecular formula $C_{21}H_{22}N_2O_2$. Its structure contains 7 rings with 6 stereocentres.[25] This molecular formula was established in the early 1830s.[26] Given that from this molecular formula one could propose millions of distinct isomers,[27] thousands of scientists became involved in the elucidation of strychnine structure to understand how the 21 carbon atoms were connected using stepwise chemical degradation for more than 100 years. The chemical structure was determined in 1948 by Woodward and Robinson and was confirmed by x-ray analysis in 1950.[27] A first total synthesis of strychnine was published in 1954.[28]

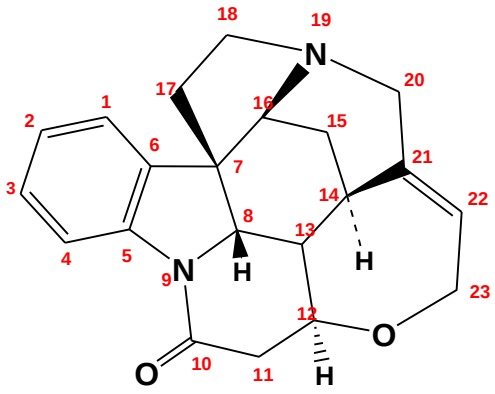

Figure 6: Structure of strychnine with numbering of atoms

1.3.2. Strychnine Pharmacokinetic Properties

Strychnine is soluble in acidic medium but poorly soluble in either water. It is absorbed very rapidly through the gastrointestinal tract, the respiratory tract and intact skin.[24] It undergoes rapid and extensive metabolism. Five metabolites formed in *vitro* by rabbit liver were determined as 2-hydroxystrychnine, strychnine *N*-oxide (major, 15%), 21-α, 22-β-dihydroxy-22-hydrostrychnine, 21, 22-epoxide and 11, 12-dehydrostrychnine. Strychnine biological half-life (in humans) is 10–12 hours. Up to 20% is excreted unchanged in the urine within 24 hours.[24]

1.3.3. Strychnine Pharmacological Actions

1.3.3.1. Strychnine as a Potent GlyR Inhibitor

The inhibitory glycine receptor is potently and selectively inhibited by strychnine.[29] While strychnine can bind to the same binding site of glycine, enabling interaction with the ligand binding site, the bulk of the molecule is thought to block the ion channel thereby inhibiting ion channel flux.[2] It acts as a competitive antagonist of glycine that results in the inhibition of Cl^- ions permeation which reduces GlyR-mediated inhibition[2] and thus causes overexcitation of spinal motor and sensory neurons (Figure 7).[30] According to the recently published crystal structure of glycine receptor, strychnine binds in a pocket at the interface between adjacent subunits, corresponding to the orthosteric binding site of glycine; both binding sites are patially overlapping (Figure 8).[3]

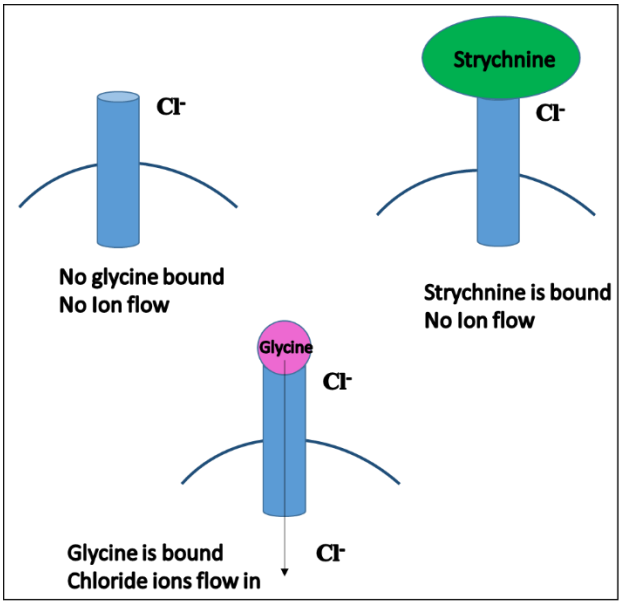

Figure 7: Schematic diagram illustrating the inhibition of GlyR and chloride ions flow after strychnine binding.

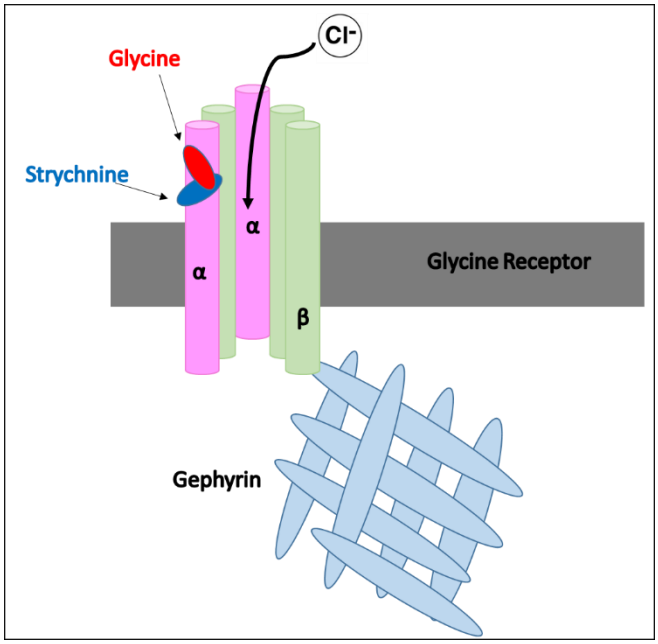

Figure 8: Binding of both glycine and strychnine at the same binding site on glycine receptors. (modified from[15] with permission).

1.3.3.2. Strychnine as an Antagonist at other Receptors

Numerous reports have provided evidence that strychnine is not only a competitive antagonist at glycine receptors but also a potent competitive antagonist at nicotinic acetylcholine receptor (nAChRs). It can inhibit cholinergic transmission at the neuromuscular junction and in sympathetic ganglia. A presynaptic nicotinic mechanism appears to account for the ability of strychnine to block the release of ACh from sympathetic ganglia and to block the release of catecholamines from adrenal medullary cells. The anticholinergic effects of strychnine in the auditory system have been observed at concentrations as low as 0.01 mM.[31] Additionally, strychnine and brucine are also well known allosteric modulators of muscarinic acetylcholine receptors.[16]

1.4. Crystal Structure of the Human Glycine Receptor Binding to Strychnine

Recently, 3.0 Å X-ray structure of the human glycine receptor α3 homopentamer in complex with a high affinity, high-specificity antagonist strychnine as well as electro-cryomicrosopy structures of the zebra fish α1 GlyR in complex with strychnine and glycine were published (Figure 9).[3, 7] This will allow exploring the binding modes of antagonists on glycine receptors.

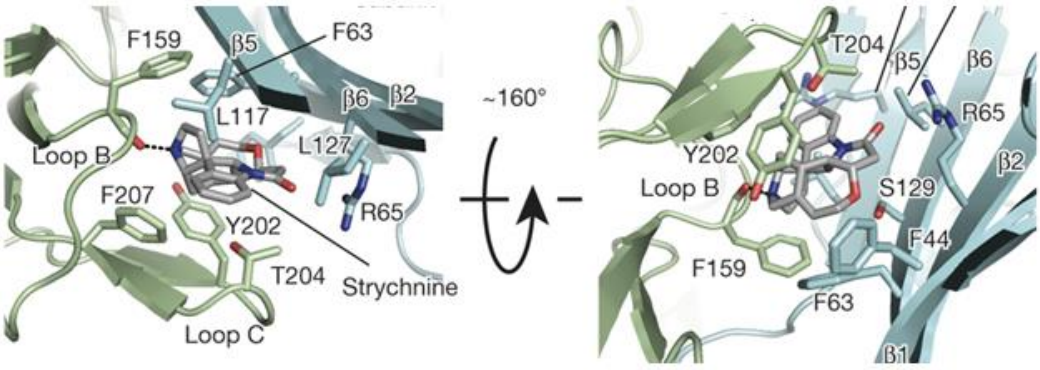

Figure 9: Orthosteric binding site of homomeric human GlyR α3 occupied by strychnine.[7] (with permission)

Two Phe residues (63 and 159) in the GlyR binding site form the hydrophobic 'base' of the binding pocket for the pyrolidine, piperidine and the tetrahydrooxepine rings including the C21=C22 double bond of strychnine. These Phe residues make hydrophobic interactions with these rings and with the π electrons of the double bond. The 'flap' of the binding pocket is composed of residues Tyr202, Thr204, and Phe207 from loop C. Moreover, the carbonyl group of Phe159 makes a hydrogen bond interaction with the tertiary amine of strychnine which is protonated at physiological pH (pKa = 8.26). The lactam oxygen also serve as a hydrogen bond acceptor in a H-bond interaction with the Arg65 (Figure 10).[7] This binding mode of strychnine indicates that the lactam group, the tertiary amine and the C21=C22 double bond are very essential structural features required for strong antagonistic activity towards GlyR.

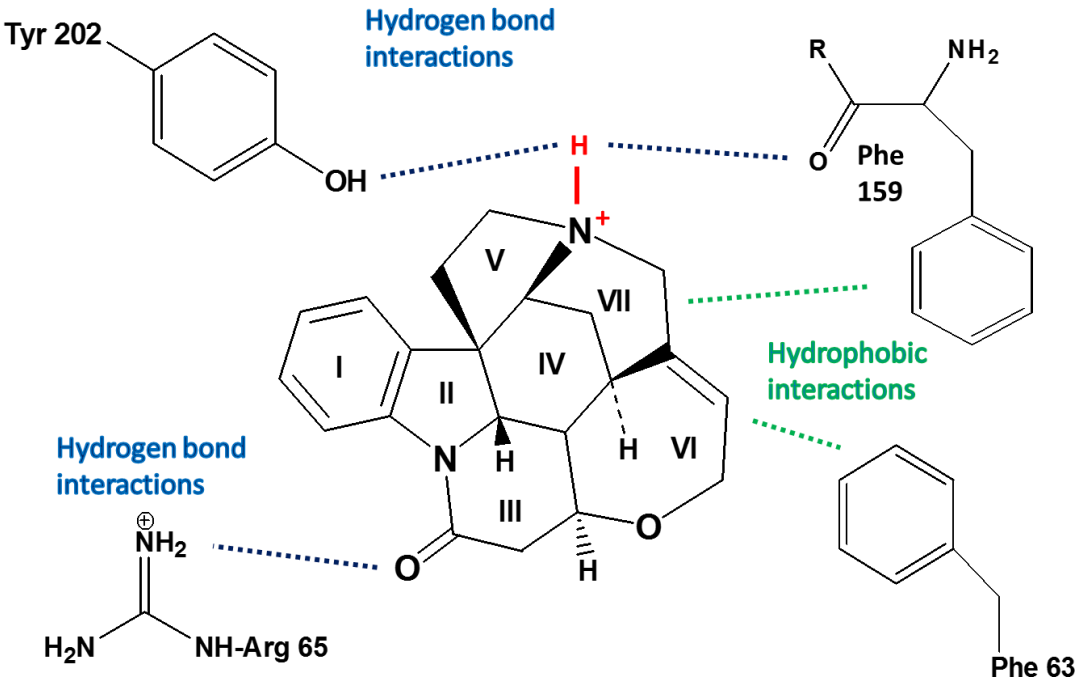

Figure 10: Binding interactions of strychnine at orthosteric binding site of homomeric human GlyR α3.[7] (with permission)

Du *et* al. suggested a similar binding mode of strychnine at zebra fish α1 GlyR. They suggested also a possible hydrogen bond between the carbonyl oxygen of strychnine and Arg81. Proximity of the same carbonyl to Thr220 (C loop), and sandwiching of strychnine's aromatic rings by Phe79 and Tyr218 further enhance interactions between the antagonist and receptor (see Figure 11).[3]

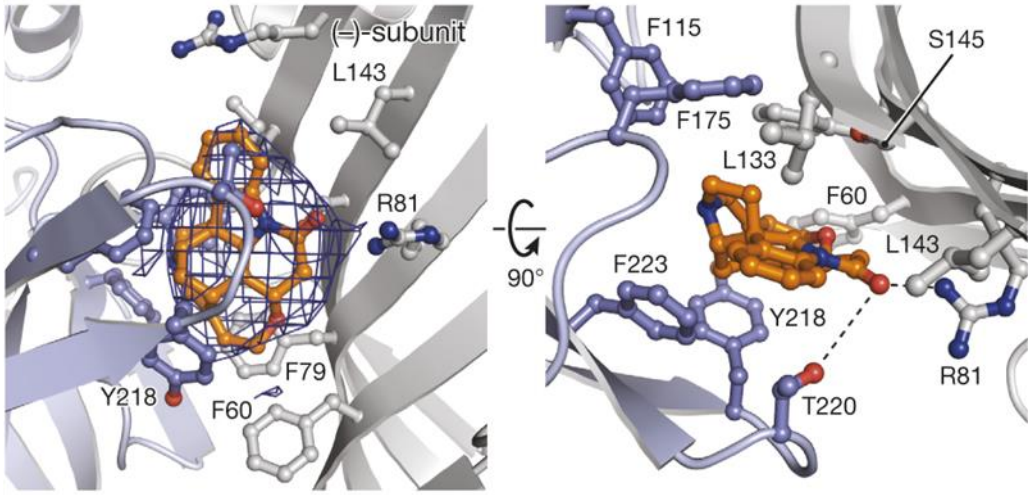

Figure 11: Cryo-microscopy structure of the orthosteric binding site of zebra fish α1 GlyR with strychnine.[3] (with permission)

1.5. Structure Activity Relationship of Strychnine

1.5.1. Strychnine Analogs with Anticonvulsive and muscle relaxant effects

In the purpose of obtaining a detailed SARs of the strychnine skeleton at GlyRs, many structural modifications were applied, however, up to now, only a limited number of pharmacological studies has been described, most of them on the convulsive effect and lethal doses in animal experiments.[32-34] In this section, the effect of various structural modification on the anticonvulsive and muscle relaxant activities is described (Figure 12).

2-aminostrychnine was reported to show high affinity for the strychnine binding sites of synaptic membranes from brain and spinal cord of rats comparable

to that of strychnine.[33] Strychnine derivatives containing the lactam group and the C21=C22 double bond were reported to be able to induce an anticonvulsive effect after subcutaneous injection in mice. Lacking of such functional groups led to a remarkable decrease in activity. Strychnidine, lacking the amido group, as well as 21, 22-dihydrostrychnine induce less convulsion compared to that of strychnine and show lethal effects in animal experiments. These findings indicate that the lactam group is responsible for the characteristic strychnine effect. The analog 21,22-dihydrostrychnidine is about twice as active and four times as toxic as strychnidine itself. When hydroxyl groups are introduced at the 21 and 22-positions as in 21,22-dihydroxy-21-22-dihydrostrychnine and 21-hydroxy-22-oxo-21,22-dihydrostrychnine, a combined convulsant and muscle-relaxant effect appeared. Introduction of an epoxy function in the 21 and 22-positions decreased the convulsant and toxic activity but no muscle-relaxant effect appeared. The decreased activity indicates that the 21,22-double bond is another important active site for the receptor. The 16-alkoxystrychnine produces both clonic and tonic convulsions. The convulsive activity and lethal effects decreased with increasing size of the alkyl substituent, whereas the unalkylated 16-hydroxy compound is the active in this series. Strychnine *N*-oxide analog showed a decreased convulsive effect, however no muscle relaxant effect appeared.[32]

Quaternary strychnine and strychnidine derivatives exhibit curiform activity but the potency is low compared to that of the curarines.[34] N-methyl strychnine, N-methyl strychnidine and N-methyl-21-22-dihydrostrychnine could produce muscle relaxant effect only. An explanation for this could be that the charged quaternary compounds cannot cross the blood brain barrier and hence cannot reach the active site in the CNS.[32]

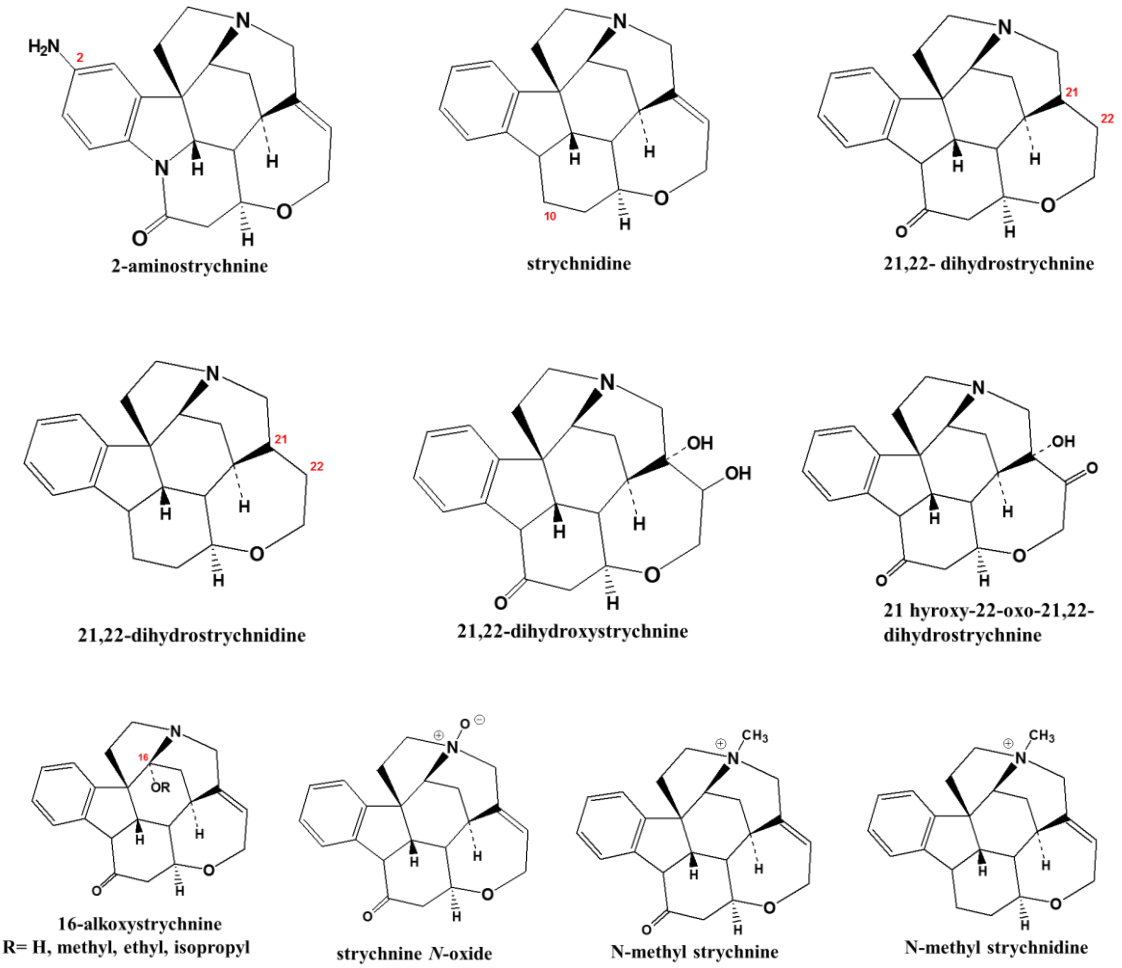

Figure 12: Structures of strychnine analogs

1.5.2. Structure Activity Relationships of Strychnine Analogs Having Activity at the GlyRs

In the course of the studies on GlyR ligands, a series of strychnine analogs as well as dimeric ligands have been characterized pharmacologically at the human α1 and α1β glycine receptor subtypes. However, none of the analogues exhibited significant selectivity for either of the two subtypes. The only modification that did not impair the antagonist potencies of the parent compounds was an E-configured hydroxyimino group at the C11-position of strychnine. However, the Z-stereoisomer, exhibited 23-fold and 16-fold lower antagonistic activities than the

corresponding E-stereoisomer at the α1 and α1β subtypes, respectively.[16] In this section, the pharmacological activities of various strychnine analogs on α1 and α1β GlyR subtypes are described (Figure 13).

Saturation of the C21=C22 double bond of strychnine to give 21,22-dihydrostrychnine resulted in significant reductions in antagonist potencies (33-fold and 10-fold compared to strychnine at α1 and α1β, respectively. This finding indicated that the presence of the C21=C22 double bond in the strychnine ring system is important for GlyR binding.[16]

Wieland Gumlich aldehyde resulted in a 58-fold and 10-fold decrease in antagonist potency at the α1 and α1β subtypes, respectively, while 2-nitrostrychnine only slightly inhibited glycine receptor signaling at a concentration of 100 μM. More strikingly, all mono- and bis-quaternary compounds were inactive at the glycine receptors (at concentrations up to 100 μM) regardless of the steric and electronic properties of their respective N19-substituents.[16] This is in agreement with the findings that quaternary strychnine derivatives exhibit actions on nicotinic receptors and are almost purely muscle relaxants.[32] Strychnine-*N*-oxide, the only compound with the positive charge on N19 fully compensated by the negatively charged oxygen atom, was inactive at both receptor subtypes. This showed the importance of cationic centres for this ligand–receptor interaction.

In summary, the lactam group, the C21=C22 bond of strychnine and the present of a cationic centre represented by the tertiary nitrogen could be identified as essential structural features required for strong antagonistic activity at glycine α1 and α1β receptors.

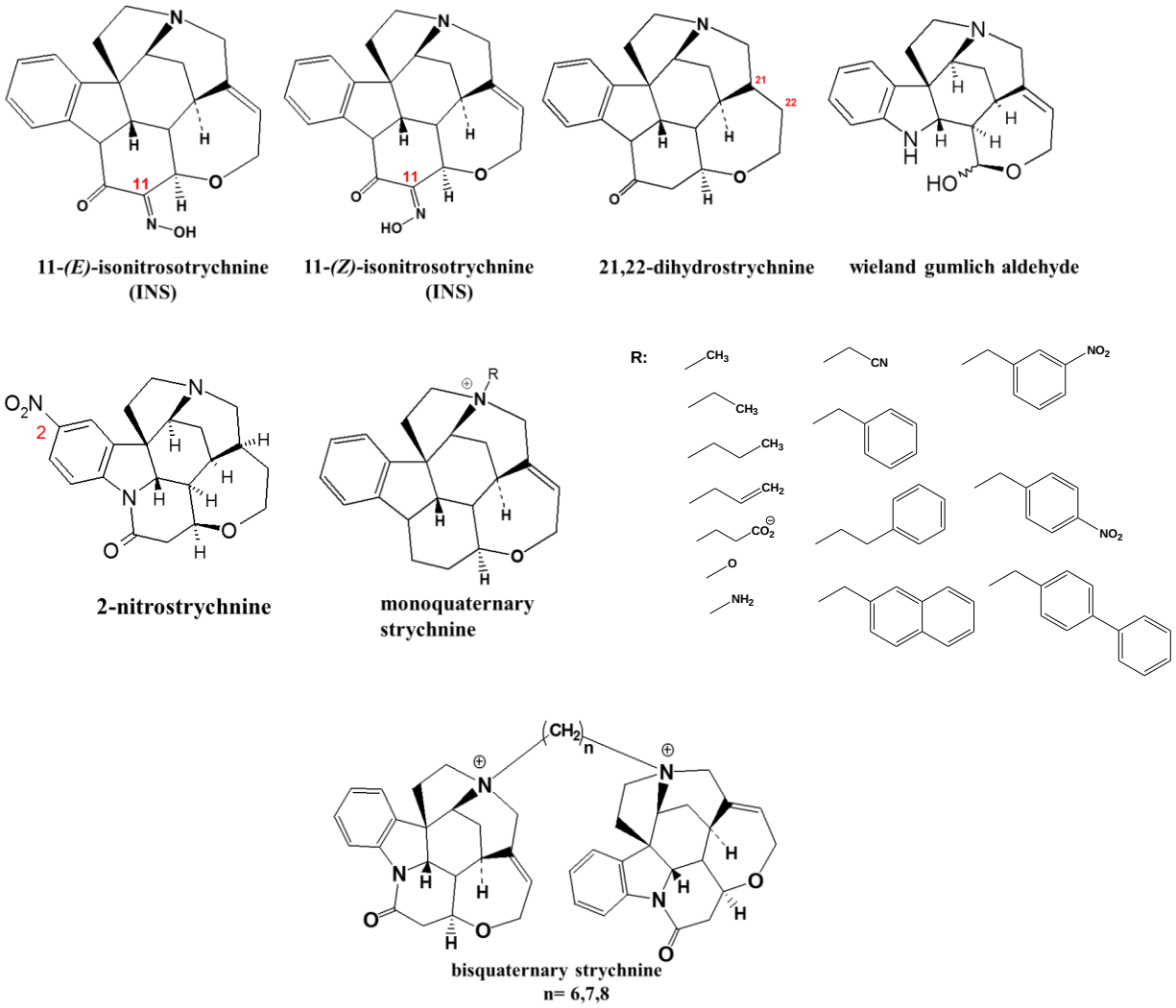

Figure 13: Structures of more strychnine analogs

1.6. Strychnine Toxicity and Detoxification

Strychnine causes characteristic and painful symptoms if it is inhaled, ingested and absorbed into the body. It has a very low lethal dose of about 1 mg/kg.[2] The first symptoms usually appear within 5 minutes to 1 hour after exposure depending on the dose, the route of exposure, and the general medical health of the person exposed.[24] Poisoning with strychnine and disruption of the normal function of hGlyRs is characterized by glycinergic disinhibition overexcitation and muscle

spasms.[8] It results also in muscular contractions and tetanus-like contractions while the person is fully conscious.[19, 35] Toxicity with strychnine results also in hyperekplexia (a rare inherited disease associated with an exaggerated startle response)[10] and seizures that have traditionally been linked to competitive antagonism of glycine receptors in the spinal cord.[36] Sensory stimulation initiates painful convulsions and arrest of respiration which can cause immediate death.[2]

Toxicity of strychnine and loss of glycinergic inhibition can be overcome by treatment with diazepam or other (GABA-A) potentiators. For example, clonazepam which potentiates (GABA-A) receptor function reduced the startle activity in hyperekplexia, while stiffness was unaffected.[2] As it was mentioned before, ivermectin, the agonist on glycine receptors, is an effective antidote of strychnine toxicity.[29]

1.7. Strychnine's Uses

Although strychnine's therapeutic uses are banned nowadays, it was claimed to have various benefits such as increasing appetite, toning skeletal musculature, increasing memory and curing snakebites. Strychnine's therapeutic uses appear to be only in very low doses. It was used as a pesticide until 1968 and a rodenticide until 2006 when its sale was banned.[37] It was found to be a miracle drug which is used as a pain-reliever and also it was used against worms and plague. In 1803, it was added to the list of malaria, female hysteria and epilepsy treatment.[23]

Small doses of strychnine were once used in medications as a stimulant, laxative, and as a treatment for other stomach ailments.[25, 38] Strychnine was also the most desired (and economically profitable) ingredients for universally popular "tonics" and this poisonous substance continued to be marketed as a tonic ingredient even into the 20th century.[23] Strychnine was used therapeutically to treat general depression, overwork, standing hypotension, urinary incontinence and nerve disorders such as polyneuritis.[39] In the late 1800s, cyclists, boxers, swimmers and

runners were taking strychnine tablets with mixtures of brandy and cocaine. Its use was not only limited to human athletes only but also the very successful Australian racehorse Phar Lap was fed strychnine, cocaine and other stimulants including caffeine.[25] Strychnine was also used by a gold-medal winner, Thomas Hicks, during the marathon at the 1904 Olympics as a performance-enhancer. After a couple of strychnine injections he died.[23, 25, 38] Because of its high toxicity and tendency to cause convulsions, the use of strychnine in medicine was eventually abandoned once safer alternatives became available.[38]

1.8. Bivalent Ligand Approach

A highly attractive approach to investigate the receptor dimerization may be provided by the utilization of bivalent ligands which can act as molecular probes simultaneously binding two adjacent binding sites of a dimer. Generally, bivalent ligands are defined as compounds that contain two pharmacophoric units separated by an appropriately designed spacer using an attachment point to connect them together (Figure 14).[40-45]

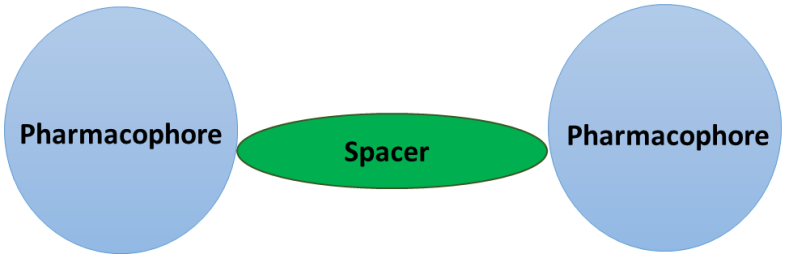

Figure 14: General structure of the bivalent ligands

The bivalent ligand approach has been widely used for G-protein coupled receptors (GPCRs). Recently, there is a growing interest in developing bivalent ligands targeting a variety of G-protein coupled receptors including opioid, dopamine, melatonin, serotonin and muscarinic receptors.[41, 46] An endogenous bivalent ligand, the bovine adrenal medulla peptide 22 (BAM22), was discovered

and shown to simultaneously bind to the two protomers of the δ-opioid receptor (OR) / sensory neuron-specific receptor (SNSR), producing a response different from that produced by the monomeric receptors which lead to increased interest in this class of ligands.[47] Therefore, this approach has become a strategy to discover the existence of GPCR dimers in native tissues and is currently applied also to ion channels[48] and transporters.[49]

1.8.1. Bivalent Ligands Benefits

It is assumed that duplication of the pharmacophoric groups according to the bivalent ligand approach leads to a supra-additive increase in potency compared to the corresponding monovalent ligand. The bivalent ligand approach in the design of ligands targeting GPCRs has proven to be promising to improve not only potency and selectivity but also the pharmacokinetic profile of compounds.[50, 51] The rationale for employing the bivalent ligand approach stems from the possibility that dimeric structures may be capable of bridging independent recognition sites (i.e. two recognition sites on a receptor dimer or one receptor and an accessory site). This results in thermodynamically more favorable binding interaction than a monovalent binding of two molecules, thus giving enhanced activity.[49, 52, 53] In other words, the binding of the first pharmacophore would increase the binding of the second pharmacophore to the dimer partner/receptor resulting in higher affinity.[43, 45, 54, 55]

It was reported that such bivalent ligands might show unusual subtype selectivity and/or interesting functional activity since the presence of the second pharmacophoric unit could allow additional ligand–receptor interactions with accessory binding sites or with the ion channel itself.[48] Moreover, dimerization can result in an increase of potency/selectivity and can interestingly improve resistance to degradation in the case of peptide agonists or antagonists.[56]

1.8.2. Some Examples of Bivalent Ligands

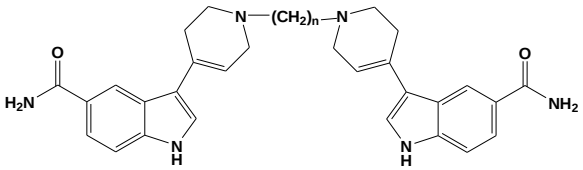

Serotonin dimer at 5-HT1B/1D receptors[57]

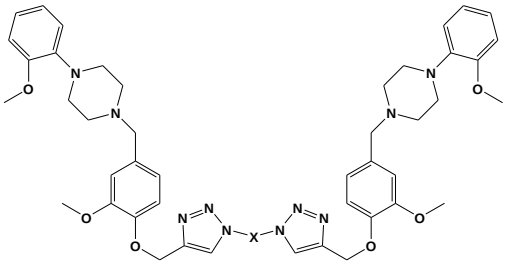

Bivalent dopamine D2 receptor ligands[58]

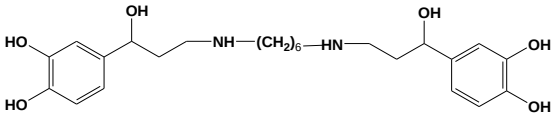

Hexoprenaline (selective β_2 adrenergic receptor agonist). It is a bivalent ligand of two noradrenaline units[59]

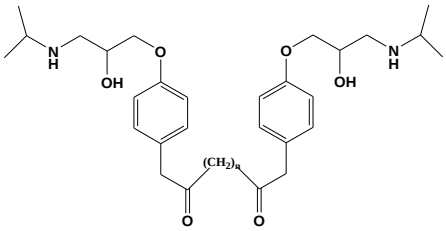

Bivalent ligand of two practolol units (β adrenergic receptor ligand)[59]

Figure 15: Some examples of bivalent ligands

1.8.3. Designing Bivalent Ligands

The design of a bivalent ligand requires consideration of several aspects, such as the choice of an appropriate pharmacophore (a monomeric ligand that is selective and able to allow attachment of a linker), the appropriate point of attachment as well as the optimization of a spacer in terms of length and adequate physicochemical properties.[45, 55, 60]

1.8.3.1. Selection of Pharmacophores

Some features must be considered when choosing the individual monomer such as the molecular bulk, the potency and the appropriate attachment point of the linker. Monomers should be generally of low/medium molecular weight (300 Da < MW <400 Da) in order to account for the significant additional bulk added through the dimerization and the attachment of linker and spacer portions. For example, the 5-HT_4 partial agonist ML10302 (Figure 16) has a molecular weight of 312.8 Da enabling the chemical bulk to be added without detrimental effects. They should also have a high affinity in the very low nanomolar range. It is observed that significant reductions in affinity occur upon the attachment of a linker and spacer portions to the original lead compound. This reduction in affinity has been shown to be up to two orders of magnitude.[45]

There are two general classifications for bivalent ligands: homobivalent, where the two pharmacophores are the same and heterobivalent having two different pharmacophores.[45, 50] For instance, in order to target 5-HT_4 receptor homodimers, a homo-bivalent ligand was developed by linking two similar pharmacophores of ML10302 (Figure 16). An example of a bivalent ligand targeting δ-κ-opioid receptors heterodimer is KDN-21. It is formed of a κ-selective antagonist (5'-guanidino naltrindole) linked to a δ-selective antagonist (naltrindole) through a poly-glycine linker. (Figure 17).[50, 55, 61]

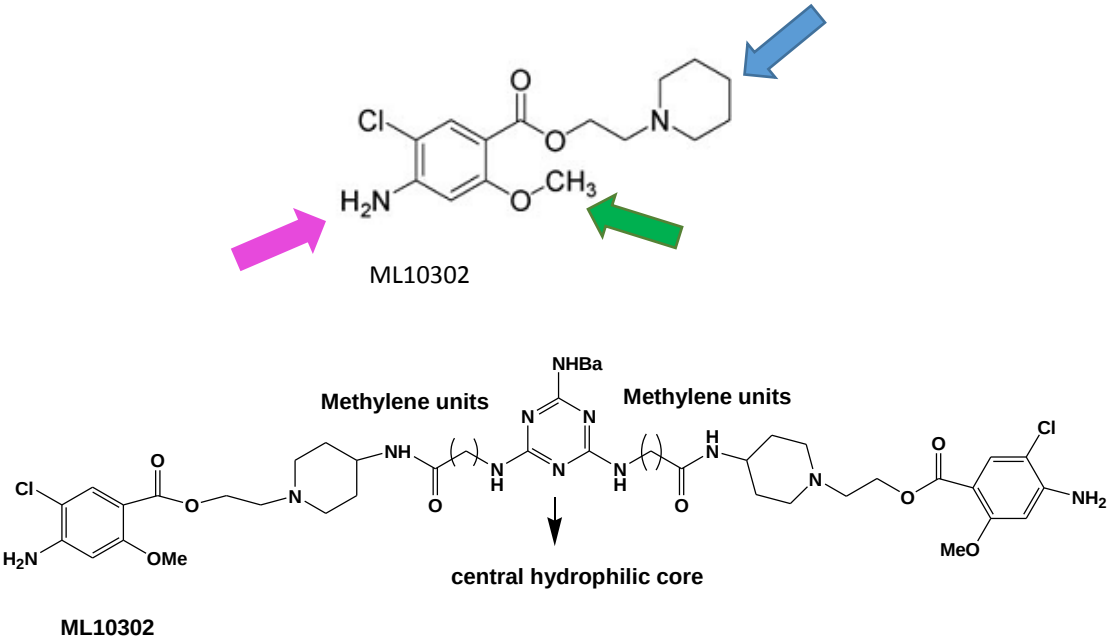

Figure 16: Structure of the monomer ML10302 with possible spacer attachment points[53] and the structure of 5-HT_4 homo-bivalent ligand based on ML10302 pharmacophores and the possible spacer

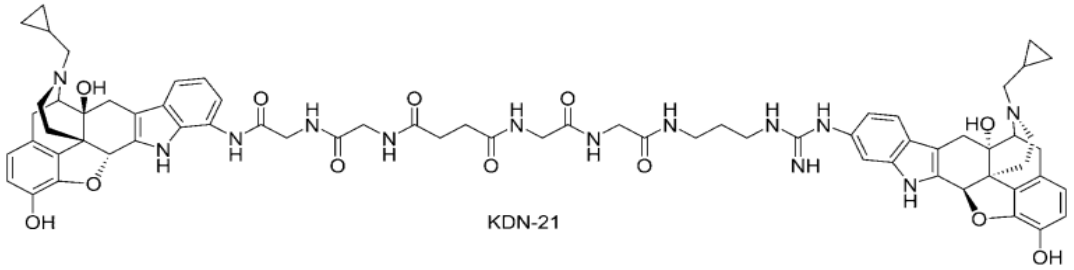

Figure 17: Structure of KDN-21, a hetero-bivalent ligand targeting δ and κ opioid receptor heterodimers attachment points.

1.8.3.2. Selection of the Attachment Point of the Linker to the Pharmacophore

The identification of the most suitable attachment point of the spacer relies on two criteria: The feasibility of chemical modifications and the compatibility of these modifications with binding properties and intrinsic activity of the respective pharmacophore.[55] Determining the best position for attachment of the linker

group can be achieved using a good understanding of the structure–activity relationships of the monovalent counterparts.[45] Preferentially applied moieties for linking two pharmacological units are hydroxyl, amine and carboxylic groups.[55] For example, there are 3 attachment points for ML10302 (Figure 16).[54]

1.8.3.3. Optimization of a Spacer Length, Conformational Flexibility and Chemical Properties

Spacer length

The length and composition of the spacer are very critical parameters for the binding mode of bivalent ligands. Although there are no rules to choose a spacer length, the optimal distance range for spacers connecting the two pharmacophores has been determined for a number of different targets, especially the opioid receptors. For example, in the synthesis of various bivalent ligands targeting opioid receptors (μ, δ and κ dimers), Portoghese et al. showed that an optimal distance for the spacer is approximately 21 atoms between pharmacophores.[62]

If the spacer is of sufficient length, both pharmacophores in a bivalent ligand may occupy distinct but very similar or identical neighboring recognition sites, or the second pharmacophore of a bivalent ligand may bridge to an adjacent accessory site which is unique to the receptor system. The ligand can simultaneously interact with two primary (orthosteric) binding sites of two neighboring protomers. They may serve as pharmacological tools to study the function of the receptor. On the other hand, the bivalent ligand may address a primary binding site and a secondary (allosteric) binding site located in close proximity of an adjacent GPCR or at the identical protomer leading to a bitopic or dualsteric binding mode.[48, 59, 63, 64] This facilitates the generation of subtype-selective agonists or antagonists because allosteric regions are frequently less conserved than the orthosteric binding pocket, which is usually very similar for all subtypes of a receptor family.

Composition and conformational flexibility of the spacer

Various spacer groups are used to connect the two pharmacophores, including polyalkyl chains, polyamide chains, polar oxygenated spacers, hydrophobic spacers, cyclic alkyl spacers, flexible aromatic containing spacers and constrained aromatic containing spacers. These spacers differ in their lipophilicity as well as the rigidity in terms of the number of rotatable bonds. The polarity of the spacer is important for the solubility of the bivalent ligand which becomes increasingly hydrophobic with increasing the spacer length e.g. for polymethylene chain. Moreover, the spacer needs to be flexible enough to allow correct positioning of each pharmacophore in the binding pocket of each protomer. However, the rigidity of the spacer is also of considerable interest as it will decrease the entropy loss upon binding of the ligand to the receptor.[45, 55]

1.9. Bivalent Ligands for Ion Channels

Dimerization of ion channels may result in different signaling characteristics, pharmacological properties and physiological function compared to monomer/homomer ion channel.[65] In this chapter, known bivalent ligands targeting ion channels are discussed.

1.9.1. Nicotinic Acetylcholine Receptor (nAChR)

nAChRs contain multiple agonist-binding sites and noncompetitive-antagonist sites. Epibatidine is the most powerful natural nicotinic agonist known. It was believed that the presence of the second epibatidine unit could allow for additional ligand–receptor interactions with accessory binding sites or with the ion channel itself. Therefore, a series of epibatidine bivalent ligands linked by an oligomethylene chain of different lengths attached to the ring nitrogen. Binding assays reveal that these four new ligands possess similar low nanomolar affinities at each of the six nAChR subtypes tested (Figure 18).[48]

Hexamethonium is a well-known bis-quaternary ammonium ligand, possessing a potent noncompetitive ganglionic nAChRs antagonist. Interestingly, elongation of the carbon linker between the ammonium head groups as in the case of decamethonium leads to the formation of a competitive antagonist for muscle-type nAChRs. It was also found that an additional cytisine in designing bivalent cytisine analogues is likely to interact with some additional sites at or near the acetylcholine binding pocket (Figure 18).[48]

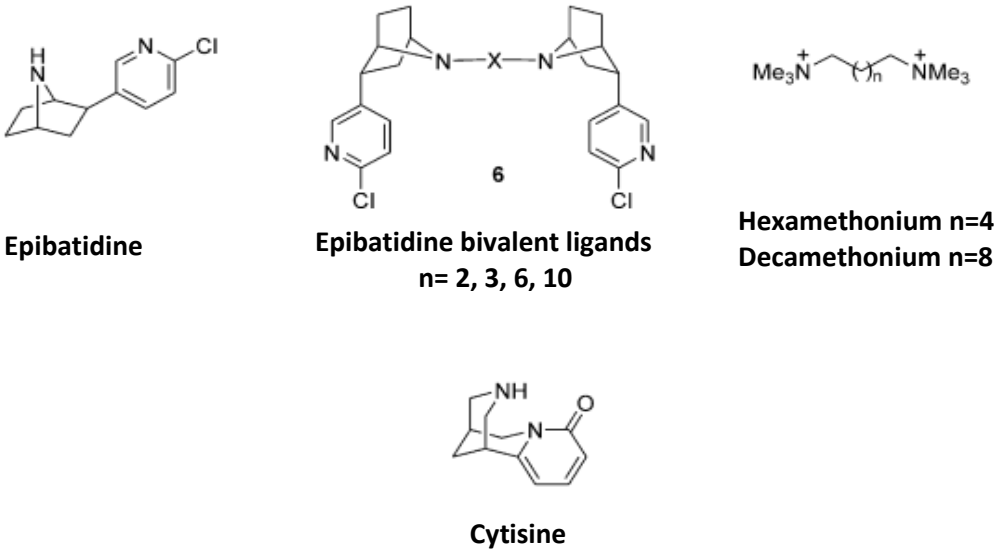

Figure 18: Nicotinic acetylcholine bivalent ligands

1.9.2. $5HT_3$ Serotonin Receptors

Bivalent ligands for $5HT_3$ receptor have been designed by linking a piperazine substituted quinolone moiety to probes, showing different functional (chemofunctional or biofunctional) features. Both the homomeric and heteromeric derivatives showed $5HT_3$ serotonin receptor affinity with concentration in the nano molar range. The results suggested that the 5-HT_3R is capable of accommodating bivalent ligands showing different spacers and that multivalency in 5-HT_3R could involve receptor domains different from the main binding site.[66]

In the design of heteromeric ligands targeting $5HT_3$, the arylpiperazine moiety, playing the role of an anchor in interacting with the main binding site of the $5\text{-}HT_3R$, was linked either to chemofunctional probes [e.g., the ureido acetic acid (UAA) moiety] or biofunctional probes [e.g., tacrine]. On the other hand, in homomeric ligand the arylpiperazine moiety is linked to another arylpiperazine anchor (MPQC) (Figure 19).[66]

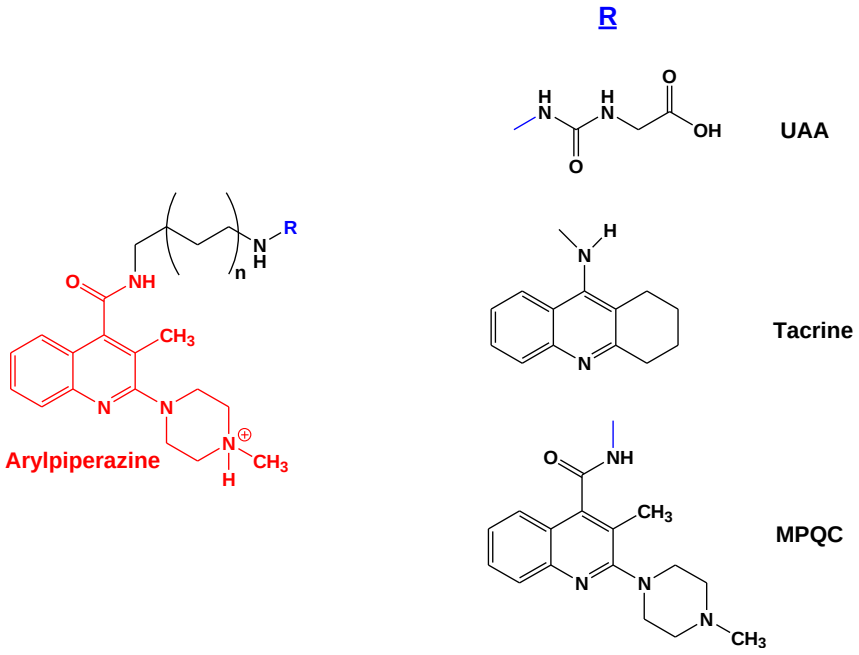

Figure 19: $5HT_3$ serotonin receptor bivalent ligands

1.9.3. $GABA_A$ Receptors

It was believed that the synthesis of dimeric ligands targeting $GABA_AR$ will exhibit enhanced selectivity and potency at the α5 $BzR/GABA_A$ subtypes with decreased side effects e.g. the bivalent ligand Xli093 exhibited selective affinity for the α5 subtype and behaved as a selective antagonist of the effects of diazepam in oocytes at this α5 subtype. Other bivalent ligands were synthesized by incorporation of two of the following pharmacophoric units (Figure 20) with different spacer length. Additionally, insertion of an oxygen atom into the linker was believed to

increase water solubility and hence enhance molecular hydrophilicity which should play an important role in the pharmacokinetic properties of the ligand.[51]

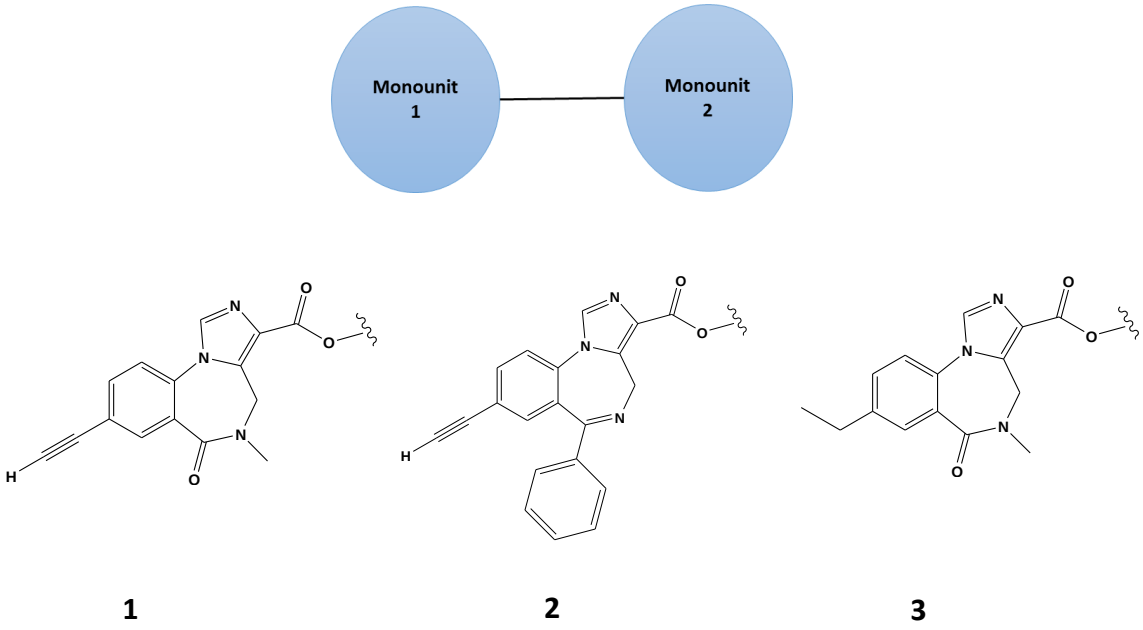

Compound	Monounit 1	Monounit 2	Spacer
Xli093	1	1	$(CH_2)_3$
A	1	1	$(CH_2)_5$
B	3	3	$(CH_2)_3$
C	1	1	CH_2OCH_2
D	2	2	$(CH_2)_2O(CH_2)_2$
E	2	2	$(CH_2)_3$

Figure 20: Some examples of $GABA_AR$ dimeric ligands

1.9.4. Glycine Receptor Dimeric Ligands

As mentioned before, 2-aminostrychnine was reported to show high affinity for the strychnine binding sites of synaptic membranes from brain and spinal cord of rats comparable to that of strychnine.[33] Recently, a series of dimeric strychnine analogs, with different spacer length, designed by linking two strychnine molecules through amino groups in position 2 was synthesized and tested in binding studies and functional assays at human α1 and α1β glycine receptors. As the bivalent ligands include amide groups in position 2 of strychnine, the reference monomeric propionamide and octanamide were prepared and pharmacologically evaluated (Figure 21).[67]

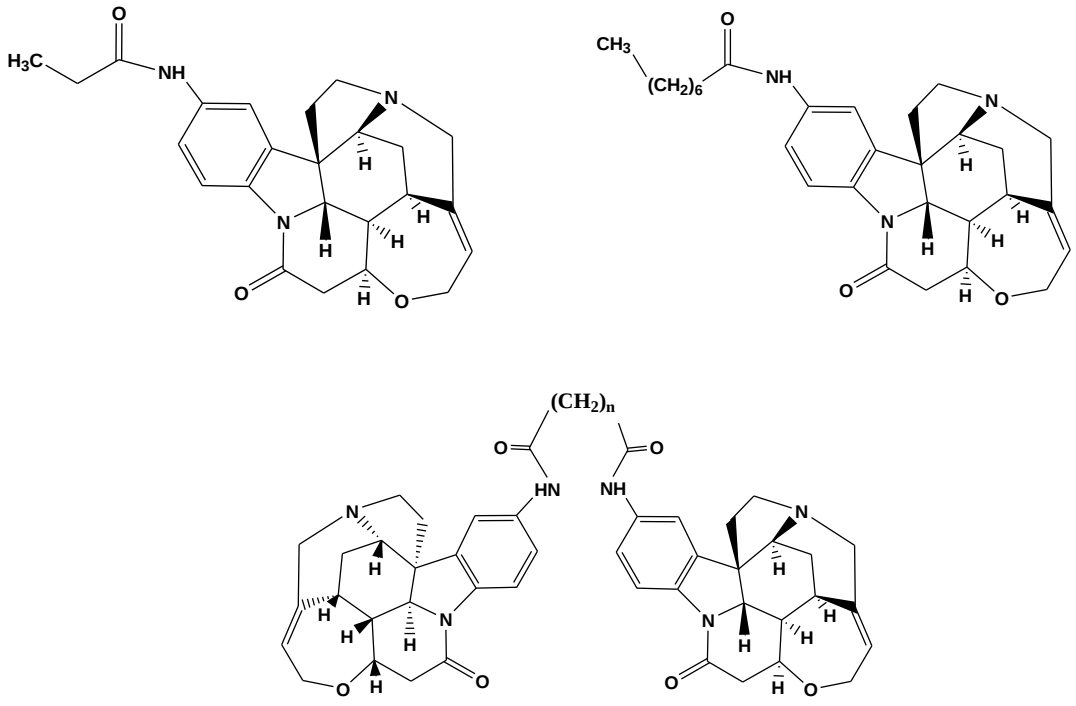

Figure 21: Structures of the reference monomeric propionamide and octanamide and structures of the bivalent ligands derived from 2-aminostrychnine. n= 2, 3, 4, 6, 8, 10

All dimeric compounds displayed comparable antagonist potencies at the two receptor subtypes with 2-aminostrychnine showing the highest 3-fold preference toward the α1 subtype. However, no subtype selectivity could be observed. Docking experiments to the strychnine binding site from the electron cryomicroscopy structure of homomeric α1 GlyRs revealed that the orientation of 2-aminostrychnine is different from that of strychnine and the essential interaction involves a hydrogen bond between the primary amino group (H-bond acceptor) and the amino group of Gly176 (H-bond donor) (Figure 22).[67]

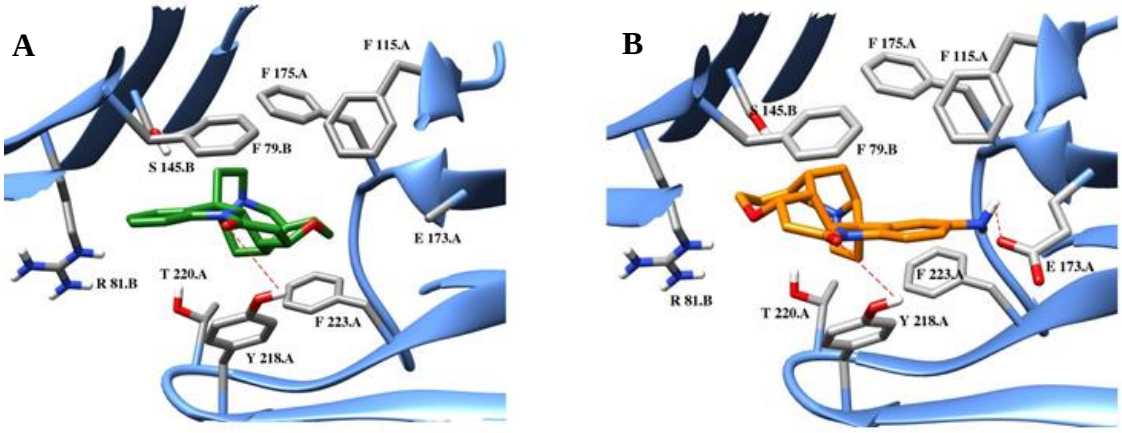

Figure 22: Strychnine (A) and 2-aminostrychnine (B) in the orthosteric binding pocket of the homomeric α1 glycine*

While the analogs with shorter $(CH_2)_n$ spacers (n = 2, 3, 4, 6, 8) were approximately 10 times less potent than the monomeric control ligands, the IC_{50} values for the compound with a $(CH_2)_{10}$ spacer were similar to those of the monomeric control compounds. Finally, the dimeric strychnine analog with the longest spacer $(CH_2)_{12}$ displayed the highest antagonistic potency at α1 and α1β.[67]

* These are preliminary results and may be subjected to modifications

2. Aim of work

Very recently, a series of dimeric strychnine analogs obtained by diamide formation of two molecules of 2-amino strychnine with dicarboxylates of different chain length was pharmacologically evaluated at human α1 and α1β glycine receptors in a functional fluorescence-based assay, in a whole cell patch-clamp assay, and in [^{3}H]strychnine binding studies. None of the dimeric analogs was superior to strychnine and all of them displayed comparable antagonist potencies at the two receptor subtypes in both the FMP and patch-clamp assays.[67]

The aim of this work was the synthesis and pharmacological evaluation of a new series of dimeric strychnine analogs. In order to explore a possible alternative attachment point for the spacer, the structure-activity relationships of strychnine at GlyR, will be first extended to include the analogs which have only been examined in animal studies (convulsive and lethal effect in mice)[32], and in radioligand binding assays at synaptic membranes of rats.[33]

It was reported that the introduction of the E-configured hydroximino group at C11 of strychnine resulted in twicely increased binding to both α1 and α1β glycine receptors[16], making the oxime hydroxyl group a suitable anchor group for the attachment of a spacer connecting two molecules of E-configured hydroximino group at C11. To explore how an alkyl spacer affects the antagonistic potency of the parent oxime, it was aimed to synthesize and pharmacologically evaluate a series of oxime ethers with alkyl groups of different length and size to derive the SAR study.

Moreover, 11-aminostrychnine, and the corresponding propionamide were aimed to be prepared and pharmacologically evaluated in order to examine the influence of the amide function at C11 as potential linker (Figure 23).

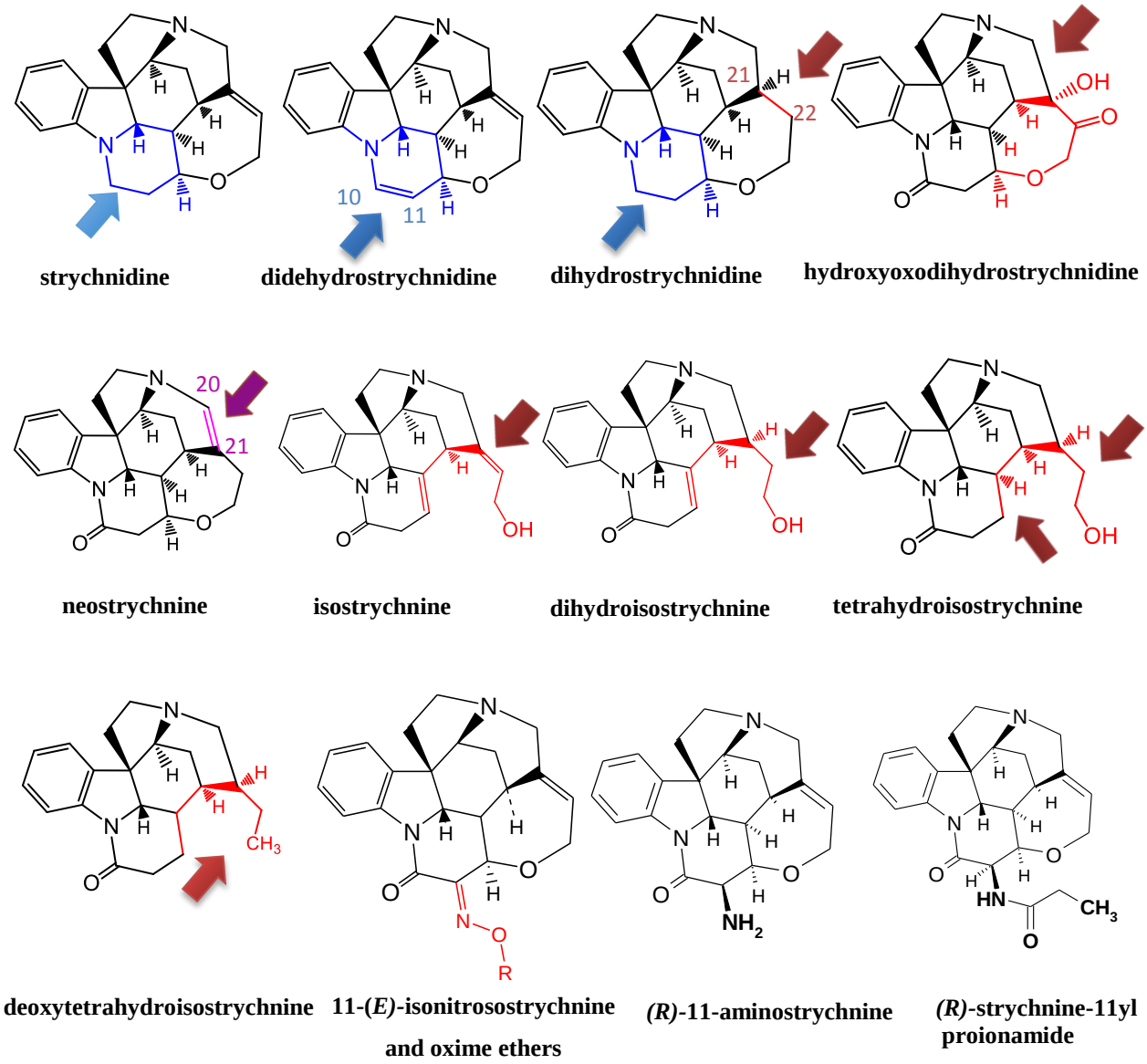

Figure 23: Structures of 9 strychnine derivatives, *(R)*-11-aminostrychnine, *(R)*-Strychnine-11yl propionamide, 11-*(E)*-isonitrososstrychnine and 11 oxime ether

Based on the pharmacological results of the potential strychnine-derived analogs such as the oxime ethers, isostrychnine, *(R)*-11-aminostrychnine, *(R)*-strychnine-11yl propionamide, the analogs showing the highest antagonist potency should be chosen as the pharmacophoric unit for the synthesis of a new series of bivalent ligands targeting GlyRs. The potential structures are shown in Fig 24.

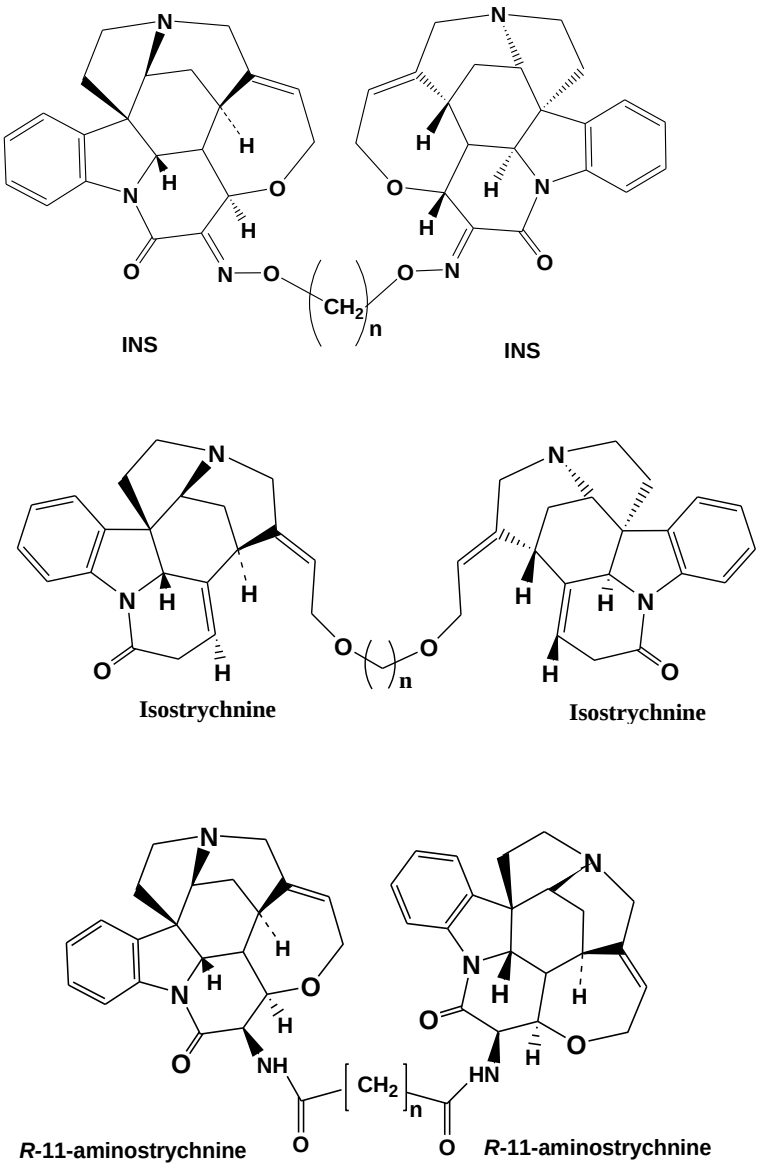

Figure 24: Structures of potential series of strychnine-derived bivalent ligands of GlyRs

3. References

1. Lynch, J. W. Molecular structure and function of the glycine receptor chloride channel. *Physiol Rev* **2004**, 84, 1051-95.
2. Breitinger, H. G.; Becker, C. M. The inhibitory glycine receptor: prospects for a therapeutic orphan. *Curr Pharm Des* **1998**, 4, 315-34.
3. Du, J.; Lu, W.; Wu, S.; Cheng, Y.; Gouaux, E. Glycine receptor mechanism elucidated by electron cryo-microscopy. *Nature* **2015**, 526, 224-9.
4. Patrick, G. L. An Introduction to Medicinal Chemistry, chapter 4, 4th ed.; Spencer, J., Ed. Oxford University Press: New York **2008**, 48-50.
5. Lippincott, W.; Wilkins, M. J. M., Richard, A. Harvey, Pamela C. Champe Pharmacology, chapter 8, 2nd ed.; **2000**, 33-34.
6. Betz, H.; Laube, B. Glycine receptors: recent insights into their structural organization and functional diversity. *J Neurochem* **2006**, 97, 1600-10.
7. Huang, X.; Chen, H.; Michelsen, K.; Schneider, S.; Shaffer, P. L. Crystal structure of human glycine receptor-alpha3 bound to antagonist strychnine. *Nature* **2015**, 526, 277-80.
8. Kirsch, J. Glycinergic transmission. *Cell Tissue Res* **2006**, 326, 535-40.
9. Breitinger, H. G.; Becker, C. M. The inhibitory glycine receptor-simple views of a complicated channel. *Chembiochem* **2002**, 3, 1042-52.
10. Yu, R.; Hurdiss, E.; Greiner, T.; Lape, R.; Sivilotti, L.; Biggin, P. C. Agonist and antagonist binding in human glycine receptors. *Biochemistry* **2014**. 53, 6041-51.
11. Sébastien D.; Becker, C. M.; Betz, H. Minireviews: Inhibitory Glycine Receptors: An Update. *J Biol Chem* **2012**, 287, 40216-40223.
12. Miyazawa, A.; Fujiyoshi, Y.; Unwin, N. Structure and gating mechanism of the acetylcholine receptor pore. *Nature* **2003**, 423, 949-955.

13. Kuhse, J.; Laube, B.; Magalei, D.; Betz, H. Assembly of the inhibitory glycine receptor: identification of amino acid sequence motifs governing subunit stoichiometry. *Neuron* **1993**, 11, 1049-56.
14. Graham, B. A.; Tadros, M. A.; Schofield, P. R.; Callister, R. J. Probing glycine receptor stoichiometry in superficial dorsal horn neurones using the spasmodic mouse. *J Physiol* **2011**, 589, 2459-74.
15. Betz, H.; Langosch, D.; Rundstrom, N.; Bormann, J.; Kuryatov, A.; Kuhse, J.; Schmieden, V.; Matzenbach, B.; Kirsch, J. Structure and biology of inhibitory glycine receptors. *Ann N Y Acad Sci* **1993**, 707, 109-15.
16. Jensen, A. A.; Gharagozloo, P.; Birdsall, N. J.; Zlotos, D. P. Pharmacological characterisation of strychnine and brucine analogues at glycine and alpha7 nicotinic acetylcholine receptors. *Eur J Pharmacol* **2006**, 539, 27-33.
17. Rajendra, S.; Lynch, J. W.; Schofield, P. R. The glycine receptor. *Pharmacol Ther* **1997**, 73, 121 -46.
18. Komatsu, H.; Furuya, Y.; Sawada, K.; Asada, T. Involvement of the strychnine-sensitive glycine receptor in the anxiolytic effects of GlyT1 inhibitors on maternal separation-induced ultrasonic vocalization in rat pups. *Eur J Pharmacol* **2015**, 746, 252-7.
19. Betz, H.; Becker, C-M. The mammalian glycine receptor: biology and structure of a neuronal chloride channel protein. *Neurochem Int* **1988**, 13, 137–146.
20. Schmieden, V.; Betz, H. Pharmacology of the inhibitory glycine receptor: agonist and antagonist actions of amino acids and piperidine carboxylic acid compounds. *Mol Pharmacol* **1995,** 48, 919-27.
21. Breitinger, U.; Raafat, K. M.; Breitinger, H. G. Glucose is a positive modulator for the activation of human recombinant glycine receptors. *J Neurochem* **2015**, 134, 1055-66.

22. Blednov, Y. A.; Benavidez, J. M.; Black, M.; Leiter, C. R.; OsterndorffKahanek, E.; Harris, R. A. Glycine receptors containing alpha2 or alpha3 subunits regulate specific ethanol-mediated behaviors. *J Pharmacol Exp Ther* **2015**, 353, 181 -91.
23. Roth, K., Strychnine: From Isolation to Total Synthesis – Part 1. *Chem Unserer Zeit* **2011**, 45, 202–218.
24. Makarovsky, I.; Markel, G.; Hoffman, A.; Schein, O.; Brosh-Nissimov, T.; Tashma, Z.; Dushnitsky, T.; Eisenkraft, A. Strychnine-a killer from the past. *Isr Med Assoc J* **2008**, 10, 142-5.
25. Woodward, R. B.; Ollis, A.; Hunger, H. U.; Dafniker and K. Schenker, Comparative total synthesis of strychnine. *Tetrahedron.* **1963**, 19, 247–288.
26. Regnault, V., Neue Untersuchungen über die Zusammensetzung der organischen Basen. *Eur J Or Chem* **1838,** 26, 10-41.
27. Roth, K. Strychnine: From Isolation to Total Synthesis - Part 2. *Chem Unserer Zeit* **2011**, 45, 202–218
28. Woodward, R. B.; Ollis, A.; Hunger, H. U.; Daeniker, K.; Schenker, The total synthesis of strychnine. *J Am Chem. Soc* **1954**, 76, 4749-4751.
29. Maher, A.; Radwan, R.; Breitinger, H. G. In vivo protection against strychnine toxicity in mice by the glycine receptor agonist ivermectin. *Biomed Res Int* **2014**, 2014, 640790.
30. Kuhse, J.; Betz, H.; Kirsch, J. The inhibitory glycine receptor: architecture, synaptic localization and molecular pathology of a postsynaptic ion-channel complex. *Curr Opin Neurobiol* **1995**, 5, 318-23.
31. Matsubayashi, H.; Alkondon, M.; Pereira, F. R.; Karen, L.; Swanson, X. A. Strychnine: A Potent Competitive Antagonist of a-Bungarotoxin-Sensitive Nicotinic Acetylcholine Receptors in Rat Hippocampal Neurons. *J Pharmacol Exp Ther* **1998**, 284, 904-913.

32. Iskander, G. M.; Bohlin, L. Structure-activity relationship of strychnine derivatives modified in the non-aromatic part. *Acta Pharm Suec* **1978**, 15, 431-8.
33. Mackerer, C. R.; Kochman, R. L.; Shen, T. F.; Hershenson, F. M. The binding of strychnine and strychnine analogs to synaptic membranes of rat brainstem and spinal cord. *J Pharmacol Exp Ther* **1977**, 201, 326-31.
34. Karrer, P.; Eugster, C. H.; Waser, P. Über Curarewirkung einiger Strychnidin- und Dihydrostrychnidin-chlor-alkylate. *Helv Chim Acta* **1949,** 32, 2381-2385
35. Van Berlo, I. R.; Arbouw, M. E.; Bles, C. M. Strychnine poisoning: uncommon, but does still happen. *Ned Tijdschr Geneeskd* **2015,** 159, A8877.
36. Beitz, A.; Alice, A.; Larson, J. Glycine Potentiates Strychnine-Induced Convulsions: Role of NMDA Receptors. *J. Neurosci* **1988**, 8, 3822-3828.
37. Parker, A. J.; Lee, J. B.; Redman, J.; Jolliffe, L. Strychnine poisoning: gone but not forgotten. *Emerg Med J* **2011**, 28, 84.
38. Michael S.; Bahrke Charles, Y. In Performance-Enhancing Substances in Sport and Exercise, Human Kinetics. *Br J sports Med* **2005**, 39, 687.
39. Cantrell, F. L. Look what I found! Poison hunting on eBay. *Clin Toxicol (Phila)* **2005**, 43, 375-9.
40. Chojnacki, J. E.; Liu, K.; Saathoff, J. M.; Zhang, S. Bivalent ligands incorporating curcumin and diosgenin as multifunctional compounds against Alzheimer's disease. *Bioorg Med Chem* **2015,** 23, 7324-31.
41. Deekonda, S.; Wugalter, L.; Rankin, D.; Largent-Milnes, T. M.; Davis, P.; Wang, Y.; Bassirirad, N. M.; Lai, J.; Kulkarni, V.; Vanderah, T. W.; Porreca, F.; Hruby, V. J. Design and synthesis of novel bivalent ligands (MOR and DOR) by conjugation of enkephalin analogues with 4-anilidopiperidine derivatives. *Bioorg Med Chem Lett* **2015**, 25, 4683-8.

42. Devi, L. A. Heterodimerization of G-protein-coupled receptors: pharmacology, signaling and trafficking. *Trends Pharmacol Sci* **2001**, 22, 532-7. 46.
43. Glass, M.; Govindpani, K.; Furkert, D. P.; Hurst, D. P.; Reggio, P. H.; Flanagan, J. U. One for the Price of Two. Are Bivalent Ligands Targeting Cannabinoid Receptor Dimers Capable of Simultaneously Binding to both Receptors. *Trends Pharmacol Sci* **2016**, 37, 353-63.
44. Schmitz, J.; Van der Mey, D.; Bermudez, M.; Klockner, J.; Schrage, R.; Kostenis, E.; Trankle, C.; Wolber, G.; Mohr, K.; Holzgrabe, U. Dualsteric muscarinic antagonists--orthosteric binding pose controls allosteric subtype selectivity. *J Med Chem* **2014,** 57, 6739-50.
45. Shonberg, J.; Scammells, P. J.; Capuano, B. Design strategies for bivalent ligands targeting GPCRs. *ChemMedChem* **2011**, 6, 963-74.
46. Anne Sophie, J., Samy, A.; Habib, M.; Dodda, B. R.; Mina, N.; Morcos, F.; Mirna, S. S.; Sarah, T.; Paula A. W.; Ralf, J.; Zlotos, P. D. N1 -linked melatonin dimers as bivalent ligands targeting dimeric melatonin receptors. *MedChemCommun* **2014,** 5, 792.
47. Breit, A.; Gagnidze, K.; Devi, L. A.; Lagace, M.; Bouvier, M., Simultaneous activation of the delta opioid receptor (deltaOR)/sensory neuron-specific receptor-4 (SNSR-4) hetero-oligomer by the mixed bivalent agonist bovine adrenal medulla peptide 22 activates SNSR-4 but inhibits deltaOR signaling. *Mol Pharmacol* **2006**, 70, 686-96.
48. Kozikowski, P.; Wei, Y.; Xiao, K. J.; Kellar, A. Synthesis and pharmacological characterization of bivalent ligands of epibatidine at neuronal nicotinic acetylcholine receptors. *Bioorg Med Chem Lett* **2004,** 14, 1855-1858.
49. Decker, M.; Lehmann, J. Agonistic and antagonistic bivalent ligands for serotonin and dopamine receptors including their transporters. *Curr Top Med Chem* **2007,** 7, 347-53.

50. Berque-Bestel, I.; Lezoualch, F.; Jockers, R. Bivalent ligands as specific pharmacological tools for G protein-coupled receptor dimers. *Curr Drug Discov Technol* **2008**, 5, 312-8.
51. Han, D.; Holger Forsterling, F.; Li, X.; Deschamps, J. R.; Parrish, D.; Cao, H.; Rallapalli, S.; Clayton, T.; Teng, Y.; Majumder, S.; Sankar, S.; Roth, B. L.; Sieghart, W.; Furtmuller, R.; Rowlett, J. K.; Weed, M. R.; Cook, J. M. A study of the structure-activity relationship of GABA(A)-benzodiazepine receptor bivalent ligands by conformational analysis with low temperature NMR and X-ray analysis. *Bioorg Med Chem* **2008**, 16, 8853-62.
52. Haviv, H.; Wong, D. M.; Silman, I.; Sussman, J. L. Bivalent ligands derived from Huperzine A as acetylcholinesterase inhibitors. *Curr Top Med Chem* **2007**, 7, 375-87.
53. Nowak, I., Probing the membrane targeting C1 subdomains of PKC with bivalent ligands. *Curr Top Med Chem* **2007**, 7, 355-62.
54. Prati, F.; Uliassi, E.; Bolognesi, M. L. Two diseases, one approach: multitarget drug discovery in Alzheimer's and neglected tropical diseases. *MedChemCommun* **2014,** 5, 853-861.
55. Hiller, C.; Kuhhorn, J.; Gmeiner, P. Class A G-protein-coupled receptor (GPCR) dimers and bivalent ligands. *J Med Chem* **2013,** 56, 6542-59.
56. Cheronis, J. C.; Whalley, E. T.; Allen, L. G.; Loy, S. D.; Elder, M. W.; Duggan, M. J.; Gross, K. L.; Blodgett, J. K. Design, synthesis, and in vitro activity of bis(succinimido)hexane peptide heterodimers with combined B1 and B2 antagonist activity. *J Med Chem* **1994**, 37, 348-55.
57. Birnkammer, T.; Spickenreither, A.; Brunskole, I.; Lopuch, M.; Kagermeier, N.; Bernhardt, G.; Dove, S.; Seifert, R.; Elz, S.; Buschauer, A. The bivalent ligand approach leads to highly potent and selective acylguanidine-type histamine H2 receptor agonists. *J Med Chem* **2012,** 55, 1147-60.

58. Yuan, Y.; Arnatt, C. K.; Li, G.; Haney, K. M.; Ding, D.; Jacob, J. C.; Selley, D. E.; Zhang, Y. Design and synthesis of a bivalent ligand to explore the putative heterodimerization of the mu opioid receptor and the chemokine receptor CCR5. *Org Biomol Chem* **2012**, 10, 2633-46.
59. Halazy, S. G-protein coupled receptors bivalent ligands and drug design. *Expert Opin Ther Pat* **1999**, 9, 431-446.
60. Mohr, K.; Schmitz, J.; Schrage, R.; Tränkle, C.; Holzgrabe, U., Molecular alliance-from orthosteric and allosteric ligands to dualsteric/bitopic agonists at G protein coupled receptors. *Angew Chem Int Ed Engl* **2013**, 52, 508-16.
61. Bhushan, R. G.; Sharma, S. K.; Xie, Z.; Daniels, D. J.; Portoghese, P. S. A bivalent ligand (KDN-21) reveals spinal delta and kappa opioid receptors are organized as heterodimers that give rise to delta(1) and kappa(2) phenotypes. Selective targeting of delta-kappa heterodimers. *J Med Chem* **2004**, 47, 2969- 72.
62. Portoghese, P. S., Bivalent ligands and the message-address concept in the design of selective opioid receptor antagonists. *Trends Pharmacol Sci* **1989,** 10, 230-5.
63. Farde, L.; Ito, H.; Swahn, C. G.; Pike, V. W.; Halldin, C. Quantitative analyses of carbonyl-carbon-11-WAY-100635 binding to central 5-hydroxytryptamine-1A receptors in man. *J Nucl Med* **1998**, 39, 1965-71.
64. Mohr, K.; Tränkle, C.; Kostenis, E.; Barocelli, E.; De Amici, M.; Holzgrabe, U. Rational design of dualsteric GPCR ligands: quests and promise. *Br J Pharmacol* **2010**, 159, 997-1008.
65. Kelly, A. B.; Patwardhan, A. M.; Akopian, A. N. Receptor and Channel Heteromers as Pain Targets. *Pharmaceuticals* **2012,** 5, 249-278.
66. Cappelli, A. M.; Paolino, M.; Gallelli, M.; Anzini, A.; Mennuni, M.; Rienzo, M. D.; Menziani, F.; Vomero, M. C. Bivalent Ligands for the Serotonin 5- HT3 Receptor. *ACS Med Chem Lett* **2011**, 2, 571-6.

67. Banoub, M. M. F. C2-Linked Dimeric Strychnine Analogs as Bivalent Ligands Targeting Glycine Receptors. Master of Science in Pharmaceutical Chemistry, German University in Cairo, Cairo, **2016**.

4. Results

4.1. Structure–Activity Relationships of Strychnine Analogs at Glycine Receptors

Amal M. Y. Mohsen, Eberhard Heller, Ulrike Holzgrabe, Anders A. Jensen, and Darius P. Zlotos*

This manuscript has been accepted in *CHEMISTRY & BIODIVERSITY* – Vol. 11 (2014)

Paper I

Abstract

Nine strychnine derivatives including neostrychnine, strychnidine, isostrychnine, 21,22-dihydro-21-hydroxy-22-oxo-strychnine, and several hydrogenated analogs were synthesized, and their antagonistic activities at human α1 and α1β glycine receptors were evaluated. Isostrychnine has shown the best pharmacological profile exhibiting an IC_{50} value of 1.6 μM at α1 glycine receptors and 3.7-fold preference towards the α1 subtype. SAR Analysis indicates that the lactam moiety and the C(21)=C(22) bond in strychnine are essential structural features for its high antagonistic potency at glycine receptors

Introduction

Strychnine (**1**), the major alkaloid from the plant *Strychnos nux vomica*, exhibits pharmacological activity at several neurotransmitter receptors, including a number of ligand-gated ion channels. Its most pronounced pharmacological action is a strong antagonistic activity at glycine receptors (GlyRs), often referred to as ‘strychnine-sensitive glycine receptors’, which are anionic chloride channels linked

to hyperpolarization and inhibition of neuronal firing.[1-3] Strychnine displays nanomolar K_i values at recombinant and native GlyRs in binding and functional assays.[2,3]

Although dozens of simple structural analogs of strychnine are known, only a limited number of pharmacological studies has been reported to date, most of them on the convulsive effect and lethal doses in animal experiments.[4-7] In the course of our studies on GlyR ligands, we have recently reported the functional properties of five tertiary and twelve quaternary strychnine analogs at α1 and α1β GlyRs.[8] While all quaternary compounds were inactive, the tertiary analogs 2-nitrostrychnine, 21,22-dihydrostrychnine, Wieland–Gumlich aldehyde, and (Z)-11-isonitrososstrychnine displayed reduced antagonistic potencies at both GlyRs, when compared to strychnine. The only structure modification that did not impair the activity of the parent compound was an (E)-configurated hydroxyimino group at C(11) (compound **2**). However, none of the analogs exhibited pronounced selectivity towards α1 or α1β receptors (Fig. 1).

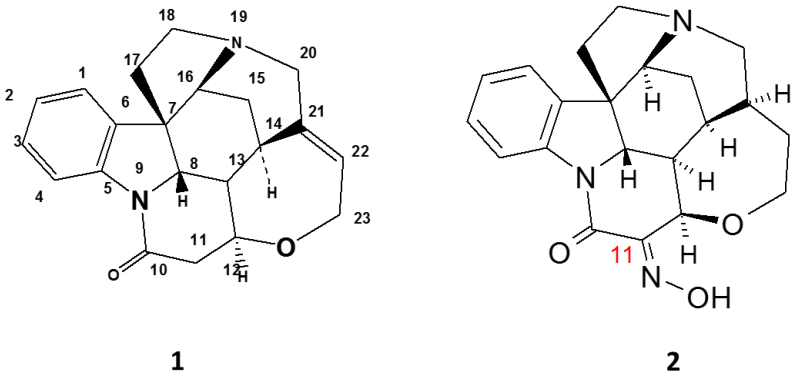

1 **2**

Fig. 1. Structures of strychnine (**1**) and (E)-11-isonitrososstrychnine (**2**)

To obtain more detailed SARs of the strychnine skeleton at GlyRs, nine tertiary strychnine derivatives (Fig. 2) were synthesized and pharmacologically evaluated in this study. The structure modifications involve the formal removal of the lactam O-atom (strychnidine (**3**)), introduction of a C(10)=C(11) bond into strychnidine (10,11- didehydrostrychnidine (**4**)), hydrogenation of the C(21)=C(22) bond in strychnidine (21,22-dihydrostrychnidine (**5**)), oxidation of the C(21)=C(22) bond (21,22-dihydro-21- hydroxy-22-oxostrychnine (**6**)), relocation of the C(21)=C(22) bond to C(20)=C(21) (neostrychnine (**7**)), opening of the tetrahydrooxepine ring (isostrychnine (**8**)), hydrogenation of the C(21)=C(22) bond of isostrychnine (21,22-dihydroisostrychnine (**9**)), hydrogenation of both C=C bonds of **8** (12,13,21,22-tetrahydroisostrychnine (**10**)), and removal of the OH group in **10** resulting in 23-deoxy-12,13,21,22-tetrahydroisostrychnine (**11**).

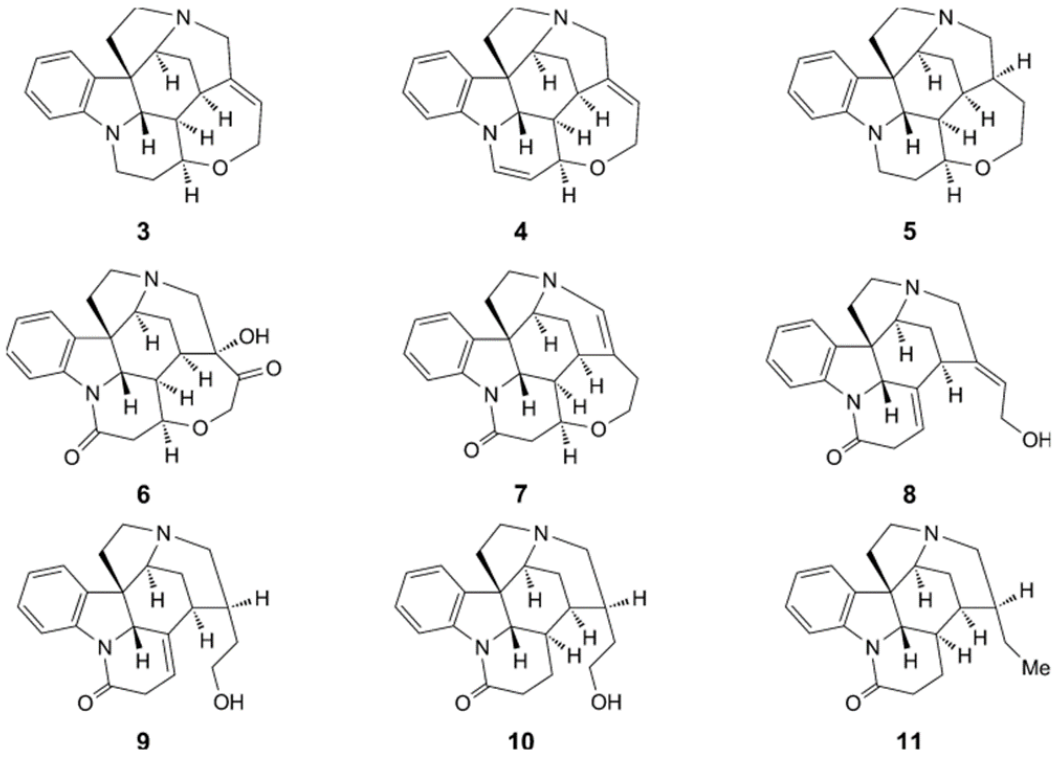

Fig. 2. Structures of the strychnine analogs **3 –11** studied in this work

Results

- Chemistry

Strychnidine (**3**) and 10, 11-didehydrostrychnidine (**4**) were synthesized by $LiAlH_4$ reduction of strychnine according to the procedure by Swan and Wilcock.[9] 21,22-Dihydrostrychnidine (**5**), previously reported to be accessible by $LiAlH_4$ reduction of 21,22-dihydrostrychnine[7], was synthesized by a more convenient approach using borane-THF as reducing agent. 21, 22-Dihydro-21-hydroxy-22-oxostrychnine (**6**) was prepared by oxidation of strychnine with KMnO4 in acetone [7]. Neostrychnine (**7**) was obtained according to a modified procedure by Chakravarti and Robinson[10] by heating strychnine in xylene with Pd/C 10% instead of the originally employed Raney-Ni. Isostrychnine (**8**) was prepared by heating strychnine in H_2O at 180° under microwave irradiation. 12,13,21,22-Tetrahydroisostrychnine (**10**) was obtained according to our previously reported procedure by hydrogenation of strychnine under microwave irradiation in H_2O at 180° and 60 bar H_2 pressure with PtO_2 as catalyst.[11] 21, 22-Dihydroisostrychnine (**9**) and 23-deoxy-12, 13, 21, 22-tetrahydroisostrychnine (**11**) were isolated as side-products of the latter reaction. Our alternative procedures for the synthesis of **5** and **7 –11** are described in the Exper. Part.

- Pharmacology

The functional properties of strychnine and the nine strychnine analogs as GlyR antagonists were characterized at the human α1 and α1β receptor subtypes. The receptors were transiently expressed in tsA201 cells, and their abilities to inhibit the glycine induced response in the *FLIPR*® membrane potential blue assay were determined. The IC_{50} values obtained for the compounds are compiled in the Table.

Table. Functional Properties of the Strychnine Analogs at the Human α1 and α1β GlyRs Transiently Expressed in tsA201 Cells in the **FLIPR**® Membrane Potential

Blue Assay. The EC_{50} values for glycine and the IC_{50} values for the analogs are given in µm with pEC_{50} ± S.E.M. and pIC_{50} ± S.E.M. values in brackets, respectively. In the antagonist experiments, EC_{50} concentrations of glycine as agonist were used. Data are the means of 3–4 individual experiments performed in duplicate.

	α1	α1β
	EC_{50} [pEC_{50} ± S.E.M.] µM	
Glycine	50 [4.30 ± 0.04]	35 [4.45± 0.04]
	IC_{50} [pIC_{50} ± S.E.M.] µM	
Strychnine (1)	0.16 [6.80 ± 0.08]	0.62 [6.21 ± 0.10]
Strychnidine (3)	~30 [~4.5]	~30 [~4.5]
10,11-Didehydrostrychnidine (4)	~50 [~4.3]	~100 [~4.0]
21,22-Dihydrostrychnidine (5)	~30 [~4.5]	~30 [~4.5]
21,22- dihydro -21-hyroxy-22-oxostrychnine (6)	11 [4.96 ± 0.05]	~30 [~4.5]
Neostrychnine (7)	~30 [~4.5]	~100 [~4.0]
Isostrychnine (8)	1.6 [5.79 ± 0.12]	5.9 [5.23 ± 0.14]
21,22-Dihydroisostrychnine (9)	~30 [~4.5]	~30 [~4.5]
12,13,21,22-Tetrahydroisostrychnine (10)	~100 [~4.0]	~100 [~4.0]
23-Deoxy-12,13,21,22-tetrahydroisostrychnine (11)	~100 [~4.0]	~300 [~3.5]

Discussion

Strychnine is the prototypical competitive antagonist of GlyRs displaying nanomolar affinities at recombinant and native receptors. However, it is not able to differentiate between the homomeric glycine receptor subtypes consisting exclusively of α subunits (α1 – α4), and the heteromeric ones assembled from α and β subunits (α1β, α2β, α3β, and α4β). In the *FLIPR*® membrane potential blue assay, strychnine displayed only a slight four-fold preference for α1 (IC_{50} = 0.16 µM) over α1β receptors (IC_{50} = 0.62 µM). In the search for potent competitive antagonists displaying selectivity towards the homomeric or heterodimeric GlyR subtypes, the functional properties of nine strychnine analogs obtained by simple structure modifications of the parent compound have been examined. The data are compiled in the Table. Although none of the derivatives was superior to strychnine, SAR enabled the identification of the structural elements that are essential for high antagonistic potency at α1 and α1β receptors.

Strychnidine **3** and didehydrostrychnidine **4** are formally obtained from the parent compound by removal of the lactam O-atom and additional introduction of a C(10)=C(11) bond into the former lactam ring, respectively. Compounds **3** and **4** displayed *ca*. 200-fold and *ca*. 300-fold lower antagonistic potencies at α1 receptors, and *ca*. 50-fold and *ca.* 150-fold lower activities at α1β receptors, respectively, when compared to strychnine. Saturation of the C(21)=C(22) bond of **3** maintained the low inhibitory activity at both α1 and α1β. The resulting dihydrostrychnidine **5** exhibited the same IC_{50} values as strychnidine at both subtypes (IC_{50} *ca*. 30 µM). The findings indicated that the lactam moiety of strychnine was an essential structural feature for the antagonistic activity at GlyRs. Relocation of the C(21)=C(22) bond of strychnine to C(20)=C(21) to give neostrychnine **7** was also detrimental for the inhibitory action at both GlyRs (α1: IC_{50} ~30 µM; α1β: IC_{50} *ca.* 100 µm). Moreover, oxidation of the C(21)=C(22) bond to a 21-hydroxy-22-oxo moiety to give compound **6** also resulted in significantly decreased antagonistic potency at α1 (IC_{50} 11 µM) and α1β (IC_{50} *ca.* 30 µM), revealing the C(21)=C(22) bond as another essential structural motif for the action at GlyRs. The latter conclusion is supported by the finding that hydrogenation of strychnine to the 21, 22-dihydro analog was previously reported to cause 30-fold and 10-fold decreased binding for α1 and α1β, respectively.[8] In accordance with these findings, **3** and 21, 22-dihydrostrychnine are known to possess considerably lower convulsive and lethal effects than strychnine in animal experiments.[6,7] Isostrychnine (**8**) is a ring-opened analog of the parent compound in which both structural features important for the antagonistic action at GlyRs, i.e. , the lactam ring and the C(21)=C(22) bond, are still present. Indeed, isostrychnine is the most potent analog in the series displaying IC_{50} values of 1.6 and 5.9 µM at α1 and α1β, respectively.

Although ten times less potent than strychnine, it maintains the three-fold preference towards the α1 subtype. As expected, the saturated analogs lacking the C(21)=C(22) bond, **9** (α1: IC_{50} *ca.* 30 µM; α1β: IC_{50} *ca*. 30 µM), and **10** (α1: IC_{50} *ca.* 100 µM;

α1β: IC_{50} *ca.* 100 μM) exhibited considerably reduced antagonistic potencies. Interestingly, the formal removal of the OH group from **10** to give **11** (α1: IC_{50} *ca.* 100 μM; α1β: IC_{50} *ca.* 300 μM) had no influence on the inhibitory activity.

In summary, the lactam group and the C (21)=C(22) bond of strychnine could be identified as essential structural features required for strong antagonistic activity at glycine α1 and α1βreceptors. The absence of one of these structural elements or changes of their relative spatial orientation result in reduced antagonistic potency. The findings are important for the future design of potent strychnine derived GlyR antagonists.

Experimental Part

General. Column chromatography (CC): silica gel 60 (SiO_2, 0.063–0.200 mm; Merck). M.p.: cap. melting-point apparatus (Gallenkamp, Sanyo); uncorrected. ^{1}H- and ^{13}C-NMR spectra: *Bruker AV-400* spectrometer; δ in ppm rel. to $CDCl_3$ as internal standard, *J* in Hz. EI-MS: *Finnigan MAT 90*; in m/z.

21,22-Dihydrostrychnidine (**5**). Borane/THF soln. (1M; 8 ml) was added dropwise to a stirred soln. of 21,22-dihydrostrychnine (500 mg, 1.54 mmol) in dry THF (100 ml) at r.t. The mixture was heated under reflux for 7 h, allowed to cool, and 2 M aq. HCl (4 ml) was added dropwise under ice cooling. After heating for 30 min under reflux, the mixture was basified under ice cooling with 25% aq. NH_3 and extracted with CH_2Cl_2. The combined org. layers were washed with H_2O (3X15 ml), dried ($MgSO_4$), and evaporated under reduced pressure. The residue was purified by CC (SiO_2; $CHCl_3$/MeOH/25% aq. NH_3 100: 10:1) to yield **5** (80 mg, 16%). White solid M.p. 216–218 °C ([7]: 221–224 °C, [12]: 212–214 °C) ^{1}H-NMR ($CDCl_3$, 400 MHz): 7.08 (*ddd*, *J* = 7.6, 7.6, 0.8, H-C(2)); 7.01 (*dd*, *J* =7.4, 0.8, H-C(4)); 6.69 (*ddd*, *J* = 7.6,7.4, 0.9, H-C(3)); 6.43 (*d*, *J* = 7.6, H-C(1)); 3.97 (*ddd*, *J* = 13.0, 3.9, 3.9, H_a-C(23)); 3.84 (*d*, *J* =11.7, H-C(8)); 3.72 (*ddd*, *J* = 6.2, 6.2, 3.6, H-C(12)); 3.58–3.45 (*m*, H_b-C(23), H_a-C(20)); 3.42 (*t*, *J*= 3.0, H-C(16)); 3.14 (*ddd*, *J* = 12.1, 10.0, 8.1, H_a-C(18)); 3.07–2.91 (*m*, H_a-C(10), H_b-C(20)); 2.85 (*J* =12.1, 8.5, 3.5, H_b-C(18));

2.54 (*J*=13.6, 8.5, 8.1, H_a-C(17)); 2.40–2.29 (*m*, H_b-C(10), H-C(14)); 2.10–1.93 (*m*, H_a-C(15), H_a-C(11), H_a-C(22), H-C(21)); 1.89 – 1.68 (*m*, H_b-C(11), H_b-C(15), H_b-C(17), H-C(13)); 1.65 (*ddd*, *J* =14.0, 3.7, 3.7, H_b-C(22)). ^{13}C-NMR ($CDCl_3$, 100 MHz): 151.2 (C(5)); 134.3 (C(6)); 128.0 (C(2)); 122.0 (C(4)); 118.3 (C(3)); 107.8 (C(1)); 78.9 (C(12)); 68.7 (C(8)); 68.5 (C(23)); 62.0 (C(16)); 58.2 (C(10)); 54.1 (C(18)); 51.9 (C(7)); 47.0 (C(13)); 41.6 (C(20)); 41.4 (C(17)); 35.3 (C(14)); 34.6 (C(22)); 31.4 (C(15)); 31.2 (C(21)); 28.7 (C(11). EI-MS: 323.1 (27), 322.1 (100, M^+), 180.1(20).

Neostrychnine (=20,21-Didehydro-21, 22-dihydrostrychnidin-10-one; **7**). Strychnine (1; 300 mg, 0.90 mmol) and Pd/C 10% (200 mg) were heated under reflux in xylene (50 ml) for 3 h. Pd/C was filtered off through a pad of Celite®545 and washed with xylene. The filtrates were combined, the solvent was removed in vacuo, and the residue was purified by CC (SiO_2; $CHCl_3$/MeOH/25% aq. NH_3 100: 10:1) to give **7** (65 mg, 22 %). White solid. M.p. 216–218 °C ([10]: 228 °C). ^{1}H-NMR: in accordance with those reported in.[13] ^{13}C-NMR ($CDCl_3$, 100 MHz): 170.4 (C=O); 141.6 (C(5)); 135.7 (C(20)); 134.4 (C(6)); 128.4 (C(1)); 124.5 (C(2)); 122.0 (C(3)); 116.1 (C(4)); 112.3 (C(21)); 77.5 (C(12)); 67.8 (C(23)); 65.2 (C(8)); 59.7 (C(16)); 53.9 (C(13)); 53.6 (C(7)); 52.6 (C(18)); 46.8 (C(17)); 41.5 (C(11)); 34.5 (C(22)); 28.6 (C(14)); 27.4 (C(15)). EI-MS: 335.1 (23), 334.1 (100, M^+), 277 (22), 167 (26), 149 (47).

Isostrychnine(=(3aR,11bS,12S,14E)-14-(2-Hydroxyethylidene) 2, 3, 10, 12, 13, 13a- hexahydro-9H,11bH-1,12-ethanopyrido[1,2,3-lm]pyrrolo[2,3-d]carbazol-9-one;8). Strychnine (**1**; 1 g, 3.00 mmol) was suspended in H_2O (180 ml), and the mixture was heated for 1 h at 180 °C under microwave irradiation (heating rate, 5 min from 258 to 180 °C). H_2O was evaporated, and the residue was subjected to CC (SiO_2; $CHCl_3$/MeOH/25% aq. NH_3 100: 10: 1) to give 175 mg (17%) of a 3.4:1 mixture of **8** and its C(11)=C(12) bond isomer as indicated by ^{1}H-NMR. The latter was further purified by CC (SiO_2; CH_2Cl_2/MeOH 100: 15) to give **8** (75 mg, 7%).

White solid. M.p. 218–220 °C ([14]: 214–215 °C, [15]: 223–224 °C) ^{1}H- and ^{13}C-NMR: in accordance with those reported in.[16] EI-MS: 335.1 (19), 334.1 (78, M^+), 316.1 (100), 303.1 (81), 220.1 (43), 167.1 (46).

12,13,21,22-Tetrahydroisostrychnine(=(3aR, 11aR, 11bS, 12S)- 14- (2 Hydroxyethyl)- 2, 3, 10, 11, 11a, 12, 13, 13a-octahydro-9H, 11bH-1,12 ethanopyrido [1,2,3-lm]pyrrolo[2,3d]carbazol-9-one; **10**). Strychnine (**1**; 6.00 mmol, 2.00 g) was dissolved in 200 ml of 10% aq. AcOH, 0.2 g of PtO_2 was added, and the mixture was hydrogenated in a high pressure microwave reactor[11] at 270° and 60 bar H_2 pressure for 4.5 h (heating rate, 10 min 25 °C to 270 °C). After cooling to 25 °C, the catalyst was filtered off, and the solvent was evaporated. The residue was treated with 150 ml of 2.0 m NaOH, extracted with CH_2Cl_2 (3 X120 ml), and dried ($MgSO_4$). The solvent was evaporated, and the residue was purified by CC (SiO_2; (R_f ($CHCl_3$/ MeOH/25% aq. NH_3 100: 10:1) 0.10) to give **10** (1.05 g, 52%). Colorless foam. . $[\alpha]_D^{23}$ = -23.0° (c = 2.0, $CHCl_3$) ([17]: $[\alpha]_D^{23}$ = -24.5, $CHCl_3$). ^{1}H-NMR ($CDCl_3$, 400 MHz): 8.11 (*d*, *J* =7.9, H-C(4)); 7.25–7.15 (*m*, H-C(1), H-C(3)); 7.10 (*t*, *J* =7.4, H-C(2)); 4.06 (*d*, *J*=5.5, H-C(8)); 3.68 (*t*, *J*=6.3, H-C(23)); 3.09 (*td*, *J*=11.9, 7.2, H_a-C(11)); 2.99 (*dd*, *J*= 11.9, 6.9, H_b-C(11)); 2.92 (*dd*, *J*=10.7, 3.6, H_a-C(20)); 2.88 (*m*, H-C(16)); 2.49 (*m*, H-C(18)); 2.27–2.43 (*m*, H-C(12), H_b-C(21)); 2.07–2.18 (*m*, H_a-C(17), H-C(13)); 1.95 (*m*, H-C(21)); 1.65 –1.80 (*m*, H-C(14), CH_2(15), H_b-C(17)); 1.53 (*m*, H_a-C(22)); 1.43 (*m*, H_b-C(22)). ^{13}C-NMR ($CDCl_3$, 100 MHz): 169.2 (C=O); 141.1 (C(5)); 138.8 (C(6)); 127.9 (C(3)); 125.1 (C(2)); 122.0 (C(1)); 117.7 (C(4)); 67.5 (C(8)); 67.0 (C(16)); 60.2 (C(23)); 55.3 (C(22)); 52.8 (C(7)); 50.4 (C(11)); 37.8 (C(12)); 37.7 (C(21)); 34.7 (C(22)); 32.1 (C(14)); 29.7 (C(18)); 28.7 (C(17)); 26.8 (C(13)); 26.6 (C(15)).

21,22-Dihydroisostrychnine(=(3aR,11bS,12S)-14-(2-Hydroxyethyl) 2, 3, 10, 12,13,13a-hexahydro-9H,11bH-1,12-ethanopyrido[1,2,3-lm]pyrrolo[2,3 d]carbazol-9-one; **9**). Compound **9** (100 mg, 5%) was obtained as a minor fraction during the purification of **10** by CC (SiO_2; R_f ($CHCl_3$/MeOH/25% aq. NH_3 100: 10:

1) 0.15). White solid. M.p. 243–245 °C ([17]: 244–246 °C). ^{1}H-NMR ($CDCl_3$, 400 MHz): 8.10 (*d*, *J* =7.7, H-C(4)); 7.24–7.15 (*m*, H-C(1), H-C(3)); 7.07 (*td*, *J*=7.5, 1.0, H-C(2)); 5.75 (*m*, H-C(12)); 4.25 (*t*, *J*=2.9, H-C(8)); 3.71 (*td*, *J*=6.4, 2.0, H-C(23)); 3.39 (*t*, *J* =3.0, H-C(16)); 3.24–2.90 (*m*, H_a-C(11), H_a-C(18), H_b-C(21), H_a-C(20), H_b-C(11)); 2.53 (*m*, H-C(14)); 2.45 (*m*, H_a-C(7)); 2.30 (*ddd*, *J* =13.9, 9.0, 1.5, H_b-C(17)); 2.14–2.03 (*m*, H_a-C(15), H-C(21)); 1.79 (*t*, *J*=12.1, H_b-C(20)); 1.59–1.48 (*m*, H_a-C(22), H_b-C(15)); 1.35 (*dddd*, *J*= 13.5, 6.7, 6.7, 6.7, H_b-C(22). ^{13}C-NMR ($CDCl_3$, 100 MHz): 168.7 (C=O); 141.2 (C(5)); 141.1 (C(13)); 136.3 (C(6)); 128.2 (C(3)); 124.4 (C(2)); 122.4 (C(12)); 122.3 (C(1)); 114.4 (C(4)); 70.8 (C(8)); 65.4 (C(16)); 60.0 (C(23)); 54.6 (C(11)); 53.7 (C(20)); 51.7 (C(7)); 48.7 (C(17)); 37.3 (C(18)); 36.7 (C(14)); 36.1 (C(21)); 35.4 (C(22)); 27.4 (C(15)). EI-MS: 337.1 (23), 336.1 (78, *M*+), 316.1 (30), 305.1 (33), 291.1 (42), 220.1 (45), 167.1 (49), 149.0 (69).

23-Deoxy-12,13,21,22-tetrahydroisostrychnine (=3aR,11aR,11bS,12S)-14-Ethyl-2,3,10,11,11a,12,13,13a-octahydro-9H,11bH-1,12-ethanopyrido[1,2,3-lm]pyrrolo[2,3 d] carbazol-9-one ; **11**). Compound **11** (75 mg, 4%) was obtained as a minor fraction during the purification of **10** by CC (SiO_2; R_f ($CHCl_3$/MeOH/25% aq. NH_3 100:10: 1) 0.49). White foam. M.p. 125–130 °C ([18]: 174–176 °C). ^{1}H-NMR ($CDCl_3$, 400 MHz): 8.10 (*d*, *J*= 7.8, H-C(4)); 7.23–7.15 (*m*, H-C(1), H-C(3)); 7.09 (*td*, *J*=7.4, 1.0, H-C(2)); 4.04 (*d*, *J*=.5, HC(8)); 3.09 (*m*, H_a-C(11)); 2.99 (*m*, H_b-C(11)); 2.92–2.86 (*m*, H_a-C(20), H-C(16)); 2.53–2.47 (*m*, CH_2(18)); 2.40–2.26 (*m*, CH*2*(12), H_b-C(20)); 2.16–2.06 (*m*, H_a-C(17), H-C(14)); 1.75–1.61 (*m*, CH_2(15), H-C(13), H_b-C(17), H-C(21)); 1.31 –1.17 (*m*, CH_2(22)); 0.93 (*t*, *J* =7.4, Me(23)). ^{13}C-NMR ($CDCl_3$, 100 MHz): 168.2 (C=O); 140.2 (C(5)); 138.0 (C(6)); 126.8 (C(23)); 124.0 (C(2)); 121.0 (C(1)); 116.7 (C(4)); 66.6 (C(8)); 66.2 (C(16)); 54.3 (C(11)); 51.9 (C(7)); 49.3 (C(20)); 41.6 (C(13)); 36.8 (C(12)); 30.2 (C(21)); 28.7 (C(18)); 27.6 (C(15)); 22.7 (C(17)); 22.5 (C(14)); 23.3 (C(22)); 10.8 (Me(23)). EI-MS: 323.1 (10), 322.1 (44, M^+), 316.1 (30), 167.0 (36), 149.0 (100), 124.1(65).

FLIPR® *Membrane Potential Blue Assay.* The functional characterization of the strychnine analogs were performed by the FLIPR® membrane potential blue assay *(Molecular Devices).*[3] TsA-201 Cells transiently transfected with cDNAs encoding for α1 or α1β GlyRs were split into poly-D-lysine-coated black 96-wells plates with clear bottom (*BD Biosciences*, Bedford, MA). Later (16 –24 h), the medium was aspirated, and the cells were washed with 100 µl of *Krebs* buffer (140 mM NaCl/4.7 mM KCl/2.5 mM $CaCl_2$/1.2 mM $MgCl_2$/11 mM *HEPES*/10 mM D-glucose; pH 7.4). *Krebs* buffer (50 µl) was added to the wells (in the antagonist experiments, various concentrations of the antagonist were dissolved in the buffer), and then an additional 50 µl of *Krebs* buffer supplemented with the FMP assay dye (1 mg/ml) was added to each well. Then, the plate was incubated at 37° in a humidified 5% CO_2 incubator for 30 min and assayed in a *NOVO*star® plate reader (*BMG Labtechnologies,* DE-Offenburg), measuring emission (in fluorescence units (FU)) at 560 nm caused by excitation at 530 nm before and up to 1 min after addition of 33 µl of agonist soln. The experiments were performed in duplicate at least three times for each compound at each receptor using an EC_{50} concentration of glycine as agonist.

References of the manuscript

1. Lynch, J. W. Molecular structure and function of the glycine receptor chloride channel. *Physiol Rev* **2004,** 84, 1051-95
2. Laube, B.; Maksay, G.; Schemm, R.; Betz, H. Modulation of glycine receptor function: a novel approach for therapeutic intervention at inhibitory synapses. *Trends Pharmacol Sci* **2002**, 23, 519-27
3. Jensen, A. A.; Kristiansen, U. Functional characterisation of the human alpha1 glycine receptor in a fluorescence-based membrane potential assay. *Biochem Pharmacol* **2004**, 67, 1789-99.

4. Karrer, P.; Eugster, C. H.; Waser, P. Über Curarewirkung einiger Strychnidin- und Dihydrostrychnidin-chlor-alkylate. *Helv Chim Acta* **1949**, 32, 2381-87.
5. Szabo, L.; Weimann, L. Data examining the relationship between the chemical structure and biological effects of strychnine. Analysis of functional groups and produce the required derivatives. *Acta Pharm Hung* **1965**, 35, 26-33
6. Szabo, L.; Weimann, L.; Clauder, O.; Data examining the relationship between the chemical structure and biological effects of strychnine. The dihydroindole nitrogen role in the biological effect. *Acta Pharm Hung* **1968,** 38, 84-90.
7. Iskander, G. M.; Bohlin, L. Structure-activity relationship of strychnine derivatives modified in the non-aromatic part. *Acta Pharm Suec*. **1978**, 15, 431-8.
8. Jensen, A. A.; Gharagozloo, P.; Birsdall, N. J. M.; Zlotos, D. P. Pharmacological characterization of strychnine and brucine analogues at glycine and alpha 7 nicotinic acetylcholine receptors. *Eur J Pharmacol* **2006**, 539, 27-33.
9. Swan, G. A.; Wilcock, J. D. 10,11-Didehydrostrychnidine. *J Chem Soc Perkin Trans* **1972,** 1, 1068-1070.
10. Chakravarti, R. N.; Robinson, R. Strychnine and brucine; the preparation of neostrychnine and neobrucine. *J Chem Soc* **1947**, 78-80.
11. E. Heller, A.; Gutmann, G.; Hiltensperger, W.; Lautenschläger, M. J.; Lohse, C.; Schirmeister, T.; Seufert, F.; Zlotos, D. P.; Holzgrabe, U. Mikrowellen-Extraktionen und -Synthesen von Naturstoffen. *G.I.T Laboratory Journal* **2013,** 1-2, 32.
12. Oxford, A. E.; Perkin, W. H.; Robinson, R. The Alkaloids: Chemistry and Physiology *J Chem Soc* **1927**, 2389.

13. Luther, J. D.; Valentini J.; Carter, J. C. Proton magnetic resonance spectra and assignments of neostrychnine and 18-oxostrychnine. *J Magn Reson* **1974**, 15, 132-41.
14. Pictet, A.; Bacovescu, A. Over Isostrychnine. *Chem Ber* **1905**, 38, 2787-92.
15. Leuchs, H.; Nietschke, Strychnos alkaloids: Preparation of isostrychnine. *Chem Ber* **1922**, 55B, 3171-4.
16. Mori, M.; Nakanishi, M.; Kajishima, J.; Sato, Y. A novel and general synthetic pathway to strychnos indole alkaloids: total syntheses of (-)-tubifoline, (-)-dehydrotubifoline, and (-)-strychnine using palladium-catalyzed asymmetric allylic substitution. *J Am Chem Soc* **2003,** 125, 9801-7.
17. Leuchs, H.; Schulte, H. Strychnos alkaloids: A third isomer of strychnine and derivatives of isobrucine. *Chem Ber* **1942,** 75B, 1522-8.
18. Leuchs, H.; Schulte, H. Strychnos alkaloids: The behavior of strychnine and dihydrostrychnine toward hydrobromic acid. *Chem Ber* **1942**, 75B, 573-9.

4.2. Oxime Ethers of (E)-11-Isonitrososstrychnine as Highly Potent Glycine Receptor Antagonists

Manuscript is in revision in the *Journal of Natural Products*

Paper II

Amal M. Y. Mohsen,† Edita Sarukhanyan,‡ Ulrike Breitinger,† Carmen Villmann,§ Maha M. Banoub, † Hans-Georg Breitinger,† Thomas Dandekar, ‡ Ulrike Holzgrabe, ⊥ Anders A. Jensen, ‖ and Darius P. Zlotos *,†

†Faculty of Pharmacy and Biotechnology, The German University in Cairo, New Cairo City, 11835 Cairo, Egypt

‡ Biocenter, Bioinformatics, University of Würzburg, 97074 Würzburg, Germany

§ Institute of Clinical Neurobiology, University of Würzburg, 97078 Würzburg, Germany

⊥ Institute of Pharmacy and Food Chemistry, University of Würzburg, 97074 Würzburg, Germany

‖Department of Drug Design and Pharmacology, Faculty of Health and Medical Sciences, University of Copenhagen, DK-2100 Copenhagen, Denmark

* Corresponding author

*E-mail: darius.zlotos@guc.edu.eg. Tel: +20 2 2758 1041. Fax: +20 2 2758 1041.

ABSTRACT:

A series of (*E*)-11-isonitrosostrychnine oxime ethers as well as pseudostrychnine, pseudostrychnine methyl ether, 2-aminostrychnine, strychnine-2-yl propionamide, and 18-oxostrychnine, were synthesized and evaluated pharmacologically at human α1 and α1β glycine receptors in a functional fluorescence-based assay, in a whole cell patch-clamp assay, and in [^{3}H]strychnine binding studies. 2-aminostrychnine and the methyl, allyl, and propargyl oxime ethers were the most potent α1 and α1β antagonists in the series, displaying IC_{50} values similar to those of strychnine at the two receptors. Docking experiments using a high resolution structure of the α1 glycine receptor indicated that while the oxime ethers adopt the same orientation as strychnine in the orthosteric binding site of the receptor, the arrangement of 2-aminostrychnine in the site is different. The findings are a valuable extension of SARs of strychnine at α1 and α1β receptors.

Strychnine, the major alkaloid from the plant *Strychnos nux vomica*, exhibits pharmacological activity at several neurotransmitter receptors, including a number of ligand-gated ion channels, such as muscle-type and neuronal nicotinic acetylcholine receptors and glycine receptors (GlyRs). The major pharmacological action of strychnine is a strong antagonistic activity at the latter receptors, which consequently often are referred to as 'strychnine-sensitive GlyRs.[1,2,3] The GlyRs are anion-selective channels that mediate inhibitory synaptic transmission in the spinal cord and brainstem, and they are believed to play crucial roles in motor coordination and pain signal transmission.[4,5] Disruption of the normal GlyR function caused by heritable mutations is associated with neuromotor disorders such as hyperekplexia or some forms of spasticity.[5,6,7,8] The GlyRs are pentameric subunit complexes belonging to the superfamily of Cys-loop receptors and exist either as homomers comprised of α subunits or heteromers that contain both α and β subunits.[9] While four α-subunit isoforms are known (α1 -α4), only one β subunit has been identified. The precise distribution of different subunits is specific to different parts of the central nervous system.[10, 11]

For a long time, understanding of the molecular mechanisms of GlyR function has been hampered by a lack of high-resolution structures of the receptors, and only recently homology models based on structures of other Cys-loop receptors have been available.[12] Very recently, however, electro cryo-microscopy structures of the zebra fish α1 GlyR in complex with strychnine and glycine[13] and a crystal structure of human α3 GlyR in complex with strychnine[14] have been published, providing a detailed insight into the molecular recognition of agonists and antagonists and mechanisms of GlyR activation and inactivation.

As a natural product, strychnine has been optimized for strong interactions with biological macromolecules through evolutionary selection. Indeed, it displays high nanomolar binding affinity and inhibitory potency at recombinant and native GlyRs in binding studies and functional assays.[2,3,15] In previous structure-activity relationships (SAR) studies any structural change to strychnine, including *N*-

quaternization, C-2-nitration, lactam reduction, hydrogenation, oxidation or relocation of the C-21-C-22 double bond, and opening of the tetrahydrooxepine ring, has been reported to decrease the antagonist activity at GlyRs.[16,17,18] The only structure modification reported not to impair the activity of the parent compound is the introduction of an (*E)*-configured hydroxyimino group at C-11 to give (*E*)-isonitrososstrychnine (**1**). Similar to strychnine, none of these analogs have exhibited selectivity between homomeric α1 and heteromeric α1β receptors.

In the present study, the synthesis and extensive pharmacological evaluation of a series of oxime ethers, formally obtained from (*E*)-isonitrososstrychnine **1** by replacement of the hydroxy group with alkoxy substituents of different size and polarity, is described. Moreover, to extend the SAR of strychnine, the functional properties of 2-aminostrychnine (**2**), 2- propionamidostrychnine (**3**), the quaternary *N*-propyl strychnine (**4**), the minor *Strychnos* alkaloid pseudostrychnine (**5**),[19,20] 18-oxostrychnine (**6**), and 16-methoxystrychnine (**7**) have been characterized at homomeric (α1) and heteromeric (α1β) GlyRs. The SAR findings are discussed based on docking experiments using the high-resolution structure of α1 GlyR with strychnine occupying its orthosteric binding site.[13]

RESULTS AND DISCUSSION

The structures of the strychnine analogues studied in this work are shown in Chart 1 and Scheme 1. (*E)*-11-Oximinostrychnine **1** was obtained by nitrosation of strychnine using *tert*-butyl nitrite/*tert*-BuOK as previously reported.[21] 2-aminostrychnine **2** was synthesized in a two step approach by nitration of strychnine and subsequent reduction of the introduced nitro group using $SnCl_2$.[22] 2-Propionamidostrychnine **3** was obtained by acylation of 2-aminostrychnine using propionic acid anhydride. *N*-Propyl strychnine bromide **4** was prepared by quaternization of strychnine using *n*-propyl bromide as previously reported.[23] Pseudostrychnine **5** and 18-oxostrychnine **6** were synthesized from strychnine *N*-

oxide using $K_2Cr_2O_7$ according to a modified procedure by Rosenmund *et al.*[24] 16-Methoxystrychnine **7** was obtained by o-methylation of pseudostrychnine **5** using iodomethane. The oxime ethers **8a-k** were synthesized by *O*-alkylation of **1** using NaH as a base and an appropriate alkylating agent. The functional properties of compounds **2-7**, **8a-k** and the reference ligands strychnine and isonitrososstrychnine **1** were characterized at the human α1 and α1β receptor subtypes in the fluorescence-based FLIPR^{TM} Membrane Potential Blue (FMP) Assay. Here, the receptors were transiently expressed in tsA201 cells, and the abilities of the compounds to inhibit the response induced by glycine EC50 (EC40-EC60) in the cells were determined.[25] The expression of homogenous populations of α1 and α1β receptors in the cells was verified on a routinely basis using picrotoxin, which as previously reported displays ~100-fold higher antagonist potency at α1 than at α1β in this assay.[26] The *IC*50 values determined for the compounds are given in Table 1.

Chart 1. Structural Formulas of Strychnine and its Analogues **1-7**

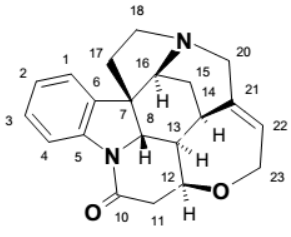

strychnine

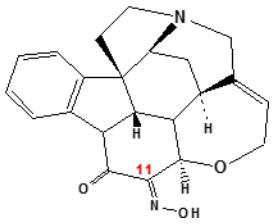

11-(E)-isonitrosotrychnine 1

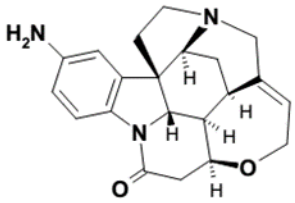

2

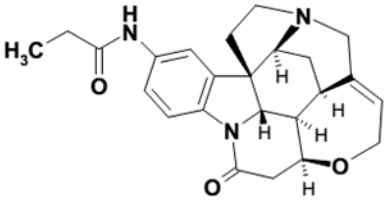

3

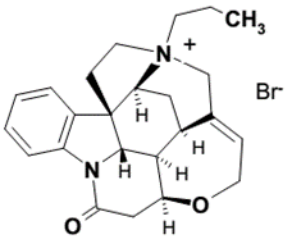

4

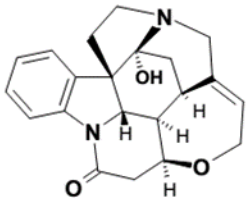

pseudostrychnine **5**

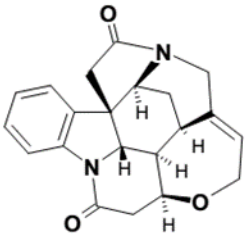

6

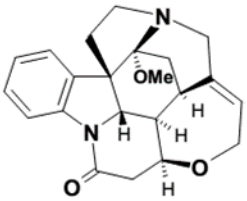

7

Scheme 1

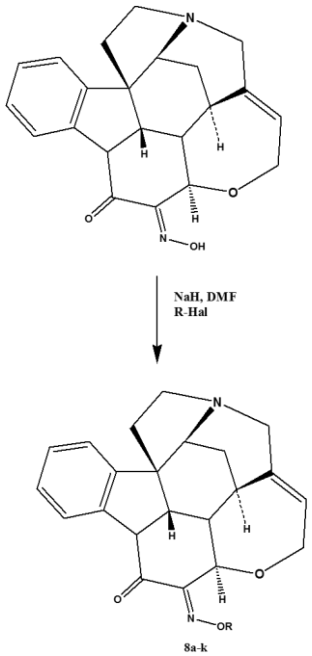

	R
8a	$-CH_3$
8b	$-(CH_2)_2CH_3$
8c	$-(CH_2)_3CH_3$
8d	$-CH_2CH(CH_3)_2$
8e	$-CH_2Ph$
8f	$-(CH_2)_4CH_3$
8g	$-(CH_2)_2Ph$
8h	$-CH_2-CH=CH_2$
8i	$-CH_2-C\equiv CH$
8j	$-CH_2CO_2CH_3$
8k	$-(CH_2)_4CO_2CH_3$

Table 1. Pharmacological Characterization of the Compounds at α1 and α1β GlyRs

	IC_{50} [μM] FMP assay[a]		IC_{50} [μM] patch-clamp assay[b]	
	α1	α1β	α1	α1β
strychnine	**0.093** [7.03 ± 0.09]	**0.18** [6.74 ± 0.06]	**0.051** ± 0.005	**0.058** ± 0.003
1	**0.097** [7.01 ± 0.03]	**0.21** [6.67 ± 0.10]	**0.082** ± 0.010	**0.080** ± 0.008
2	**0.077** [7.11 ± 0.08]	**0.27** [6.56 ± 0.05]	**0.076** ± 0.009	**0.097** ± 0.011
3	**0.54** [6.27 ± 0.05]	**0.94** [6.03 ± 0.08]	**0.201** ± 0.019	**0.311** ± 0.039
4	**10** [4.98 ± 0.07]	**13** [4.87 ± 0.05]	**4.59** ± 0.41	**6.53** ± 0.59
5	~**100** [~4.0]	~**100** [~4.0]		
6	**6.9** [5.16 ± 0.04]	**9.8** [5.00 ± 0.16]		
7	**7.3** [5.06 ± 0.09]	**13** [4.87 ± 0.08]		
8a	**0.10** [6.98 ± 0.09]	**0.21** [6.67 ± 0.05]	**0.075** ± 0.008	**0.056** ± 0.011
8b	**0.11** [6.94 ± 0.09]	**0.35** [6.45 ± 0.08]	**0.109** ± 0.009	**0.116** ± 0.018
8c	**0.37** [6.42 ± 0.05]	**0.88** [6.06 ± 0.03]	-	-
8d	**0.26** [6.58 ± 0.07]	**1.10** [5.95 ± 0.06]	-	-
8e	**0.17** [6.78 ± 0.13]	**0.31** [6.51 ± 0.06]	-	-
8f	**0.25** [6.61 ± 0.10]	**0.71** [6.15 ± 0.08]	-	-
8g	**0.69** [6.15 ± 0.07]	**0.78** [6.11 ± 0.08]	-	--
8h	**0.095** [7.02 ± 0.03]	**0.15** [6.80 ± 0.04]	**0.049** ± 0.004	**0.046** ± 0.0049
8i	**0.052** [7.29 ± 0.10]	**0.24** [6.62 ± 0.13]	**0.059** ± 0.008	**0.043** ± 0.007
8j	**0.22** [6.65 ± 0.09]	**0.67** [6.18 ± 0.06]	-	-
8k	**0.72** [6.15 ± 0.04]	**1.50** [5.83 ± 0.08]	-	-

[a]Functional properties of the compounds at the human α1 and α1β GlyRs transiently expressed in tsA201 cells in the FLIPR™ Membrane Potential Blue (FMP) assay. EC_{50} (EC_{40}-EC_{60}) concentrations of glycine were used as agonist at the two receptors (EC_{50} = 42 μM at α1, EC_{50} = 23 μM at α1β. The IC_{50} values for the analogues represent the antagonistic potency and are given in μM with pIC_{50} ± S.E.M in brackets. Data are given as the means based on n=3-4.

[b]Direct inhibition of glycine-mediated currents was measured using whole-cell patch clamp recordings from HEK293 cells transiently transfected with GlyR α1 or α1/β cDNA. After determination of EC_{50}, strychnine derivatives in varying concentrations were perfused over GlyR-expressing cells and inhibition curves constructed from whole-cell current amplitudes measured in the presence and absence of inhibitor at EC_{50} concentrations of glycine. IC_{50} values were determined from inhibition curves constructed from a nonlinear fit to dose-response data using 3 - 5 cells per inhibitor. Data are given as means ± SD.

Previous SAR studies have identified the lactam carbonyl group, the tertiary amino group and the C21=C22 double bond in strychnine as essential structural elements required for its strong antagonistic activity at homo- and heteromeric GlyRs.[16-18] These findings are in agreement with the recently published high-resolution structures of strychnine bound to the homomeric α1 and α3 GlyRs.[13,14] The residues critical for strychnine binding are identical in the two receptors, resulting in the same antagonist binding mode. The strychnine binding site of the homomeric α1 receptor is shown in Fig. 1. The binding interactions between strychnine and the receptor include hydrogen bonds between the protonated tertiary amine of strychnine and the backbone carbonyl group of Phe175, and between the lactam oxygen of strychnine and the guanidinium group of Arg81 and a hydroxyl group of Thr220. Moreover, the benzene rings of Phe79, Phe175, and Phe223 are involved in interactions with hydrophobic parts of the strychnine molecule, such as the aromatic ring, methylene groups CH_2-17, CH_2-18, and the C21=C22 double bond (see Fig. 1).

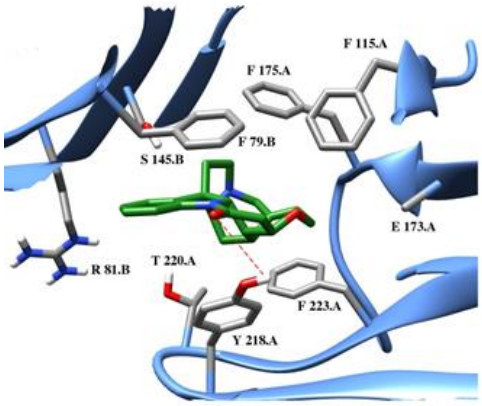

Figure 1. Graphical representation of the antagonist binding pocket of the homomeric α1 GlyR with bound strychnine (green)

The residues essential for strychnine binding are conserved among the α and β subunits of GlyRs, with the exception that α Phe207 is replaced by a Tyr in the β subunit.[14] Consequently, it is hardly surprising that neither strychnine nor any of the

analogues in this study displayed substantial selectivity toward α1 or α1β receptors. In the FMP assay, all compounds either displayed comparable antagonist potencies at the two receptors or slightly higher potency at the homomeric receptor with 2-aminostrychnine **2,** and the *n*-propyl, isobutyl, and *n*-pentyl oxime 10 ethers **8b**, **8d,** and **8f**, respectively, showing the highest preference toward the α1 subtype (3-4-fold).

While the lactam group and the C21=C22 double bond are present in all strychnine analogues examined in this study, two analogues lack the tertiary amino group, namely the quaternary *n*-propyl derivative **4** and 18-oxostrychnine **6** in which *N*-19 is a part of an amide function. Consequently, for both compounds, *N*-19 can not exist in a protonated form required for its action as a hydrogen bond donor, which is reflected in the antagonist potencies of **4** and **6** (IC_{50} ~10 μM) being approximately 100-fold lower than those of strychnine (IC_{50} ~ 0.1 μM) at both α1 and α1β.

2-Aminostrychnine **2** and pseudostrychnine (16 hydroxystrychnine) **5**, a minor alkaloid from *Strychnos nux vomica*[27] and *Strychnos icaya*,[28] have previously been identified as high affinity ligands for the strychnine binding sites in synaptic membranes from brain and spinal cord of rats.[15] Radioligand displacement experiments using [^{3}H]strychnine revealed almost identical dissociation constants for strychnine (K_i = 12 nM) and pseudostrychnine (Ki = 10 nM), and only slightly reduced affinity for 2-aminostrychnine (Ki = 18 nM).[15] Surprisingly, pseudostrychnine **5** displayed very low antagonist potency (IC_{50} ~ 100 μM) at both GlyRs in the FMP assay. The corresponding 16-methoxy analogue **7** was also a weak GlyRs inhibitor (IC_{50} ~ 10 μM) with ~100-fold lower antagonist potencies than strychnine.

For 2-aminostrychnine **2**, the IC_{50} values determined in the FMP assay correlate very well with the previously reported binding affinity data.[15] Compound **2** exhibited strong inhibition of α1 (IC_{50} = 97 nM) and α1β (IC_{50} = 270 nM)

receptors, thus being equipotent to strychnine at both subtypes. As discussed later, docking experiments revealed that the orientation of 2-aminostrychnine in the antagonist binding pocket is different from that of strychnine due to a hydrogen bond between the primary amino group and the carbonyl group of Glu173 (see Fig. 2).

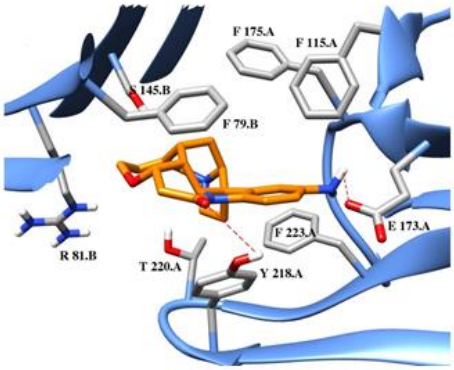

Figure 2. Graphical representation of the antagonist binding pocket of the homomeric α1 GlyR with bound 2-aminostrychnine **2** (orange)

For the propionamide **3** (*N*-acylated 2-aminostrychnine), the corresponding H-bond is not possible resulting in a significantly lower antagonistic potency at α1 (IC_{50} = 540 nM) and α1β (IC_{50} = 940 nM) receptors. Isonitrososstrychnine **1** has been previously reported to exert strong antagonistic action at GlyRs.[17] In the FMP assay it displayed almost identical IC_{50} values (α1: 97 nM; α1β: 210 nM) to strychnine. An equally high inhibition was observed for its methyl ether **8a** (α1: IC_{50} = 100 nM; α1β: IC_{50} = 210 nM). The effect of increasing the size of the oxime ether substituent on the antagonist potency was examined in the series of ligands **8a-i**. While the *n*-propyl analogue **8b** maintained the high antagonist potency (α1: IC_{50} = 110 nM; α1β: IC_{50} = 350 nM), further increasing the size of the alkyl substituent (**8c-g**, R = *n*-butyl, *iso*-butyl, benzyl, *n*-pentyl, phenylethyl) gradually reduced the GlyR activity of the analogs. For example, **8g** bearing a bulky phenylethyl substituent exhibited ~5-fold higher IC_{50} values at the GlyRs (690 nM (α1) and 780 nM (α1β) than those of the methyl analogue **8a.** A terminal methyl ester group did not

significantly change the antagonist potencies in the oxime ether series as indicated by the *IC*50 values of the methyl acetate **8j** (α1: 220 nM; α1β: 720 nM) and the methyl valerate **8k** (α1: 720 nM; α1β: 1,500 nM), the latter being less potent because of the longer spacer between the oxime ether oxygen and the ester carbonyl group.

Introduction of a double or triple bond into the propyl group of **8b** significantly improved antagonistic potency. The resulting allyl (**8h**) and propargyl (**8i**) analogues are among the most potent GlyR antagonists published to date displaying IC_{50} values of 95 nM (α1) and 150 nM (α1β); and 52 nM (α1) and 240 nM (α1β), respectively. These findings indicate that the strychnine binding site at GlyRs comprises an additional lipophilic pocket located close to C-11 of strychnine, and the groups best accommodated in this pocket are E-allyl- and E-propargyl oxime ethers (Figure 3).

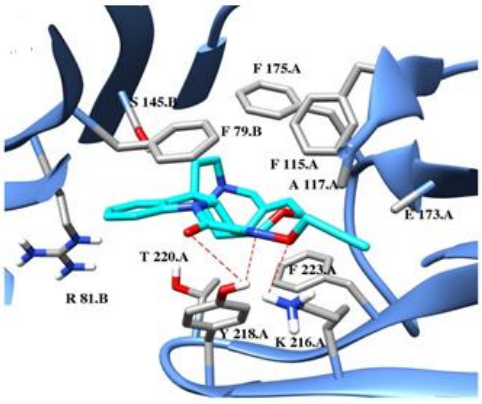

Figure 3. Graphical representation of the antagonist binding pocket of the homomeric α1 GlyR with bound propargyl oxime ether **8i** (cyan)

The analogues displaying the highest antagonist potencies in the FMP assay (**1**, **2**, **8a**, **8b**, **8h**, **8i**) and the less potent antagonists **3** and **4** were tested in whole-cell patch-clamp assays at α1 and α1β GlyRs recombinantly expressed in HEK 293 cells. This method records ion channel-mediated transmembrane currents directly and thus allows direct insight into the inhibition of GlyR function.[29] While the FMP assay generates an equilibrium of all receptor states (free, ligand-bound, inhibitor-

bound, active, desensitized), the patch-clamp technique observes receptor activation and inhibition in a pre-equilibrium situation, where receptor desensitization, i.e. the transition into an inactive refractory state is excluded.[29] The concentration-dependent reduction of GlyR currents in the presence of strychnine derivatives was used to construct concentration-inhibition curves and determine functional IC_{50} values.[30,31]

The IC_{50} values (Table 1) obtained in the patch-clamp recordings generally correlate well with those from the FMP assay confirming the SAR conclusions drawn so far and indicating that affinity of strychnine analogues for active and desensitized receptor states is similar. For most analogues, the IC_{50} values were slightly lower and none of the ligands showed preference toward α1 subtype.

In order to confirm that the antagonist potencies obtained for the strychnine analogs in the two functional studies correlate with their binding affinities at the receptors, compounds **1**, **3**, **8a**, **8b**, and **8h** were subjected to radioligand binding experiments at α1 receptors recombinantly expressed in HEK293 cells using [^{3}H]strychnine as radioligand. The displacement curves are shown in Figure 4. The binding affinities for the analogues (K_i values) are given in Table 2. Isonitrososstrychnine **1** that was found to be equipotent to strychnine in both functional assays also exhibited comparable binding affinity (K_i = 40 nM) to the parent compound (K_i = 23 nM). 2-Propionamidostrychnine **3** that was 3-fold less potent than strychnine in both functional assays, displayed a 3-fold decreased binding affinity (K_i =67 nM) compared to strychnine in the binding assay. Surprisingly, the oxime ethers **8a**, **8b**, and **8h** that exhibited antagonistic potencies similar to that of strychnine in both functional assays, showed significantly reduced binding affinity compared to the parent compound (**8a** K_i =189 nM; **8b** K_i = 241 nM; **8h** K_i = 371 nM).

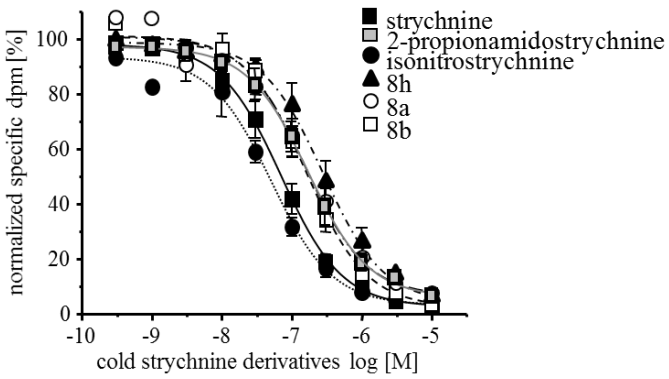

Figure 4. Displacement curves for strychnine, 2-propionamidostrychnine, isonitrososstrychnine, 8h, 8a, 8b

Table 2. Binding Affinities of Selective Compounds for the Human α1 GlyRs Expressed in HEK293 Cells Obtained in Competition Radioligand Binding Assays Using [^{3}H]strychnine

	K_i [nM] ± SEM
strychnine	23 ± 6
1	40 ± 4
3	67 ± 17
8a	189 ± 30
8b	241 ± 67
8h	370 ± 116

To determine the binding modes of the novel analogues, strychnine and its most potent analogues 2-aminostrychnine **2,** and the propargyl oxime **8i** were docked into the orthosteric binding site of high resolution structure of homomeric α1 GlyR (3JAD).[13] Simulations were performed for each compound separately using Autodock 4.2.6.[32] Rigid-protein docking was employed as it gave a better correlation between the calculated free energy values and experimental inhibition constants than flexible docking.

A graphical representation of strychnine at its active site is shown in Figure 1. The binding pocket is composed of the residues Phe115, Phe79, Phe175, Phe223, Gly176, Tyr218, Thr220, Arg81 and Ser145. The majority of these are aromatic residues form a hydrophobic environment interacting with the lipophilic parts of the strychnine molecule, such as the aromatic ring, methylene groups CH_2-17, CH_2-18, and the C-21-C-22 double bond. The strongest polar interaction is a hydrogen bond (3.4 Å) between the lactam oxygen of strychnine and the OH group of Tyr218. Docking results of the most potent strychnine oxime ethers revealed the same orientation of the strychnine skeleton as for the parent compound. As shown for the propargyl oxime ether **8i** (Fig. 3), in addition to all interactions already found for strychnine, the nitrogen and oxygen atoms of the oxime ether moiety make hydrogen bonds with the hydroxyl group of Tyr218, and the propargyl group occupies a pocket surrounded by Glu173, Ala117, and Lys216.

In contrast, 2-aminostrychnine **2** adopts a different arrangement in the binding pocket, which seems to be induced by a hydrogen bond between the primary amino group of 2-aminostrychnine and the carboxylate group of Glu173, (Fig. 2). Another polar interaction is a H-bond between the lactam oxygen and the OH group of Tyr218.

The fact that **2** despite this different binding mode to the orthosteric site in GlyR exhibits potent antagonism is interesting, and we propose that the compound

because of its different arrangement in the binding pocket could constitute an interesting lead for future series of analogs.

In summary, a series of (*E*)-11-isonitrosostrychnine oxime ethers was synthesized and characterized as antagonists at homomeric and heteromeric glycine receptors in the FMP assay, in a whole cell patch-clamp assay, and in [^{3}H]strychnine binding studies. The most potent antagonists in the series bear methyl, allyl, and propargyl substituents. While the methyl and allyl analogues **8a** and **8h** were equipotent to strychnine, the propargyl oxime ether **8i** was a slightly more potent antagonist than the parent compound. Moreover, 2-aminostrychnine **2**, previously reported to show high affinity for the strychnine binding sites of rat synaptic membranes, was found to display antagonistic potency similar to that of strychnine at the GlyRs, and this analog seems to exert its antagonism through a different binding mode to the orthosteric sites of the receptors. The findings provide a valuable extension of the SARs of strychnine at α1 and α1β receptors and are important for the design of bivalent ligands targeting glycine receptors which currently are under investigation.

Experimental Section

General Experimental Procedures. Melting points were determined using a capillary melting point apparatus (Gallenkamp, Sanyo) and are uncorrected. Bruker AV-400 spectrometer was used to obtain ^{1}H NMR and ^{13}C NMR spectra, respectively. ^{1}H NMR chemical shifts are referred to $CHCl_3$ (7.26 ppm) and DMSO-d_6 (2.50 ppm). ^{13}C NMR chemical shifts are referred to $CDCl_3$ (77.26 ppm) and DMSO-d_6 (39.52 ppm). The NMR resonances were assigned by means of COSY, and HMQC experiments. ESI mass spectra were determined on an Agilent 1100 MS systems. Elemental analyses were performed by the microanalytical section of the Institute of Inorganic Chemistry, University of Würzburg. All reactions were carried out under an argon atmosphere. Column chromatography was carried out on silica

gel 60 (0.063–0.200 mm) obtained from Merck. 2-Aminostrychnine **2** was synthesized by nitration of strychnine and reduction of the resulting 2-nitrostrychnine using $SnCl_2$ as reported in ref.[22] *N*-Propylstrychnine bromide **4** was prepared as previously described.[23]

***N*-(Strychnin-2yl) propionamide (3).** Propionic anhydride (4.4 mL) was dropwise added to the solution of 2-aminostrychnine (290 mg, 0.83 mmol) and triethylamine (2.53 mL) in dry CH_2Cl_2 (20 mL). After stirring for 2 h at room temperature, the solvent was removed under reduced pressure and the residue was subjected to column chromatography ($CHCl_3$−MeOH−25%NH_3, 100:10:1) to give **2** (256 mg, 76%) as colorless solid; ^{1}H NMR (400 MHz, $CDCl_3$) δ 7.99 (1H, d, *J* = 8.6 Hz, H-4),7.60 (1H, d, *J* = 1.9 Hz, H-1), 7.42 (1H, s, NH), 7.14 (1H, dd, *J* = 8.6, 1.9 Hz, H-3), 5.87 (1H, t, *J* = 6.0 Hz, H-22), 4.26 (1H, dt, *J* = 8.4, 3.3 Hz, H-12), 4.13 (1H, dd, *J* = 13.8, 6.9 Hz, H-23a), 4.04 (1H, dd, *J* = 13.8, 6.0 Hz, H-23b), 3.92 (1H, s, H-16), 3.84 (1H, d, *J* = 10.5 Hz, H-8), 3.67 (1H, dd, *J* = 14.8, 1.0 Hz, H-20a), 3.19 – 3.06 (3H, m, H-11a, H-14, H-18a), 2.83 (1H, td, *J* = 10.1, 7.7 Hz, H-18b), 2.72 – 2.60 (2H, m, H-11b, H-20b), 2.37 (2H, q, *J* = 7.5 Hz, - C<u>H</u>$_2$CH$_3$),2.34 – 2.28 (1H, m, H-17a),1.95 – 1.81 (2H, m, H-15a, H-15b), 1.42 (1H, d, *J* = 14.4 Hz, H-17b), 1.25-1.22 (1H, m, H-13), 1.23 (3H, t, *J* = 7.5 Hz, -CH$_2$C<u>H</u>$_3$); ^{13}C NMR (100 MHz, $CDCl_3$) δ 171.76 (C, C=O), 168.92 (C, C-10), 140.42 (C, C-5), 138.36 (C, C-21), 134.51 (C, C-6), 133.59 (C C-2), 126.93 (CH, C-22), 119.83 (CH, C-3), 116.12 (CH,C-4), 114.40 (CH,C-1), 77.45 (CH, C-12) ,64.43 (CH_2, C-23), 60.21 (CH, C-16), 59.91 (CH, C-8), 52.51 (CH_2, C-20), 51.88 (C, C-7), 50.13 (CH_2, C-18), 48.03 (CH, C-13), 42.56 (CH_2, C-15), 42.17 (CH_2, C-11), 31.40 (CH, C-14), 30.45 (CH_2, -<u>C</u>H$_2$CH$_3$), 26.71 (CH_2, C-17), 9.50 (CH_3, -CH$_2$<u>C</u>H$_3$), ESI MS *m/z* 405.8 [M]+ (100%); *anal*. C 71.00, H 6.86, N 10.15%, calcd for $C_{24}H_{27}N_3O_3$ C 71.09, H 6.71, N 10.36%.

Pseudostrychnine (5) and **18-Oxostrychnine (6)** A solution of $K_2Cr_2O_7$ (6 mg, 0.02 mmol) in 2 mL H_2O was added to a solution of strychnine-*N*-oxide (200 mg, 0.57 mmol) in 10 mL H_2O and 5 mL dioxane and the reaction mixture was heated

under reflux for 2 h. After cooling to room temp, the solvent was removed under reduced pressure. 4 mL H_2O and 10 mL warm 1N HCl were added to the residue and the insoluble brown material was filtered off and subjected to column chromatography (CH_2Cl_2-MeOH-25%NH_3, 100: 5: 0.5) to give compound **6** (70 mg, 35.3%). The filtrate was neutralized to pH 9 using 25% ammonia and water was removed under reduced pressure. The white solid residue was subjected to column chromatography on silica gel (CH_2Cl_2-acetone, 3:1) to give pseudostrychnine **5** (50 mg, 25.0%).

Pseudostrychnine (5): colorless solid, mp 263 ^oC (Lit. 263^oC)[24]; ^1H NMR (400 MHz, $CDCl_3$) δ 8.09 – 8.01 (1H, m, H-4), 7.82 (1H, dd, *J* = 7.8, 0.9 Hz, H-1), 7.23 – 7.15 (1H, m, H-3), 7.00 (1H, dd, *J* = 5.1, 2.5 Hz, H-2), 5.88 (1H, t, *J* = 6.2 Hz, H-22), 4.21 (1H, dt, *J* = 8.4, 3.6 Hz, H-12), 4.09 (1H, dd, *J* = 13.9, 6.9 Hz, H-23a), 3.98 (1H, dd, *J* = 13.9, 6.1 Hz, H-23b), 3.85 (1H, dd, H-20a), 3.77 (1H, d, *J* = 10.6 Hz, H-8), 3.20 (1H, d, *J* = 11.0 Hz, H-14), 3.18 – 3.13 (1H, m, H-18a), 3.08 – 3.00 (1H, m, H-11a), 2.85 – 2.72 (2H, m, H-18b, H-20b), 2.57 (1H, dd, *J* = 17.4, 3.6 Hz, H-11b), 2.301 – 2.162 (2H, m, H-15a, H-17a), 1.831 – 1.680 (2H, m, H-15b, H-17b), 1.31 (1H, ddd, *J* = 13.0, 8.2, 4.8 Hz, H-13); ^{13}C NMR (101 MHz, $CDCl_3$) δ 170.3 (C, C=O), 169.0 (C, C-10), 142.0 (C, C-5), 138.9 (C, C-21), 131.8 (C, C-6), 128.7 (CH, C-2), 127.4 (CH, C-3), 124.3 (CH, C-22), 115.7 (CH, C-4), 92.5 (C, C-16), 77.3 (CH, C-12), 65.2 (CH_2, C-23), 60.4 (CH, C-8), 56.6 (C, C-7), 52.8 (CH_2, C-20), 48.7 (CH, C-13), 48.4 (CH_2, C-18), 42.7 (CH_2, C-11), 39.8 (CH_2, C-17), 35.0 (CH_2, C-15), 33.4 (CH, C-14); ESI MS *m/z* =350.2 $[M]^+$

18-Oxostrychnine (6): colorless solid, mp 330 ^0C (Lit. 334 ^0C)[24]; ^1H NMR (400 MHz, $CDCl_3$) δ 8.05 (1H, d, *J* = 8.1 Hz, H-4), 7.273 – 7.190 (2H, m, H-1, H-3), 7.06 (1H, td, *J* = 7.5, 1.0 Hz, H-2), 5.93 (1H, t, *J* = 6.4 Hz, H-22), 4.44 (1H, d, *J* = 3.8 Hz, H-16), 4.26 (1H, d, *J* = 14.2 Hz, H-17a), 4.20 (1H, dt, *J* = 8.3, 4.1 Hz, H-12), 4.05 (1H, dd, *J* = 13.8, 7.0 Hz, H-23a), 3.99 – 3.92 (1H, m, H-23b), 3.88 (1H, d, *J* = 10.5 Hz, H-8), 3.54 (1H, t, *J* = 10.5 Hz, H-17b), 3.24 (1H, m, H-14), 3.03 (1H, dd, *J* = 16.9, 8.5 Hz, H-11a), 2.64 (1H, d, *J* = 15.8 Hz, H-20a), 2.56 (1H, dd, *J* =

16.9, 4.2 Hz, H-11b), 2.44 (1H, d, *J* = 15.8 Hz, H-20b), 2.37 (1H, dt, *J* = 14.6, 4.4 Hz, H-15a), 1.60 – 1.54 (1H, m, H-15b), 1.23 (1H, dd, *J* = 7.0, 3.4 Hz, H-13); ^{13}C NMR (101 MHz, $CDCl_3$) δ 176.6 (C, C=O), 169.3 (C, C=O), 143.0 (C, C-5), 139.8 (C, C-21), 129.3 (CH, C-1), 128.2 (C, C-6) 127.4 (CH, C-22), 124.5 (CH, C-2), 122.1 (CH_2, C-3), 117.0 (CH, C-4), 77.6 (CH_2, C-11), 64.6 (CH_2, C-23), 60.46 (CH, C-8), 56.9 (CH, C-16), 53.8 (C, C-7), 50.9 (CH_2, C-20), 47.7 (CH, C-13), 43.9 (CH_2, C-17), 42.0 (CH, C-12), 30.6 (CH, C-14), 26.5 (CH_2, C-15); ESI MS *m/z* = 348.2 $[M-2]^+$

16-Methoxystrychnine (**7**). A solution of **5** (80 mg, 0.22 mmol) in dry DMF (4 mL) was added dropwise to a stirred suspension of sodium hydride (5 mg, 0.22 mmol 60% dispersion in mineral oil) in dry DMF (2 mL) at 0 ^{0}C. After stirring at 0 ^{0}C for 30 min., iodomethane (0.01 mL, 0.16 mmol) was added. The resulting mixture was stirred at room temp for further 16 h. The solvent was removed under reduced pressure and the residue was subjected to column chromatography (CH_2Cl_2 - acetone, 3:1) to give **7** (22 mg, 27.4%) as colourless solid.; ^{1}H NMR (400 MHz, $CDCl_3$) δ 5.96 (1H, t, *J* = 6.2 Hz, H-22), 4.35 (1H, d, *J* = 11.3 Hz, H-12), 4.25 – 4.22 (1H, m, H-8), 4.19 (1H, dd, *J* = 12.6, 5.4 Hz, H-23a), 4.02 – 3.95 (1H, m, H-23b), 3.41 (1H, m, H-14), 3.25 – 3.18 (1H, m, H-20a), 3.13 (1H, d, *J* = 10.2 Hz, H-20b), 3.07 (1H, dd, *J* = 11.8, 6.4 Hz, H-11a), 2.99 (1H, dd, *J* = 13.9, 3.9 Hz, H-17a), 2.95 (1H, dd, *J* = 13.9, 3.9 Hz, H-15a), 2.71 – 2.67 (1H, m, H-11b), 2.64 – 2.54 (1H, m, H-18a), 2.21 – 2.13 (2H, m, H-15b, H-17b), 2.10 (3H, s, O-C$\underline{H}_3$), 1.72 – 1.64 (1H, m, H-18b), 1.65 – 1.60 (1H, m, H-13);^{13}C NMR (101 MHz, $CDCl_3$) δ 167.1 (C, C=O), 141.5 (C, C-5) , 139.8 (C, C-21), 133.1 (C, C-6), 130.3 (CH, C-22), 128.4 (CH, C-3), 126.5 (CH, C-2), 124.3 (CH, C-1), 115.9 (CH, C-4), 77.9 (CH, C-8), 65.20 (CH_2, C-23), 62.9 (CH_2, C-20), 59.2 (CH, C-12), 54.7 (C, C-7), 47.1 (CH_2, C-18), 45.8 (CH, C-13), 42.7 (CH_2, C-17), 42.0 (CH_2, C-11), 43.3 (CH_2, C-15), 40.1 (C, O$\underline{C}H_3$), 35.7 (CH, C-14); ESI MS *m/z* = 364.2 $[M]^+$; mp 226 ^{0}C; *anal.* C 72.92, H 6.50, N 7.34%, calcd for $C_{22}H_{24}N_2O_3$ C 72.51, H 6.64, N 7.69%.

General procedures for the Synthesis of the Oxime Ethers 8a-k. A solution of **1** (500 mg, 1.4 mmol) in dry DMF (4 mL) was added dropwise to a stirred suspension of sodium hydride (0.03 g, 1.4 mmol, 60% dispersion in mineral oil) in dry DMF (3 mL) at 0 ^{o}C. After stirring at 0 ^{o}C for 30 min., the respective alkyl halide (0.32 mmol) was dropwise added. After stirring at room temperature for 16 hrs, the reaction mixture was concentrated under reduced pressure and the residue was subjected to column chromatography using CH_2Cl_2-MeOH-25%NH_3 (100:5:0.5) as eluent unless otherwise stated.

***(E)*-11-(Methoxyimino)strychnine (8a)** (60 mg, 12 %) was obtained from **1** and iodomethane (0.02 mL) as a pale yellow solid; ^{1}H NMR (400 MHz, DMSO-d_6) δ 8.03 (1H, d, *J* = 7.7 Hz, H-4), 7.39 (1H, d, *J* = 7.0 Hz, H-2), 7.34 – 7.28 (1H, m, H-3), 7.17 (1H, td, *J* = 7.5, 0.9 Hz, H-1), 5.73 (1H, t, *J* = 4.9 Hz, H-22), 4.85 (1H, d, *J* = 2.4 Hz, H-12), 4.092 – 4.013 (2H,m, H-23a, H-23b), 3.97 (3H, s, C$\underline{H_3}$), 3.93 (1H, d, *J* = 10.8 Hz, H-8), 3.80 (1H, dd, *J* = 12.1 Hz, H-16), 3.49 (1H, d, *J* = 14.2 Hz, H-20a), 2.96 – 2.96 (1H, m, H-14), 2.93 – 2.87 (1H, m, H-18a), 2.63 – 2.57 (1H, m, H-18b), 2.50 (1H, d, *J* = 14.2 Hz, H-20b), 2.26 – 2.14 (1H, m, H-15a), 1.79 (1H, m, H-17a), 1.64 – 1.57 (1H, m, H-13), 1.51 (ddd, *J* = 10.8, 2.6 Hz, H-17b), 1.27 (1H, ddd, *J* = 14.3 Hz, H-15b); ^{13}C-NMR(100 MHz, DMSO-d_6) δ 158.2 (C, C=O), 149.5 (C, C=N), 142.2 (C, C5), 140.4 (C, C21), 134.1 (C, C6), 128.2 (CH, C-3), 126.6 (CH, C-22), 124.6 (CH, C-1), 122.8 (CH, C-2), 114.8 (CH, C-4), 75.4 (CH, C-12), 65.3 (CH_2, C-23), 63.6 (CH_3, O-C$\underline{H_3}$), 59.5 (CH, C-16), 58.8 (CH, C-8), 52.4 (CH_2, C-20), 51.2 (C, C7), 49.4 (CH_2, C-18), 44.5 (CH, C-13), 42.8 (CH_2, C-17), 31.3 (CH, C-14), 26.4 (CH_2, C-15); ESI MS: *m/z* 377.6 $[M]^+$; mp 181 ^{o}C; *anal.* C 69.42, H 6.30, N 10.64%, calcd for $C_{22}H_{23}N_3O_3$ C 70.01, H 6.14, N 11.13%.

***(E)*-11-(Propyloxyimino)strychnine (8b)** (130 mg, 25%) was obtained from **1** and *n*-propylbromide (0.03 mL) in the presence of KI (1 mg) as white solid. ^{1}H NMR (400 MHz, DMSO-d_6) δ 4.28 (2H, t, *J* = 6.4 Hz, OC$H_2$$CH_2CH_3$), 1.74 (2H, m, $OCH_2CH_2CH_3$), 0.99 (3H, t, *J* = 7.4 Hz, -$OCH_2CH_2CH_3$), *δ* and *J*-values for all other hydrogen atoms coincide with the values for the corresponding atoms of **8a** within

±0.04 ppm and ± 0.1 Hz, respectively; ^{13}C-NMR(100 MHz, DMSO-d_6) 77.0 (O*C*$H_2CH_2CH_3$), 22.1 (OCH_2*C*H_2CH_3), 10.0 (CH_3, OCH_2CH_2*C*H_3), chemical shifts for all other carbon atoms coincide with the δ values for the corresponding atoms of **8a** within ±0.1 ppm; ESI: *m/z* 405.4 $[M]^+$; mp 182 ^oC; *anal.* C 69.63, H 6.41, N 9.98%, calcd for $C_{24}H_{27}N_3O_3$ C 71.09, H 6.71, N 10.36%.

***(E)*-11-(Butyloxyimino)strychnine (8c) (**40 mg, 7.3%) was obtained from **1** and *n*-butyl bromide (0.03 mL) in the presence of KI (1 mg) as brown solid. ^{1}H NMR (400 MHz, $CDCl_3$) δ 8.17 (1H, d, *J* = 8.0 Hz, H-3), 8.00 (1H, s, H-1), 7.30 – 7.23 (1H, m, H-4), 7.11 (1H, t, *J* = 7.1 Hz, H-2), 5.89 (1H, s, H-22), 4.95 (1H, d, *J* = 2.4 Hz, H-12), 4.46 – 4.36 (2H, m, OC*H*$_2$(CH_2)$_2CH_3$), 4.28 (1H, dd, *J* = 13.9, 7.1 Hz, H-23a), 4.17 (1H, d, *J* = 10.6 Hz, H-8), 4.11 (1H, dd, *J* = 13.9, 5.7 Hz, H-23b), 3.96 (1H, s, H-16), 3.70 (1H, d, *J* = 14.6 Hz, H-20a), 3.14 (1H, dd, *J* = 16.8, 8.2 Hz, H-18a), 3.06 (1H, s, H-14), 2.84 (1H, d, *J* = 5.0 Hz, H-18b), 2.68 (1H, d, *J* = 14.6 Hz, H-20b), 2.39 (1H, dt, *J* = 14.4, 4.2 Hz, H-15a), 1.92 – 1.85 (2H, m, H-17), 1.79 – 1.70 (2H, m, OCH_2C*H*$_2CH_2CH_3$), 1.56 – 1.38 (4H, m, O(CH_2)$_2$C*H*$_2CH_3$, H-13, H-15b), 0.99 – 0.90 (3H, m, CH_3);^{13}C NMR (101 MHz, $CDCl_3$) δ 159.2 (C, C=O), 149.5 (C, C=N), 142.7 (C, C-5), 139.5 (C, C-21), 133.1 (C, C-6), 129.4 (C, C-3), 127.4 (CH, C-22), 125.2 (C, C-1), 122.1 (C, C-4), 116.6 (C, C-1), 77.3 (CH_2, O*C*H$_2$(CH_2)$_2CH_3$), 76.3 (CH, C-12), 66.5 (CH_2, C-23), 60.1 (CH, C-16), 58.6 (CH, C-8), 53.5 (C, C-7), 52.8 (CH_2, C-20), 49.9 (CH_2, C-18), 45.8 (CH, C-13), 43.3 (CH_2, C-17), 32.8 (CH, C-14), 30.6 (CH_2, CH_2C*H*$_2CH_2CH_3$), 27.1 (CH_2, C-15), 19.5 (CH_2, O(CH_2)$_2$C*H*$_2CH_3$), 14.1 (CH_3, CH_3) ESI MS *m/z* 419.4 $[M]^+$; mp 121 ^{0}C; *anal.* C 71.32, H 6.52, N 9.72%, calcd for $C_{25}H_{29}N_3O_3$ C 71.58, H 6.97, N 10.02%.

***(E)*-11-(Isobutyloxyimino)strychnine (8d)** (30mg, 5.5%) was obtained from **1** and 1-bromo-2-methylpropane (0.04 mL)) in the presence of KI (1 mg) as white solid; ^{1}H NMR (400 MHz, $CDCl_3$) δ 4.13 – 4.08 (2H, m, OC*H*$_2$CH(CH_3)$_2$), 2.02 (1H, m, OCH_2C*H*(CH_3)$_2$)), 0.91 (6H,dd, *J* = 6.6, 5.8 Hz, OCH_2CH(C*H*$_3$)$_2$)), *δ* and *J*-values for all other hydrogen atoms coincide with the values for the corresponding atoms of **8c** within ±0.04 ppm and ± 0.1 Hz, respectively; ^{13}C NMR (100 MHz, $CDCl_3$) δ

83.0 (CH_2, O*C*H_2CH(CH_3)$_2$), 28.7 (CH, OCH$_2$*C*H(CH_3)$_2$), 19.2 (CH_3, OCH$_2$CH(*C*H_3)$_2$), chemical shifts for all other carbon atoms coincide with the δ values for the corresponding atoms of **8c** within ±0.1 ppm; ESI MS *m/z* 419.5 $[M]^+$; mp 121 ^{0}C; *anal.* C 71.42, H 6.66, N 9.78%, calcd for $C_{25}H_{29}N_3O_3$ C 71.58, H 6.97, N 10.02%.

***(E)*-11-(Benzyloxyimino)strychnine (8e)** (45mg, 9%) was obtained from **1** and benzylbromide (0.04 mL)) as white solid; eluate for column chromatography CH_2Cl_2-MeOH (100 : 7), ^{1}H NMR (400 MHz, $CDCl_3$) δ 7.43 – 7.32 (5H, m, $CH_2C_6H_5$), 5.57 (1H, d, *J* = 12.3 Hz, HC*H*C_6H_5), 5.43 (1H, d, *J* = 12.3 Hz, *H*CHC_6H_5),), *δ* and *J*-values for all other hydrogen atoms coincide with the values for the corresponding atoms of **8c** within ±0.04 ppm and ± 0.1 Hz, respectively; ^{13}C NMR (100 MHz, $CDCl_3$) δ 136.9 (C, CH_2C_{ar}), 128.7 (CH, 2x CH_2C*C*H_{ar}), 128.2 (C, CH_2*C*CHCHCH_{ar}), 128.1 (CH, 2x CH_2*C*CHCH_{ar}); chemical shifts for all other carbon atoms coincide with the δ values for the corresponding atoms of **8c** within ±0.1 ppm; ESI MS *m/z* 453.4 $[M]^+$; mp 144 ^{0}C; *anal.* C 73.53, H 5.88, N 8.77%, calcd for $C_{28}H_{27}N_3O_3$ C 74.15, H 6.00, N 9.26%.

***(E)*-11-(Pentyloxyimino)strychnine (8f) (**100 mg, 18%) was obtained from **1** and *n*-pentyl bromide (0.04 mL) in the presence of KI (1 mg) as white solid, ^{1}H NMR (400 MHz, $CDCl_3$) δ 4.43 – 4.32 (2H, m, OC*H*$_2$(CH_2)$_3$$CH_3$), 1.73 (2H, m, OCH$_2$C*H*$_2$($CH_2$)$_2$$CH_3$), 1.40 – 1.31 (4H, m, OCH$_2$CH$_2$(C*H*$_2$)$_2$$CH_3$), 0.92 – 0.86 (3H, m, O(CH_2)$_4$$CH_3$) *δ* and *J*-values for all other hydrogen atoms coincide with the values for the corresponding atoms of **8c** within ±0.04 ppm and ± 0.1 Hz, respectively; ^{13}C NMR (100 MHz, $CDCl_3$) δ 76.9 (CH_2, O*C*H_2(CH_2)$_3$$CH_3$), 29.0 ($CH_2$, OCH$_2$*C*$H_2$($CH_2$)$_2$$CH_3$), 28.1 ($CH_2$, O($CH_2$)$_2$*C*$H_2CH_2CH_3$), 22.4 ($CH_2$,O($CH_2$)$_3$*C*$H_2CH_3$), 14.1 ($CH_3$, *C*$H_3$), chemical shifts for all other carbon atoms coincide with the δ values for the corresponding atoms of **8c** within ±0.1 ppm; ESI MS *m/z* 433.5 $[M]^+$; mp 109 ^{0}C; *anal.* C 73.53, H 5.88, N 8.77%, calcd for $C_{26}H_{31}N_3O_3$ C 73.40, H 5.80, N 8.69%.

***(E)*-11-[(Phenylethyl)imino]strychnine (8g) (**33 mg, 6%) was obtained from **1** and 2-phenylethyl bromide (0.044 mL) as white solid, eluate for column chromatography CH_2Cl_2-MeOH (100 : 7), ^{1}H NMR (400 MHz, $CDCl_3$) δ 7.30 – 7.09 (5H, m, $CH_2C_6H_5$), 4.69 – 4.55 (2H,m, $OCH_2CH_2C_6H_5$), 3.12 – 3.04 (2H, m, $OCH_2CH_2C_6H_5$),) δ and *J*-values for all other hydrogen atoms coincide with the values for the corresponding atoms of **8c** within ±0.02 ppm and ± 0.1 Hz, respectively; ^{13}C NMR (100 MHz, $CDCl_3$) δ 138.6 (C, CH_2C_{ar}), 129.3 (CH, 2x CH_2CCH_{ar}), 129.2 (C, $CH_2CCHCHCH_{ar}$), 128.6 (CH, 2x CH_2CCHCH_{ar}); 77.6 (CH_2, $OCH_2CH_2C_6H_5$), 35.7 (CH_2, $OCH_2CH_2C_6H_5$), chemical shifts for all other carbon atoms coincide with the δ values for the corresponding atoms of **8c** within ±0.1 ppm; ESI MS *m/z* 467.6 $[M]^+$; mp 189 ^{0}C; *anal*. C 73.74, H 6.61, N 8.58%, calcd for $C_{29}H_{29}N_3O_3$, C 74.50, H 6.25, N 8.99%.

***(E)*-11-(Allyloxyimino)strychnine (8h) (**45 mg, 9%) was obtained from **1** and allyl bromide (0.03 mL) as pale yellow solid, ^{1}H NMR (400 MHz, $CDCl_3$) δ 6.10 – 6.00 (1H, m, $CH=CH_2$), 5.39 (1H,ddd, *J* = 17.3, 3.2, 1.6 Hz, $CH=CHH$), 5.27 (1H, dd, *J* = 10.5, 1.4 Hz, $CH=CHH$), 4.98 – 4.86 (2H, m, $CH_2CH=CH_2$), δ and *J*-values for all other hydrogen atoms coincide with the values for the corresponding atoms of **8c** within ±0.04 ppm and ± 0.1 Hz, respectively; ^{13}C NMR (100 MHz, $CDCl_3$) δ 133.2 (CH, $CH=CH_2$), 118.6 (CH_2, $CH=CH_2$), 77.9 (CH_2, $CH_2CH=CH_2$), chemical shifts for all other carbon atoms coincide with the δ values for the corresponding atoms of **8c** within ±0.1 ppm; ESI MS *m/z* 402.4 $[M-1]^+$; mp 161 ^{0}C; *anal*. C 70.42, H 6.30, N 9.70%, calcd for $C_{24}H_{25}N_3O_3$, C 71.44, H 6.25, N 10.41%.

***(E)*-11-(Propargyloxyimino)strychnine (8i) (**130 mg, 25%) was obtained from **1** and propargyl chloride (0.023 mL) the presence of KI (1 mg) as pale brown solid. ^{1}H NMR (400 MHz, $CDCl_3$) δ 4.95 – 4.92 (3H, m, $CH_2C{\equiv}CH$, H-12), 2.47 (1H, t, *J* = 2.4 Hz, $C{\equiv}CH$), δ and *J*-values for all other hydrogen atoms coincide with the values for the corresponding atoms of **8c** within ±0.04 ppm and ± 0.1 Hz, respectively; ^{13}C NMR (100 MHz, $CDCl_3$) δ 78.5 (CH, $C{\equiv}CH$), 63.9 (CH_2,

CH_2C≡CH), chemical shifts for all other carbon atoms coincide with the δ values for the corresponding atoms of **8c** within ±0.1 ppm; ESI MS *m/z* 401.4 $[M]^+$; mp 148 ^{0}C; *anal*. C 71.42, H 6.12, N 10.06%, calcd for $C_{24}H_{23}N_3O_3$, C 71.80, H 5.77, N 10.47%.

***(E)*-11-[(Methoxycarbonylmethyl)oxyimino]strychnine (8j) (**130 mg, 23%) was obtained from **1** and methyl bromoacetate (0.03 mL) as pale brown solid. ^{1}H NMR (400 MHz, $CDCl_3$) δ 4.99 (1H, d, *J* = 16.5 Hz, C*H*HCO_2CH_3), 4.90 (1H, d, *J* = 16.5 Hz, CH*H*CO_2CH_3), 3.74 (3H, s, OC*H*$_3$), *δ* and *J*-values for all other hydrogen atoms coincide with the values for the corresponding atoms of **8c** within ±0.02 ppm and ± 0.1 Hz, respectively; ^{13}C NMR (100 MHz, $CDCl_3$) δ 169.3 (C, *C*$OOCH_3$), 72.2 (CH_2, *C*$H_2CO_2CH_3$), 52.2 (CH_3, OCH_3), chemical shifts for all other carbon atoms coincide with the δ values for the corresponding atoms of **8c** within ±0.1 ppm; ESI MS: *m/z* 435.4 $[M]^+$; mp 233 ^{0}C; *anal*. C 65.48, H 6.24, N 9.58%, calcd for $C_{24}H_{25}N_3O_5$, C 66.19, H 5.79, N 9.65%.

***(E)*-11-[(Methoxycarbonylbutyl)oxyimino]strychnine (8k) (**100 mg, 16%) was obtained from **1** and methyl 5-bromovalerate (0.05 mL) as white solid. ^{1}H NMR (400 MHz, $CDCl_3$) δ 4.42 – 4.30 (2H, m, OC*H*$_2$$(CH_2)_3CO_2CH_3$), 3.64 (3H, s, OCH_3), 2.39 – 2-33 (2H, m, O$(CH_2)_3$C*H*$_2CO_2CH_3$), 1.78 -1.72 (2H, m, OCH_2C*H*$_2$$(CH_2)_2CO_2CH_3$), 1.48 – 1.44 (2H, m, O$(CH_2)_3$C*H*$_2CO_2CH_3$), *δ* and *J*-values for all other hydrogen atoms coincide with the values for the corresponding atoms of **8c** within ±0.02 ppm and ± 0.1 Hz, respectively; ^{13}C NMR (100 MHz, $CDCl_3$) δ 174.0 (C, *C*$OOCH_3$), 76.9 (CH_2, O*C*$H_2$$(CH_2)_3CO_2CH_3$), 51.5 ($CH_3$, OCH_3), 43.4 (CH_2, O$(CH_2)_3$*C*$H_2CO_2CH_3$), 27.2 (OCH_2C*H*$_2$$(CH_2)_2CO_2CH_3$), 21.5 ($CH_2$, O$(CH_2)_3$C*H*$_2CO_2CH_3$), chemical shifts for all other carbon atoms coincide with the δ values for the corresponding atoms of **8c** within ±0.1 ppm; ESI MS: *m/z* 477.5 $[M]^+$; mp 115 ^{0}C; *anal*. C 67.81, H 6.43, N 9.58%, calcd for $C_{24}H_{25}N_3O_5$, C 67.91, H 6.54, N 9.48%.

FLIPR™ Membrane Potential Blue assay. The functional characterization of the strychnine analogues was performed in the *FLIPR*™ Membrane Potential Blue assay (Molecular Devices).[25] The tsA201 cells were maintained in Dulbecco's Modified Eagle Medium + Glutamax™-I, supplemented with 10% foetal bovine serum, 100 units/ml penicillin and 100 µg/ml streptomycin at 37 °C in a humidified 5% CO_2 atmosphere. The cells were split into 10 cm (2×10^6 cells) tissue culture plates and transfected the following day with a total of 8 µg cDNA using Polyfect® Transfection Reagent according to the protocol of the manufacturer (Qiagen, Hilden, Germany). The following day, the cells were split into poly-D-lysine-coated black 96-wells plates with clear bottom (BD Biosciences, Bedford, MA). 16-24 h later the medium was aspirated, and the cells were washed with 100 µl Krebs buffer [140 mM NaCl/4.7 mM KCl/2.5 mM $CaCl_2$/1.2 mM $MgCl_2$/11 mM HEPES/10 mM D-Glucose, pH 7.4]. 50 µl Krebs buffer was added to the wells (in the antagonist experiments, various concentrations of the antagonist were dissolved in the buffer) and then an additional 50 µl Krebs buffer supplemented with the FMP assay dye (1 mg/ml) was added to each well. Then the plate was incubated at 37 °C in a humidified 5% CO_2 incubator for 30 min and then assayed in a FlexStation3 Benchtop Multi-Mode Microplate Reader (Molecular Devices) measuring emission at 565 nm [in fluorescence units (FU)] caused by excitation at 525 nm a total of 90 sec before and after addition of 33 µl agonist solution in Krebs buffer. The experiments were performed in duplicate at least three times for each compound at each receptor using an EC_{50} (EC_{40}-EC_{60}) concentration of glycine as agonist.

Single-cell patch-clamp assay. The direct activity of strychnine derivatives on GlyR ion channel function was assessed using whole cell patch-clamp recording techniques. HEK293 cells were grown in 10 cm tissue culture Petri dishes in MEM (Sigma, Deisenhofen, Germany) supplemented with 10 % FBS (Invitrogen, Karlsruhe, Germany) and 5000 i.u. Penicillin/Streptomycin at 5 % CO_2 and 37 °C in a water saturated atmosphere. For experiments, cells were plated on poly-L-lysine

treated glass coverslips in 6 cm dishes. Transfection was performed 1 day after cell passage using Gen-Carrier (Epoch Lifesciences, Sugarland, TX, USA): 1.3 µg of receptor cDNA, 1.3 µg of green fluorescence protein cDNA and 2.6 µl of GenCarrier were used, following the manufacturer's instructions. Measurements were performed 2 to 4 days after transfection.

Current responses from GlyR-transfected HEK293 cells were measured at room temperature (21°C – 23°C) at a holding potential of -50 mV. Whole-cell recordings were performed using a HEKA EPC10 amplifier (HEKA Electronics, Lambrecht, Germany) controlled by Pulse software (HEKA Electronics). Recording pipettes were pulled from borosilicate glass tubes (World Precision Instruments, Berlin, Germany) using a Sutter P-97 horizontal puller (Sutter, Novato, CA). Solutions were applied using an Octaflow system (NPI electronics, Tamm, Germany), where cells were bathed in a laminar flow of buffer, giving a time resolution for solution exchange and re-equilibration of about 100 ms. The external buffer consisted of 135 mM NaCl, 5.5 mM KCl, 2 mM $CaCl_2$, 1.0 mM $MgCl_2$, and 10 mM Hepes (pH adjusted to 7.4 with NaOH); the internal buffer was 140 mM CsCl, 1.0 mM $CaCl_2$, 2.0 mM $MgCl_2$, 5.0 mM EGTA, and 10 mM Hepes (pH adjusted to 7.2 with CsOH). Dose-response curves for GlyR activation by glycine were calculated from a fit to the Hill equation $\frac{I_{glycine}}{I_{sat}} = \frac{[Glycine]^{nHill}}{[Glycine]^{nHill} + EC_{50}{}^{nHill}}$ using a nonlinear algorithm in Microcal Origin (Additive, Friedrichsdorf, Germany). Here, $I_{glycine}$ is the current amplitude at a given glycine concentration, I_{sat} is the maximum current amplitude at saturating concentrations of glycine, EC_{50} is the glycine concentration at half-maximal current responses, and *n*Hill is the Hill coefficient. Currents from each individual cell were normalized to the maximum response at saturating glycine concentrations. Inhibition curves were determined from varying the concentration of strychnine derivatives in the presence of 50 □M glycine (ca. EC_{50}) using 4 to 5 cells per each inhibitor. IC_{50} values were determined from inhibition curves constructed using a non-linear fit to the equation $I_{obs} = I_{max} / [1 + ([I]/IC_{50})]$, where

I_{obs} is the observed current at any given concentration of inhibitor, I_{max} is the maximum current amplitude observed in the absence of inhibitor, and [I] is the concentration of inhibitor. In all experiments EC_{50} values were determined for each individual cell from a non-linear fit of dose response data to the logistic equation (above). All data are given as means ± SEM.

Radioligand binding studies

Cell line and transfection. Transiently transfected tsA201 (=HEK293) cells hold in Dulbecco's Modified Eagle Medium + Glutamax™-I (2 mM), supplemented with 10% foetal bovine serum, 1 mM sodium pyruvate, 1% Pen/Strep at 37 °C in a humidified 5% CO_2 atmosphere were used for the experiments. Cells were transfected with a modified calcium phosphate precipitation method (10 µg plasmid GlyR α1 DNA, 50 µl 2.5 M $CaCl_2$, 440 µl 0.1 x TE-buffer, 500 µl HBS-transfection buffer (50 mM HEPES, 12 mM dextrose, 10 mM KCl, 28 mM NaCl, 1.5 mM Na_2HPO_4, pH 6.95), mixed, incubated for 20 min at room temperature, drop-wise given to cells), washed with medium 12 h post-transfection. Following 48 h post-transfection, cells were harvested.

Membrane protein preparation - Cell pellets from transfected cells were homogenized in potassium phosphate buffer (buffer H = 10 mM potassium phosphate, pH 7.4, protease inhibitor tablet complete, Roche, Mannheim, Germany). Following homogenization, protein suspension was centrifuged at 30.000 x g for 20 min. After a repeating step of homogenization and centrifugation, the membrane pellet was resuspended in buffer B (25 mM potassium phosphate, 200 mM KCl). GlyR α1 expression was verified using immunostaining with a pan- antibody following Western blotting.

Radioligand-binding assay. 80 µg of GlyR protein have been used for sample preparation in a radioligand-binding assay. In order to determine the binding

affinities of the strychnine analogues, all compounds have been diluted to concentrations of 10.000, 3.000, 1.000, 300, 100, 30, 10, 1, 0.3 nM and incubated with 80 µg of GlyR protein for 30 min on ice (all data points were done in triplicates). 9.6 nM [^{3}H] strychnine was added and incubated with the suspension for additional 30 min on ice. The suspension was filtered through GC/F glass microfiber filters (preincubated in buffer B + 0.5% BSA) and washed twice with buffer B, dried and resuspended in scintillation liquid. All samples were analysed in a Tri-Carb Liquid Scintillation Counter (Perkin Elmer, Rodgau, Germany).

Molecular Modeling

Molecular Structure preparation. The 3D coordinates for the α1 GlyR in a complex with strychnine reported by Du *et. al*.[13] were retrieved from the RCSB Protein Data Bank (http://www.rcsb.org, reference code 3JAD). Only protein molecules were used for the docking, while all non-protein moieties were discarded. The 3D coordinates for strychnine have been obtained from PubChem (https://pubchem.ncbi.nlm.nih.gov/; CID 441071). The 3D structures of compounds **2** and **8i** were generated based on the X-ray crystallography structure of strychnine[33] using a conformational searching method implemented in Tridant™.[34] For the visualization of molecular structures UCSF Chimera software was employed.[35]

Molecular Docking

To examine the binding modes of strychnine derivatives to GlyR, molecular docking was performed using the AutoDock software (version 4.2.6, available at http://autodock.scripps.edu). The AutoDock Tools (ADT) were used to generate input parameter files for docking. For the current study the protein was considered as a rigid molecule, while ligands contained rotatable bonds. The volume of the grid box was set as 60 x 60 x 60 with a 0.375 Å spacing (default value). The centre of the grid box was placed so that it included the important amino acids responsible for strychnine binding (Phe223 Phe79 Phe115 Phe175 Ser145 Gly176 Tyr218 Arg81 and Thr220) (see Figure 1). The number of docking runs was fixed to 50.

Acknowledgements. This work was partially funded by Bundesministerium für Bildung und Forschung (BMBF) and Deutscher Akademischer Austauschdienst (DAAD). A. A. J. thanks the Novo Nordisk Foundation for financial support.

Supporting Information. ^{1}H and ^{13}C NMR spectra of compounds **2,3, 5-7**, **8a-8k**. Displacement curves for [^{3}H]strychnine binding experiments of compounds **1**, **3**, **8a**, **8b**, and **8h.** This material is available free of charge via the Internet at http://pubs.acs.org.

REFERENCES

1. Lynch, J.W. Molecular structure and function of the glycine receptor chloride channel. *Physiol Rev* **2004**, 84, 1051–1095.
2. Laube, B.; Maksay, G.; Schemm, R.; Betz, H. Modulation of glycine receptor function: a novel approach for therapeutic intervention at inhibitory synapses *Trends Pharmacol Sci* **2002**, 23,519–527.
3. Jensen, A. A.; Kristiansen, U. Functional characterisation of the human alpha1 glycine receptor in a fluorescence-based membrane potential assay *Biochem Pharmacol* **2004**, 67, 1789–1799.
4. Lynch, J.; Callister, R. Glycine receptors: a new therapeutic target in pain pathways *Curr Opin Invest Drugs* **2006**, 7, 48−53.
5. Breitinger, H. G. Glycine Receptors **2014** In: eLS. *John Wiley & Sons* Ltd, Chichester.http://www.els.net.[doi:10.1002/9780470015902.a0000236.pub]
6. Breitinger, H. G.; Becker, C. M. The inhibitory glycine receptor: prospects for a therapeutic orphan *Curr Pharm Design* **1998**, 4, 315-334.
7. Bode, A.; Lynch, J. The impact of human hyperekplexia mutations on glycine receptor structure and function *Mol Brain* **2014**, 7, 2.

8. Schaefer, N.; Langlhofer, G; Kluck, C. J.; Villmann, C. Glycine receptor mouse mutants: model systems for human hyperekplexia. *Br J Pharmacol* **2013**, 170, 933–952.
9. Langosch, D.; Thomas, L.; Betz, H. Conserved quaternary structure of ligand-gated ion channels: the postsynaptic glycine receptor is a pentamer. *Proc Natl Acad Sci U.S.A.* **1988**, 85, 7394−7398.
10. Watanabe, E.; Akagi, H. Distribution patterns of mRNAs encoding glycine receptor channels in the developing rat spinal cord. *Neurosci Res* **1995**, 23, 377−382.
11. Lynch J. W. Native glycine receptor subtypes and their physiological roles. *Neuropharmacol* **2009**, 56, 303-309.
12. Yu, R.; Hurdiss, E.; Greiner, T.; Lape, R.; Sivilotti, L.; Biggin, P. C. Agonist and antagonist binding in human glycine receptors. *Biochemistry* **2014**, 53, 6041-6051.
13. Du, J.; Lü, W.; Wu, S.; Cheng, Y.; Gouaux, E. Glycine receptor mechanism elucidated by electron cryo-microscopy. *Nature* **2015**, 526, 224-229.
14. Huang, X.; Chen, H.; Michelsen, K.; Schneider, S.; Shaffer, P. L. Crystal structure of human glycine receptor-alpha3 bound to antagonist strychnine. *Nature* **2015**, 526, 277-280.
15. Mackerer, C. R.; Kochman, R. L.; Shen, T. F.; Hershenson, F. M. *J.* The binding of strychnine and strychnine analogs to synaptic membranes of rat brainstem and spinal cord. *Pharmacol Exp Ther* **1977**, 201, 326-331.
16. Iskander, G. M.; Bohlin, L. Structure-activity relationship of strychnine derivatives modified in the non-aromatic part. *Acta Pharm Suec* **1978**, 15, 431-438.
17. Jensen, A. A.; Gharagozloo, P.; Birsdall, N. J. M.; Zlotos, D. P. Pharmacological characterisation of strychnine and brucine analogues at glycine and alpha7 nicotinic acetylcholine receptors. *Eur J Pharmacol* **2006**, 539, 27-33.

18. Mohsen, A. M. Y.; Heller, E.; Holzgrabe, U.; Zlotos, D. P. Structure-activity relationships of strychnine analogs at glycine receptors. *Chem Biodiversity* **2014**, 11, 1256-1262.
19. Warnat, H. Über drei neue Strychnos-alkaloide. *Helv Chim Acta* **1931**, 14, 997-1007.
20. Bisset, N. G.; Walker, M. D. Alkaloids from the stem bark of Strychnos ignatii. *Phytochemistry* **1974**, 13, 525-526.
21. Zlotos, D. P.; Buller, S.; Stiefl, N., Baumann, K.; Mohr, K. Probing the pharmacophore for allosteric ligands of muscarinic M2 receptors: SAR and QSAR studies in a series of bisquaternary salts of caracurine V and related ring systems. *J Med Chem* **2004**, 47, 3561- 3571.
22. Pingping, T.; Silver-Catalyzed Late-Stage Fluorination. *J Am Chem Soc* **2010**, 132, 12150-12154.
23. Gharagozloo, P.; Lazareno, S.; Popham, A.; Birdsall, N. J. M. Allosteric interactions of quaternary strychnine and brucine derivatives with muscarinic acetylcholine receptors. *J Med Chem* **1999**, 42, 438- 445.
24. Rosenmund, P.; Schmitt, M-P.; Franke, H. Vomicin aus Strychnine. *Liebigs Ann Chem* **1980,** 6**,** 895-907
25. Jensen, A. A. Functional characterisation of human glycine receptors in a fluorescence-based high throughput screening assay. *Eur J Pharmacol* **2005**, 521, 39-42.
26. Jensen, A. A.; Bergmann, M. L.; Sander, T.; Balle, T. Ginkgolide X is a potent antagonist of anionic Cys-loop receptors with a unique selectivity profile at glycine receptors. *J Biol Chem* **2010**, 285, 10141-10153
27. Philippe, G; De Mol, P.; Zeches-Hanrot, M.; Nuzillard, J-M.; Tits, M-H.; Angenot, L.; Frederich, M. Study of the interaction of antiplasmodial strychnine derivatives with the glycine receptor. *Phytochemistry* **2003**, 62, 623-629.

28. Ma, L.; Yang, X-W.; Xu, W.; Cai, B-C.; Hattori, M. *Planta Medica* **2009**, 75, 631-634.
29. Hess G. P. Determination of the chemical mechanism of neurotransmitter receptor-mediated reactions by rapid chemical kinetic techniques. *Biochemistry* **1993**, 32, 989-1000.
30. Breitinger H. G.; Geetha N.: Hess G. P. Inhibition of the serotonin 5-HT_3 receptor by nicotine, cocaine, and fluoxetine investigated by rapid chemical kinetic techniques. *Biochemistry* **2001**, 40**,** 8419-8429
31. Raafat, K.; Breitinger, U.; Mahran, L.; Ayoub, N.; Breitinger, H.-G. Synergistic inhibition of glycinergic transmission in vitro and in vivo by flavonoids and strychnine. *Toxicol Sci* **2010,** 118, 171-182.
32. *AutoDock* version 4.2.6. http://autodock.scripps.edu
33. Mostad, A. Structural study of the strychnine molecule in crystals of the free base and of the nitric acid complex. *Acta Chemica Scandinavica*b **1985**, B39, 705-716.
34. Tridant V. Wavefunction, Inc. Irvine, CA 92612, USA, **2006**
35. Pettersen, E. F.; Goddard, T. D.; Huang, C. C.; Couch, G. S.; Greenblatt, D. M.; Meng, E. C.; Ferrin, T. E. UCSF Chimera--a visualization system for exploratory research and analysis. *J Comput Chem* **2004**, 25, 1605−1612.

4.3. Dimeric Strychnine Analogs as Bivalent Ligands Targeting Glycine Receptors

Abstract A series of C11-linked dimeric strychnine analogs as well as *(R)*-11-aminostrychnine and *(R)*-strychnine-11-yl propionamide were synthesized and pharmacologically evaluated at human α1 and α1β glycine receptors transiently expressed in tsA201 cells in the FLIPR™ Membrane Potential Blue Assay. The strychnine dimers were designed to bind simultaneously to two α-subunits of the pentameric receptors and increase receptor affinity and potency. All the synthesized dimeric compounds displayed comparable antagonist potencies at the two receptor subtypes and none of them was superior to strychnine. Compound **4e** that contains a 10 carbons spacer is as potent as strychnine. These findings suggest that only one strychnine molecule of the dimeric strychnine analogs can bind to the receptor.

Introduction

The inhibitory glycine receptor is potently and selectively inhibited by the natural alkaloid strychnine. Binding of strychnine to GlyR results in the blocking of the Cl^- ion channel thereby inhibition of Cl^- ions permeation. This results in reducing GlyR-mediated inhibition and thus causes overexcitation of spinal motor and sensory neurons.[1] Being a competitive antagonist, strychnine and glycine bind to the same binding site, enabling interaction with the ligand binding site. The bulk of the strychnine molecule is thought to block the ion channel.[2] Glycine receptors are ligand gated ion channels that are present in the spinal cord and brain stem where they are mainly involved in the regulation of motor functions. Additionally, they are found in sensory pathways of the spinal cord, including pain fibers, as well as the auditory and visual system.[2-4] GlyRs topology and the amino acid composition of GlyR subunits classify this receptor as a member of the Cys–loop receptors. They are named Cys-loop receptors for the extracellular domain (ECD) of each subunit, as it possess a characteristic 13-residue loop formed by a disulfide bond between two cysteine (Cys) residues.[5-7] GlyR complex is composed of two glycosylated integral membrane proteins of 48 kDa (α) and 58 kDa (β) and a peripheral membrane protein of 93 kDa (gephyrin). There are four known isoforms of the α-subunit (α1 -4) of GlyR while there is a single β-subunit. Glycine receptors can be homomeric that include only α subunits or heteromeric which contains both α and β subunits.[3, 8, 9]

For a long time, the knowledge of the molecular mechanism of GlyRs inactivation by strychnine were insufficient due to the lack of high-resolution structures of the receptor. Up till recently, only homology models based on structures of other Cys-loop receptors have been available. In 2015, 3.0 Å X-ray structure of the human glycine receptor-α3 homopentamer in complex with the high affinity, high-specificity antagonist strychnine, as well as electro cryo-microscopy structures of the zebra fish α1-GlyR in complex with strychnine and glycine were published.[4,5] Such information provided detailed insight into the molecular

recognition of agonists and antagonists and mechanisms of GlyR activation and inactivation. This will consequently allow exploration of the binding modes of antagonists on glycine receptors.

A highly attractive approach to investigate receptor dimerization might be the utilization of bivalent ligands. Generally, bivalent ligands contain two pharmacophoric units separated by an appropriately designed spacer to connect them. It is expected that duplication of the pharmacophoric groups according to the bivalent ligand approach leads to a supra-additive increase in potency compared to the corresponding monovalent ligand. When designed as strychnine dimers, they should be able to bind simultaneously to two α-subunits of the pentameric receptors, causing a possibly stronger inhibition compared to the monomeric strychnine.[10-14]

Various approaches to the synthesis of dimeric strychnine analogs were examined. It was of interest at first to explore the synthesis of bivalent ligands starting from 11-*(E)*-isonitrosotrychnine which was previously reported to have a twicely increased in binding to both α1 and α1β glycine receptors.[15] The oxime hydroxyl group was chosen as a point of attachment of a spacer to connect two molecules of isonitrostrychnine at C11. These approaches were unsuccessful for a wide range of attempted direct o-alkylation reactions of two molecules of isonitrososstrychnine using dialkylhalides. The failure of all of these reactions was ascribed to the highly basic tertiary nitrogen in strychnine which is very reactive and is easily quaternized with alkylhalides. The quaternary strychnine derivatives were reported to be inactive at both glycine receptor subtypes.[15] Further attempts in the synthesis of bivalent analogs through formation of oxime ester functional group connecting two 11-*(E)*-isonitrostrychnine molecules and diacids were unsuccessfull too.

Very recently, a series of dimeric strychnine analogs obtained by diamide formation of two molecules of 2-aminostrychnine with dicarboxylates of different chain lengths was pharmacologically evaluated at human α1 and α1β glycine

receptors in a functional fluorescence-based assay, in a whole cell patch-clamp assay, and in [^{3}H]strychnine binding studies. None of the synthesized bivalent compounds was found to be superior to strychnine,[16] therefore there is a need to explore other possible attachment points in order to connect two strychnine molecules with a spacer more properly.

In the present study, a newly developed method for the synthesis of a series of bivalent strychnine ligands formally obtained from 11-(*E*)-isonitrosostrychnine **1** by reduction of the oxime functional group to the corresponding amine **2** followed by coupling of the amine with the diacids is described. To examine the optimal spacer length for bridging the ion channel, a series of ligands with different lengths of the spacer 2-12 **(4a-f)** has been prepared. Moreover, the monomeric reference compound, *(R)*-strychnine-11-yl propionamide **3,** whose structure represents half the molecule of the bivalent compound **4b** has been synthesized and pharmacologically evaluated (Figure 1).

Figure 1. Structural Formulas of Strychnine and its Analogs **1-3, 4a-f**

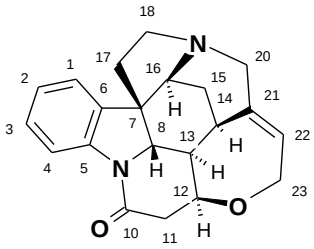

Strychnine

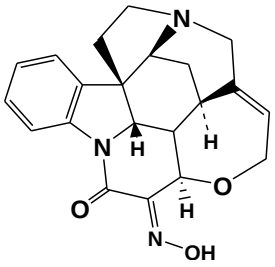

11-*(E)*-Isonitrososstrychnine 1

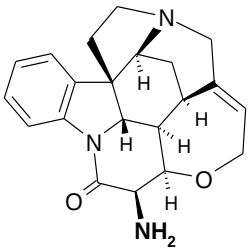

***(R)*-11-aminostrychnine (2)**

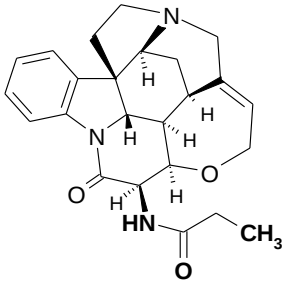

***(R)*-strychnine-11-yl propionamide (3)**

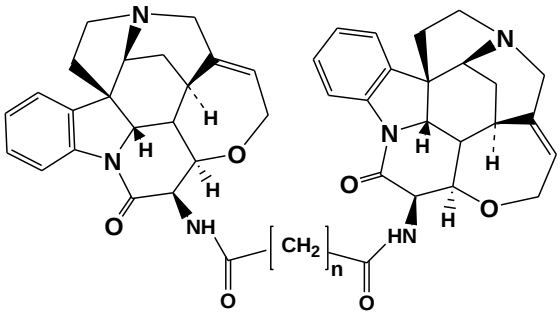

n= 2, 4a
n=4, 4b
n=6, 4c
n=8, 4d
n=10, 4e
n=12, 4f

Bivalent ligands

Results and discussion

The synthesis of the bivalent strychnine analogs studied in this work is shown in Scheme 1. Such dimeric strychnine analogs were designed by linking two strychnine molecules through amino groups in position 11. 11-(*E*)-isonitrosostrychnine **1** was obtained by nitrosation of strychnine using *tert*-butyl nitrite/*tert*-BuOK as previously reported.[17] The reduction of the oxime group of **1** to give (R)-11-aminostrychnine **2** was achieved using zinc powder and HCl according to earlier published procedure to synthesize 11-aminobrucine.[18] The spacer was then introduced by amide formation between two molecules of **2** and one molecule of aliphatic dicarboxylate of different spacer lengths using 1-[Bis(dimethylamino)methylene]-1H-1,2,3-triazolo[4,5-b]pyridinium 3-oxid hexafluorophosphate (HATU) as a coupling reagent. As the bivalent ligands include amide groups in position 11 of strychnine, the reference monomeric propionamide **3** was prepared too and pharmacologically evaluated.

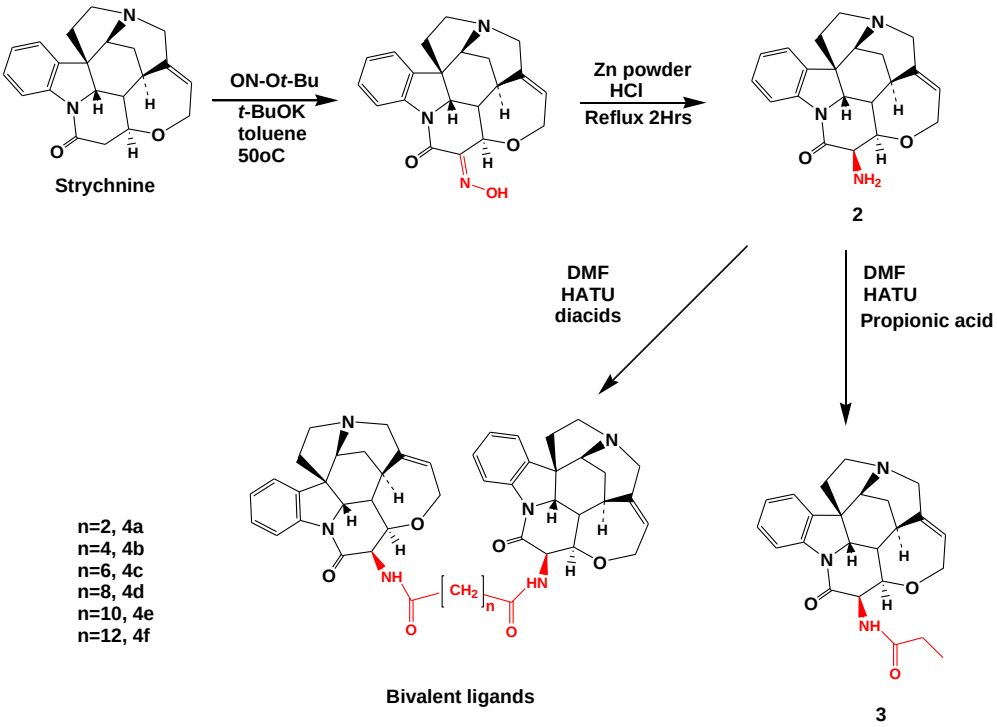

Scheme 1: Synthetic plan for the bivalent strychnine ligand

Determining the absolute configuration of C-11.

The absolute configuration of C11 in *(R)*-strychnine-11-yl-propionamide was determined by NMR spectroscopy. This was only possible for propionamide and not for the *(R)*-11-aminostrychine due to signal overlapping. The H-11 resonance signal of the propionamide appeared as doublet of doublets at δ 4.80 ppm with coupling constants of 5.1 and 8.3 Hz. H-11 couples with the adjacent H-12 which appeared as doublet signal with coupling constant of 5.1 Hz. These coupling constants indicates cis orientation of H-11 and H-12 hydrogens (Figure 2). The adjacent NH signal appeared at 6.65 ppm as a doublet with coupling constant = 8.3 Hz. These findings confirm that the absolute configuration of C-11 is *(R)*. In the 600 MHz 2D NOESY experiment, a strong NOE between H-11 and H-12 which confirms the orientation (Figure 3).

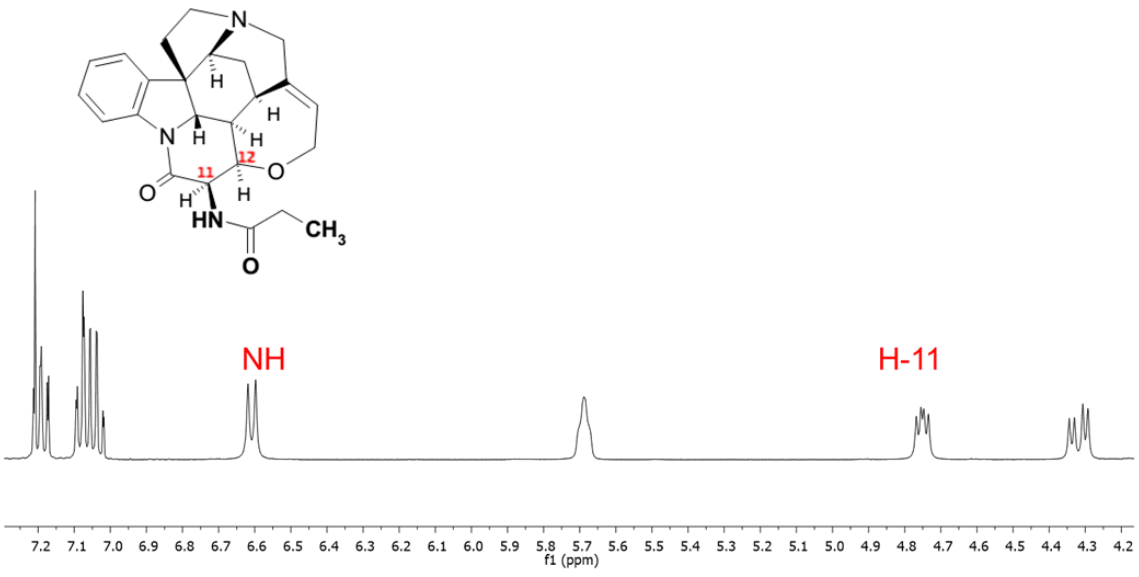

Figure 2 ^{1}H-NMR spectrum (400 MHz, $CDCl_3$) of *(R)*-strychnine-11-yl propionamide

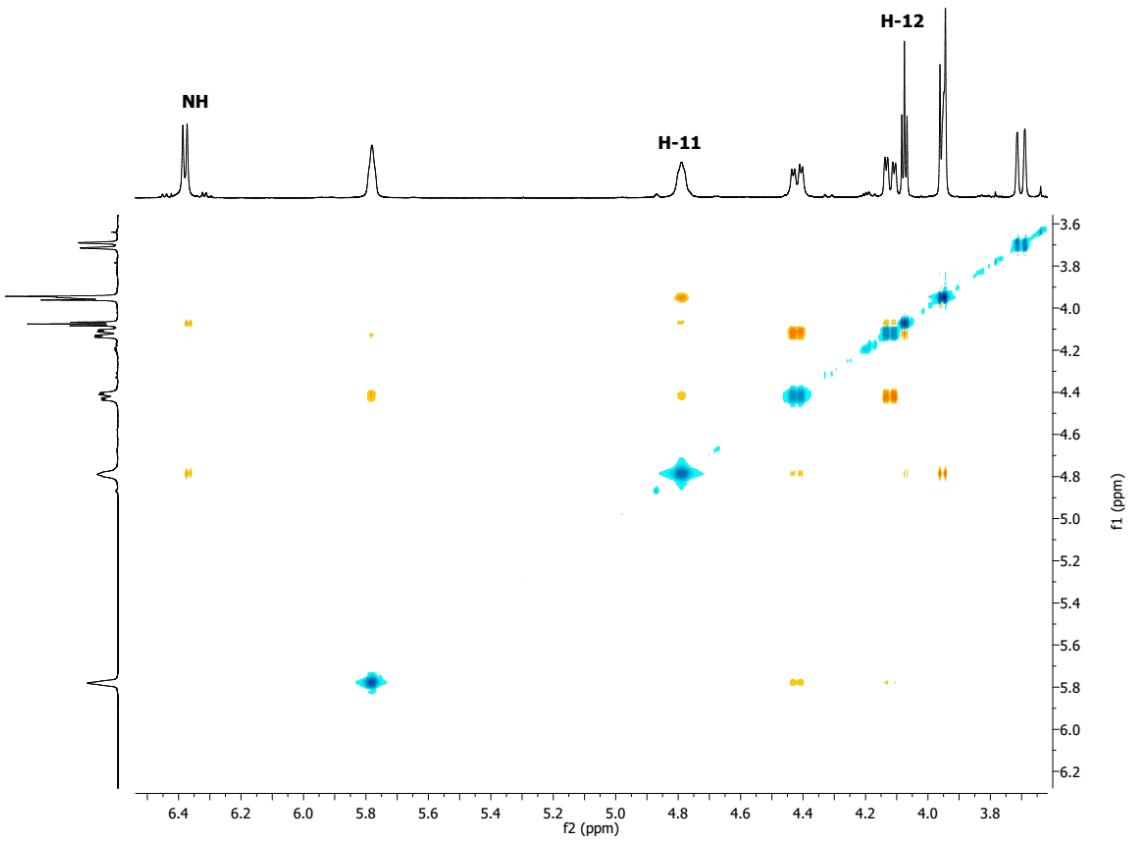

Figure 3: NOESY of *(R)*-strychnine-11-yl propionamide

The functional properties of compounds **2-3, 4a-f** were characterized at the human α1 and α1β receptor subtypes in the fluorescence-based FLIPRTM Membrane Potential Blue (FMP) Assay.[15] Here, the receptors were transiently expressed in tsA201 cells and the abilities of the compounds to inhibit the response induced by glycine EC50 (EC_{40}-EC_{60}) in the cells were determined. The expression of homogenous populations of α1 and α1β receptors in the two cell populations was verified on a routinely basis using picrotoxin, which as previously reported displays 100-fold higher antagonist potency at α1 than at α1β in this assay.[19] The IC_{50} values determined for the compounds are given in Table 1.

Table 1. Pharmacological Characterization of the Compounds at α1 and α1β GlyRs

	α1	α1β
	EC_{50} [pEC_{50} ± S.E.M.]	
Glycine	**42** [4.37 ± 0.02]	**26** [4.59 ± 0.05]
	IC_{50} [pIC_{50} ± S.E.M.] $IC_{50}/IC_{50}^{strychnine}$ (μM)	IC_{50} [pIC_{50} ± S.E.M.] IC_{50}/IC_{50}^{s} (μM)
Strychnine	**0.15** [6.82 ± 0.05] -	**0.51** [6.29 ± 0.05] -
2	**3.8** [5.42 ± 0.03] 4.7	**7.9** [5.10 ± 0.09] 4.3
3	**0.71** [6.15 ± 0.10] 25	**2.2** [5.66 ± 0.04] 15
4a, (n=2)	**0.21** [6.67 ± 0.02] 1.4	**1.2** [5.91 ± 0.08] 2.4
4b, (n=4)	**0.37** [6.43 ± 0.02] 2.5	**1.4** [5.87 ± 0.03] 2.7
4c, (n=6)	**0.42** [6.38 ± 0.02] 2.8	**0.90** [6.04 ± 0.06] 1.8
4d, (n=8)	**0.40** [6.40 ± 0.08] 2.7	**0.96** [6.02 ± 0.11] 1.9
4e, (n=10)	**0.15** [6.82 ± 0.08] 1	**0.68** [6.17 ± 0.09] 1.3
4f, (n=12)	**0.4**3 [6.37 ± 0.05] 2.9	**2.7** [5.56 ± 0.06] 5.3

[a] The concentration-inhibition curve was not completed at concentrations up to 100 μM. The IC_{50} value is estimated from the fitted curve.

The concentration of glycine that gives half-maximal response (effective concentration EC_{50}) and the concentration of the strychnine analogues where the response is reduced by half (inhibitory concentration IC_{50}) are given in μM. The EC_{50} for glycine is determined based on the fitted concentration-response curve based on the determined responses for 8 different concentrations. The IC_{50} values for strychnine and its analogs were determined based on the fitted concentration-inhibition curves of the determined responses measured for glycine (EC_{80}) in the absence or in the presence of eight different antagonist concentrations. In the presence of increasing concentrations of strychnine (or one of the strychnine analogs), this fixed concentration of glycine elicits lower fluorescent responses. The antagonist properties were determined using glycine EC_{70}-EC_{90} as agonist. EC_{80} (a range from EC_{70}-EC_{90}) was used in order to have a robust glycine-induced response to be antagonized by the antagonists. The ratios of the IC_{50} values of compared to the IC_{50} values of strychnine at the respective receptors are given for the sake of comparison.

Previously, the essential structural elements required for strong antagonistic action of strychnine at homo- and heteromeric GlyRs were described to be the lactam carbonyl group, the tertiary amino group as well as the C21=C22 double bond.[15,20,21] All the synthesized compounds bearing the three structural elements displayed antagonist potencies at the two receptor subtypes comparable to strychnine. However, the lack of subtype selectivity is almost the same among the newly synthesized bivalent ligands, as residues essential for strychnine binding are conserved among the α and β subunits of GlyRs.

(R)-11-Aminostrychnine **2** showed a 30 fold and 15 fold lower antagonistic potency compared to strychnine at α1 and α1β, respectively. This is in agreement with the previous findings data indicating that the strychnine binding site at GlyRs may comprise an additional lipophilic pocket that allow interactions with C-11 on strychnine, and the compounds best accommodated in this pocket are those which bear a lipophilic group in C-11. Consequently, *(R)*-11-aminostrychnine, bearing the polar amino group at position 11, shows lower potency than strychnine.

For the acylated *(R)*-11-aminostrychnine analog **3**, the H-bond which was reported to be between the lactam carbonyl group and the Arg residue in the receptor binding site[4] is much weaker. That might be attributed to the reduced electron density on the oxygen atom resulting in approximately 5-fold lower antagonistic potency at both receptor subtypes compared to strychnine.

Regarding, the series of bivalent ligands **4a-f**, a weak correlation between the spacer length and activity was observed. All the dimeric ligands showed non-significant difference in potency to that of strychnine and none of them was superior to strychnine. Moreover, the reference monomeric compound **3** containing an ethylene spacer displayed about 5 fold decrease in potency compared to strychnine. When comparing compound **3** to the dimeric ligand containing double the number of spacer atoms $(CH_2)_4$, a 3-fold increase in potency was observed. The dimer containing $(CH_2)_{10}$ spacer length was found to be equipotent to strychnine. This

similar potency suggests that the "second" strychnine moiety of the dimer might not make any significant contacts with the receptor. Instead, the 'additional' strychnine molecule in the dimer probably protrudes from the orthosteric binding sites of the receptor. This may suggest that these dimers could not be accommodated by the binding site of the GlyR and that only one molecule of strychnine can activate the receptor. In other words, two strychnine molecules cannot simultaneously bind to the receptor.

On the other hand, the role of molecular size in ligand efficiency should also be considered. Ligand efficiency assesses the quality of the ligands (binding energy/non-hydrogen atoms)[23] to make them more effective. When the ligand efficiency of the dimeric derivatives is considered, this will result in a drop in the efficiency of these compounds since they have higher number of non-hydrogen atoms compared to strychnine or the monomer **3**.

As a conclusion, the bivalent compounds will remain an important tools to study the binding interactions within the GlyRs. Other points of attachments or anchor groups may be examined which could result in an increase in the potency. It is also of interest to examine the incorporation of other spacers that have different polarity such as the incorporation of polyamide spacers. This would probably increase the solubility and the pharmacokinetic properties of these compounds.

Experimental section

General Experimental Procedures. Melting points were determined using a capillary melting point apparatus (Gallenkamp, Sanyo) and are uncorrected. Bruker AV-400 spectrometer was used to obtain ^{1}H NMR and ^{13}C NMR spectra, respectively. ^{1}H NMR chemical shifts are referred to $CHCl_3$ (7.26 ppm) and DMSO-d_6 (2.50 ppm). ^{13}C NMR chemical shifts are referred to $CDCl_3$ (77.26 ppm) and DMSO-d_6 (39.52 ppm). The NMR resonances were assigned by means of COSY and HMQC experiments. Mass spectrometric analysis (HPLC-ESI-MS) was performed on a TSQ quantum (Thermo Electron Corporation) instrument equipped with an ESI source and a triple quadrupole mass detector (Thermo Finnigan, San Jose, CA). The MS detection was carried out at a spray voltage of 4.2 kV, a nitrogen sheath gas pressure of 4.0105 Pa, an auxiliary gas pressure of 1.0105 Pa, a capillary temperature of 400 C, capillary voltage of 35 V, and source CID of 10 V. All samples were injected by autosampler (Surveyor, Thermo Finnigan) with an injection volume of 10 µL. A RP C18 NUCLEODUR 100-3 (125 mm x 3 mm) column (Macherey-Nagel) was used as stationary phase. The solvent system consisted of water containing 0.1% aqueous TFA (A) and 0.1% TFA in acetonitrile (B). HPLC-method: flow rate 400 µL/min. The percentage of B started at an initial of 5%, was increased up to 100% during 16 min, kept at 100% for 2 min, and flushed back to the 5% in 2 min. All masses were reported as those of the protonated parent ions. The purity of the tested compounds as determined by HPLC coupled with mass spectroscopy and were higher than 95% purity. All reactions were carried out under an argon atmosphere. Column chromatography was carried out on silica gel 60 (0.063–0.200 mm) obtained from Merck. The NMR data of the strychnine nucleus of all the bivalent ligands is nearly identical. This will be indicated by "chemical shifts and coupling constants for all other hydrogen atoms coincide with the δ values for the corresponding atoms of compound **4a** within ±0.04 ppm and ± 0.1 Hz, respectively" for the ^{1}H NMR and by "chemical shifts for all other carbon atoms

coincide with the δ values for the corresponding atoms of **4a** within ±0.1 ppm" for ^{13}C NMR.

(11*R*)-11-aminostrychnine (2). Zinc powder (6g, 0.1 mole) was added to a suspension of 11-*(E)*-isonitrososstrychnine **1** (600 mg, 1.65 mmole) in EtOH: H_2O (45 mL, 2:1). HCl (1 N) (0.3 mL, 10 mmole) was added dropwise to the suspension and the reaction mixture was stirred at 0 °C. After 2 h, the reaction mixture was heated under reflux for another 2 h. Zinc was filtered over Celite and washed with EtOH, and the solvent was removed under reduced pressure. Water (50 mL) was added to the residue and the medium was neutralized to pH 9 using ammonia (25%). The product was extracted with $CHCl_3$ (5 x 100 mL). The combined organic layers were washed with water and dried over Na_2SO_4 and the solvent was removed in vacuo. The residue was subjected to column chromatography using silica gel (CH_2Cl_2-MeOH-25%NH_3, 100:3:0.3) to give **2** (350 mg, 66 .77%) as yellow solid, mp 237 ^{0}C; ^{1}H NMR (Acetone d_6) δ 8.03 (1H, d, *J* = 7.7 Hz, H-1), 7.39 (1H, d, *J* = 7.0 Hz, H-4), 7.34 – 7.28 (1H, m, H-3), 7.17 (1H, td, *J* = 7.5, 0.9 Hz, H-2), 5.93 (1H, t, *J* = 11.6 Hz, H-22), 4.33 (1H, d, *J* = 4.0 Hz, H-12), 4.14 – 4.09 (2H, m, *J* = 4.6 Hz, H-23), 4.04 - 3.87 (3H, m, *J* = 8.6 Hz, H-8, H-16, H-11), 3.70 (1H, d, *J* = 14.8 Hz, H-20a), 3.28 (1H, s, H-14), 3.19 – 3.10 (1H, m, H-18a), 2.89 (1H, ddd, *J* = 12.2, 10.0, 6.2 Hz, H-18b), 2.72 (1H, d, *J* = 14.8 Hz, H-20b), 2.36 (1H, dt, *J* = 14.3, 4.3 Hz, H-15a), 1.90 – 1.80 (2H, m, H-17), 1.51 – 1.36 (2H, m, H-15b, H-13); ^{13}C NMR (Acetone d_6) δ 167.7 (C, C=O), 142.7 (C, C-21), 140.7 (C, C-5), 133.3 (C, C-6), 128.3 (C, C-3), 127.5 (CH,C-22), 123.9 (C, C-2), 122.7 (C, C-4), 115.9 (C, C-1), 86.1 (CH, C-12), 68.7 (CH, C-11), 63.9 (CH_2, C-23), 60.5 (CH, C-16), 60.2 (CH, C-8), 52.1 (CH_2, C-20), 51.9 (CH_2, C-18), 50.3 (C, C-7), 47.8 (CH, C-13), 42.3 (CH_2, C-17), 31.1 (CH, C-14), 26.4 (CH_2, C-15), ESI MS *m/z* 405.49.

(11*R*)-*N*-(Strychnin-11yl)-propanamide (3) A mixture of propionic acid (2 mmole, 0.14 mL), HATU (700 mg, 2 mmole), DIPEA (0.7 mL, 4 mmole) in dry

dichloromethane (10 mL) was stirred at room temperature for 30 mins. A solution of **1** (350 mg, 1 mmole) in dry dichrolomethane (10 mL) was added and stirred for 12 h. Afterwards, the mixture was diluted with water (50 mL) and the product was extracted with dichloromethane (3x 100). The combined organic layers were dried over Na_2SO_4 and the solvent was removed in vacuo. The residue was subjected to column chromatography using silica gel (CH_2Cl_2-MeOH-25%NH_3,100:5:0.5) to give the corresponding amide **3** (60 mg, 14.8 %) as white solid, mp 188 ^{0}C ; ^{1}H NMR ($CDCl_3$) δ 8.00 (1H, d, *J* = 8.0 Hz, H-1), 7.24 (1H, dt, *J* = 8.1, 1.8 Hz, H-3), 7.11-7.23 (2H, m, H-4, H-2), 6.65 (1H, d, *J* = 8.2 Hz, NH), 5.74 (1H, s, H-22), 4.80 (1H, dd, *J* = 8.3, 5.1 Hz, H-11), 4.37 (1H, dd, *J* = 14.2, 5.8 Hz, H-23a), 4.08 (1H, dd, *J* = 14.2, 4.3 Hz, H-23b), 4.04 (1H, t, *J* = 5.0 Hz, H-12), 3.91 (1H, d, *J* = 10.6 Hz, H-8), 3.88 (1H, d, *J* = 10.4 Hz, H-16), 3.64 (1H, d, *J* = 14.8 Hz, H-20a), 3.23 – 3.15 (1H, m, H-18a), 3.02 (1H, s, H-14), 2.82 – 2.77 (1H, m, H-18b), 2.67 (1H, d, *J* = 14.8 Hz, H-20b), 2.44 – 2.34 (2H, m, NH-C=O-C$\underline{H_2}$-CH_3), 2.30 – 2.21 (1H, m, H-15a), 1.91 – 1.78 (2H, m, H-17), 1.33 – 1.15 (5H, m, H-13, H-15b, NH-C=O-CH_2-C$\underline{H_3}$); ^{13}C NMR ($CDCl_3$) δ 174.6 (C, NH-$\underline{C}$=O), 168.17 (C, C=O), 141.77 (C, C-21), 138.53 (C, C-5), 132.96 (C, C-6), 128.7 (C, C-3), 126.9 (CH, C-22), 124.8 (C, C-2), 122.6 (C, C-4), 117.0 (C, C-1), 83.1 (CH, C-12), 64.4 (CH_2, C-23), 60.8 (CH, C-8), 59.9 (CH, C-16), 56.6 (CH, C-11), 52.9 (CH_2, C-20), 52.1 (C, C-7), 50.2 (CH_2, C18), 48.3 (CH, C-13), 42.3 (CH_2, C-17), 30.8 (CH, C-14), 29.3 (CH_2, NH-C=O-$\underline{C}H_2$-CH_3) , 26.6 (CH, C-15), 9.6 (CH3, C=O-CH_2-$\underline{C}H_3$); ESI MS *m/z* 349.43.

General procedures for the synthesis of compounds 4a-f.

HATU (700 mg, 2 mmole) and DIPEA (0.7 mL, 4 mmole) were added to a solution of the corresponding dicarboxylic acid (0.33 mmole) in dry dichloromethane (20 mL). The mixture was stirred at room temperature for 30 min. Afterwards, a solution of **2** (350 mg, 1 mmole) in dry dichloromethane (10 mL) was added and the reaction mixture was stirred for 12 h. The solvent was evaporated in vacuo and the residue was subjected to column chromatography using silica gel (CH_2Cl_2-MeOH-25%NH_3, 100:5:0.5) to give the corresponding bivalent amide.

***(R,R)-N,N'*-Bis(strychnine-11yl)-butanediamide (4a)** (20 mg, 2.5 %) was obtained from succinic acid (40 mg) as a white solid, mp 239 ^{0}C; ^{1}H NMR (MeOD) δ 7.94 (2H, d, *J* = 7.8 Hz, H-1), 7.29 – 7.20 (4H, m, H-3, H-4), 7.17 – 7.11 (2H, m, H-2), 5.98 (2H, s, H-22), 4.68 (2H, d, *J* = 4.2 Hz, H-11), 4.25 (2H, m, H-12, H-23), 3.96 (2H, d, *J* = 10.6 Hz, H-8), 3.78 (2H, d, *J* = 13.1 Hz, H-16), 3.65 (2H, d, *J* = 2.7 Hz, H-20a), 3.21 – 3.11 (4H, m, *J* = 10.7 Hz, H-18a, H-14), 2.96 – 2.85 (2H, m, H-18b), 2.85 – 2.75 (2H, m, H-20b), 2.75 – 2.64 (4H, m, NH-C=O-C$\underline{H_2}$-), 2.22 (2H, dt, *J* = 13.3, 3.8 Hz, H-15a), 1.90 (2H, dd, *J* = 12.7, 5.8 Hz, H-17a), 1.83 – 1.74 (2H, m, H-17b), 1.05 – 0.96 (2H, m, H-13), 0.91 (2H, dt, *J* = 13.3, 6.0 Hz, H-15b); ^{13}C NMR (MeOD) δ 174.1 (C, NH-$\underline{C}$=O), 168.6 (C,C=O) , 141.5 (C, C-21), 138.9 (C, C-5), 133.1 (C, C-6) , 128.5 (C, C-3), 128.4 (CH, C-22), 124.8 (C, C-2), 122.5 (C, C-4), 116.2 (C, C-1), 82.8 (CH, C-12), 63.8 (CH_2, C-23), 60.1 (CH, C-8), 59.7 (CH, C-16), 58.2 (CH, C-11), 52.1 (C, C-7), 51.8 (CH_2, C-20), 49.7 (CH_2, C-18), 48.4 (CH, C-13), 42.3 (CH_2, C-17), 33.2 (CH_2, NH-C=O-$\underline{C}H_2$), 30.6 (CH, C-14), 25.5 (CH_2, C-15); ESI MS *m/z* 780.91.

***(R,R)-N,N'*-Bis(strychnine-11yl)-hexanediamide (4b)** (80 mg, 9.8%) was obtained from adipic acid (50 mg) as a white solid, mp 249 ^{0}C; ^{1}H NMR (MeOD) δ 8.02 (2H, t, *J* = 6.3 Hz, H-1), 7.37 – 7.32 (2H, m, H-3), 7.30 – 7.27 (2H, m, H-4), 7.20 (2H, td, *J* = 7.5, 1.0 Hz, H-2), 5.97 (2H, s, H-22), 4.89 (2H, d, *J* = 4.8 Hz, H-

11), 4.30 – 4.12 (6H, m, H-23, H-12), 3.98 (2H, t, *J* = 8.3 Hz, H-8), 3.80 (2H, d, *J* = 10.3 Hz, H-16), 3.66 (2H, d, *J* = 15.0 Hz, H-20a), 3.17 (2H, dd, *J* = 10.3, 7.4 Hz, H-18a), 2.91 (2H, ddd, *J* = 12.5, 6.3, 4.3 Hz, H-18b), 2.85 (2H, s, H-14), 2.80 (2H, d, *J* = 14.8 Hz, H-20b), 2.70 (2H, dt, *J* = 15.2, 5.4 Hz, NH-C=O-C<u>H</u>-H-CH_2-), 2.41 (2H, ddd, *J* = 14.9, 10.1, 4.9 Hz, NH-C=O-CH-<u>H</u>-CH_2-), 2.14 (2H, ddd, *J* = 14.7, 5.8, 2.4 Hz, H-15a), 1.85 (6H, dtd, *J* = 20.2, 12.7, 6.6 Hz, H-17, NH-C=O-CH_2-C<u>H</u>-H-), 1.70 – 1.63 (2H, m, NH-C=O-CH_2-CH-<u>H</u>-), 0.81 – 0.67 (4H, m, H-13, H-15b); ^{13}C NMR (MeOD) δ 174.5 (C, NH-<u>C</u>=O), 168.8 (C, C=O), 141.4 (C, C-5), 133.1 (C, C-5), 128.7 (C, C-3), 128.5 (CH, C-22), 124.9 (C, C-2), 122.8 (C, C-4), 116.4 (C, C-1), 82.5 (CH, C-12), 63.6 (CH_2, C-23), 60.1 (CH, C-8), 59.6 (CH, C-16), 57.2 (CH, C-11), 51.8 (C, C-7), 51.4 (CH_2, C18), 49.9 (CH_2, C20), 48.4 (CH, C-13), 42.1 (CH_2, C17), 35.7 (CH_2, NH-C=O-<u>C</u>H_2-CH_2-), 30.2 (CH, C-14), 25.2 (CH_2, C-15), 24.9 (NH-C=O-CH_2-<u>C</u>H_2-); ESI MS *m/z* 808.96.

***(R,R)*-*N*,*N*'-Bis(strychnine-11yl)-octanediamide (4c)** (100 mg, 11.9%) was obtained from suberic acid (50 mg) as a white solid, mp 200 ^{0}C; ^{1}H NMR (MeOD) δ 2.45 (4H, ddd, *J* = 22.4, 14.1, 7.0 Hz, NH-C=O-C<u>H</u>$_2$-CH_2-CH_2-), 1.81 (6H, dtd, *J* = 26.4, 12.8, 6.7 Hz, H-17b, NH-C=O-CH_2-C<u>H</u>$_2$-CH_2-), 1.58 – 1.50 (4H, m, NH-C=O-CH_2-CH_2-C<u>H</u>$_2$-), chemical shifts and coupling constants for all other hydrogen atoms coincide with the δ values for the corresponding atoms of **4a** within ±0.04 ppm and ± 0.1 Hz, respectively; ^{13}C NMR (MeOD) δ 35.2 (CH_2, NH-C=O-<u>C</u>H_2-CH_2-CH_2-), 27.7(CH_2, NH-C=O-CH_2-CH_2-<u>C</u>H_2-), 25.9(CH_2, NH-C=O-CH_2-<u>C</u>H_2-CH_2-), chemical shifts for all other carbon atoms coincide with the δ values for the corresponding atoms of **4a** within ±0.1 ppm; ESI MS *m/z* 837.02.

***(R,R)-N,N'*-Bis(strychnine-11yl)-decanediamide (4d)** (20 mg, 2.31%) was obtained from sebacic acid (66 mg) as a magenta solid, 223 ^{0}C; ^{1}H NMR (MeOD) δ 2.42 – 2.37 (4H, m, NH-C=O-C<u>H$_2$</u>-CH$_2$-CH$_2$-CH$_2$-), 1.79 – 1.69 (6H, m, H-15a, NH-C=O-CH$_2$-C<u>H$_2$</u>-CH$_2$-CH$_2$-), 1.46 (6H, s, H-15b, NH-C=O-CH$_2$-CH$_2$-C<u>H$_2$</u>-CH$_2$-), 1.33 (6H, d, *J* = 5.4 Hz, H-13, NH-C=O-CH$_2$-CH$_2$-CH$_2$-C<u>H$_2$</u>-), chemical shifts and coupling constants for all other hydrogen atoms coincide with the δ values for the corresponding atoms of **4a** within ±0.04 ppm and ± 0.1 Hz, respectively ; ^{13}C NMR (MeOD) δ 35.6 (NH-C=O-<u>C</u>H$_2$-CH$_2$-CH$_2$-CH$_2$), 28.9 (NH-C=O-CH$_2$-<u>C</u>H$_2$-CH$_2$-CH$_2$-), 28.5 (NH-C=O-CH$_2$-CH$_2$-<u>C</u>H$_2$-CH$_2$-), 25.7 (NH-C=O-CH$_2$-CH$_2$-CH$_2$-<u>C</u>H$_2$-), chemical shifts for all other carbon atoms coincide with the δ values for the corresponding atoms of **4a** within ±0.1 ppm; ESI MS *m/z* 865.07.

***(R,R)-N,N'*-Bis(strychnine-11yl)-dodecanediamide (4e)** (80 mg, 8.95%) was obtained from dodecanedioic acid (76 mg) as a white solid, 174 ^{0}C; ^{1}H NMR (MeOD) δ 3.11 – 2.96 (6H, m, H-18b, NH-C=O-C<u>H$_2$</u>-CH$_2$-CH$_2$-CH$_2$-CH$_2$-), 2.39 (6H, m, H-15a, NH-C=O-CH$_2$-C<u>H$_2$</u>-CH$_2$-CH$_2$-CH$_2$-), 1.77 – 1.70 (4H, m, NH-C=O-CH$_2$-CH$_2$-C<u>H$_2$</u>-CH$_2$-CH$_2$-), 1.40 – 1.13 (12H, m, H-15b, H-13, NH-C=O-CH$_2$-CH$_2$-CH$_2$-C<u>H$_2$</u>-C<u>H$_2$</u>-), chemical shifts and coupling constants for all other hydrogen atoms coincide with the δ values for the corresponding atoms of **4a** within ±0.04 ppm and ± 0.1 Hz, respectively; ^{13}C NMR (MeOD) δ 43.8 (CH$_2$, NH-C=O-<u>C</u>H$_2$-CH$_2$-CH$_2$-CH$_2$-CH$_2$-), 35.7 (CH$_2$, NH-C=O-CH$_2$-<u>C</u>H$_2$-CH$_2$-CH$_2$-CH$_2$-), 29.4 (CH$_2$, NH-C=O-CH$_2$-CH$_2$-CH$_2$-<u>C</u>H$_2$-CH$_2$-), 28.8 (CH$_2$, NH-C=O-CH$_2$-CH$_2$-CH$_2$-CH$_2$-<u>C</u>H$_2$-), 25.8 (CH$_2$, NH-C=O-CH$_2$-CH$_2$-<u>C</u>H$_2$-CH$_2$-CH$_2$-), chemical shifts for all other carbon atoms coincide with the δ values for the corresponding atoms of **4a** within ±0.1 ppm; ESI MS *m/z* 893.12.

***(R,R)-N,N'*-Bis(strychnine-11yl)-tetradecanediamide (4f)** (25 mg, 2.71%) was obtained from tetradecanedioic acid (85 mg) as a magenta solid, mp 191 ^{0}C; ^{1}H NMR (MeOD) δ 2.37 (6H, dd, *J* = 7.7, 6.6 Hz, H-15a, NH-C=O-C$\underline{H_2}$-CH_2-CH_2-CH_2-CH_2-CH_2-), 1.76 – 1.68 (4H, m, NH-C=O-CH_2-C$\underline{H_2}$-CH_2-CH_2-CH_2-CH_2-), 1.51 – 1.39 (20H, m, H-13, H-15b, NH-C=O-CH_2-CH_2-C$\underline{H_2}$-C$\underline{H_2}$-C$\underline{H_2}$-C$\underline{H_2}$), chemical shifts and coupling constants for all other hydrogen atoms coincide with the δ values for the corresponding atoms of **4a** within ±0.04 ppm and ± 0.1 Hz, respectively; ^{13}C NMR (MeOD) δ 35.7 (CH_2, NH-C=O-$\underline{C}H_2$-CH_2-CH_2-CH_2-CH_2-CH_2-), 29.4 (CH_2, NH-C=O-CH_2-CH_2-$\underline{C}H_2$-CH_2-CH_2-CH_2-), 29.2 (CH_2, NH-C=O-CH_2-CH_2-CH_2-$\underline{C}H_2$-CH_2-CH_2-), 28.9 (CH_2, NH-C=O-CH_2-CH_2-CH_2-CH_2-$\underline{C}H_2$-CH_2-), 28.8 (CH_2, NH-C=O-CH_2-CH_2-CH_2-CH_2-CH_2-$\underline{C}H_2$-), 25.9 (CH_2, NH-C=O-CH_2-$\underline{C}H_2$-CH_2-CH_2-CH_2-CH_2-), chemical shifts for all other carbon atoms coincide with the δ values for the corresponding atoms of **4a** within ±0.1 ppm; ESI MS *m/z* 921.18.

FLIPR™ Membrane Potential Blue assay.

The functional characterization of the strychnine analogs was performed in the *FLIPR*™ Membrane Potential Blue assay (Molecular Devices).[22] The tsA201 cells were used and supplemented with 10% foetal bovine serum, 100 units/ml penicillin and 100 μg/ml streptomycin at 37 °C in a humidified atmosphere. Afterwards, the medium was aspirated, and the cells were washed with 100 μl Krebs buffer. Then the plate was incubated for 30 min and then the emission was measured at 565 nm [in fluorescence units (FU)] caused by excitation at 525 nm a total of 90 sec before and after addition of 33 μl agonist solution in Krebs buffer. EC_{80} (a range from EC_{70}-EC_{90}) was used in order to have a robust glycine-induced response to be antagonized by the antagonists.

References

1. Kuhse, J.; Betz, H.; Kirsch, J. The inhibitory glycine receptor: architecture, synaptic localization and molecular pathology of a postsynaptic ion-channel complex. *Curr Opin Neurobiol* **1995**, 5, 318-23.
2. Breitinger, H. G.; Becker, C. M. The inhibitory glycine receptor: prospects for a therapeutic orphan. *Curr Pharm Des* **1998**, 4, 315-34.
3. Kirsch, J. Glycinergic transmission. *Cell Tissue Res* **2006**, 326, 535-40.
4. Huang, X.; Chen, H.; Michelsen, K.; Schneider, S.; Shaffer, P. L. Crystal structure of human glycine receptor-alpha3 bound to antagonist strychnine. *Nature* **2015**, 526, 277-80.
5. Du, J.; Lu, W.; Wu, S.; Cheng, Y.; Gouaux, E. Glycine receptor mechanism elucidated by electron cryo-microscopy. *Nature* **2015**, 526, 224-9.
6. Lippincott, W.; Wilkins, M. J. M., Richard, A. Harvey, Pamela C. Champe Pharmacology, chapter 8, 2nd ed. **2000**, 33-34.
7. Yu, R.; Hurdiss, E.; Greiner, T.; Lape, R.; Sivilotti, L.; Biggin, P. C. Agonist and antagonist binding in human glycine receptors. *Biochemistry* **2014**. 53, 6041-51.
8. Miyazawa, A.; Fujiyoshi, Y.; Unwin, N. Structure and gating mechanism of the acetylcholine receptor pore. *Nature* **2003**, 423, 949-55.
9. Kuhse, J.; Laube, B.; Magalei, D.; Betz, H. Assembly of the inhibitory glycine receptor: identification of amino acid sequence motifs governing subunit stoichiometry. *Neuron* **1993**, 11, 1049-56.
10. Deekonda, S.; Wugalter, L.; Rankin, D.; Largent-Milnes, T. M.; Davis, P.; Wang, Y.; Bassirirad, N. M.; Lai, J.; Kulkarni, V.; Vanderah, T. W.; Porreca, F.; Hruby, V. J. Design and synthesis of novel bivalent ligands (MOR and DOR) by conjugation of enkephalin analogues with 4-anilidopiperidine derivatives. *Bioorg Med Chem Lett* **2015**, 25, 4683-8.
11. Glass, M.; Govindpani, K.; Furkert, D. P.; Hurst, D. P.; Reggio, P. H.; Flanagan, J. U. One for the Price of Two. Are Bivalent Ligands Targeting

Cannabinoid Receptor Dimers Capable of Simultaneously Binding to both Receptors. *Trends Pharmacol Sci* **2016**, 37, 353-63.

12. Shonberg, J.; Scammells, P. J.; Capuano, B. Design strategies for bivalent ligands targeting GPCRs. *ChemMedChem* **2011**, 6, 963-74.
13. Chojnacki, J. E.; Liu, K.; Saathoff, J. M.; Zhang, S. Bivalent ligands incorporating curcumin and diosgenin as multifunctional compounds against Alzheimer's disease. *Bioorg Med Chem* **2015,** 23, 7324-31.
14. Mohr, K.; Trankle, C.; Kostenis, E.; Barocelli, E.; De Amici, M.; Holzgrabe, U. Rational design of dualsteric GPCR ligands: quests and promise. *Br J Pharmacol* **2010**, 159, 997-1008.
15. Jensen, A. A.; Gharagozloo, P.; Birdsall, N. J.; Zlotos, D. P. Pharmacological characterisation of strychnine and brucine analogues at glycine and alpha7 nicotinic acetylcholine receptors. *Eur J Pharmacol* **2006**, 539, 27-33.
16. Banoub, M. M. F. C2-Linked Dimeric Strychnine Analogs as Bivalent Ligands Targeting Glycine Receptors. Master of Science in Pharmaceutical Chemistry, German University in Cairo, Cairo, **2016**.
17. Zlotos, D. P.; Buller, S.; Stiefl, N., Baumann, K.; Mohr, K. Probing the pharmacophore for allosteric ligands of muscarinic M2 receptors: SAR and QSAR studies in a series of bisquaternary salts of caracurine V and related ring systems. *J Med Chem* **2004**, 47, 3561- 3571.
18. Heinrich Wieland, H. M., 11-Aminobrucine und 11-Oxybrucine ober Strychnos-Alkaloide. *Liebigs Ann* **1936,** 527, 141-151.
19. Betz, H.; Langosch, D.; Rundstrom, N.; Bormann, J.; Kuryatov, A.; Kuhse, J.; Schmieden, V.; Matzenbach, B.; Kirsch, J. Structure and biology of inhibitory glycine receptors. *Ann N Y Acad Sci* **1993**, 707, 109-15.
20. Mohsen, A. M. Y.; Heller, E.; Holzgrabe, U.; Zlotos, D. P. Structure-activity relationships of strychnine analogs at glycine receptors. *Chem Biodiversity* **2014**, 11, 1256-1262.

21. Iskander, G. M.; Bohlin, L. Structure-activity relationship of strychnine derivatives modified in the non-aromatic part. *Acta Pharm Suec* **1978**, 15, 431-8.

22. Jensen, A. A. Functional characterisation of human glycine receptors in a fluorescence-based high throughput screening assay. *Eur J Pharmacol* **2005**, 521, 39-42.

23. Kuntz, I. D.; Chen, K.; Sharp, K. A.; Kollman, P. A., The maximal affinity of ligands. *Proc Natl Acad Sci* **1999,** 96, 9997-10002.

5. Overall Discussion and Conclusion

The most pronounced activity of strychnine is shown by being a direct and extremely potent competitive antagonist of glycine receptors. GlyRs mediate responses to glycine and other neurotransmitters as well as they are involved in many physiological functions including inflammatory pain sensitization and regulation of motor functions.[1] Strychnine acts by inhibition of inhibitory actions of glycine so that the excitatory synapses can then exert their action unrestrained which results in motor disturbance, increased muscle tone and overexcitation.[2, 3]

At present only a few ligands capable of differentiating between glycine receptor subtypes have been identified. Picrotoxin is a more potent antagonist of homomeric α glycine receptors than of heteromeric α1β receptors.[3-5]

Mackerer et al. has studied the binding of strychnine and strychnine analogs to synaptic membranes of rat brainstem and spinal cord.[6] For the purpose of obtaining a more detailed picture of the structure-activity relationships of strychnine, Iskander et al. studied the structure-activity relationships of strychnine analogs after subcutaneous injection in mice.[7] It was found that the binding affinity and convulsant and lethal pharmacological activities were highly correlated. 2-aminostrychnine was reported to have high affinity for the strychnine binding sites comparable to that of strychnine. Pseudostrychnine (16-hydroxystrychnine) showed very similar binding affinities to that of strychnine. Reduction of the double bond in positions 21 and 22 to give 21,22-dihydrostrychnine causes 17-fold decrease in the convulsive activity when compared to strychnine.[6] The reduction of the amide carbonyl function as in strychnidine decreased the observed convulsive and lethal effects. It seems therefore that the presence of the amide group is not only necessary, but should be part of a ring as in strychnine in order to give optimal activity.[7]

These results which were obtained from the study of the lethal and convulsive effects of strychnine analogs as well as the binding studies on animal studies are not enough to offer a clear structure-activity relationships at glycine receptors. In order to confirm and develop an "enriched" picture of the structure-activity relationships of strychnine at glycine receptors and to have a clear correlation to the previous results obtained from animal studies, a series of strychnine analogs including strychnidine, didehydrostrychnidine, dihydrostrychnidine, hydroxyoxodihydrostrychnidine, neostrychnine, isostrychnine, dihydroisostrychnine, tetrahydroisostrychnine, deoxytetrahydroisostrychnine and strychnine-*N*-propyl were synthesized and tested at α and α1β glycine receptors. Compounds with highest affinity and good pharmacological profile as well as having chemical liability to connect two molecules of strychnine were modified for the synthesis of dimeric ligands targeting glycine receptors.

In the journey of synthesizing strychnine analogs, many structural modifications were applied to strychnine at C21=C22 double bond, the lactam moiety at position 10, the tertiary nitrogen at position 19 and the tetrahydooxepine ring (Figure 25).

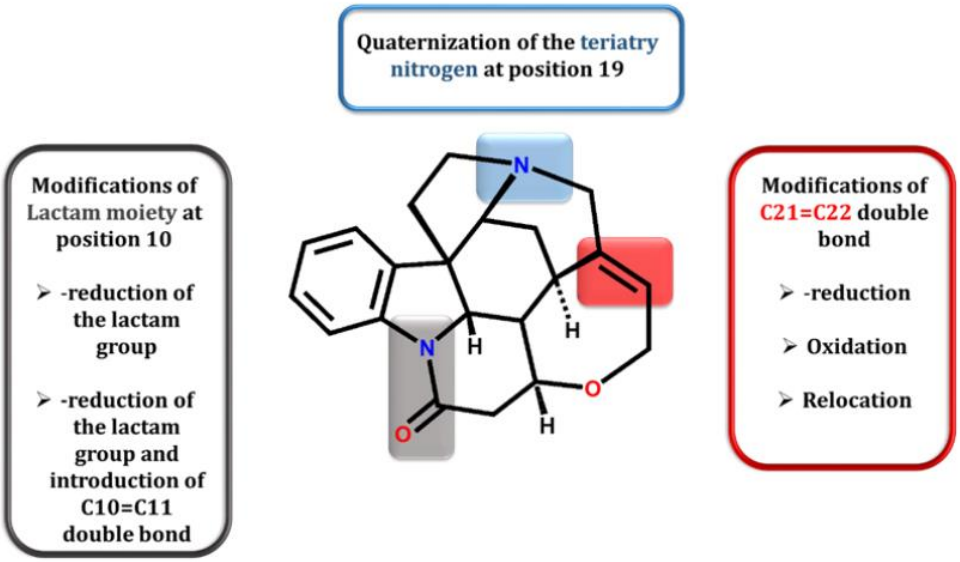

Figure 25: Structural modifications applied to strychnine

All compounds were pharmacologically evaluated at human α1 and α1β glycine receptors. The IC_{50} values of these compounds indicated that the C21=C22 double bond, the lactam moiety and the tertiary amino group are important elements for the ligand in order to be able to bind to the GlyRs. Consequently, isostrychnine is the most potent derivative in the series as the three main structural elements were maintained. These findings are in accordance with the previously published data on animal experiments and functional assays reporting that any reduction in the lactam moiety or double bond and quaternization of the tertiary amine are detrimental to the activity on GlyR.[4, 7] These results are also in agreement with the 3.0 Å X-ray structure of the human glycine receptor- α3 homopentamer as well as electro-cryomicrosopy structures of the zebra fish α1 GlyR in complex with strychnine which were published recently.[8, 9] The binding modes of strychnine on glycine receptors indicated that the presence of these three groups is crucial for better binding. Although none of the derivatives was superior to strychnine, a clear structure-activity relationships were obtained, enabling us to identify the pharmacophores needed for high antagonistic potency at α1 and α1β GlyR receptors. Accordingly, they were maintained in the synthesis of further strychnine analogs (Figure 26).

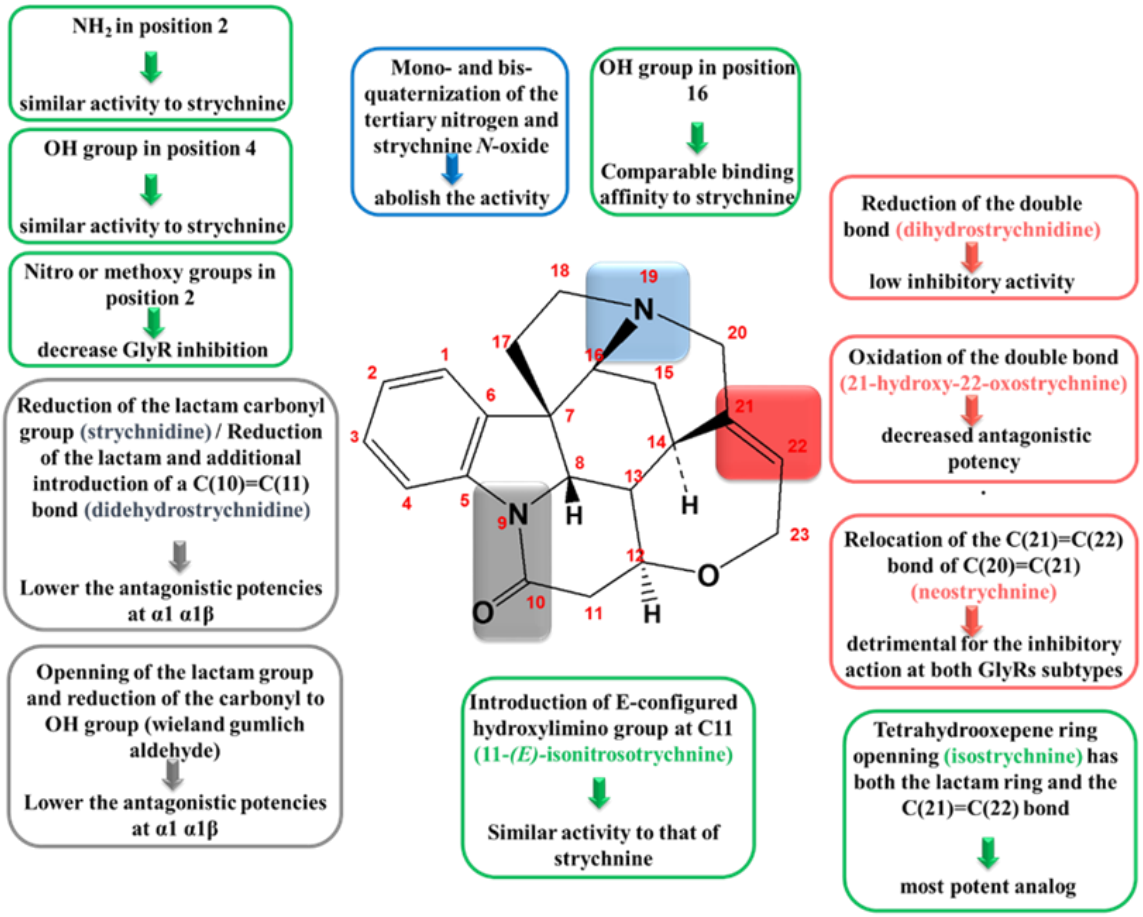

Figure 26: Structure-activity relationships of strychnine and its analogs.

The glycine receptor activity of strychnine appeared to be quite sensitive to structural modifications, since the only modification that did not impair the antagonist potencies of the strychnine was an *E*-configured hydroxyimino group at position 11 of strychnine. 11-*(E)*-isonitrostrychnine exhibited 23-fold and 16-fold higher antagonist activities than the corresponding *Z*-stereoisomer[4] which prompted us to choose the hydroxyl group of the oxime as a possible anchor group to synthesize dimeric ligands. In order to explore the GlyR pocket tolerance for oxime extension and whether it can accommodate the lipophilic spacer, a series oxime ethers of different sizes, lengths and sterical/lipophilic and electronic properties were prepared and pharmacologically evaluated. The methyl and propyl oxime ethers showed comparable potency to that of strychnine, indicating that the spacer

is not influencing the antagonistic activity. Therefore, more oxime ethers with branched substituent such as isobutyl oxime ether and with larger substituents such as butyl, pentyl, benzyl and phenylethyl oxime ethers were synthesized. The findings indicated that there may be a lipophilic pocket in the binding site that can accommodate these groups. However, this binding pocket is assumed to be not large enough to accommodate larger lipophilic groups as in benzyl and phenylethyl oxime ethers as indicated by their lower IC_{50} values. Allyl and propargyl oxime ethers were relatively the best in this series, revealing that these groups are best accommodated in the lipophilic pocket.

The bivalent ligand action were assumed that they can simultaneously bind to both receptor subunits within the pentameric complex. It was of interest to explore the synthesis of bivalent ligands starting from 11-*(E)*-isonitrosotrychnine by direct o-alkylation of two molecules of 11-*(E)*-isonitrosotrychnine using dialkylhalides. Unfortunately, this approach failed and this was ascribed to the highly reactive basic nitrogen in strychnine which is easily quaternized with very small amounts of alkylhalides. This is in accordance with the results obtained from Jensen et al. who studied the structure-activity relationships of strychnine analogs on GlyRs and reported the fact that all mono- and bisquaternary compounds were inactive at the glycine receptors (at concentrations up to 100 μM) regardless of the steric and electronic properties of their respective N-substituents.[4] This confirms again the importance of the tertiary nitrogen in the activity of strychnine.

This led to a new anchor group for the synthesis of bivalent strychnine ligands while maintaining C11 as the attachment point. *(R)*-11-aminostrychnine was synthesized and directly coupled with the diacids of different spacer lengths. However, no significant difference in potency between the dimeric compounds and strychnine. When comparing the reference monomeric propionamide containing $(CH_2)_2$ spacer to the dimeric ligand containing double the number of spacer atoms $(CH_2)_4$, a 3-fold increase in potency was observed. Since the dimer containing $(CH_2)_{10}$ spacer length was found to be equipotent to strychnine, it is assumed that

these dimers could not be accommodated by the binding site of the GlyR and that only one molecule of strychnine activates the receptor. In other words, two strychnine molecules cannot simultaneously bind to the receptor.

On the other hand, bivalent ligands will remain of a great potential and can be used as a basis to explore the binding mode of strychnine-based compounds as well as serve as a good pharmacological tools which can guide the design of more potent GlyR inhibitors. Therefore, the synthesis of bivalent ligands targeting glycine receptors will likely continue to feature as a noticeable aspect of modern medicinal chemistry. It can be considered helpful to further investigate the bivalent ligand approach through finding another more suitable point of attachment to connect two strychnine molecule. Also the nature of the spacer can be altered which may lead to further binding interactions with the receptor. This can be achieved through using e.g.: polyamide chains or polar oxygenated spacers. Despite the fact that the spacer needs to be flexible enough to allow correct positioning of each pharmacophore in the binding pocket of each subtype of the receptor, the rigidity of the spacer is also of considerable interest thermodynamically and consequently may increase the potency. This may be done by incorporation of double or triple bonds in the spacer.

6. References

1. Breitinger, H. G., Becker, C. M., The inhibitory glycine receptor: prospects for a therapeutic orphan. *Curr Pharm Des* **1998,** 4, 315-34.
2. Philippe, G.; Monique, T.; Fre´de´rich, M. About the toxicity of some Strychnos species and their alkaloids. *Toxicon* **2004,** 44, 405-416.
3. Laube, B.; Maksay, G.; Schemm, R.; Betz, H., Modulation of glycine receptor function: a novel approach for therapeutic intervention at inhibitory synapses. *Trends Pharmacol Sci* **2002,** 23, 519-27.
4. Jensen, A. A.; Gharagozloo, P.; Birdsall, N. J.; Zlotos, D. P., Pharmacological characterisation of strychnine and brucine analogues at glycine and alpha7 nicotinic acetylcholine receptors. *Eur J Pharmacol* **2006,** 539, 27-33.
5. Rajendra, S.; Lynch, J. W.; Schofield, P. R., The glycine receptor. *Pharmacol Ther* **1997,** 73, 121-46.
6. Mackerer, C. R.; Kochman, R. L.; Shen, T. F.; Hershenson, F. M., The binding of strychnine and strychnine analogs to synaptic membranes of rat brainstem and spinal cord. *J Pharmacol Exp Ther* **1977,** 201, 326-31.
7. Iskander, G. M.; Bohlin, L., Structure-activity relationship of strychnine derivatives modified in the non-aromatic part. *Acta Pharm Suec* **1978,** 15, 431-8.
8. Huang, X.; Chen, H.; Michelsen, K.; Schneider, S.; Shaffer, P. L. Crystal structure of human glycine receptor-alpha3 bound to antagonist strychnine. *Nature* **2015,** 526, 277-80.
9. Du, J.; Lu, W.; Wu, S.; Cheng, Y.; Gouaux, E., Glycine receptor mechanism elucidated by electron cryo-microscopy. *Nature* **2015,** 526, 224-9.
10. Kuntz, I. D.; Chen, K.; Sharp, K. A.; Kollman, P. A., The maximal affinity of ligands. *Proc Natl Acad Sci U S A* **1999,** 96, 9997-10002.

7. Summary

The inhibitory glycine receptors are one of the major mediators of rapid synaptic inhibition in the mammalian brainstem, spinal cord and higher brain centres. They are ligand-gated ion channels that are mainly involved in the regulation of motor functions. Dysfunction of the receptor is associated with motor disorders such as hypereklepxia or some forms of spasticity. GlyR is composed of two glycosylated integral membrane proteins α and β and a peripheral membrane protein of gephyrin. Moreover, there are four known isoforms of the α-subunit (α1-4) of GlyR while there is a single β-subunit. Glycine receptors can be homomeric including α subunits only or heteromeric containing both α and β subunits. To date, strychnine is the ligand that has the highest affinity as glycine receptor ligand. It acts as a competitive antagonist of glycine that results in the inhibition of Cl^- ions permeation and consequently reducing GlyR-mediated inhibition.

For a long time, the details of the molecular mechanism of GlyRs inactivation by strychnine were insufficient due to the lack of high-resolution structures of the receptor. Only homology models based on structures of other cys-loop receptors have been available. Recently, 3.0 Å X-ray structure of the human glycine receptor-α3 homopentamer in complex with strychnine, as well as electro cryo-microscopy structures of the zebra fish α1 GlyR in complex with strychnine and glycine were published. Such information provided detailed insight into the molecular recognition of agonists and antagonists and mechanisms of GlyR activation and inactivation.

Very recently, a series of dimeric strychnine analogs obtained by diamide formation of two molecules of 2-aminostrychnine with diacids of different chain length was pharmacologically evaluated at human α1 and α1β glycine receptors. None of the dimeric analogs was superior to strychnine.

The present work focused on the extension of the structure-activity relationships of strychnine derivatives at glycine receptors. The structural modifications that were applied to strychnine are shown in Figure 27.

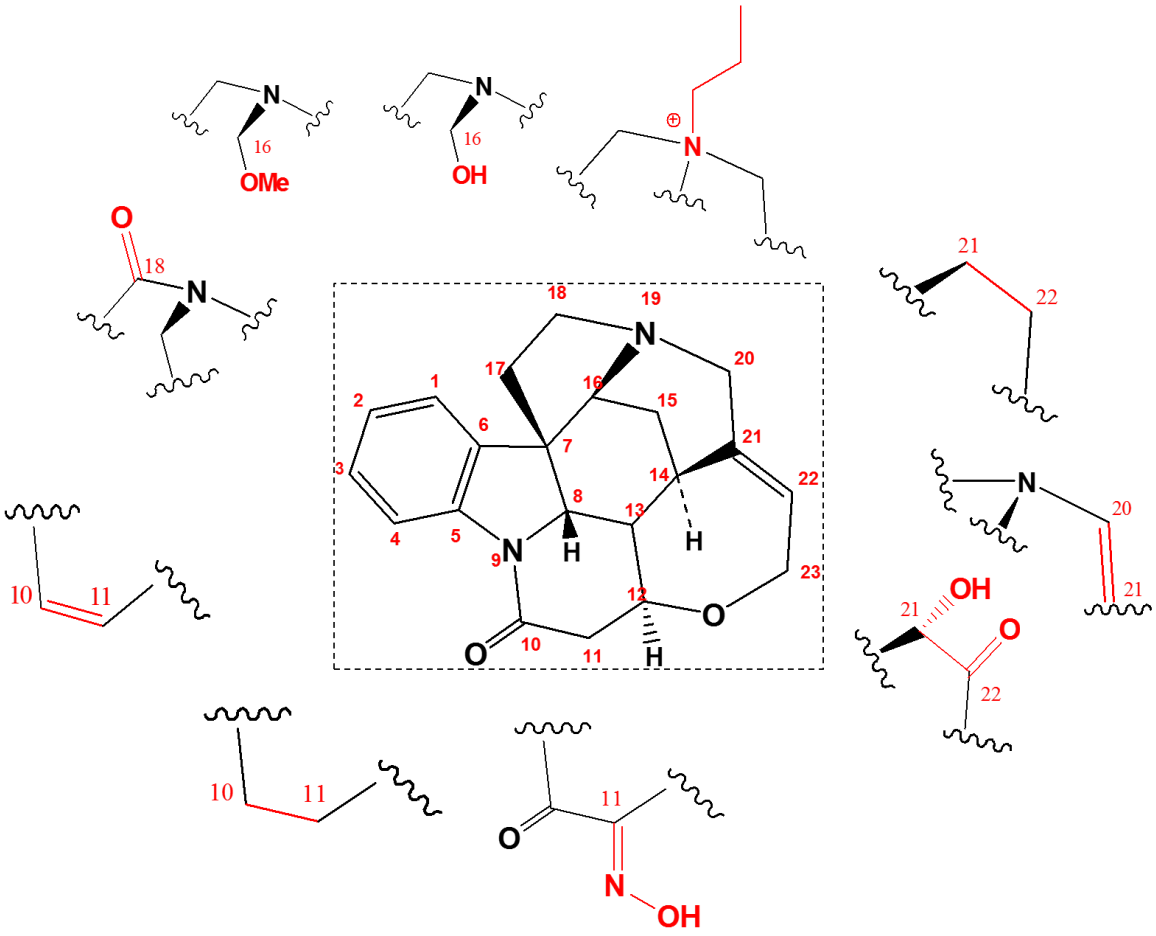

Figure 27: Structural modification applied to strychnine.

All the synthesized compounds were pharmacologically evaluated at human α1 and α1β glycine receptors in a functional FLIPR^{TM} assay and the most potent analogs were pharmacologically evaluated in a whole cell patch-clamp assay and in [^{3}H]strychnine binding studies.

It was reported that 11-*(E)*-isonitrososstrychnine displayed a 2-times increased binding to both α1 and α1β glycine receptors which prompted us to choose the hydroxyl group as a suitable attachment point to connect two 11-*(E)*-isonitrososstrychnine molecules using a spacer. In order to explore the GlyR pocket tolerance for oxime extension, a series of oxime ethers with different spacer lengths and sterical/lipophilic properties were synthesized biologically evaluated. Among all the oxime ethers, methyl, allyl and propagyl oxime ethers were the most potent antagonists displaying IC_{50} values similar to that of strychnine. These findings indicated that strychnine binding site at GlyRs comprises an additional small lipophilic pocket located in close proximity to C11 of strychnine and the groups best accommodated in this pocket are *(E)*-allyl and *(E)*-propagyl oxime ethers.

Moreover, 11-aminostrychnine, and the corresponding propionamide were prepared and pharmacologically evaluated to examine the amide function at C11 as potential linker.

A series of dimeric strychnine analogs designed by linking two strychnine molecules through amino groups in position 11 with diacids were synthesized and tested in binding studies and functional assays at human α1 and α1β glycine receptors. The synthesized bivalent ligands were designed to bind simultaneously to two α-subunits of the pentameric glycine receptors causing a possibly stronger inhibition than the monomeric strychnine. However, all the bivalent derivatives showed no significant difference in potency compared to strychnine. When comparing the reference monomeric propionamide containing ethylene spacer to the dimeric ligand containing butylene spacer, a 3-fold increase in potency was observed. Since the dimer containing $(CH_2)_{10}$ spacer length was found to be equipotent to strychnine, it is assumed that one molecule of strychnine binds to the receptor and the ‘additional’ strychnine molecule in the dimer probably protrudes from the orthosteric binding sites of the receptor.

8. Zusammenfassung

Die inhibitorischen Glycin-Rezeptoren (GlyR) gehören zu den wichtigsten Mediatoren der schnellen synaptischen Hemmung im Säugetierhirnstamm, Rückenmark und in höheren Gehirnzentren. Sie sind ligandgesteuerte Ionenkanäle, die hauptsächlich an der Regulation der motorischen Funktionen beteiligt sind. Dysfunktion des Rezeptors ist assoziiert mit motorischen Störungen wie Hyperekplexie und einigen Formen von Spastizität. GlyR sind Proteinkomplexe, die aus zwei glykosylierten integralen Membranproteinen α und β und dem peripheren Membranprotein Gephyrin bestehen. Von der α-Untereinheit sind vier Isoformen bekannt (α1-4), von der β-Untereinheit nur eine. GlyR können homomer (nur α-Untereinheiten) oder heteromer (α und ß-Untereinheiten) sein. Das Alkaloid Strychnin weist eine sehr hohe Affinität zu den GlyR auf. Es wirkt als kompetitiver Antagonist von Glycin und führt nach Bindung zu einer Hemmung des Chlorid-Ionen-Einstroms und folglich zu einer Verringerung der GlyR-vermittelten Inhibition.

Lange Zeit waren die genauen Details des molekularen Mechanismus der GlyR-Inaktivierung durch Strychnin aufgrund des Fehlens von hochauflösenden Röntgenstrukturen des Rezeptors nicht bekannt; es standen nur Homologie-Modelle basierend auf Strukturen anderer cys-Loop-Rezeptoren zur Verfügung. Vor kurzem wurden eine 3.0-Å-Röntgenstruktur des humanen GlyR (α3-Homopentamer) im Komplex mit Strychnin sowie eine Kryoelektronenmikroskopie-Struktur des Zebrafisches (α1-GlyR im Komplex mit Strychnin und Glycin) veröffentlicht. Dadurch erhielt man detailliertere Informationen über die molekulare Erkennung von Agonisten und Antagonisten sowie den Mechanismen der Aktivierung und Inaktivierung von GlyR.

Kürzlich wurde eine Reihe von dimeren Strychnin-Analoga, bei denen jeweils zwei Moleküle 2-Aminostrychnin durch Reaktion mit Disäuren unterschiedlicher

Kettenlänge zu den entsprechenden Diamiden miteinander verknüpft wurden, pharmakologisch an humanen α1- und α1β-GlyR untersucht. Keines der dimeren Analoga war Strychnin überlegen.

Die vorliegende Arbeit konzentriert sich auf der Erweiterung der Struktur-Wirkungs-Beziehungen von Strychnin-Derivaten bzgl. der Aktivität an Glycin-Rezeptoren. Die strukturellen Änderungen, die an Strychnin durchgeführt wurden, sind in Abbildung 27 dargestellt.

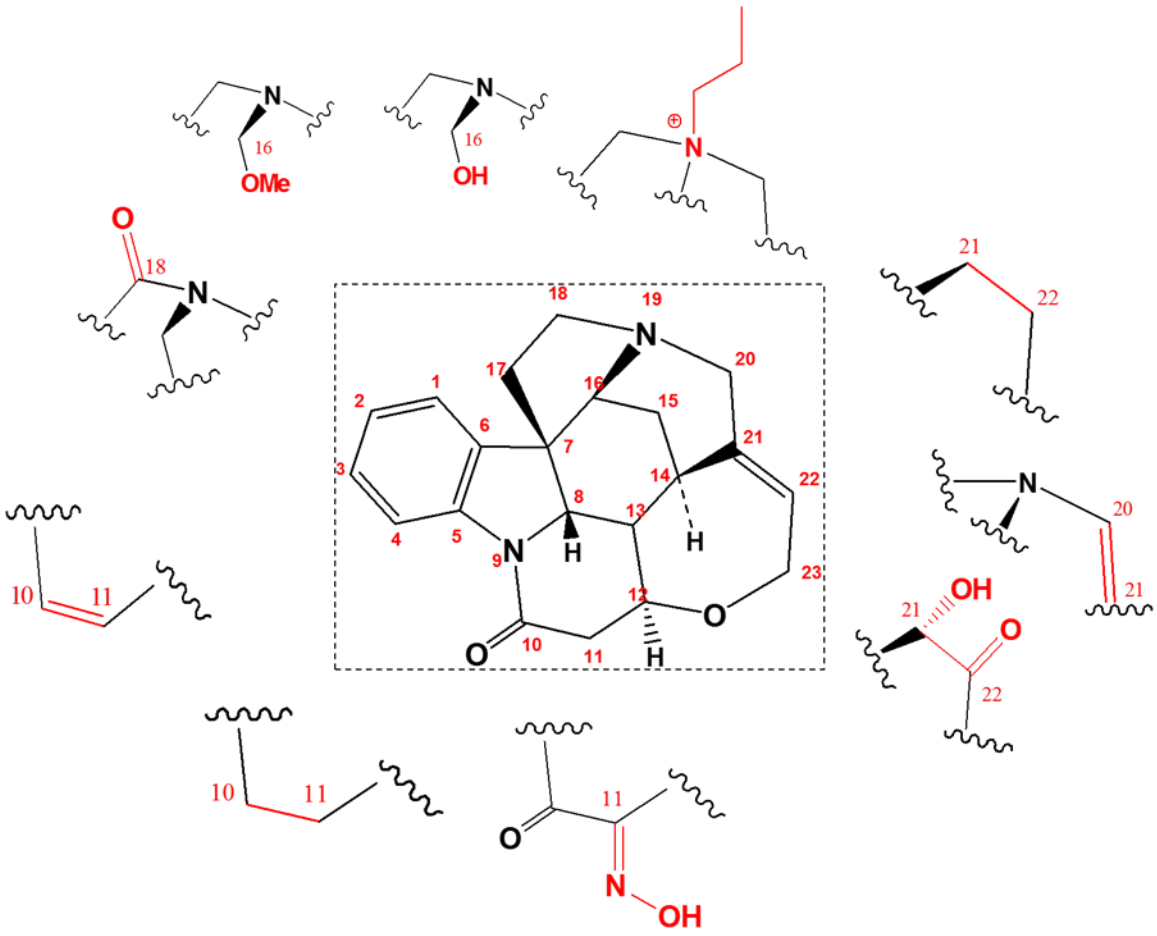

Abbildung 27: Durchgeführte strukturelle Modifikationen der Leitsubstanz Strychnin.

Alle synthetisierten Verbindungen wurden pharmakologisch an humanen α1- und α1β- GlyR mittels funktionellem FLIPR^{TM}-Test und die wirksamsten Analoga anschließend pharmakologisch mittels *Patch-Clamp*-Technik an ganzen Zellen sowie [^{3}H]Strychnin-Bindungsstudien untersucht.

In der Literatur wurde berichtet, dass 11-*(E)*-Isonitrosostrychnin eine zweifach höhere Affinität sowohl zu α1- als auch zu α1β-GlyR aufweist. Aus diesem Grund wurde eine Serie von Analoga synthetisiert, bei denen zwei Moleküle 11-(*E*)-Isonitrosostrychnin über die die Hydroxyl-Gruppe der Oxim-Gruppe mit geeigneten Spacern verknüpft wurden. Um die Größe der GlyR-Bindetasche zu überprüfen wurde zunächst eine Reihe von Oximethern, deren Alkylketten sich in Länge und Lipophilie unterscheiden, synthetisiert und pharmakologisch charakterisiert. Die wirksamsten Verbindungen waren Methyl-, Allyl- und Propargyl-Oximether, deren IC_{50}-Werte im Bereich der Leitstruktur Strychnin liegen. Diese Ergebnisse zeigten, dass die Strychnin-Bindungsstelle bei GlyR eine zusätzliche kleine lipophile Tasche aufweist, die sich in unmittelbarer Nähe zur Position 11 des Strychnins befindet, und dass der *(E)-A*llyl- und der *(E)-P*ropargyl-Oximether am besten in diese zusätzliche Bindetasche passen.

Außerdem wurden 11-Aminostrychnin und das entsprechende Strychnin-11-propionamid synthetisiert und pharmakologisch untersucht, um zu testen, ob die Aminofunktion in Position 11 als potentieller Anknüpfungspunkt für eine Dimerisierung dienen könnte. Eine Reihe von dimeren Strychnin-Analoga wurde durch Reaktion der Aminogruppen in Position 11 mit Disäuren unterschiedlicher Kettenlänge synthetisiert und in Bindungsstudien und funktionellen Tests an menschlichen α1- und α1β-GlyR untersucht. Hierbei sollte überprüft werden, ob diese dimeren Verbindungen gleichzeitig an zwei α-Untereinheiten binden können und dadurch die GlyR stärker inhibiert werden. Jedoch zeigten alle bivalenten Derivate keinen signifikanten Unterschied bezüglich der Wirksamkeit im Vergleich zu Strychnin. Vergleicht man das Monomere Strychnin-11-propionamid mit den dimeren Verbindungen, so weist das Derivat mit vier Methylengruppen als Spacer

zwar die dreifache Potenz auf, diese nimmt jedoch mit einer Verlängerung des Spacers kontinuierlich ab. Das Derivat mit zehn Methylengruppen entspricht in der Wirkung der Leitsubstanz Strychnin. Daraus lässt sich schlussfolgern, dass die dimeren Verbindungen nicht gleichzeitig zwei Untereinheiten der GlyR besetzten und nur ein Molekül Strychnin ausreicht, um den Rezeptor zu aktivieren.

9. APPENDIX

P1	**Amal M. Y. Mohsen, Eberhard Heller, Ulrike Holzgrabe, Anders A. Jensen and Darius P. Zlotos (**2014) Structure–Activity Relationships of Strychnine Analogs at Glycine Receptors. *Journal of Chemistry & Biodiversity* DOI: 10.1002/cbdv.201400110, 11: 1256-1262

Author	1	2	3	4	5
Synthetic scheme development					X
Synthesis of compounds **3-7**	X				
Synthesis of compounds **8-11**		X			X
FLIPR® Membrane Potential (FMP) Blue assay				X	
Manuscript planning	X		X		X
Manuscript writing	X				
Supervision of Amal			X		X

P2	**Amal M. Y. Mohsen, Edita Sarukhanyan, Ulrike Breitinger, Carmen Villmann, Maha M. Banoub, Hans-Georg Breitinger, Thomas Dandekar, Ulrike Holzgrabe, Anders A. Jensen, and Darius P. Zlotos** (2016) Oxime Ethers of (E)-11-Isonitrososstrychnine as Highly Potent Glycine Receptor Antagonists. This Manuscript is in revision in the *Journal of Natural Products*.

Author	1	2	3	4	5	6	7	8	9	10
Synthetic scheme development	X									X
Synthesis of compounds **1, 4-7, 8a-k**	X									
Synthesis of compounds **2,3**					X					
Revision of the experimental parts										X
Docking into the orthosteric binding site of high resolution structure of homomeric α1 GlyR (3JAD)		X					X			
Radioligand binding experiments at α1 receptors				X						
Whole-cell patch clamp technique						X				
FLIPR® Membrane Potential (FMP) Blue assay									X	
Manuscript planning	X							X		X
Manuscript writing	X									
Supervision of Amal								X		X

9.1. NMR Spectra of the Compounds Described in Chapter 4.1

Figure A1. ^{1}H ($CDCl_3$, 400 MHz), DEPT-135 and ^{13}C NMR spectra of Strychnine **1**

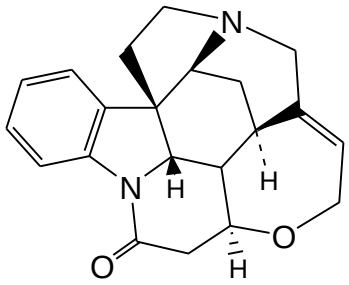

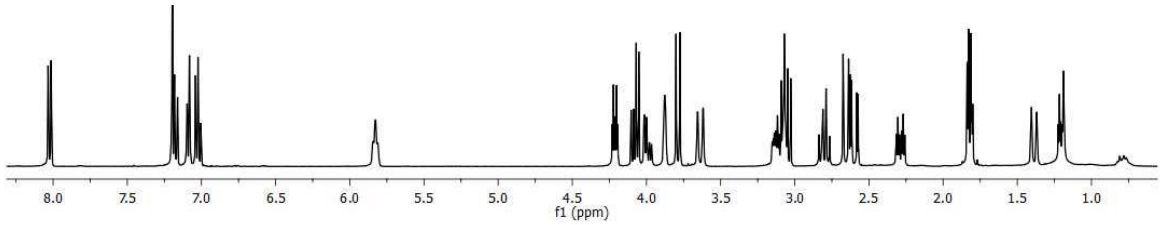

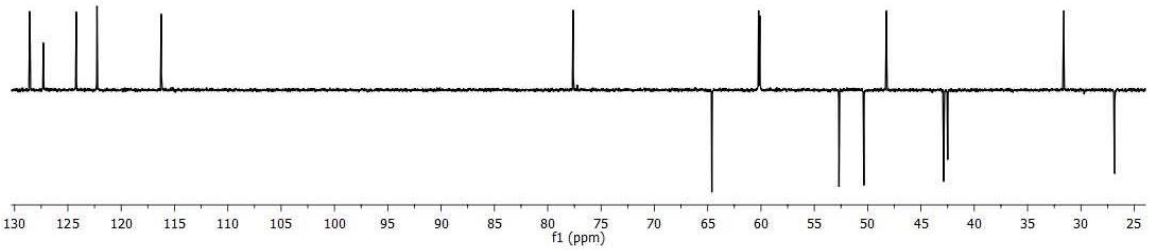

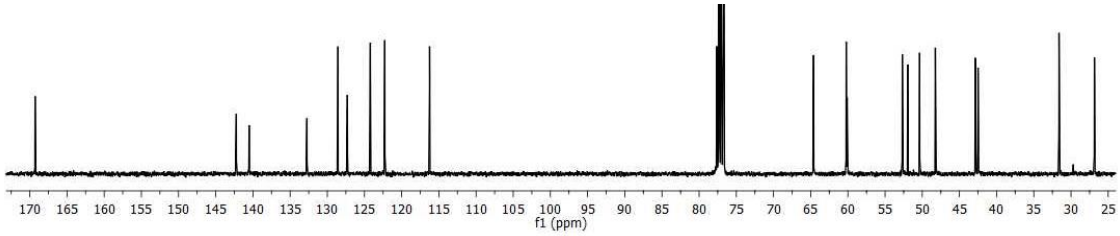

Figure A2. ^{1}H ($CDCl_3$, 400 MHz), DEPT-135 and ^{13}C NMR spectra of Strychnidine **3**

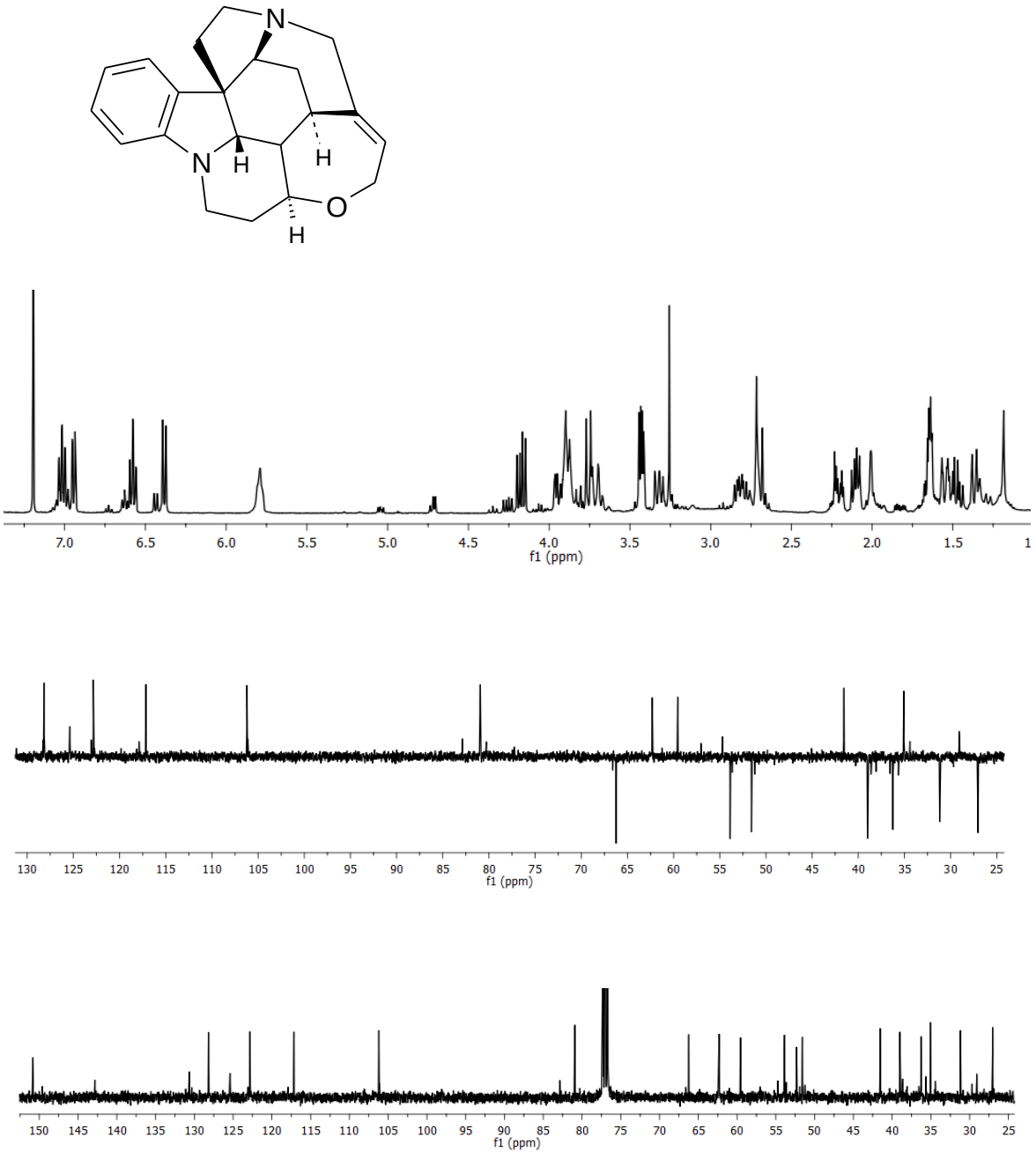

Figure A3. ^{1}H ($CDCl_3$, 400 MHz), DEPT-135 and ^{13}C NMR spectra of Didehydrostrychnidine **4**

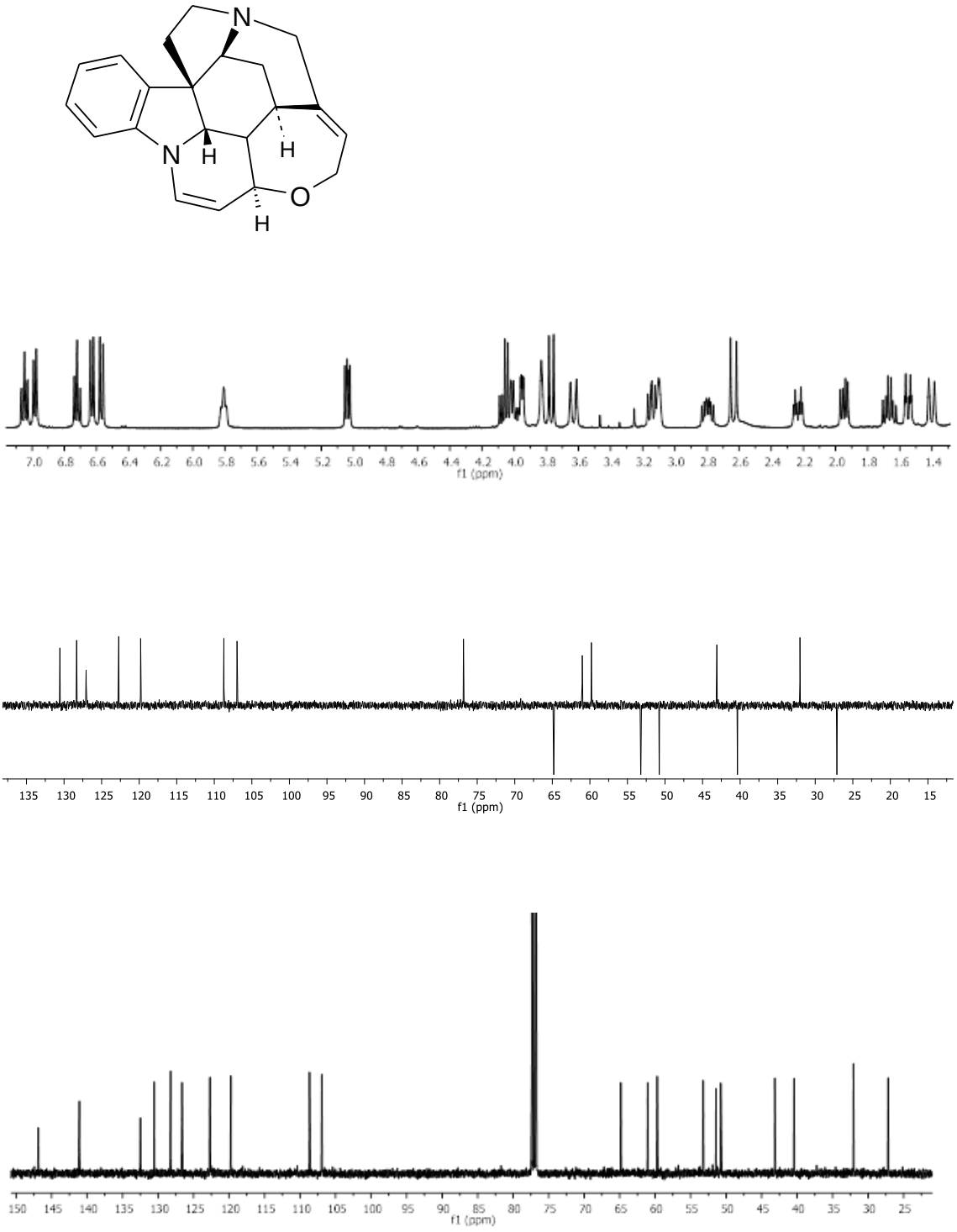

Figure A4. ^{1}H ($CDCl_3$, 400 MHz), DEPT-135 and ^{13}C NMR spectra of Dihydrostrychnidine **5**

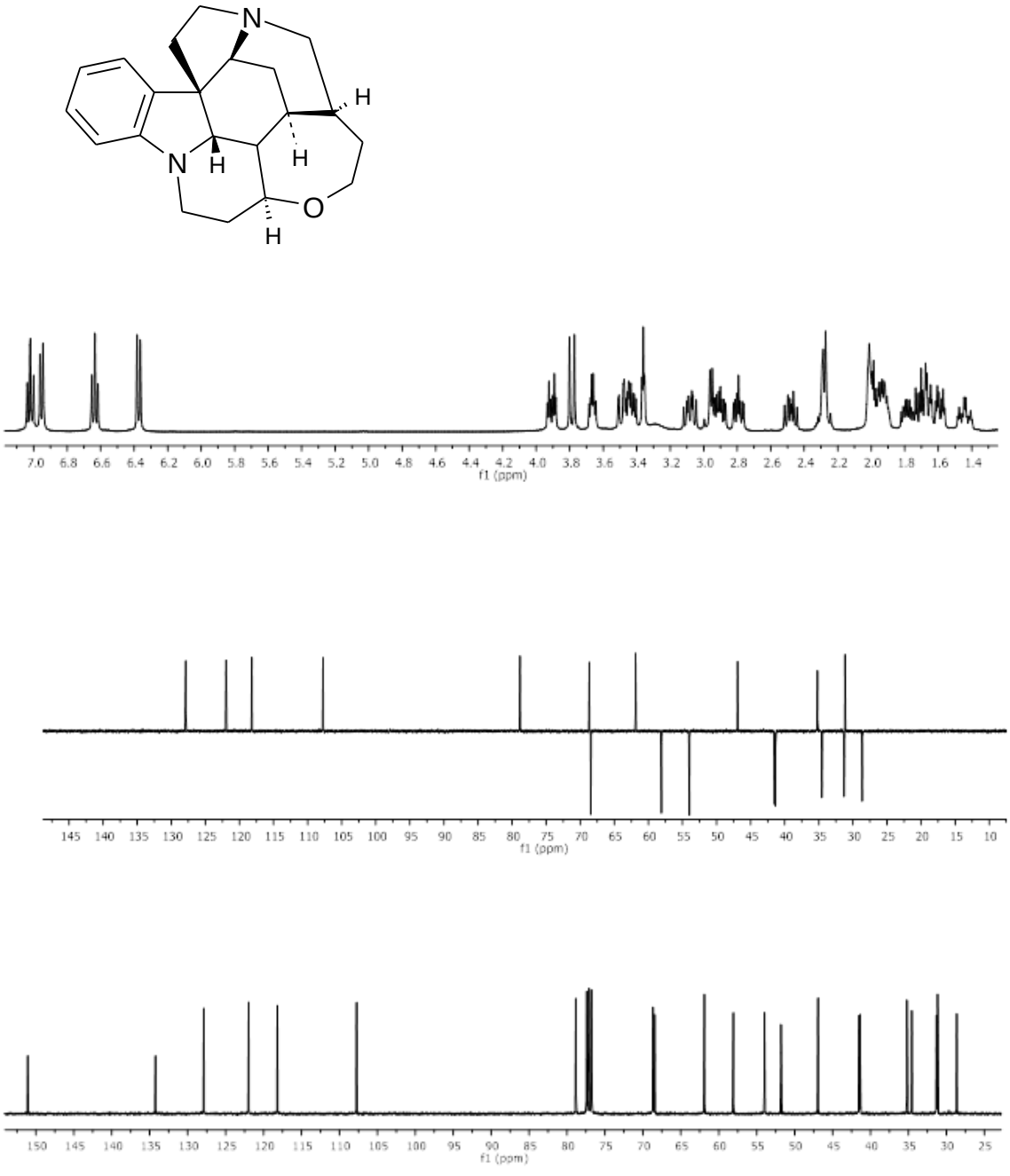

Figure A5. ^{1}H ($CDCl_3$, 400 MHz), DEPT-135 and ^{13}C NMR spectra of 21-hydroxy-22-oxo-21,22-dihydrostrychnine **6**

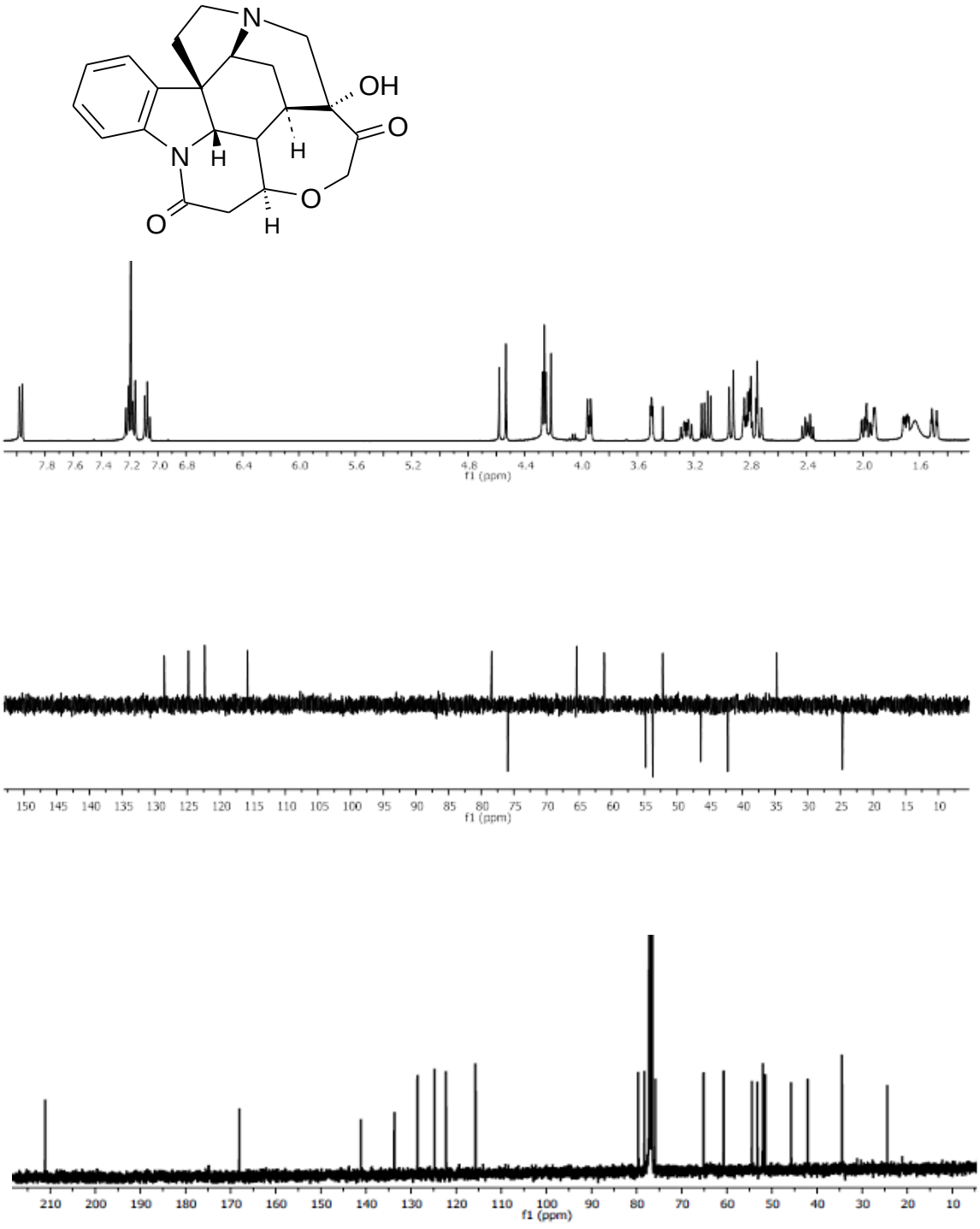

Figure A6. ^{1}H ($CDCl_3$, 400 MHz), DEPT-135 and ^{13}C NMR spectra of Neostrychnine **7**

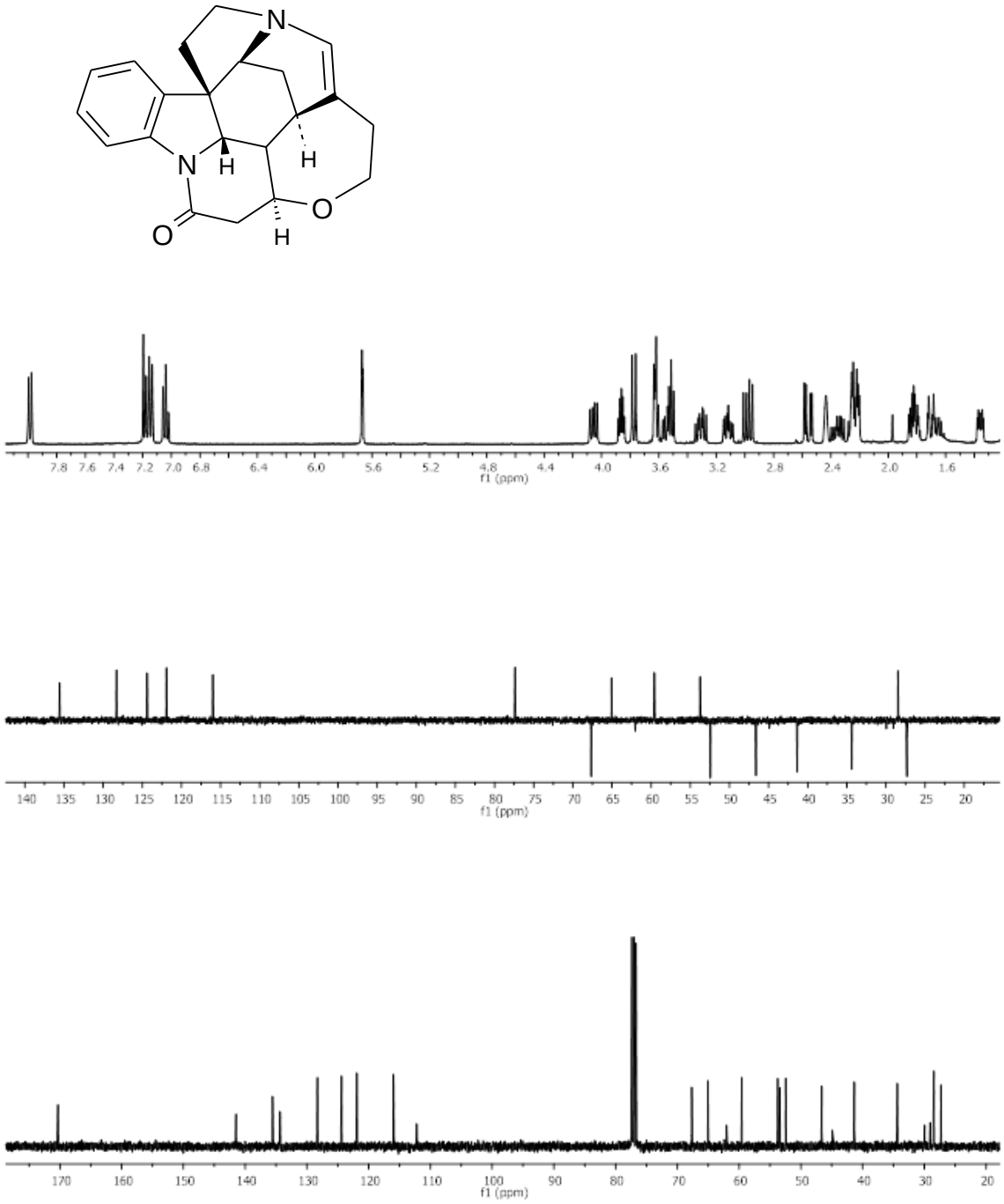

Figure A7. ^{1}H ($CDCl_3$, 400 MHz), DEPT-135 and ^{13}C NMR spectra of Isostrychnine **8**

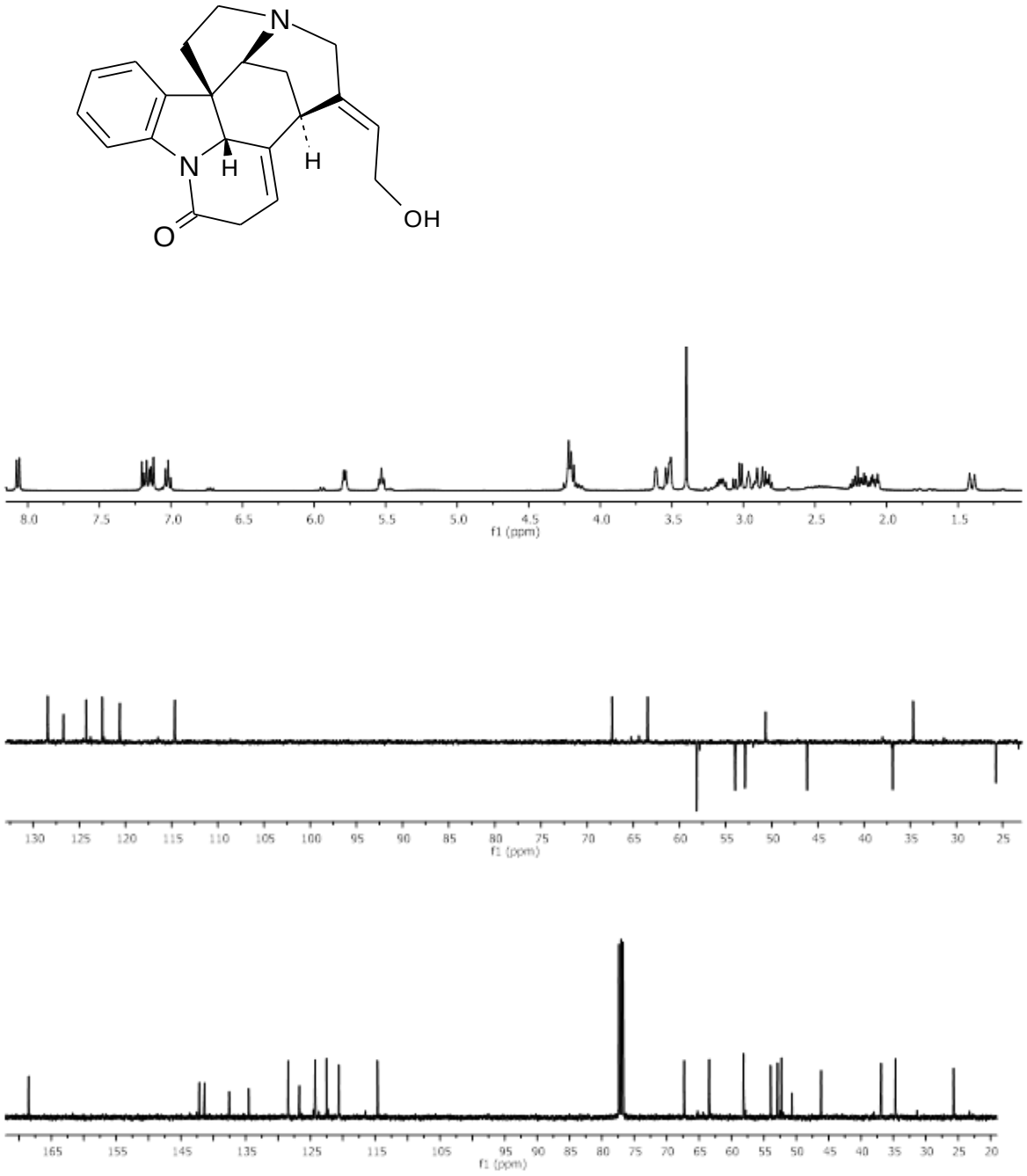

Figure A8.^{1}H ($CDCl_3$, 400 MHz), DEPT-135 and ^{13}C NMR spectra of 21,22-dihydroisostrychnine **9**

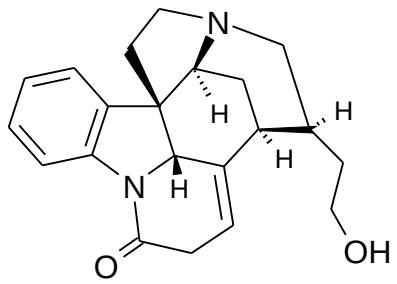

9

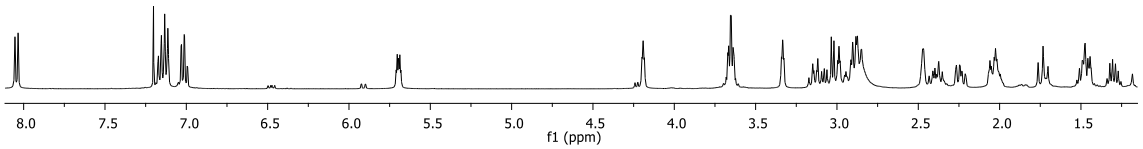

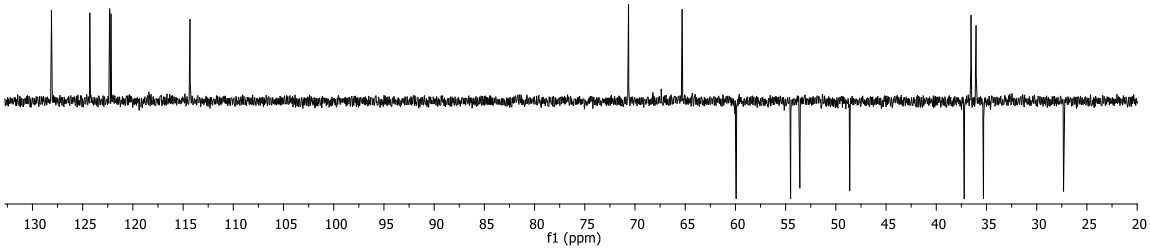

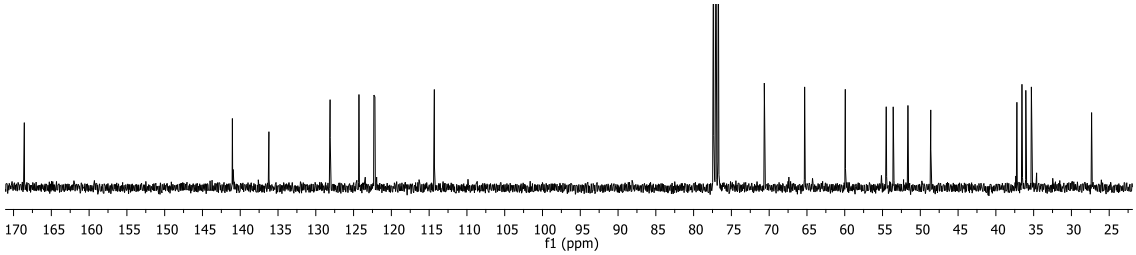

Figure A9. ^{1}H ($CDCl_3$, 400 MHz), DEPT-135 and ^{13}C NMR spectra of 12,13,21,22-tetrahydroisostrychnine **10**

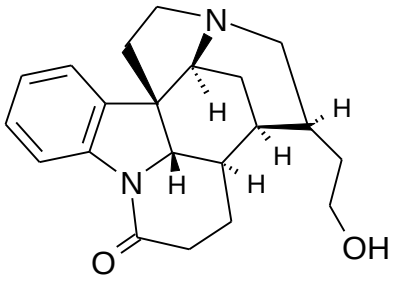

10

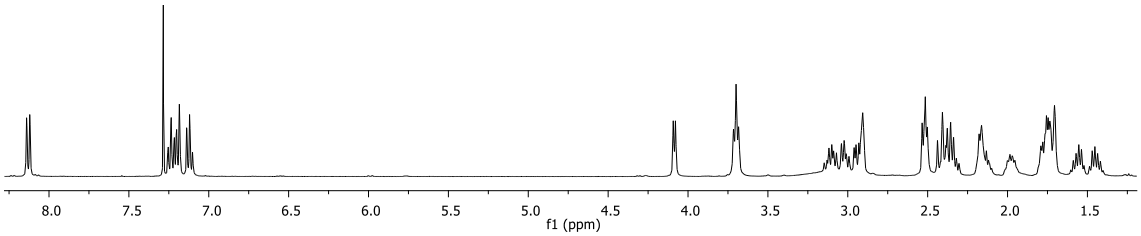

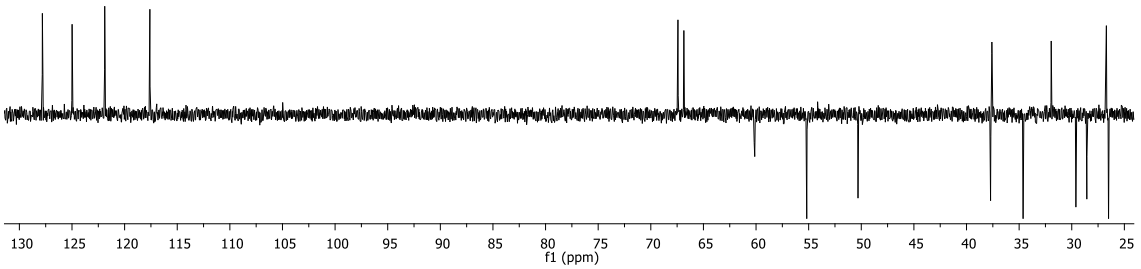

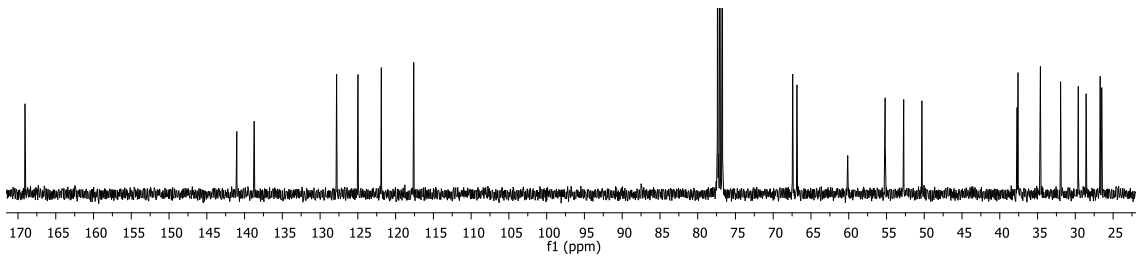

Figure A10. ^{1}H ($CDCl_3$, 400 MHz), DEPT-135 and ^{13}C NMR spectra of 23-deoxo-12,13,21,22-tetrahydroisostrychnine **11**

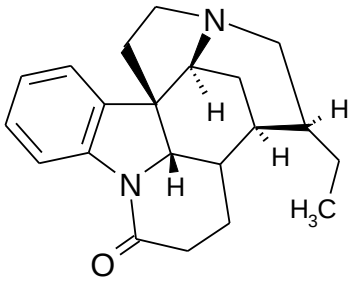

11

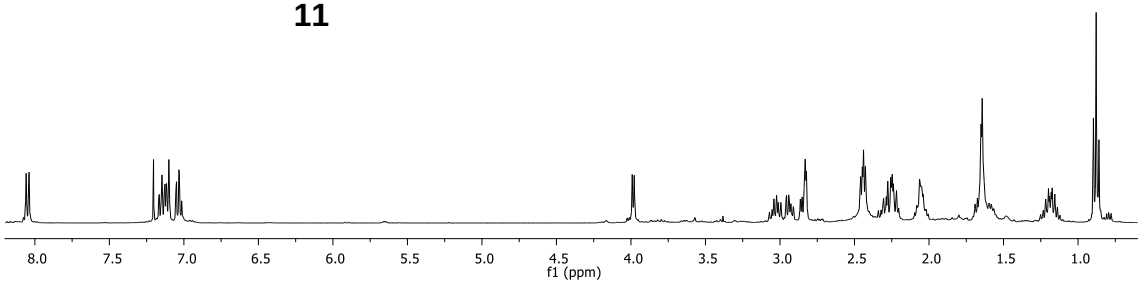

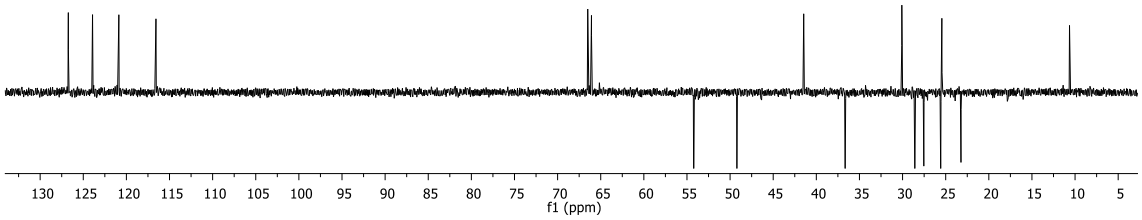

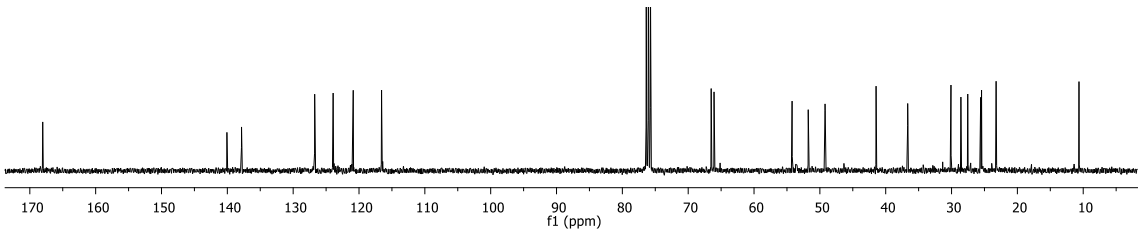

9.2. NMR Spectra of the Compounds Described in Chapter 4.2

Figure A11. ^{1}H (DMSO, 400 MHz), DEPT-135 and ^{13}C NMR spectra of Isonitrososstrychnine **1**

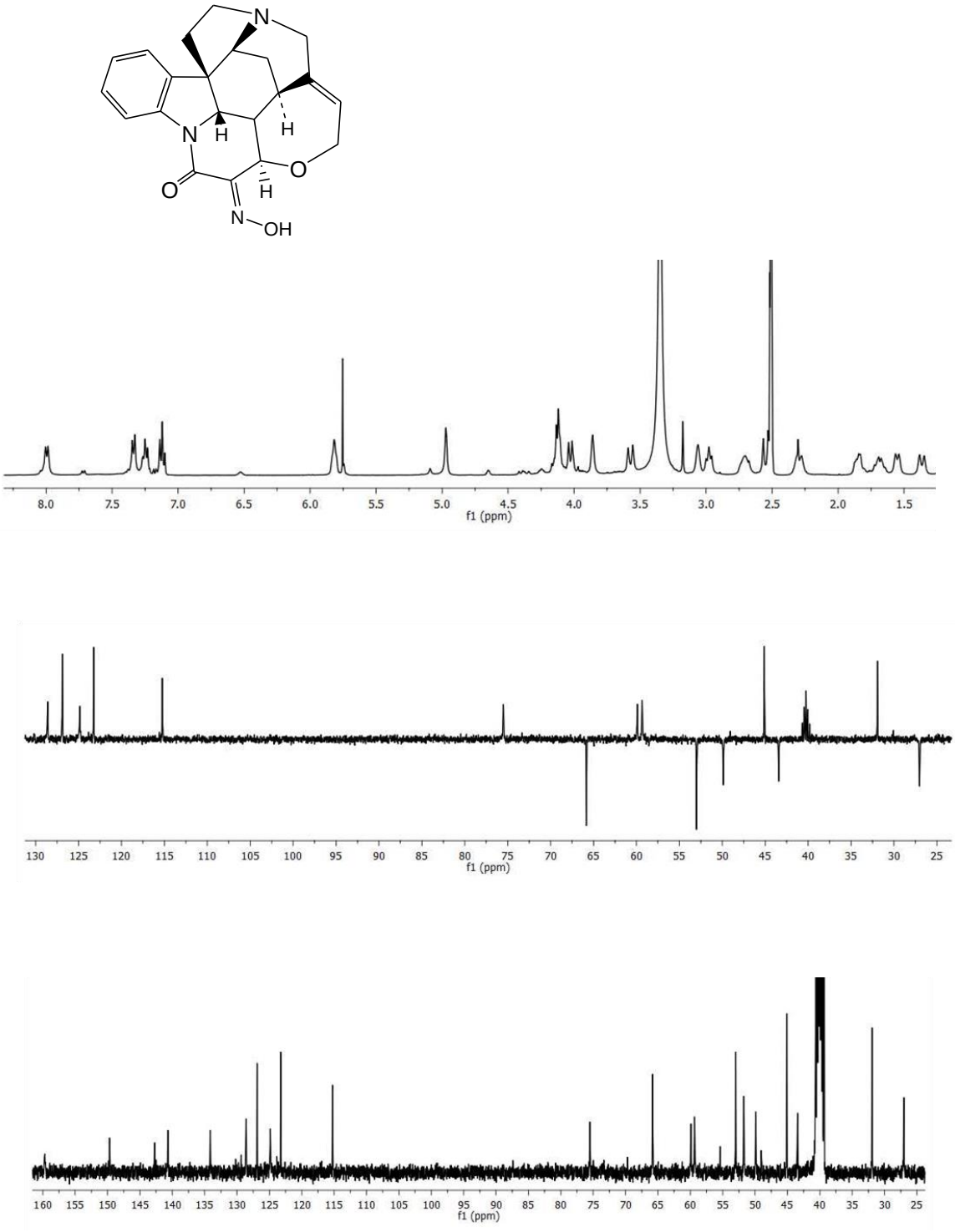

Figure A12. ^{1}H (DMSO, 400 MHz), DEPT-135 and ^{13}C NMR spectra of *N*-Propyl strychnine bromide **4**

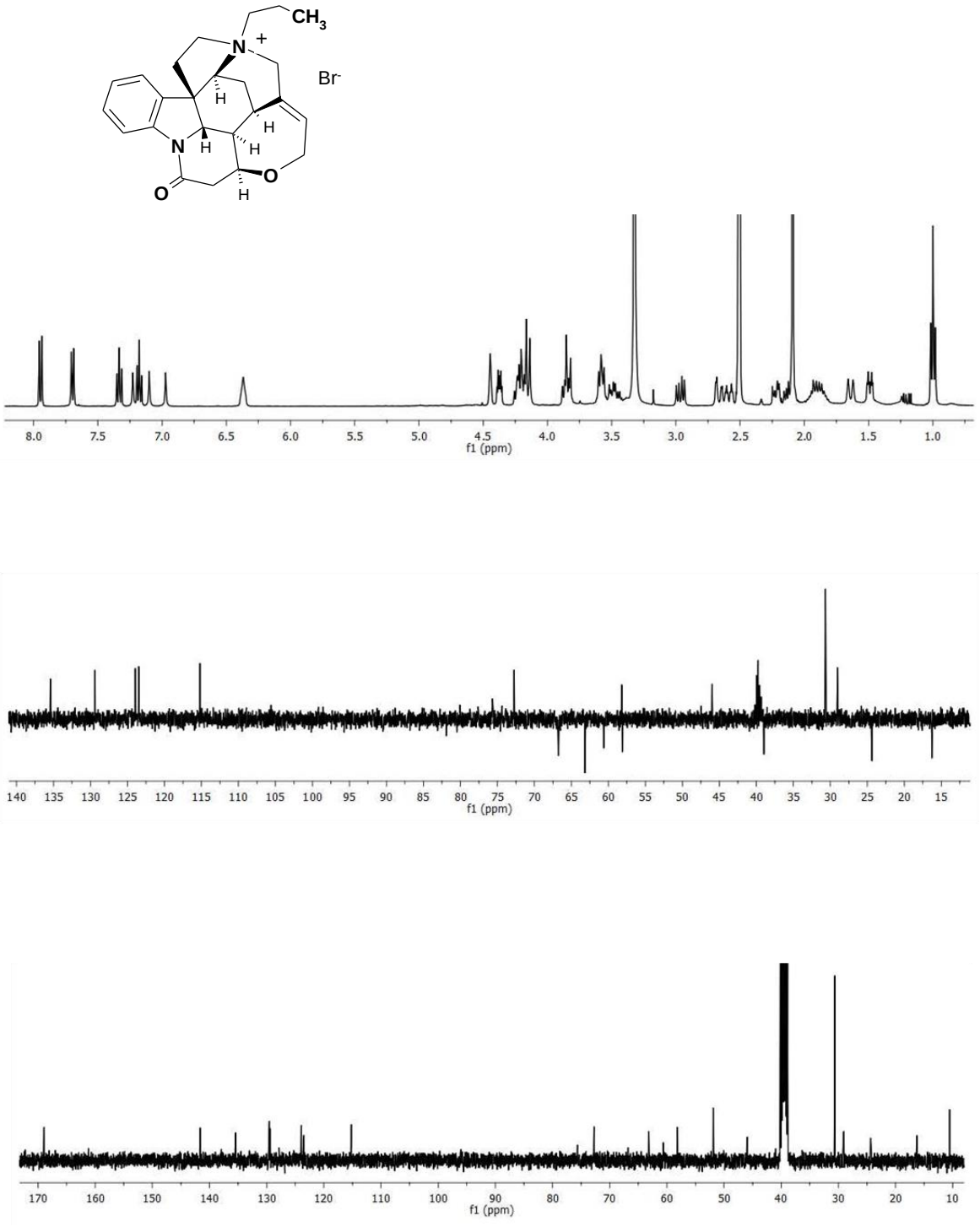

Figure A13. ^{1}H ($CDCl_3$, 400 MHz), DEPT-135 and ^{13}C NMR spectra of Pseodostrychnine **5**

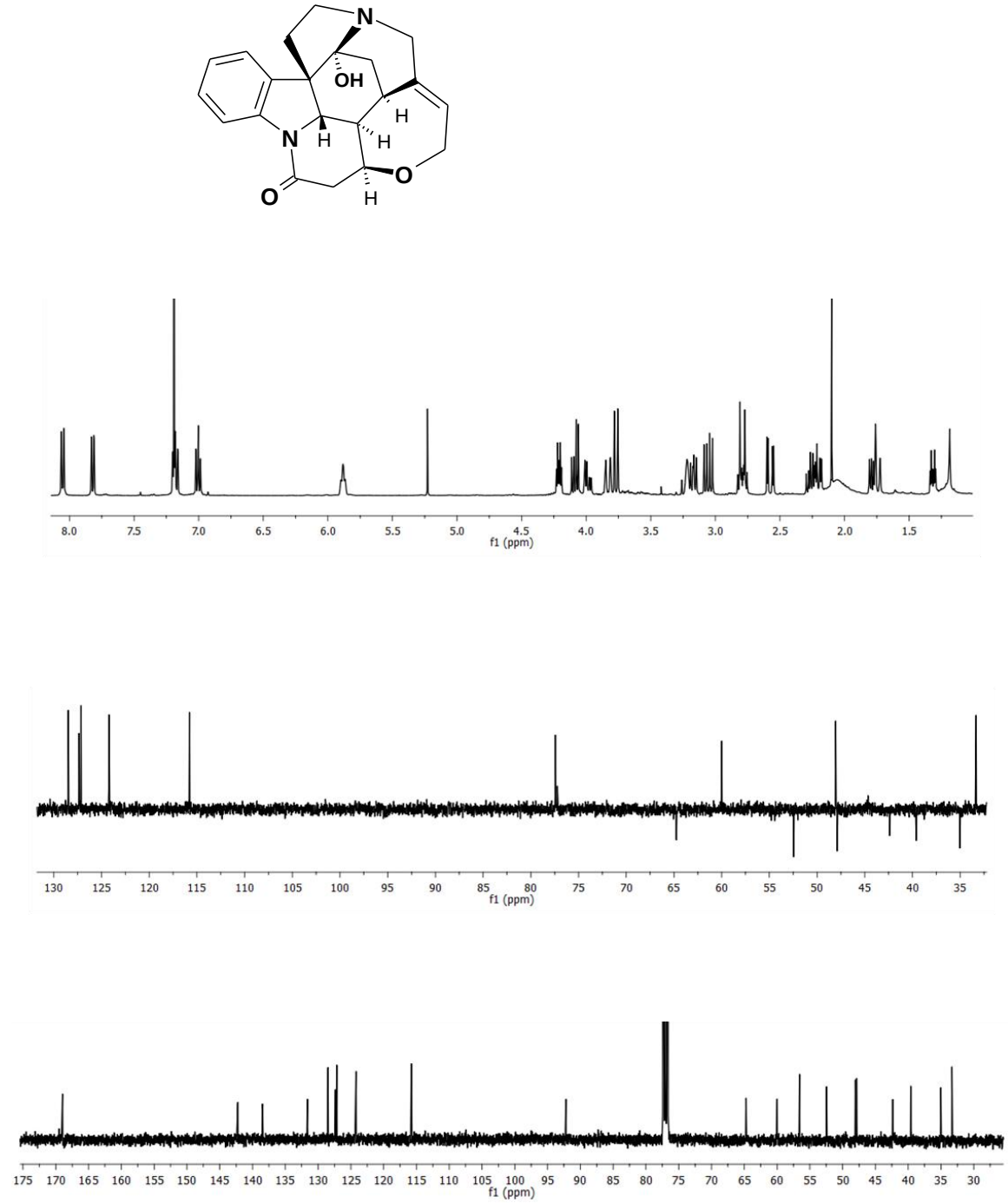

Figure A14. ^{1}H ($CDCl_3$, 400 MHz), DEPT-135 and ^{13}C NMR spectra of Oxostrychnine **6**

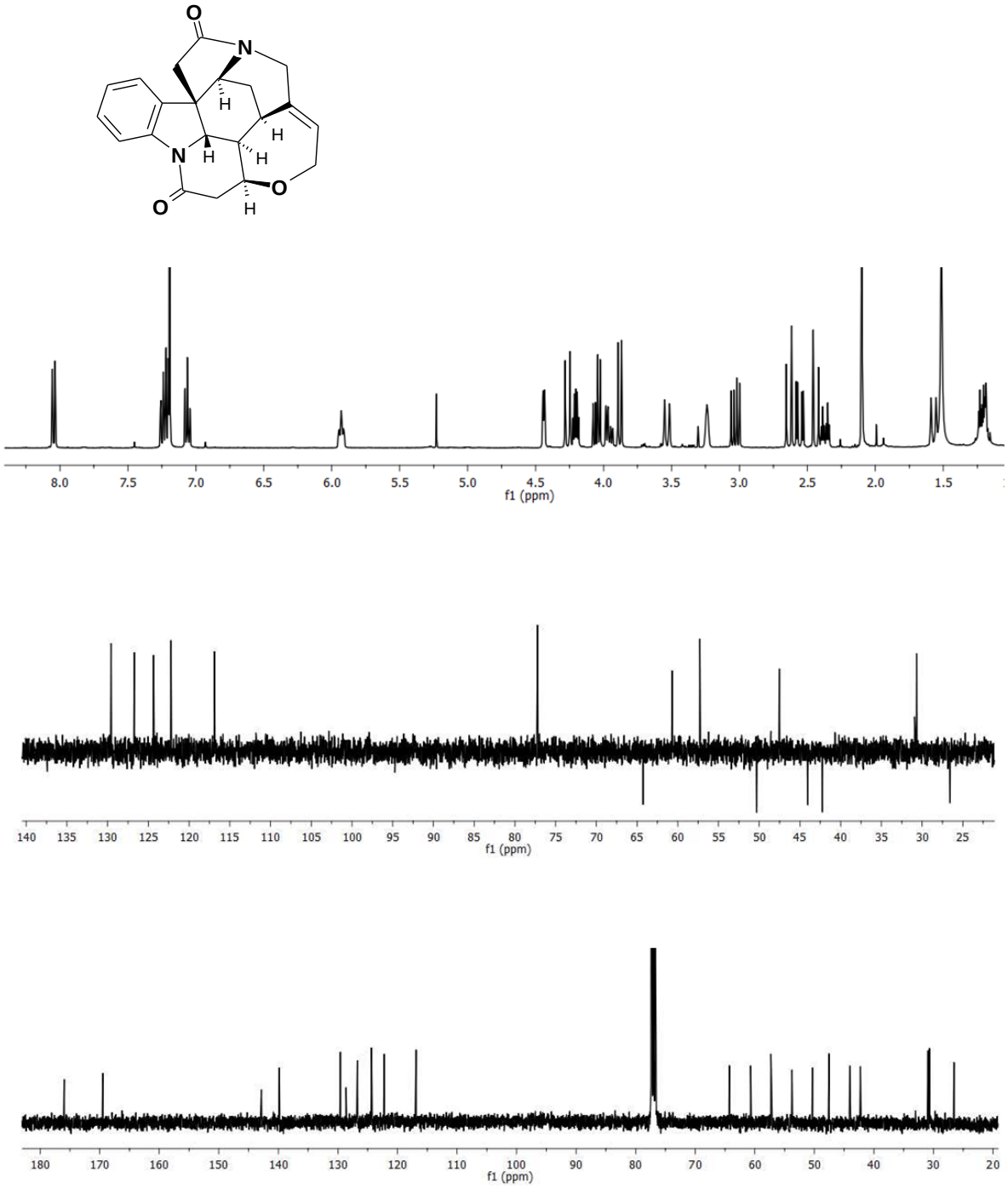

Figure A15. ^{1}H ($CDCl_3$, 400 MHz), DEPT-135 and ^{13}C NMR spectra of compound **7**

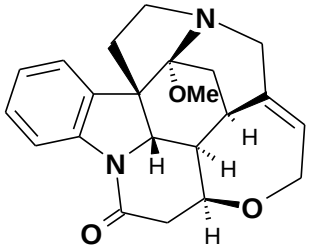

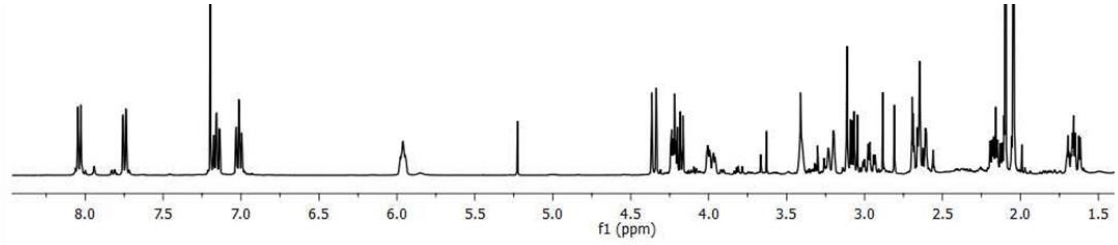

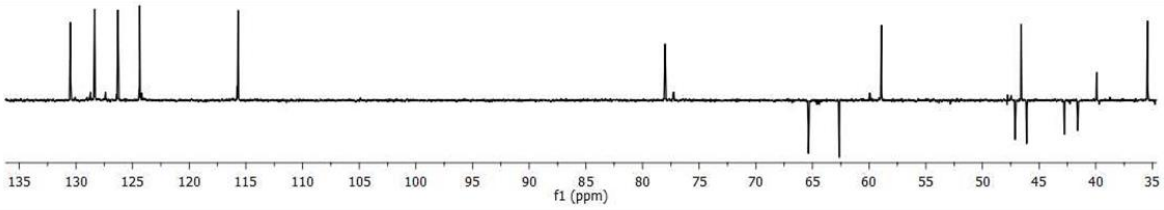

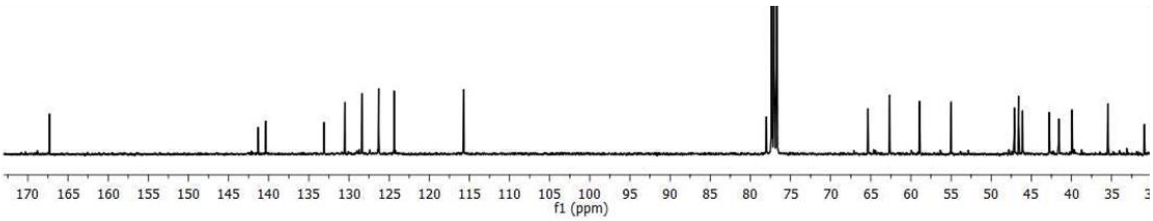

Figure A16. ^{1}H (DMSO, 400 MHz), DEPT-135 and ^{13}C NMR spectra of compound **8a**

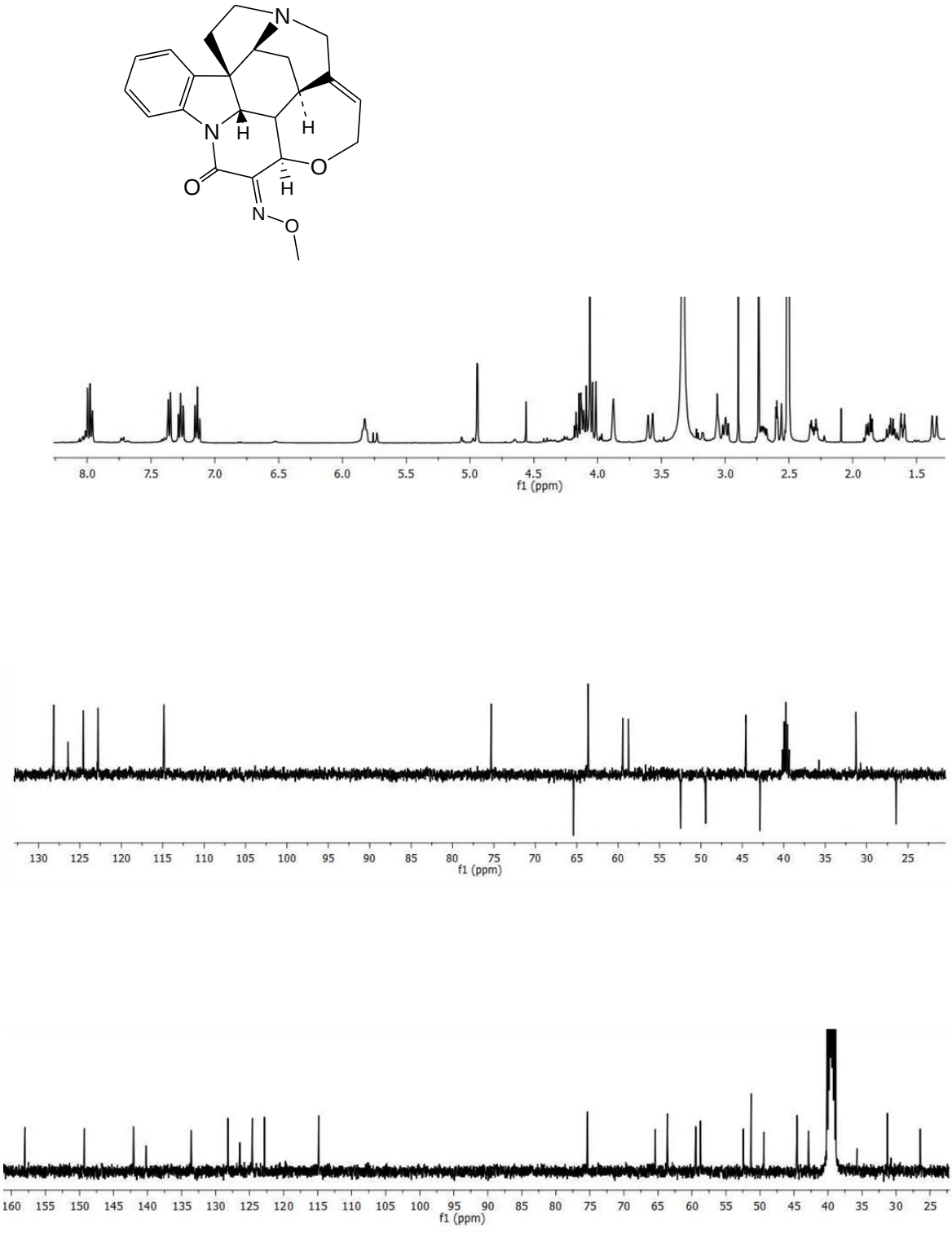

Figure A17. ^{1}H (DMSO, 400 MHz), DEPT-135 and ^{13}C NMR spectra of compound **8b**

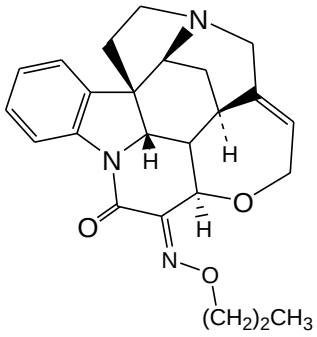

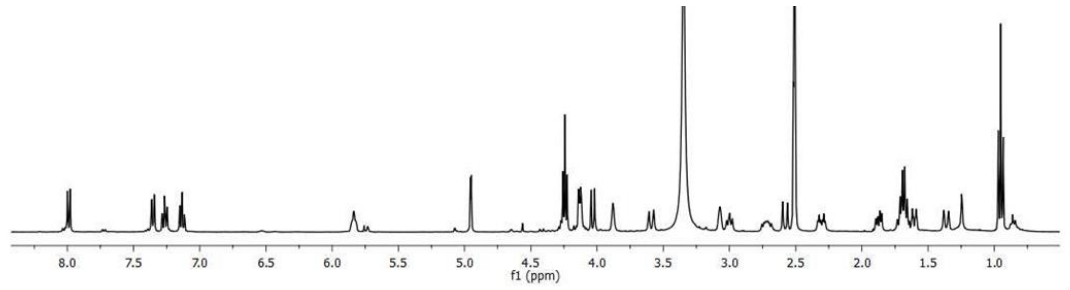

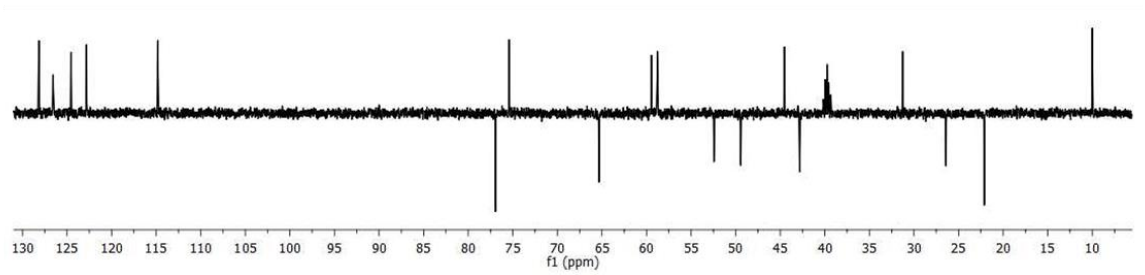

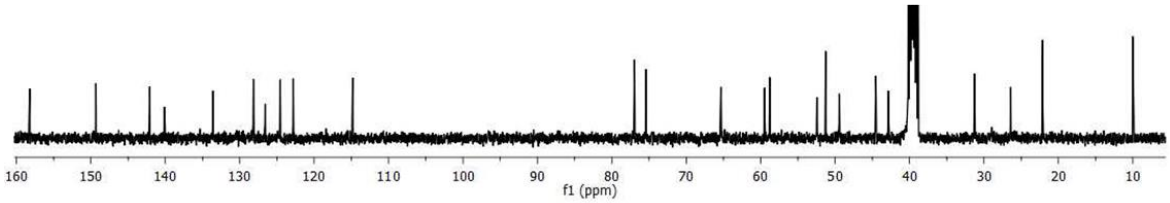

Figure A18. ^{1}H ($CDCl_3$, 400 MHz), DEPT-135 and ^{13}C NMR spectra of compound **8c**

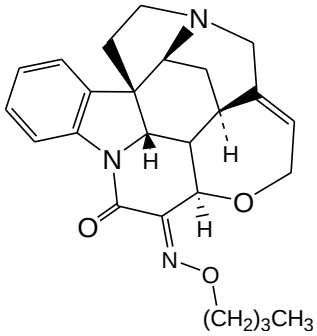

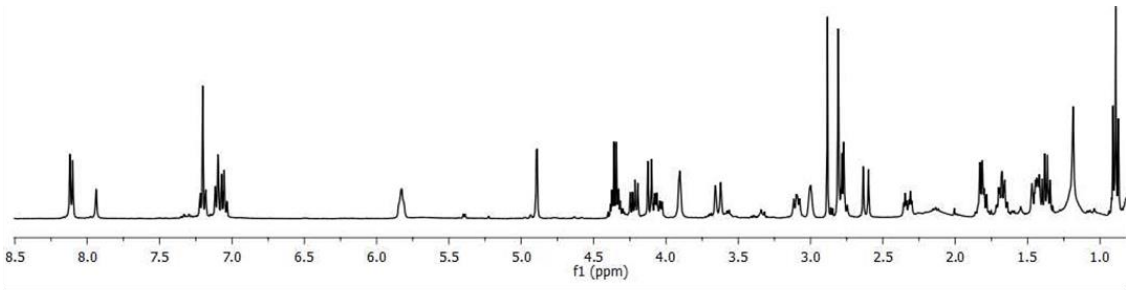

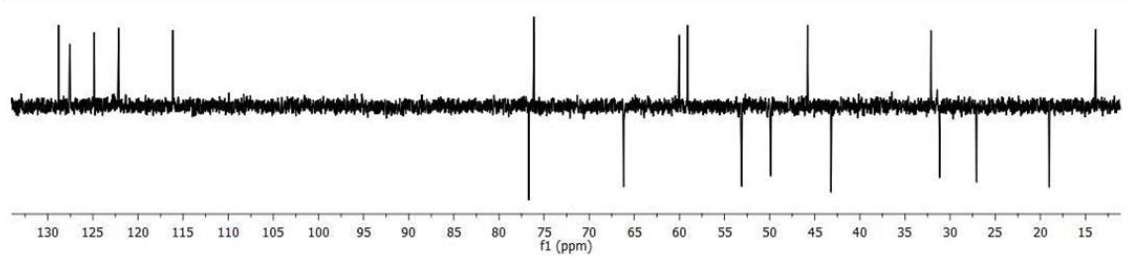

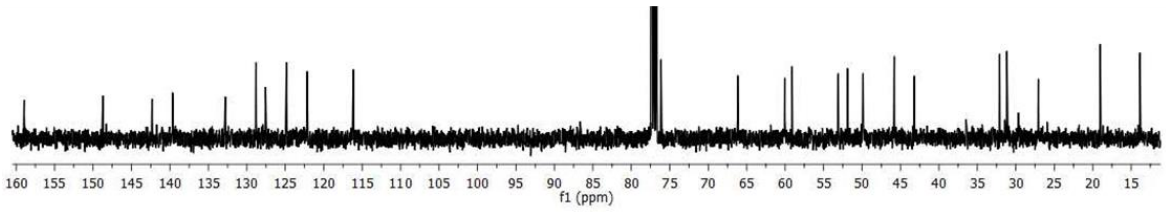

Figure A19. ^{1}H ($CDCl_3$, 400 MHz), DEPT-135 and ^{13}C NMR spectra of compound **8d**

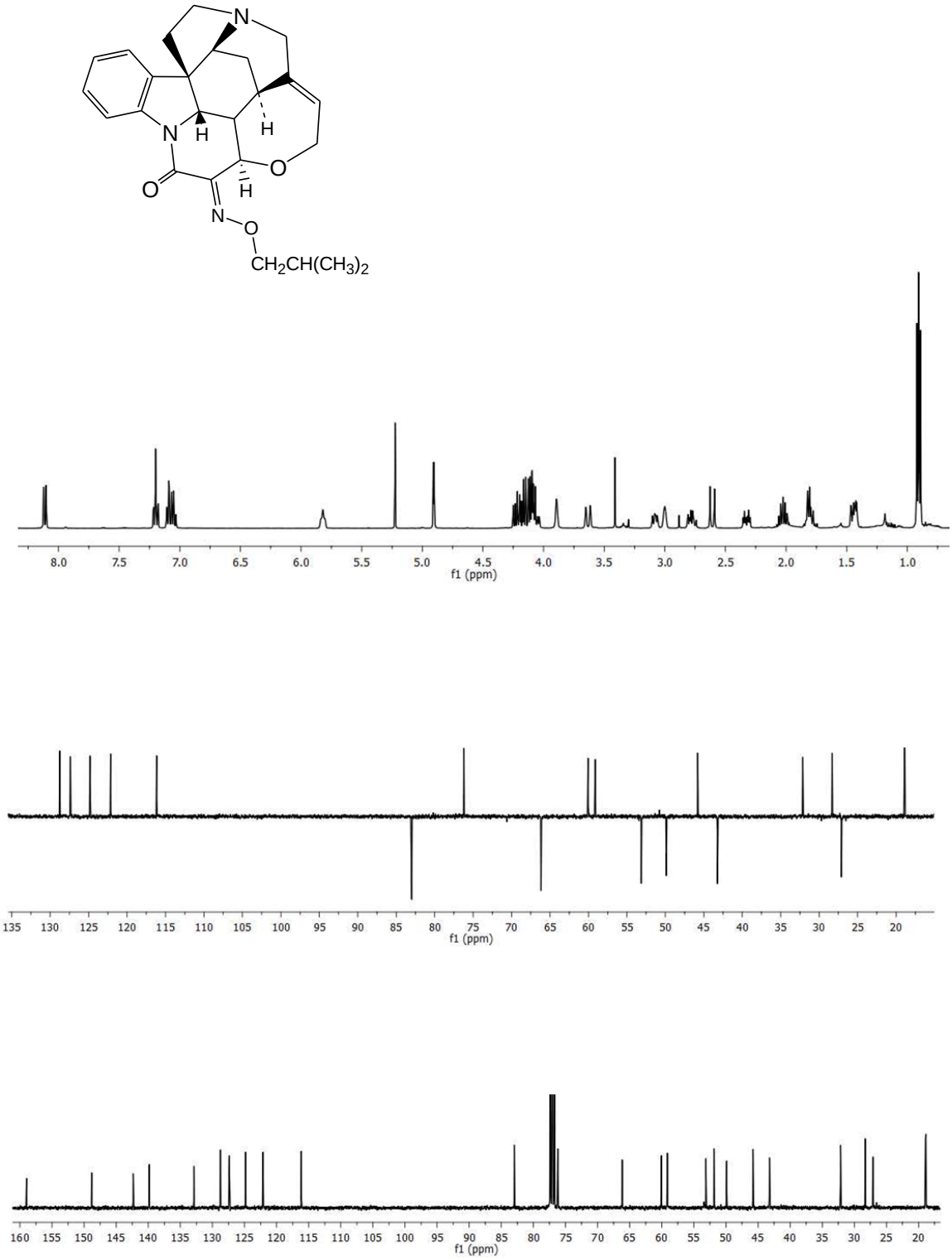

Figure A20. ^{1}H ($CDCl_3$, 400 MHz), DEPT-135 and ^{13}C NMR spectra of compound **8e**

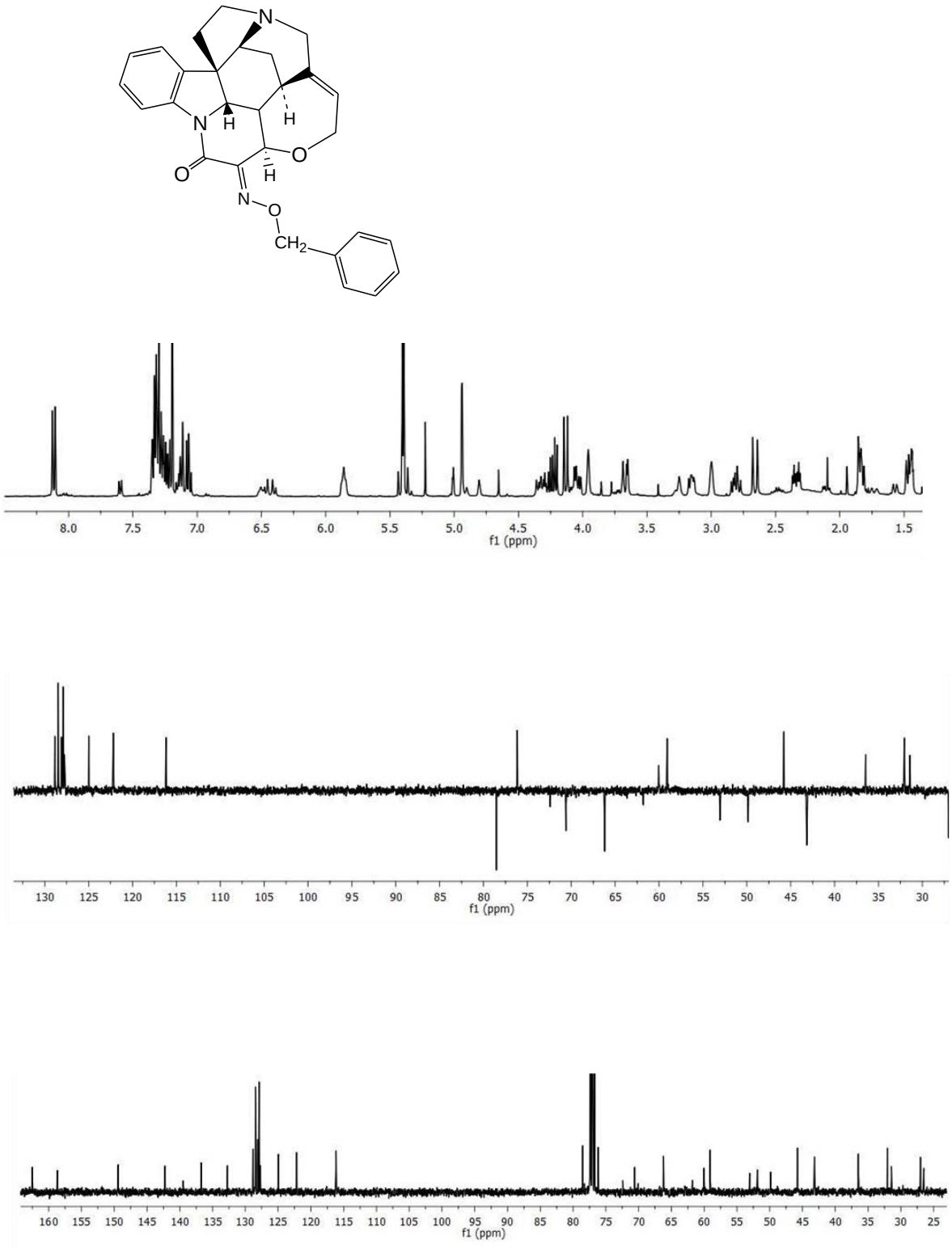

Figure A21. ^{1}H ($CDCl_3$, 400 MHz), DEPT-135 and ^{13}C NMR spectra of compound **8f**

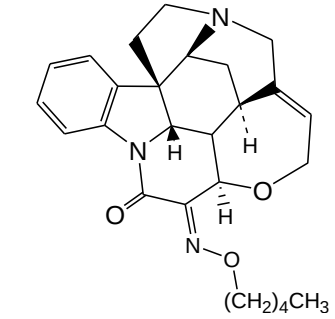

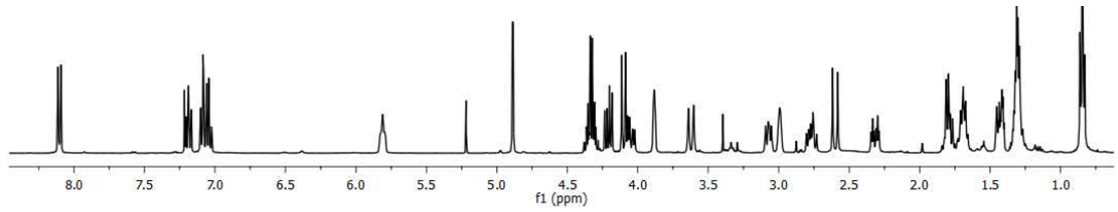

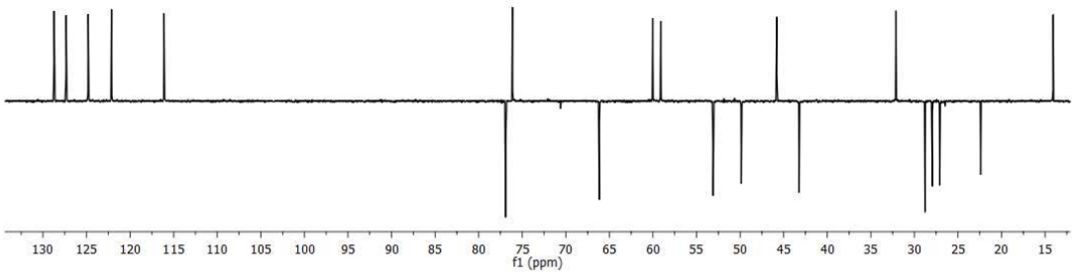

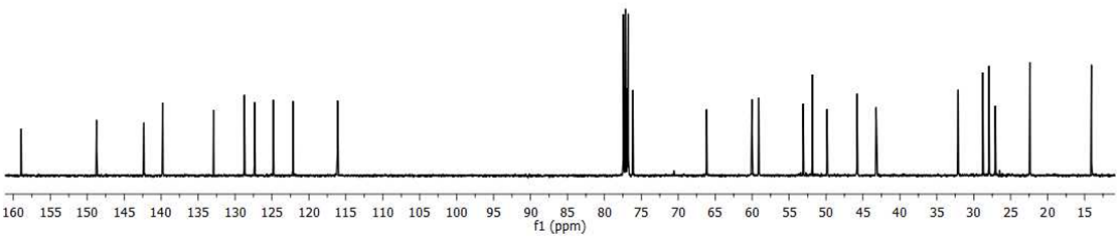

Figure A22. ^{1}H ($CDCl_3$, 400 MHz), DEPT-135 and ^{13}C NMR spectra of compound **8g**

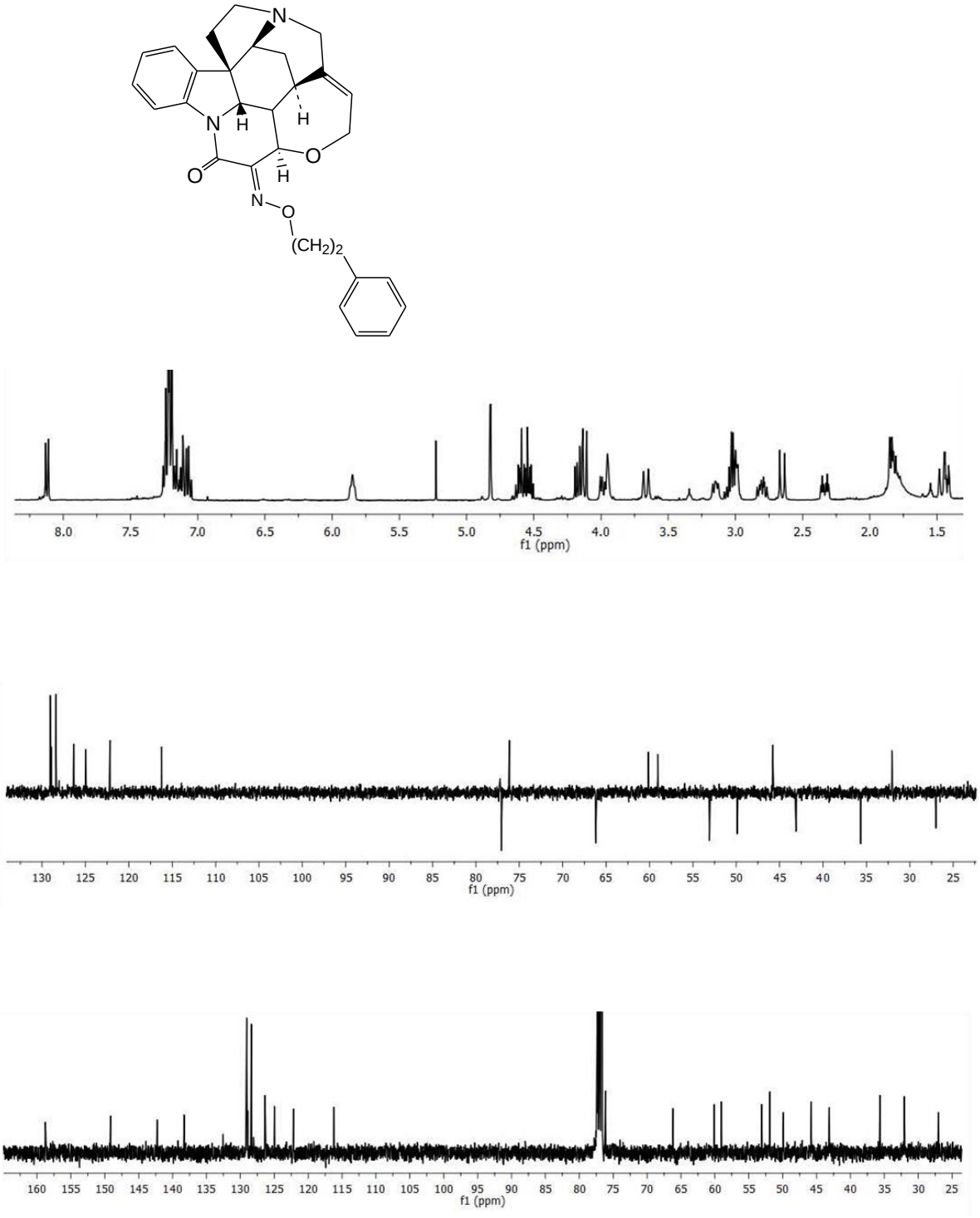

Figure A23. ^{1}H ($CDCl_3$, 400 MHz), DEPT-135 and ^{13}C NMR spectra of compound **8h**

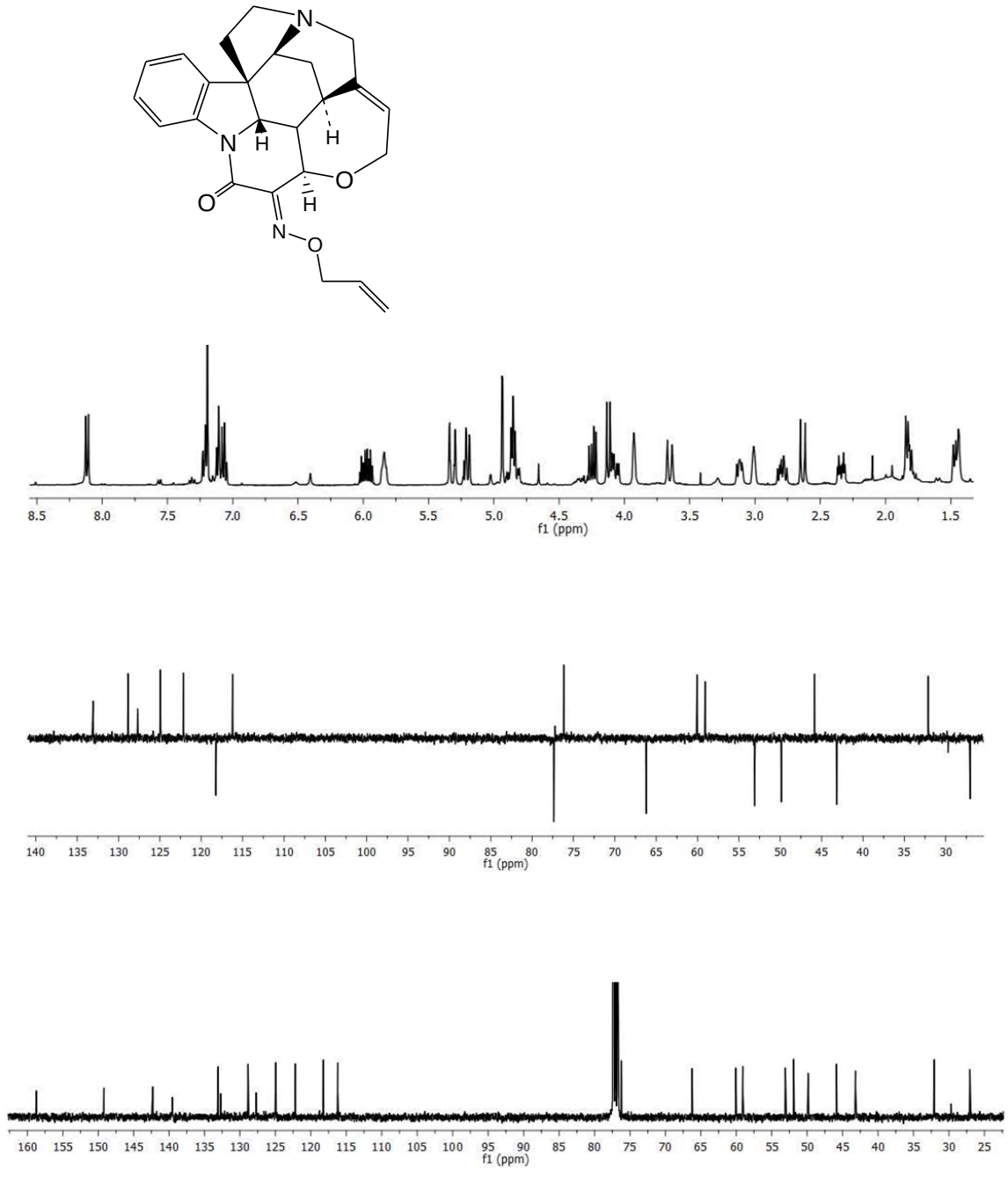

Figure A24. ^{1}H ($CDCl_3$, 400 MHz), DEPT-135 and ^{13}C NMR spectra of compound **8i**

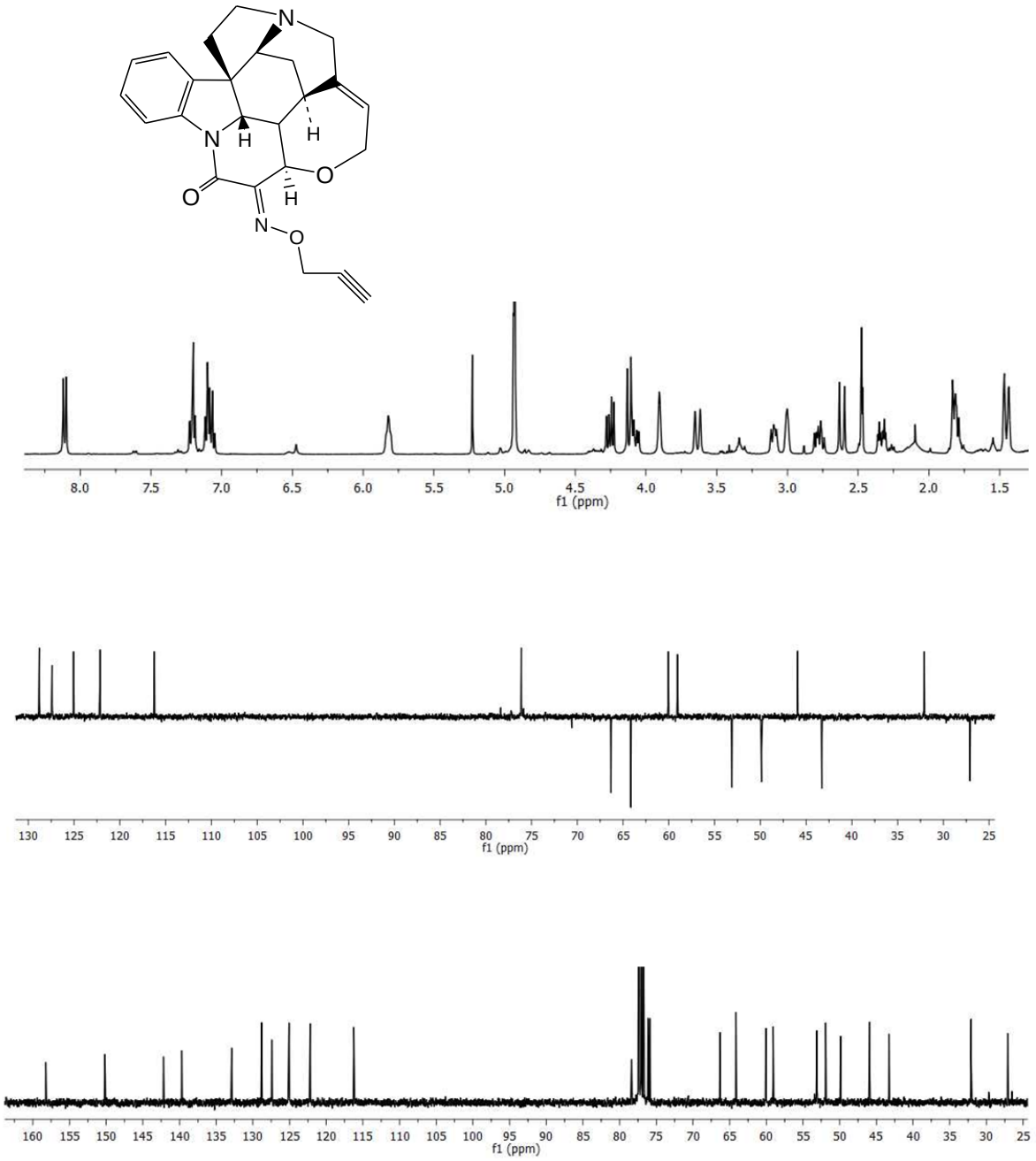

Figure A25. ^{1}H ($CDCl_3$, 400 MHz), DEPT-135 and ^{13}C NMR spectra of compound **8j**

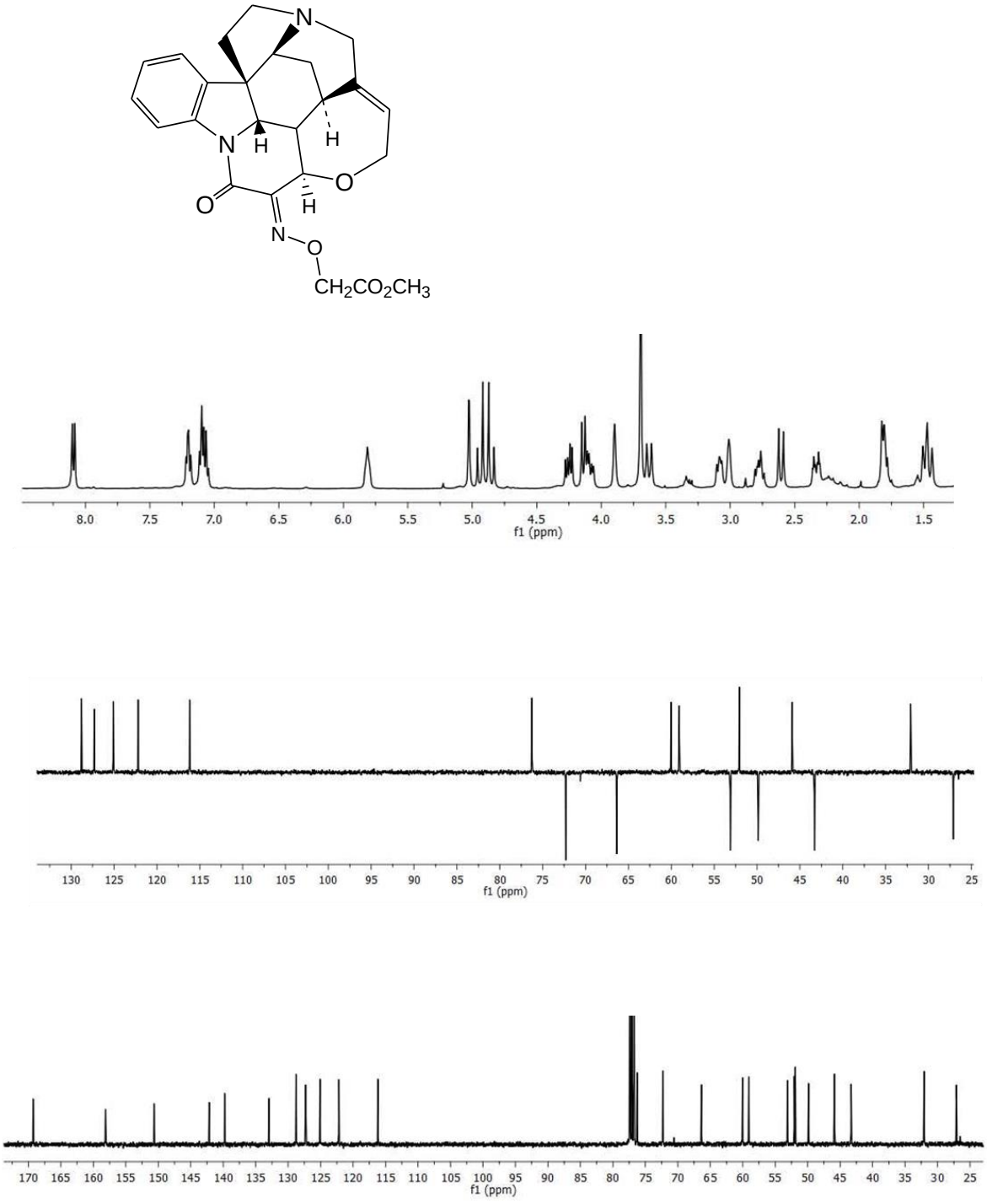

Figure A26. ^{1}H ($CDCl_3$, 400 MHz), DEPT-135 and ^{13}C NMR spectra of compound **8k**

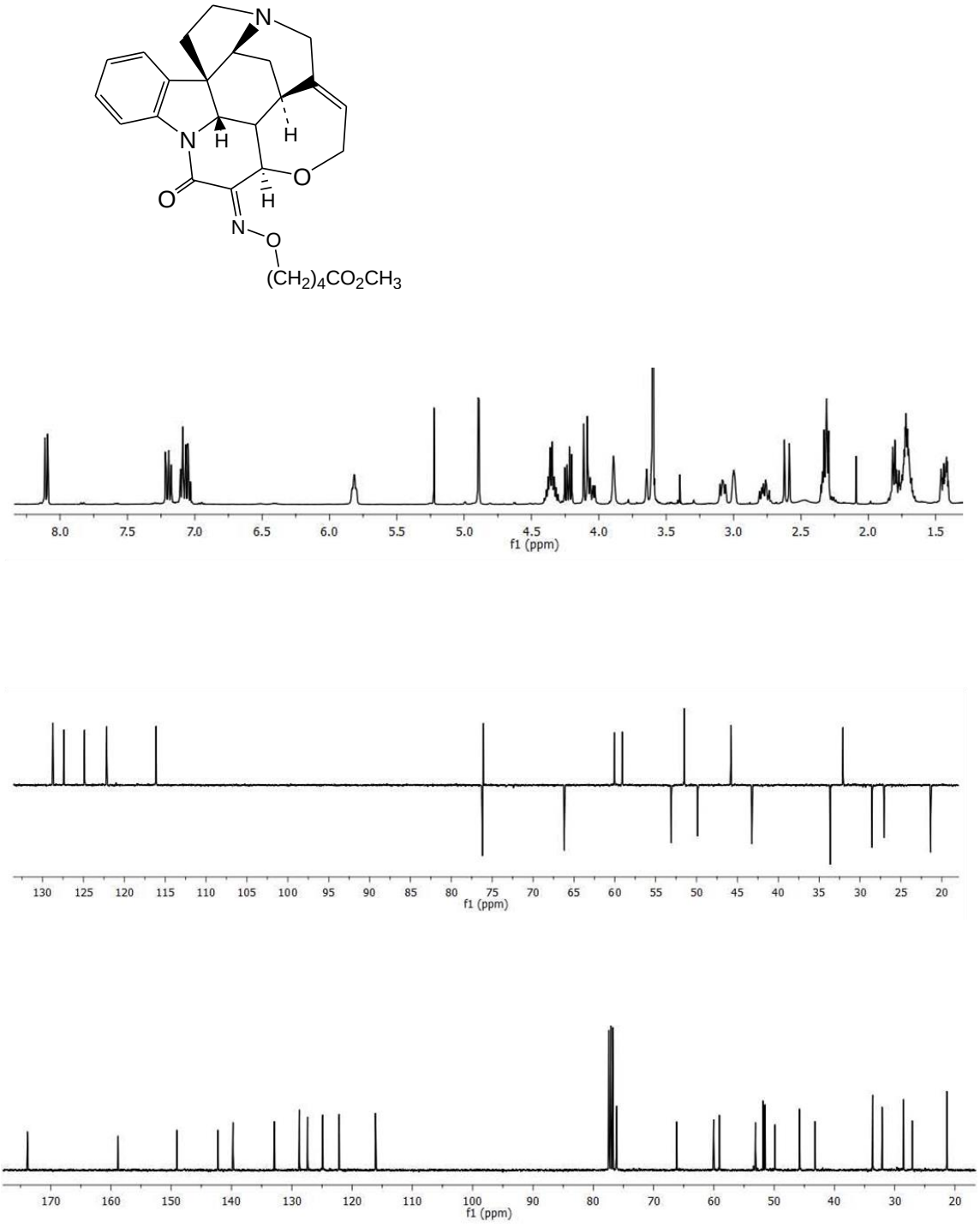

9.3. NMR Spectra of the Compounds Described in Chapter 4.3

Figure A27. ^{1}H (DMSO, 400 MHz), DEPT-135 and ^{13}C NMR spectra of 11-aminostrychnine **2**

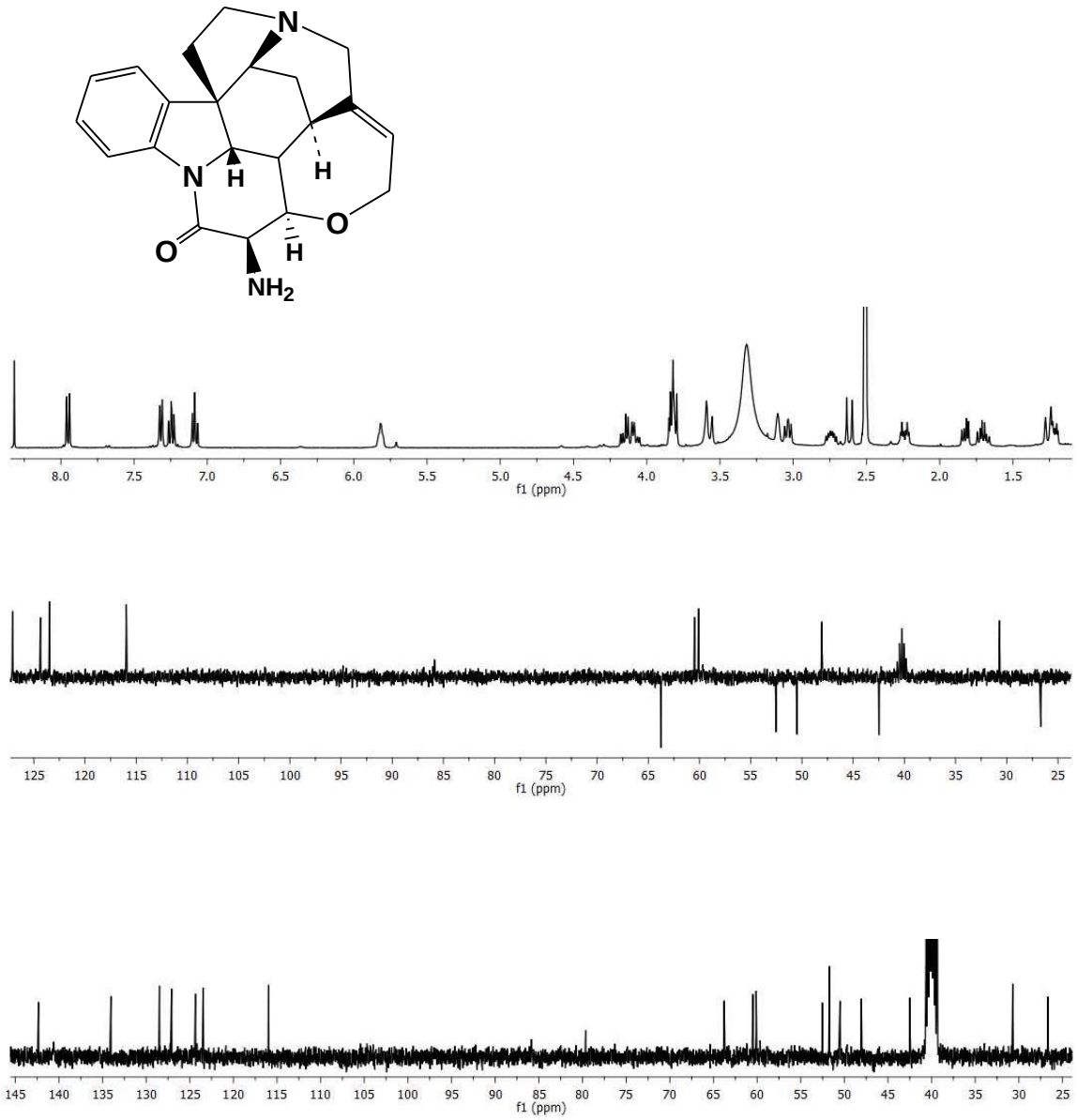

Figure A28. ^{1}H ($CDCl_3$, 400 MHz), DEPT-135 and ^{13}C NMR spectra of reference compound **3**

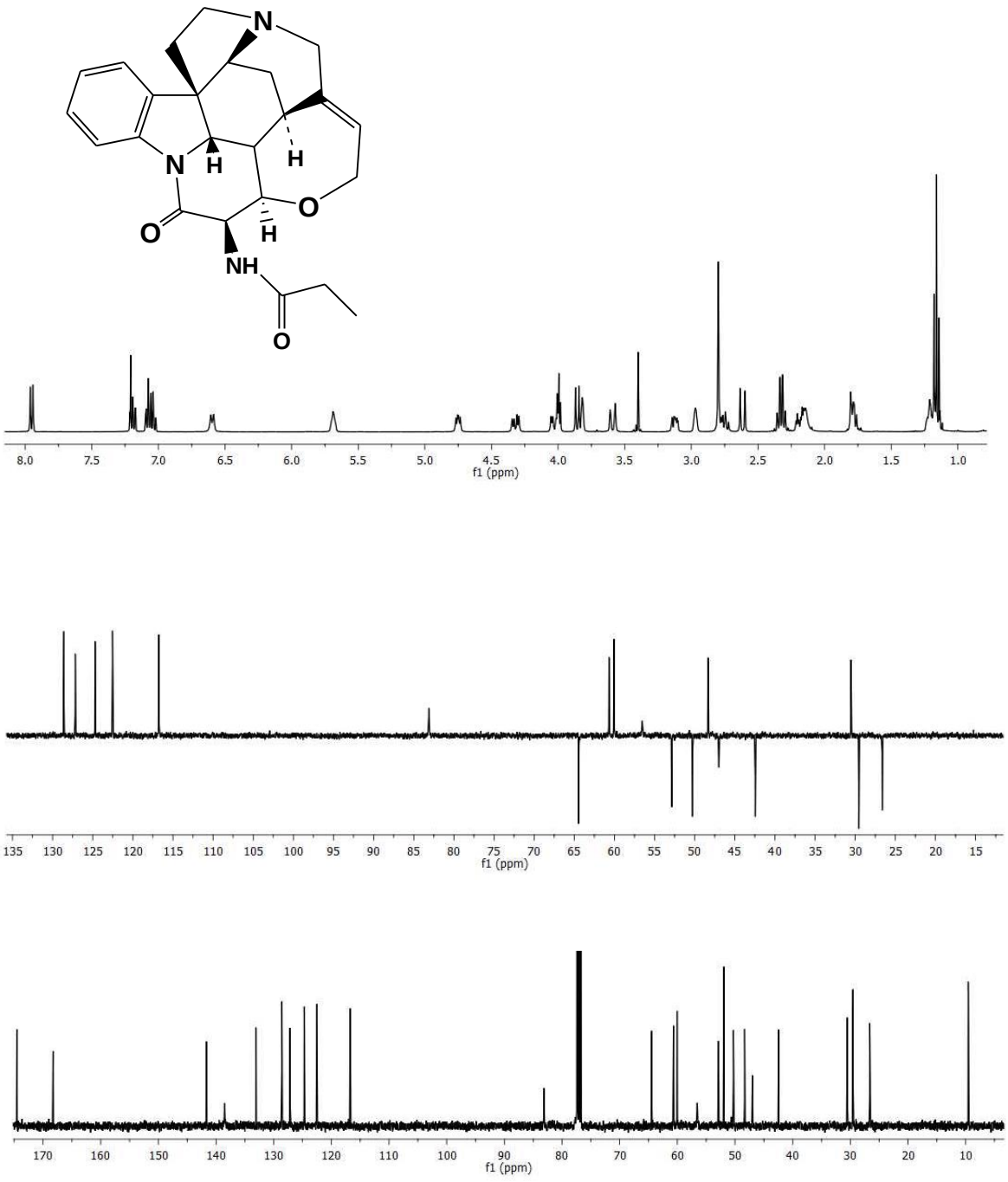

Figure A29. ^{1}H (MeOD, 101 MHz), DEPT-135 and ^{13}C NMR spectra of compound 4a

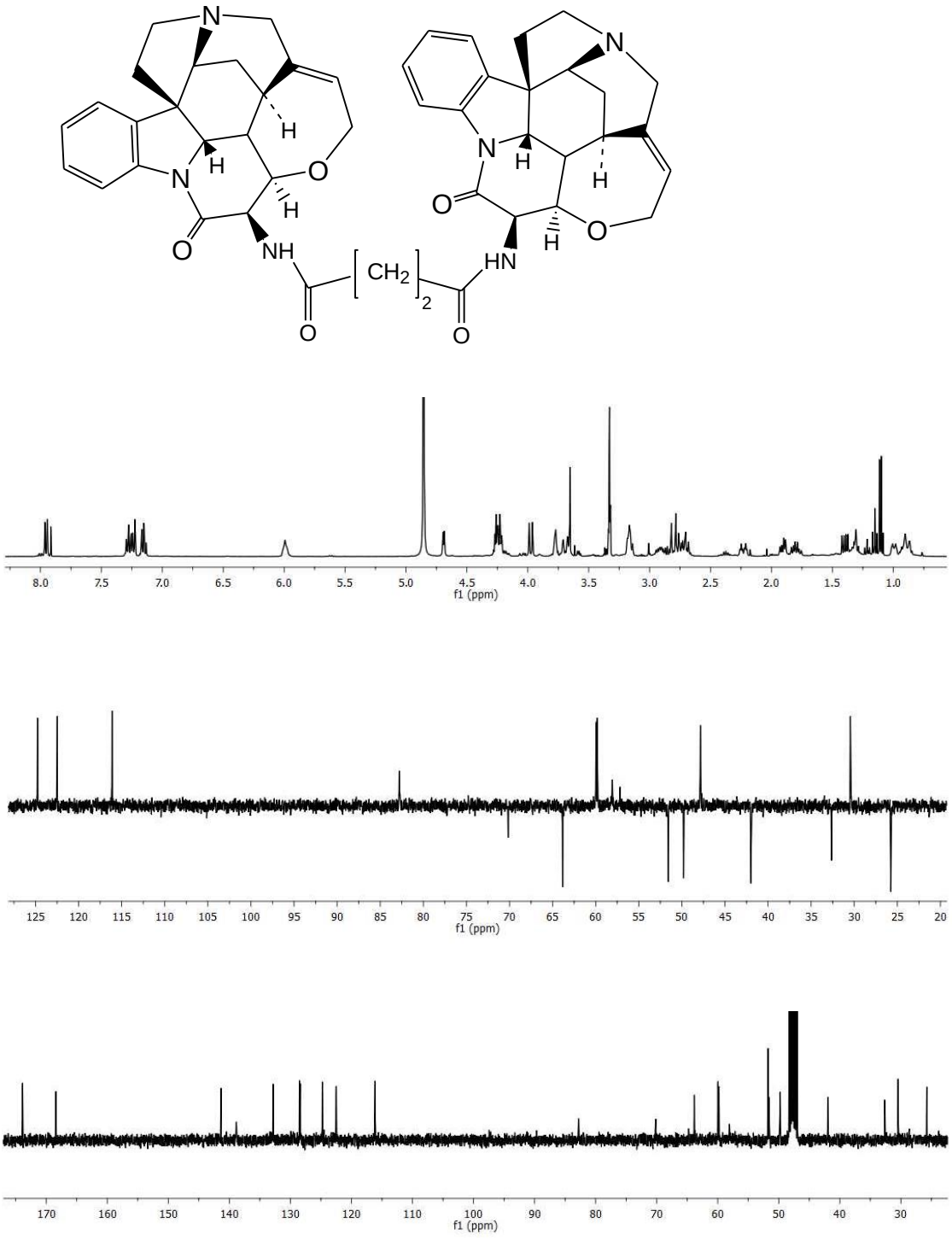

Figure A30. ^{1}H (MeOD, 101 MHz), DEPT-135 and ^{13}C NMR spectra of compound 4b

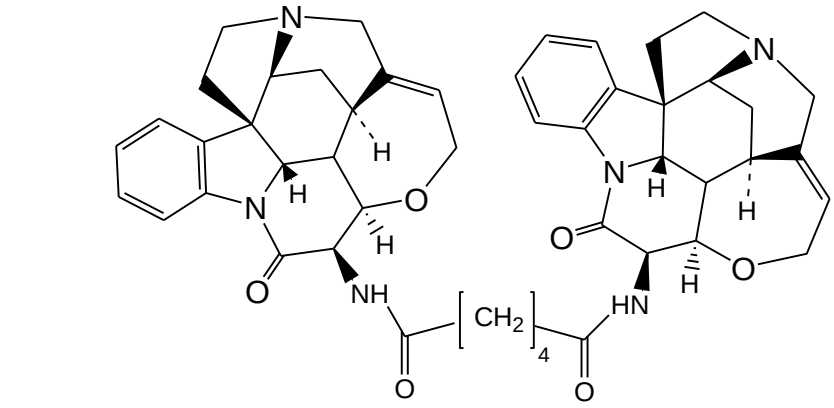

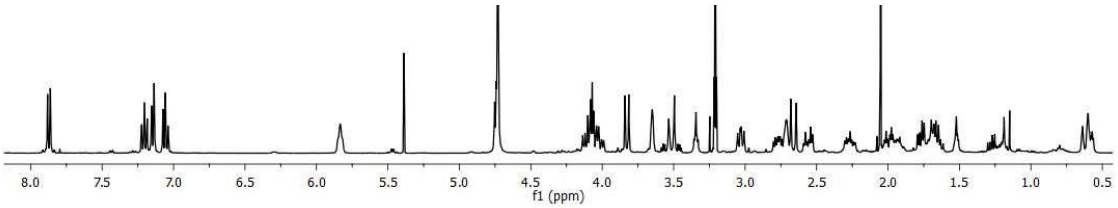

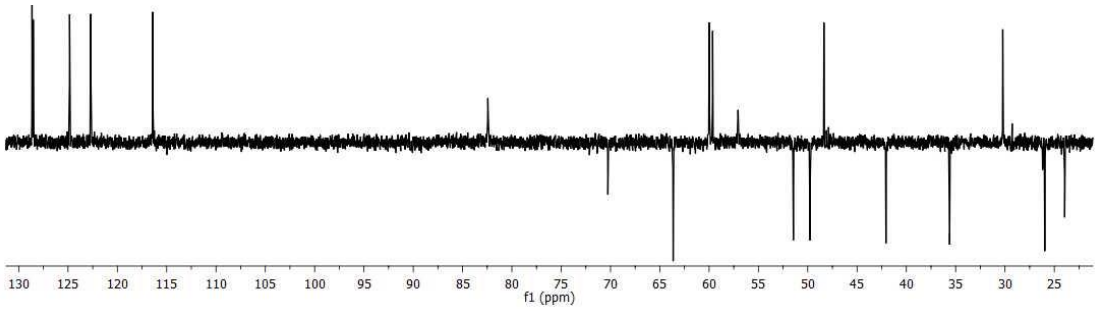

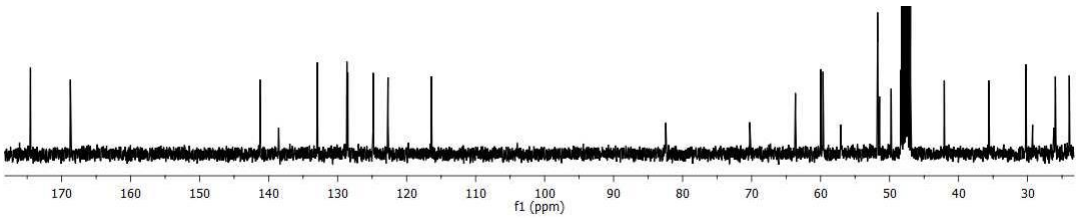

Figure A31. ^{1}H (MeOD, 101 MHz), DEPT-135 and ^{13}C NMR spectra of compound **4c**

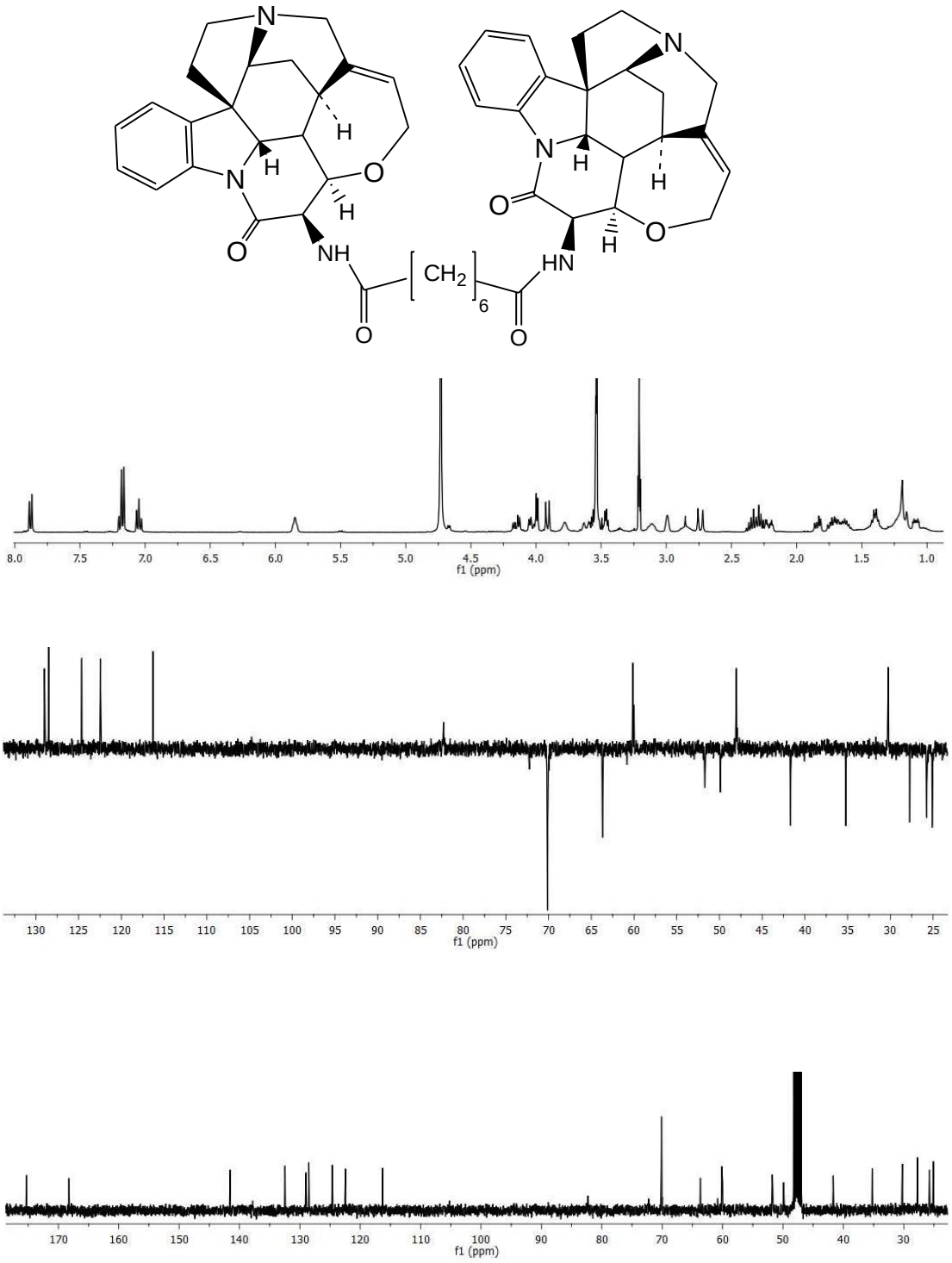

Figure A32. ^{1}H (MeOD, 101 MHz), DEPT-135 and ^{13}C NMR spectra of compound **4d**

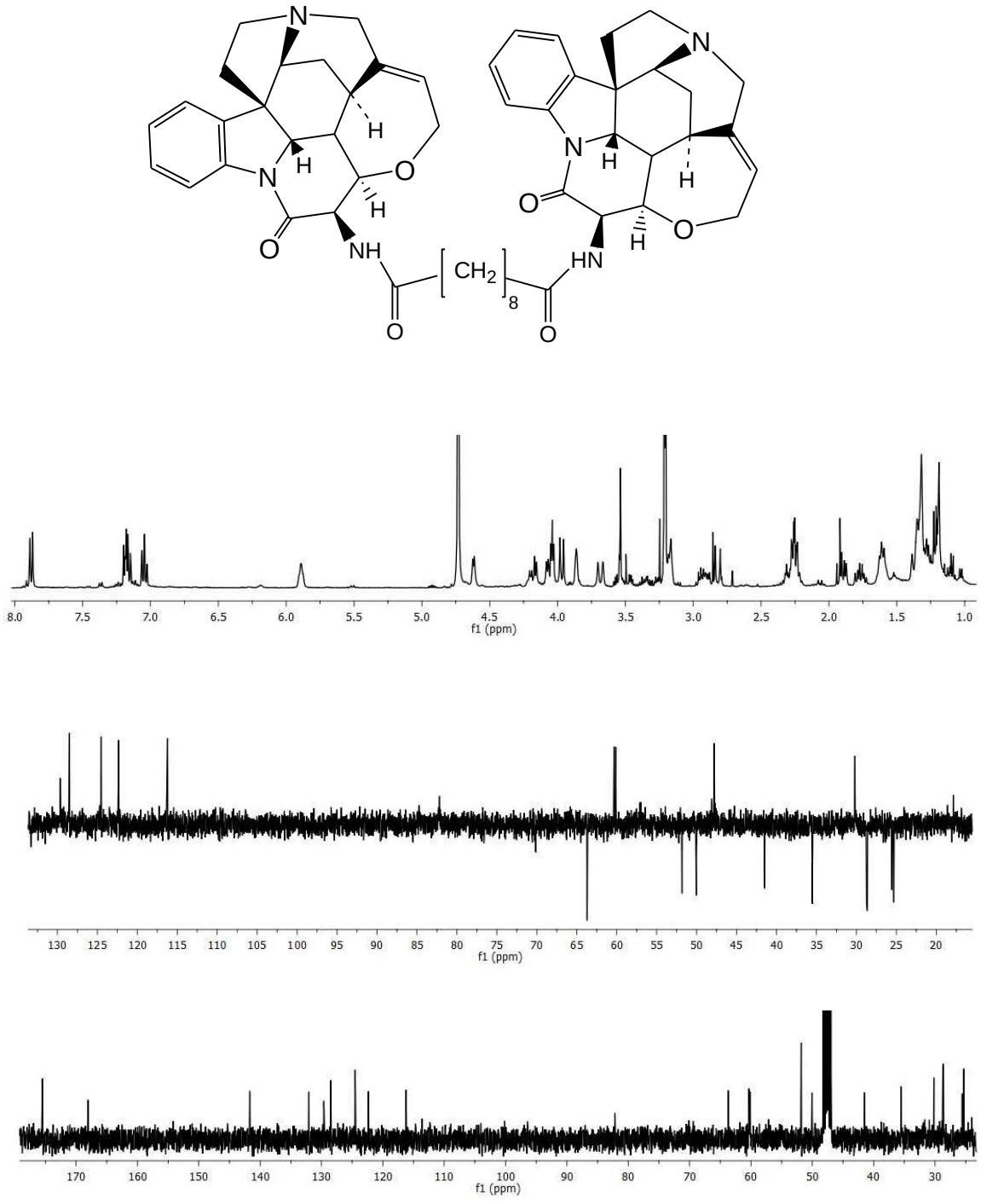

Figure A33. ^{1}H (MeOD, 101 MHz), DEPT-135 and ^{13}C NMR spectra of compound **4e**

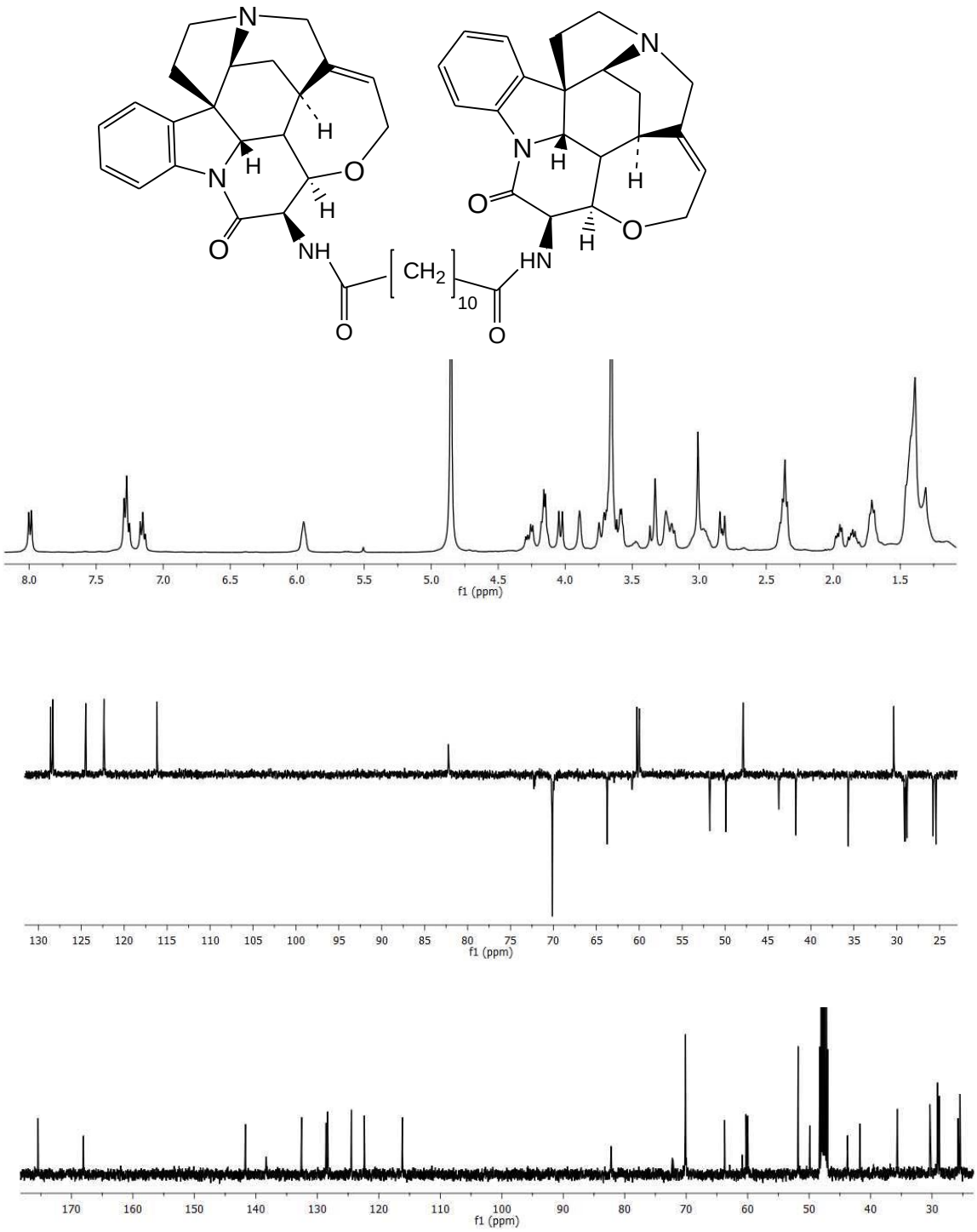

Figure A34. ^{1}H (MeOD, 101 MHz), DEPT-135 and ^{13}C NMR spectra of compound **4f**

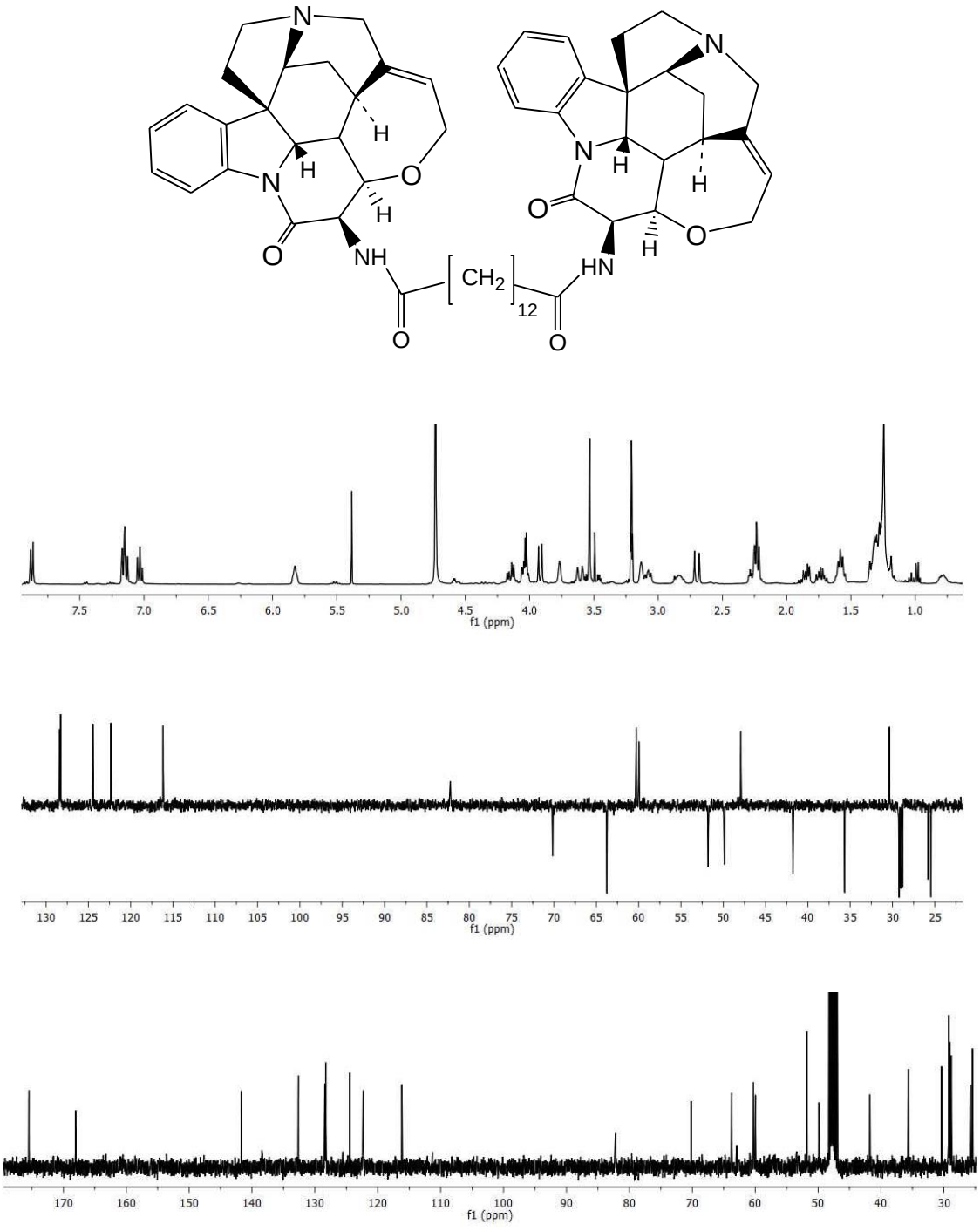

9.4. LC-MS Chromatograms of the Compounds Described in Chapter 4.3

Figure A35. LC-MS Chromatogram of compound **2**

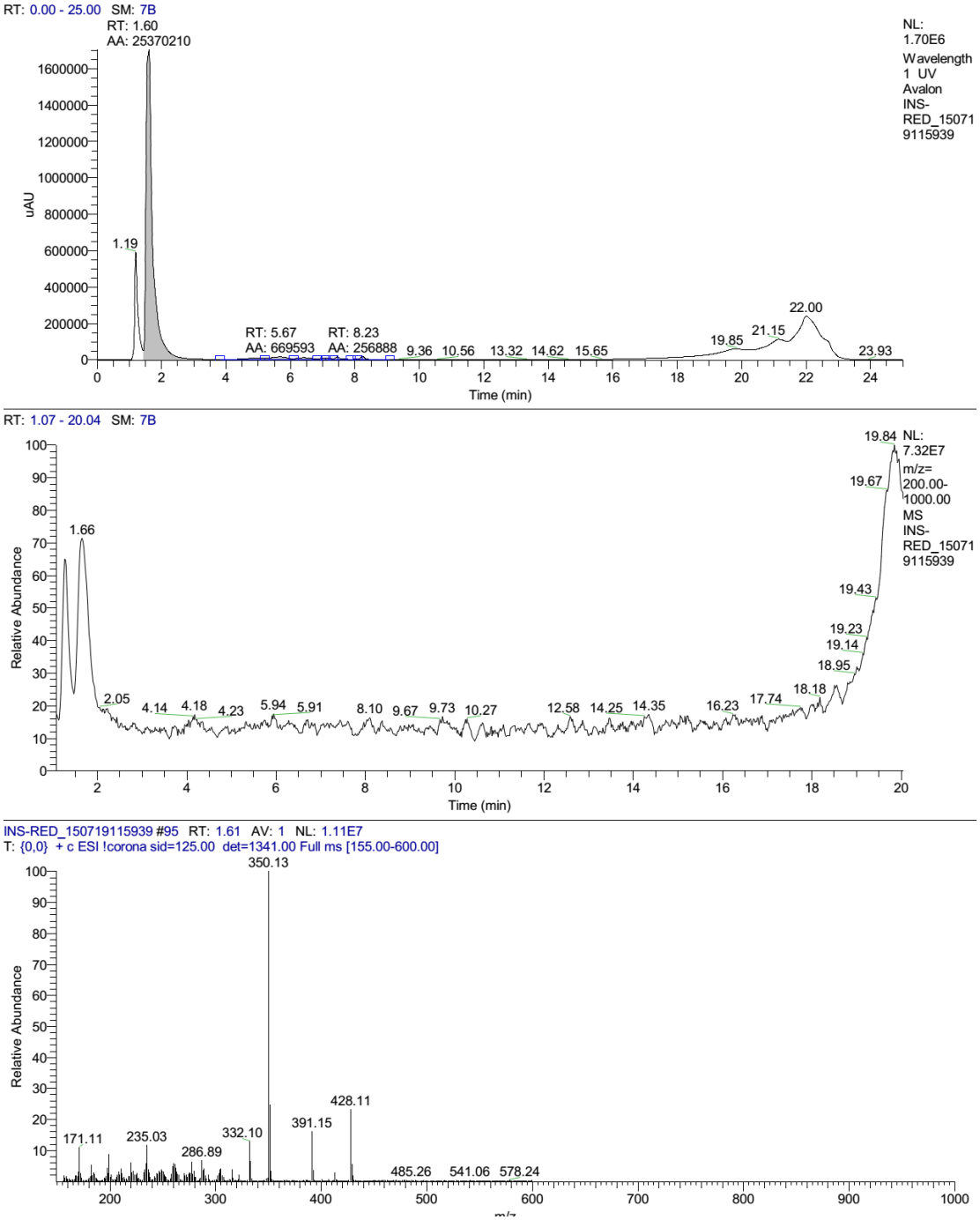

Figure A36. LC-MS Chromatogram of compound **3**

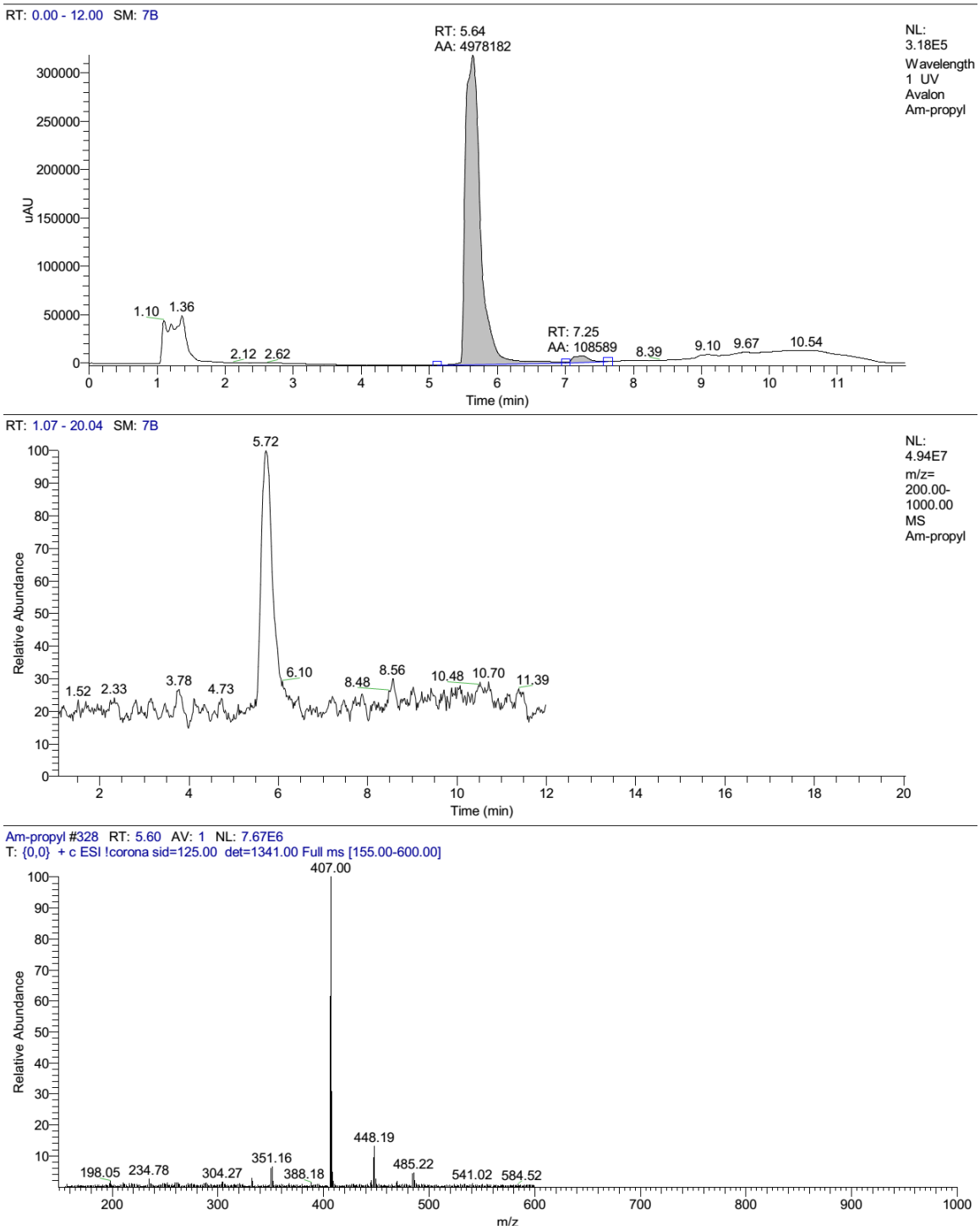

Figure A37. LC-MS Chromatogram of compound **4b**

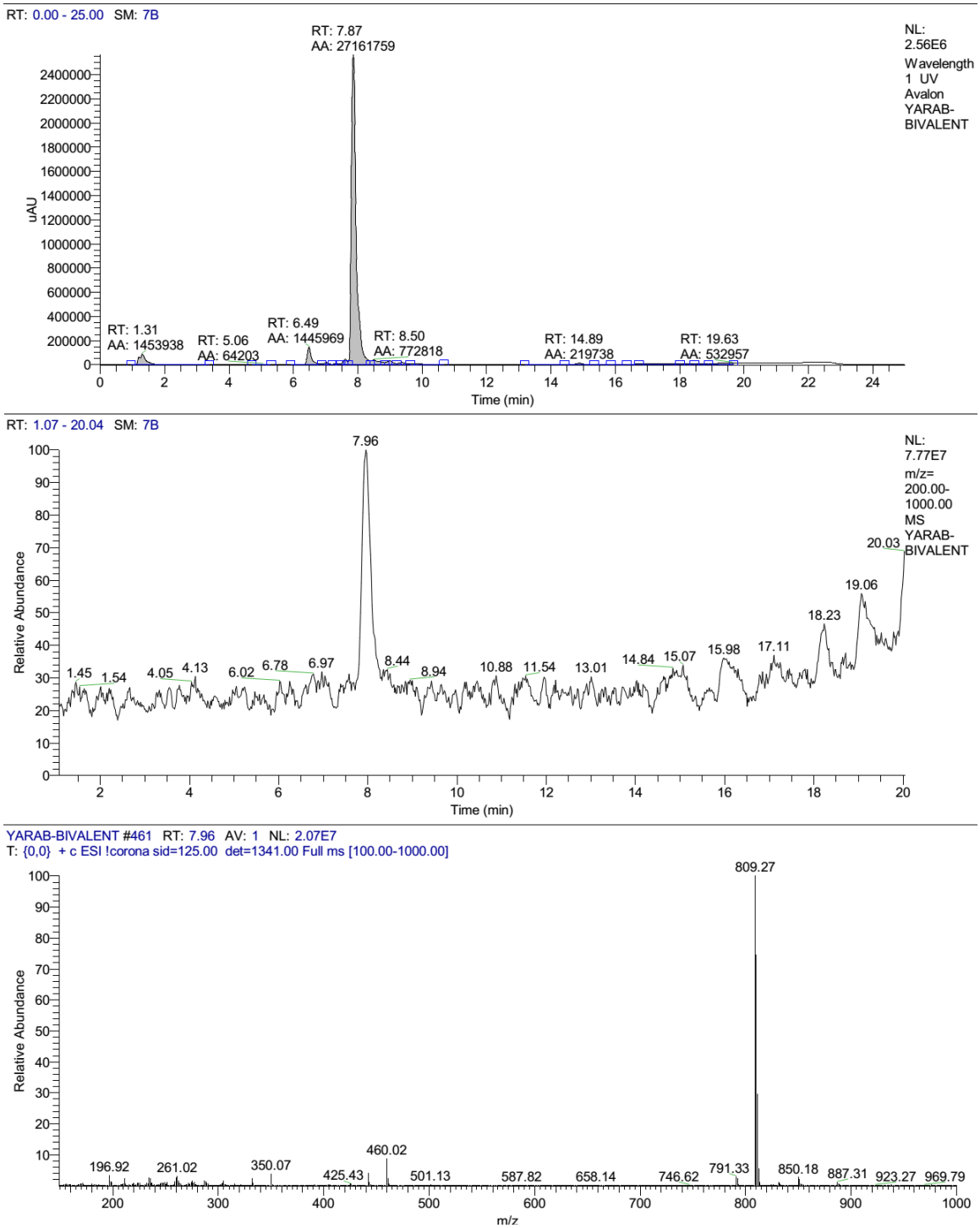

Figure A38. LC-MS Chromatogram of compound **4c**

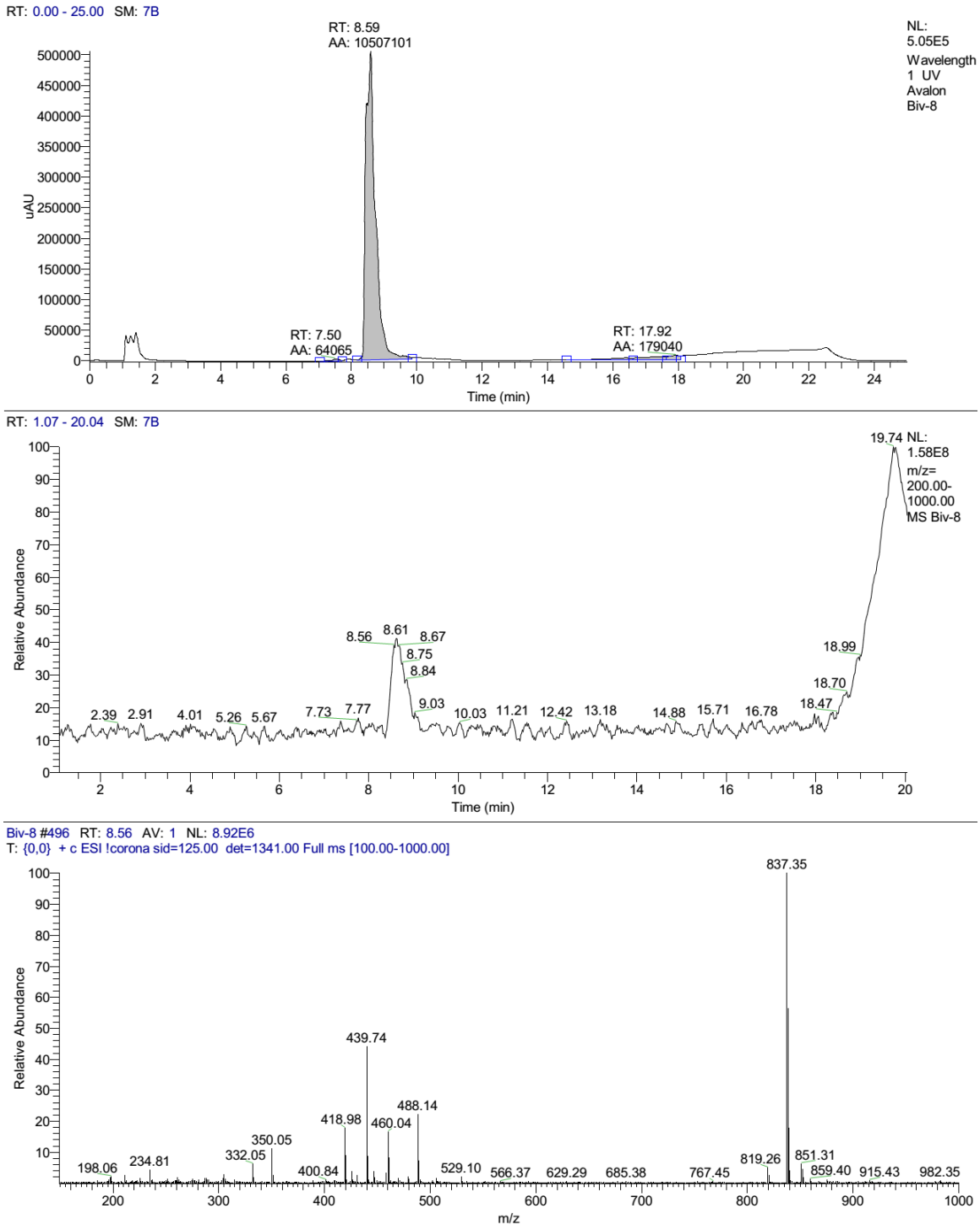

Figure A39. LC-MS Chromatogram of compound **4e**